LEABHARLANN CHOLÁISTE NA TRÍONÓIDE, BAILE ÁTHA CLIATH | TRINITY COLLEGE LIBRARY DUBLIN
Ollscoil Átha Cliath | The University of Dublin

Terms and Conditions of Use of Digitised Theses from Trinity College Library Dublin

Copyright statement

All material supplied by Trinity College Library is protected by copyright (under the Copyright and Related Rights Act, 2000 as amended) and other relevant Intellectual Property Rights. By accessing and using a Digitised Thesis from Trinity College Library you acknowledge that all Intellectual Property Rights in any Works supplied are the sole and exclusive property of the copyright and/or other IPR holder. Specific copyright holders may not be explicitly identified. Use of materials from other sources within a thesis should not be construed as a claim over them.

A non-exclusive, non-transferable licence is hereby granted to those using or reproducing, in whole or in part, the material for valid purposes, providing the copyright owners are acknowledged using the normal conventions. Where specific permission to use material is required, this is identified and such permission must be sought from the copyright holder or agency cited.

Liability statement

By using a Digitised Thesis, I accept that Trinity College Dublin bears no legal responsibility for the accuracy, legality or comprehensiveness of materials contained within the thesis, and that Trinity College Dublin accepts no liability for indirect, consequential, or incidental, damages or losses arising from use of the thesis for whatever reason. Information located in a thesis may be subject to specific use constraints, details of which may not be explicitly described. It is the responsibility of potential and actual users to be aware of such constraints and to abide by them. By making use of material from a digitised thesis, you accept these copyright and disclaimer provisions. Where it is brought to the attention of Trinity College Library that there may be a breach of copyright or other restraint, it is the policy to withdraw or take down access to a thesis while the issue is being resolved.

Access Agreement

By using a Digitised Thesis from Trinity College Library you are bound by the following Terms & Conditions. Please read them carefully.

I have read and I understand the following statement: All material supplied via a Digitised Thesis from Trinity College Library is protected by copyright and other intellectual property rights, and duplication or sale of all or part of any of a thesis is not permitted, except that material may be duplicated by you for your research use or for educational purposes in electronic or print form providing the copyright owners are acknowledged using the normal conventions. You must obtain permission for any other use. Electronic or print copies may not be offered, whether for sale or otherwise to anyone. This copy has been supplied on the understanding that it is copyright material and that no quotation from the thesis may be published without proper acknowledgement.

A CONTINUOUS FLOW ARSENIC REMOVAL SYSTEM USING SOLAR OXIDATION

Clare O'Farrell

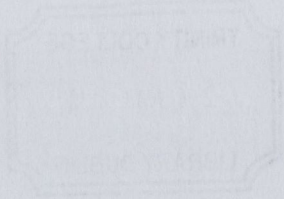

A thesis submitted for the degree of Doctor of Philosophy to the University of Dublin, Trinity College.

2012

TRINITY COLLEGE
2 4 MAY 2013
LIBRARY DUBLIN
Thesis 10038

DECLARATION

I declare that this thesis has not been submitted as an exercise for a degree at this or any other university and it is entirely my own work.

I agree to deposit this thesis in the University's open access institutional repository or allow the library to do so on my behalf, subject to Irish Copyright Legislation and Trinity College Library conditions of use and acknowledgement.

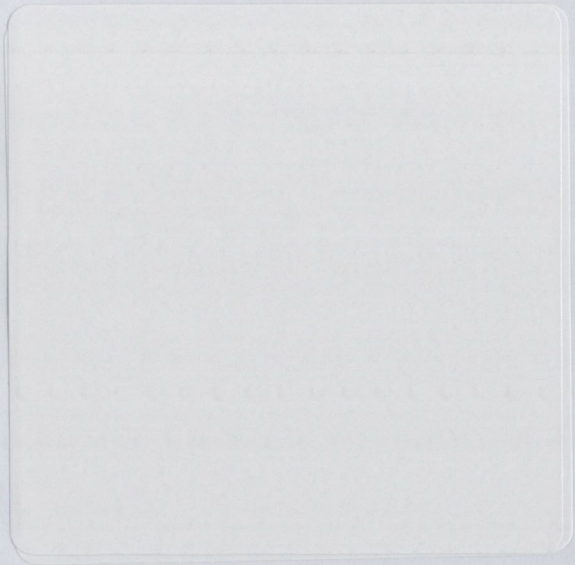

SUMMARY

It is estimated that over 100 million people worldwide are drinking water contaminated with arsenic. The World Health Organisation (WHO) set the maximum contaminant level for arsenic at 10μg/l in 1996 as it is not only carcinogenic, but is associated with numerous other potentially fatal diseases. An extensive borehole drilling programme started in the 1970s by UNICEF in Bangladesh in order to protect the local population from having to use bacterially contaminated surface waters. However, unknowingly, this caused 'the largest mass poisoning of a population in history' according to the WHO, as the groundwater extraction triggered the release of arsenic from the anaerobic sediments laid down over the years by the rivers Ganges and Brahmaputra in their delta regions.

This thesis involves an investigation of using a Solar Oxidation and Removal of Arsenic (SORAS) process in a continuous flow reactor. The SORAS process involves subjecting contaminated water to UV light to photochemically oxidize As(III) to As(V). This requires the presence of iron which generates free radicals that facilitates the oxidation. The presence of this iron, also promotes the subsequent co-precipitation with As(V) which can then be easily separated by gravity from the water. The process has been demonstrated successfully by several authors in batch scale laboratory and field experiments in transparent PET bottles (Hug *et al.* 2001; Garcia *et al.* 2004; Lara *et al.* 2006; Mukherjee *et al.* 2007).

Small and large scale experiments were carried out on compound parabolic reflectors focusing light into transparent tubing, using artificial UV lamps and natural sunlight. The main parameters involved in the process were investigated thoroughly, namely arsenic, iron, UV dose and citrate, and the effects of other water quality parameters on the efficiency of the

process were also examined. An investigation into an appropriate technology for the removal of precipitate, and the dissolution of iron from corrosion products for the required iron dose were also carried out.

At the tested flow rate of 10 l/min, on the full scale reactor, the research has shown that 7.5 kJ_{UV}/min of solar radiation is required to fall on the reactor for effective arsenic removal down to less than 10 μg/l, the WHO MCL, provided the required iron dose is present. The key factor of arsenic removal in this process is the adsorptive capacity of the iron. These large scale tests in natural sunlight proved very successful, particularly given that the UV intensities in Ireland could be half those in West Bengal. This indicates the potential of such a treatment process which could now be designed to remove arsenic down safe drinking water levels taking into account a spectrum of different local geographical and water quality parameters. To demonstrate this, an example of a full scale treatment system design was carried out for a hypothetical village in an arsenic affected region. This considered the required dissolved iron for the process and local variations in solar radiation from which the required size of the continuous flow reactor was calculated. The precipitate removal system using a flocculation channel and sedimentation basin was then also designed.

ACKNOWLEDGEMENTS

Heartfelt thanks to my supervisor, Dr. Laurence Gill, for all his help and encouragement (and craic) over the last four years. His efforts during the last few days especially were immense and above and beyond the expectations anyone could have for their supervisor, I'd say I owe you a brewery at this stage never mind a pint!

Huge thanks to all the staff in the Civil Engineering Dept. for all their assistance and camaraderie. To Patrick "Birdman" Veale especially, and Kev 'McGyver' Ryan and Dave 'go-to-man' McAuley, for their expertise with the big and little things involved in the project, for their complete willingness to drop everything when I needed them, for all the help in the lab, and for their friendship - the list could go on, my sincere thanks. Thanks also to the rest of the technical staff: to Martin Carney for lending me all of his lab tools, and to Chris O'Donovan, Eoin Dunne, Barry McElhinney, Mick Harris and Sean Downey.

I would also like to acknowledge the interns, undergrads and MSc students for their part in the project: Katherine Howett, Peter Gorman, Bernard Ward, Matthias De Cazes, Paul Coleman and Guillaume Merriaux-Mansart. Without their contributions, this would not have been possible.

To all my fellow PhD students, thanks for banter and good times. A special word of thanks to the inhabitants of room 3.9, the old crew of Niall "High Sham" O'Luanaigh, "Perfect" Dave Misstear and Rachael Stewart. The great friendship of Avril "Galway" Challoner, Ronnie "Minesweeper" O'Brien and Paddy "I've-a-story-for-you" Morrissey, and their efforts in getting the submission in are greatly appreciated. Thanks also to everyone who helped me out with the lab work, including Paul Hynds, Dave Morgan and Joanne McMahon, and my brother Seán for building the light rig. Thanks to Vikram Pakrashi, Bidisha Ghosh and Liam O'Brien for great advice and friendship, and Peter Carroll for his drawing skills. Finally, sincere thanks to Moma Kay, Elaine Casey, Beccy Morris, the lads and my family for all the support and encouragement they have given me. Andrew Lochaden, my best friend and confidant for the past 4 years, it was a pleasure to complete this venture with you. Thanks for your help with excel, help with word, help in the lab, and help with life! Und mein Schatz, iluvds.

TABLE OF CONTENTS

DECLARATION ii

SUMMARY iii

ACKNOWLEDGEMENTS v

TABLE OF CONTENTS vi

LIST OF FIGURES viii

LIST OF TABLES xiv

1. INTRODUCTION 1

1.1 Background 1

1.2 Aims and objectives 3

1.3 Scope of thesis 4

2. LITERATURE REVIEW 7

2.1 Arsenic in the environment 7

2.2 Health 18

2.3 Removal 23

2.4 Solar Oxidation and Removal of Arsenic (SORAS) 36

2.5 Continuous Flow Solar Reactors 46

2.6 Solar Disinfection 50

3. MATERIALS AND METHODS 55

3.1 Materials 55

3.2 Methods 69

4. SORAS RESULTS 79

4.1 Introduction 79

4.2 Batch scale tests 79

4.3 Continuous flow reactor profile experiments 89

4.4 Optimum iron dose experiments 91

4.5 Optimum natural citrate dose experiments 94

4.6 Optimum sodium citrate dose experiments 97

4.7 Optimum iron dose experiments (repeated without citrate) 100

4.8 Effect of other water quality parameters 110
4.9 Effect of titanium dioxide photocatalysts 122
4.10 Large Scale testing 124
4.11 Combined SORAS-SODIS experiments 133
4.12 Other testing issues 138

5. PRECIPITATE REMOVAL 141
5.1 Introduction 141
5.2 Background 141
5.3 Materials and methods 154
5.4 Results and discussion 161
5.5 Precipitate-sludge disposal 169

6. IRON DISSOLUTION 173
6.1 Introduction 173
6.2 Background 174
6.3 Materials and Methods 180
6.4 Results and discussion 184
6.5 Modelling 192

7. SUGGESTED DESIGN OF COMPLETE SYSTEM 197
7.1 Introduction 197
7.2 Sizing of continuous flow CPC SORAS reactor 199
7.3 Suggested design of coagulation-flocculation-clarification system for SORAS precipitate 203
7.4 Iron dissolution reactor 206
7.5 Optimised system 206

8. CONCLUSIONS 209
8.1 Conclusions of research 209
8.2 Recommendations for further research 214

REFERENCES 215

LIST OF FIGURES

Figure 2.1 Structure of arsenite and arsenate 8

Figure 2.2 Predominance diagram for As(V) (above) and As(III) (below)as a function of pH (Gupta and Chen, 1978) 9

Figure 2.3 Global arsenic occurrence (World Bank, 2005) 10

Figure 2.4 Arsenic distribution in the Ganges-Brahmaputra Basin. The red area indicates tubewells containing >50 µg/l, green <50 µg/l, and orange shows wells with mixed distribution of high-low As concentrations (Metral et al., 2008) 13

Figure 2.5 Arsenic occurrences in North, Central and South America (Bundschuh et al., 2011) 16

Figure 2.6 Hyperkeratosis on the palms of a villager in Bangladesh resulting from arsenic contaminated water (http://earthday.ning.com/photo/arsenichands-1?context=latest) 19

Figure 2.7 Blackfoot disease of patient in Taiwan (http://www.watchwater.de/en/products/watch-envirosorbR-filter-medias/arsensorb.html) 20

Figure 2.8 Photon flux absorbed per volume by 1 and 90 µM Fe(III)/l (Hug et al. 2001) 38

Figure 2.9 Light spectrum (http://www.jnjvisioncare.com/en_US/uv-damage-cnt1.jsp) 38

Figure 2.10 Photochemical formation of the reactive oxidants and settlement of Fe-As particles 42

Figure 2.11 World distribution of solar radiation indicating suitability of areas for solar applications (Acra et al., 1984b) 44

Figure 2.12 Profile of CPC reactor (McLoughlin et al., 2004) 48

Figure 3.1 Cross-section through reactors: (a) compound parabolic; (b) parabolic; (c) V-groove and (d) flat plate 61

Figure 3.2 Laboratory scale CPC 62

Figure 3.3 Full scale CPC 63

Figure 3.4 Cross section through large scale CPC 63

Figure 3.5 Small scale UV lamp 65

Figure 3.6 Emission spectrum of lamp, plotted with information obtained from Philips. 66

Figure 3.7 Solar radiometer 67

Figure 3.8 Example output from PMA2100 giving UV data for summer day 67

Figure 3.9 Example of pyranometers (shadow ring on left) used in measuring global radiation 68

Figure 3.10 Example output from pyranometers giving global radiation data for summer day 69

Figure 3.11 Schematic of reactor set-up 71

Figure 4.1 Plot of As remaining against initial iron dosage after 4 hours irradiation at 15 W/m^2 UVA 80

Figure 4.2 Plot of As removal against cumulative UV dose and irradiation time (initial As: 150 µg/l, Fe: 7 mg/l, lemon juice 200 µl/l) 81

Figure 4.3 Final As concentrations with and without citrate addition 84

Figure 4.4 Sample solution (a) before irradiation and (b) after irradiation and settlement 84

Figure 4.5 Plot of final arsenic concentration from 500 µg/l against initial iron dose for each photocatalyst dose after 4 hours irradiation 86

Figure 4.6 Plot of final arsenic concentration against cumulative UV dose and irradiation time (initial As: 500 µg/l, Fe: 9 mg/l, TiO_2: 10 mg/l) 87

Figure 4.7 Plot of final As concentration against cumulative UV dose and illumination time (initial As: 1000 µg/l, Fe: 9 mg/l, TiO_2: 10 mg/l) 87

Figure 4.8 Plot of final As concentration from 1000 µg/l against initial iron dosage for 1 and 10 mg/l TiO_2, with and without citrate after 4 hours irradiation at 15 W/m^2 UVA (5.25kJ_{UV}/l cumulative 88

Figure 4.9 As concentration (initial 500 µg/l) after 4 hours irradiation time in the continuous flow set-up against iron dosage for the four reactor profiles 91

Figure 4.10 As concentration vs cumulative UV dose and irradiation time under artificial lamp (initial As (a)1000 µg/l (b)500 µg/l (c)100 µg/l) 93

Figure 4.11 Plot of As concentration vs cumulative UV dose and irradiation time – the effect of natural citrate (initial As, Fe (a)1000 μg/l, 15 mg/l (b)500 μg/l, 10 mg/l (c)100 μg/l, 6 mg/l) 95

Figure 4.12 As concentration vs cumulative UV dose and irradiation time – the effect of sodium citrate (initial As, Fe (a)1000 μg/l, 15 mg/l (b)500 μg/l, 10 mg/l (c)100 μg/l, 6 mg/l) 99

Figure 4.13 As concentration vs cumulative UV dose and irradiation time without citrate (initial As (a)1000 μg/l (b)500 μg/l (c)100 μg/l) 101

Figure 4.14 Molar ratio against k1 for initial As of (a) 1000 (b) 500 (c) 100 μg/l 103

Figure 4.15 Molar ratio against k2 for initial As of (a) 1000 (b) 500 (c) 100 μg/l 104

Figure 4.16 As concentration vs cumulative UV dose (without citrate) on a log scale showing k_1 values (initial As (a)1000 μg/l (b)500 μg/l (c)100 μg/l) 107

Figure 4.17 As concentration vs cumulative UV dose (without citrate) on a log scale showing k_2 values (initial As (a)1000 μg/l (b)500 μg/l (c)100 μg/l) 108

Figure 4.18 Comparison of cumulative UV dose per litre in batch and continuous flow reactors 109

Figure 4.19 As concentration vs cumulative UV dose and irradiation time – the effect of phosphate (initial As, Fe (a)1000 μg/l, 12 mg/l (b)500 μg/l, 10 mg/l (c)100 μg/l, 5 mg/l) 113

Figure 4.20 As concentration vs cumulative UV dose and irradiation time – the effect of silicate (and phosphate) (initial As: 500 μg/l, Fe: 10 mg/l) 114

Figure 4.21 Change in pH against irradiation time 116

Figure 4.22 Change in pH over first 0.2 hours irradiation time for varying initial pH 116

Figure 4.23 As removal vs cumulative UV dose and irradiation time – effect of initial pH 117

Figure 4.24 Change in temperature vs irradiation time 118

Figure 4.25 As removal vs cumulative UV dose and irradiation time – effect of temperature 120

Figure 4.26 As removal vs cumulative UV dose and irradiation time – effect of dissolved oxygen 122

Figure 4.27 Change in DO vs time (note: irradiation time = 0.2 times total time in reactor) 122

Figure 4.28 As removal against cumulative UV dose and irradiation time (initial As: 1000 µg/l, Fe 9 mg/l, TiO_2 10 mg/l) 123

Figure 4.29 Light intensity data for 27th July 2011 (sunny day) 125

Figure 4.30 Light intensity data for 19th July 2011 (overcast day, intermittent clouds) 125

Figure 4.31 Light intensity data for southern India (Balasaraswathy et al., 2002) 126

Figure 4.32 As concentration against cumulative UV-A flux (initial As 1000 µg/l) 128

Figure 4.33 As concentration against cumulative UV-A flux (initial As 500 µg/l) 128

Figure 4.34 As concentration against cumulative UV-A flux (initial As 100 µg/l) 129

Figure 4.35 As concentration against cumulative UV-A flux (S=small scale, L=large scale) 130

Figure 4.36 The iron requirement for varying arsenic starting concentrations to reduce the As concentration down to 10 ug/l (once there has been the threshold cumulative dose of UVA) 130

Figure 4.37 Large scale reactor set up indicating locations of temperature probes 132

Figure 4.38 Temperature variation with time of day (reactor and ambient) 132

Figure 4.39 Arsenic removal during hot and cold day (initial As:1000 µg/l, Fe: 10 mg/l) 133

Figure 4.40 Plot of log decay in bacteria and remaining arsenic concentration against cumulative solar flux. Initial conditions: As 1000 µg/l, Fe 15 mg/l, E. coli 5-10 x 10^3 CFU/ml. 135

Figure 4.41 Plot of log decay in bacteria and remaining arsenic concentration against cumulative solar flux. Initial conditions: As 1000 µg/l, Fe 10 mg/l, E. coli 4-25 x 10^4 CFU/ml 136

Figure 4.42 Plot of log decay in bacteria and remaining arsenic concentration against cumulative solar flux. Initial conditions: As 1000 µg/l, Fe 5 mg/l, E. coli 1.5-2 x 10^6 CFU/ml. 136

Figure 4.43 Precipitate adhesion to reactor tubing 139

Figure 5.1 Mechanical flocculators (a) paddle mixed and (b) turbine mixed (Metcalf and Eddy, 2003) 148

Figure 5.2 (a) Vertical (over and under) baffled channel in cross section (b) Plan view of horizontal (around the end) baffled channel 150

Figure 5.3 Hydraulic jump (Smet, 2002) 150

Figure 5.4 Typical sedimentation tanks (a) horizontal flow rectangular tank (b) radial flow circular tank (c) hopper-bottomed upward flow clarifier (http://openlearn.open.ac.uk/mod/resource/view.php?id=185898) 153

Figure 5.5 Moringa oleifera seeds 155

Figure 5.6 Potato starch 156

Figure 5.7 Flocculation unit 157

Figure 5.8 Modified bottom withdrawal tube 158

Figure 5.9 Filter papers containing As-Fe sediment 161

Figure 5.10 Standard effluent (left) and effluent with MO addition (right) during flocculation 164

Figure 5.11 S-curves showing % slower than against settling velocity for the seven different fall velocity tests with and without flocculation and coagulants/polyelectrolytes 166

Figure 6.1 Diagram of iron oxide occurring and iron release (adapted from Ahmad, 2006) 175

Figure 6.2 Example of corroded iron pieces 181

Figure 6.3 Schematic of the experimental rig 182

Figure 6.4 Plot of iron dissolution against each flow through of clean water (defined as 1 hydraulic retention time) for different sized material and flow rates 185

Figure 6.5 Plot of iron dissoultion against hydraulic retention times at 0.12 l/min and 0.6 l/min for long term tests 188

Figure 6.6 Iron dissolution over time with periodic drying 190

Figure 6.7 Iron dissolution over time with periodic drying 190

Figure 6.8 Plot of modelled and experimental results of Fe (molality) against time. 196

Figure 7.1 Light intensity data for southern India (Balasaraswathy et al., 2002) 201

Figure 7.2 Full scale solar disinfection system in Kenya (Gill and Price, 2010) 202

Figure 7.3 Plan view of baffled channel flocculator 204

LIST OF TABLES

Table 2.1 Comparison of main arsenic removal methods (Feenstra et al., 2007) 31

Table 2.2 Comparison of treatment costs (National Research Council (US), 2001) 34

Table 2.3 List of reactions in the SORAS process (adapted from Hug et al., 2001) 39

Table 3.1 Tap water composition 59

Table 3.2 Reactor characteristics 64

Table 4.1 Comparison of k1 and k2 values for tested molar As:Fe ratios 105

Table 4.2 Comparison of removal coefficients (Note: k1b and k2b from study without bacteria addition) 137

Table 5.1 Factors affecting coagulation (Murcott et al., 1996) 142

Table 5.2 Advantages and disadvantages of inorganic coagulants (US Army, 2001) 143

Table 5.3 Typical G and Gt values for flocculation (Wang et al., 2004) 147

Table 5.3 Experimental conditions of the process of coagulation-flocculation-settlement chosen by various authors 147

Table 5.4 Flocculation test results giving coagulant/polyelectrolyte dosages and observations 162

Table 5.5 Fall velocity test parameters 165

Table 5.6 Settling velocities (V_{50}) for 50% removal of precipitates 168

Table 6.1 Tap water parameters used in PHREEQC 193

Table 6.2 HFO parameters (Dzombak and Morel, 1990) 194

Table 7.1 Advantages and disadvantages of household and community water treatment 198

CHAPTER 1: INTRODUCTION

1.1 Background

It is estimated that over 100 million people worldwide are drinking water contaminated with arsenic. The World Health Organisation (WHO) set the maximum contaminant level for arsenic at 10μg/l in 1996 as it is not only carcinogenic, but is associated with numerous other potentially fatal diseases. An extensive borehole drilling programme started in the 1970s by UNICEF in Bangladesh in order to protect the local population from having to use bacterially contaminated surface waters. However, unknowingly, this caused 'the largest mass poisoning of a population in history' according to the WHO, as the groundwater extraction triggered the release of arsenic from the anaerobic sediments laid down over the years by the rivers Ganges and Brahmaputra in their delta regions. Although the initial benefits of pathogen free water were seen immediately with a marked drop in the number of deaths from water-bourne diseases with diarrhoeal symptoms (e.g. dysentery) and other water-related diseases such as malaria, etc., the long-term effects of chronic arsenic ingestion have been increasingly evident. Although, the problem of arsenic has been most reported in the West Bengal / Bangladesh region it also is an issue in many other parts of the world (for example, South America), particularly for rural communities who rely on groundwater from certain geological settings for their water source.

Arsenic remediation methods vary greatly with cost, efficiency and applicability, with large scale removal plants operating successfully in countries like the USA. However, there are many problems associated with supplying arsenic free water at a household / community

level in rural areas of developing countries. The difficulties encountered due to the chemically and / or energy intensive nature of these treatment technologies, and issues related to the generation and disposal of hazardous arsenic sludge from these treatment processes render such systems economically or logistically unviable. There is a pressing need for research into appropriate technological removal methods using natural resources such as solar power, and locally available materials.

This thesis involves an investigation of using a Solar Oxidation and Removal of Arsenic (SORAS) process in a continuous flow reactor. The SORAS process involves subjecting contaminated water to UV light to photochemically oxidize As(III) to As(V). This requires the presence of iron which generates free radicals that facilitates the oxidation. The presence of this iron, also promotes the subsequent co-precipitation with As(V) which can then be easily separated by gravity from the water. The addition of small amounts of citric acid also acts to accelerate oxidation by forming iron-citrate complexes that yield further reactive oxygen species. The process has been demonstrated successfully by several authors in batch scale laboratory and field experiments in transparent PET bottles (Hug *et al.* 2001; Garcia *et al.* 2004; Lara *et al.* 2006; Mukherjee *et al.* 2007). However, a limited volume of water is produced by this process and its success relies heavily on the dedication of each individual user. A similar solar disinfection process (SODIS) using plastic bottles has been shown to give effective pathogen removal (EAWAG, 2002), however recent reports have called into question the user acceptability of the system (du Preez *et al.* 2010; Mäusezahl *et al.* 2009), with low participation levels despite promotional campaigns. Community scale continuous flow systems that utilise appropriate technology like SODIS have been put into practice (Gill and Price, 2010; Chapelon and Herrmann, 2004; Navntoft *et al.*, 2007). The

concept involves water flowing through a transparent pipe at the focal point of a compound parabolic reflector, optimally angled beneath the pipe for maximum sunlight capture. To our knowledge no attempt has been made to adapt the SORAS method to a continuous flow system. Hence, the approach taken in this research is to investigate an arsenic removal process at a semi-centralised community scale. The design must be an appropriate technology with low maintenance and energy requirements, minimal reliance on complicated mechanical or electrical processes and require minimal supply of non-local chemicals.

1.2 Aims and objectives

The overall aim of the research is to design a continuous flow oxidation process for arsenic removal, with an appropriate technology that would be suitable for a village scale water supply in a developing country.

This has been achieved via several targeted objectives as follows:

- To investigate the effect of the three main parameters (arsenic, iron and citrate) on the kinetics of the solar oxidation process in a series of batch and small-scale continuous flow tests in controlled laboratory conditions under artificial UV light
- To investigate the effect of the different reflector profiles on the kinetics of the solar oxidation process in small-scale continuous flow experiments under controlled laboratory conditions

- To investigate the effect of the three main parameters (arsenic, iron and citrate) on the kinetics of a continuous flow solar oxidation process in a full-scale reactor in varying natural sunlight
- To determine the effects of other water quality parameters (phosphate, silicate, dissolved oxygen, pH and temperature) on the kinetics of the solar oxidation process
- To investigate the possible enhancement of the process by the use of titanium dioxide photocatalyst
- To investigate the most appropriate process to remove the arsenic precipitate from the treated water leaving the SORAS reactor
- To design and test an appropriate technology which can augment the required amount of soluble iron in the water in order to optimise the SORAS process, including the development of a numerical model to simulate the iron dissolution kinetics
- To design a complete arsenic removal treatment system according to water requirements of a hypothetical rural community in West Bengal

1.3 Scope of thesis

The initial stage of this thesis involves a study and review of the relevant literature, whereby the problem of arsenic contamination in the world is detailed as well as the impacts on health. Particular attention is paid to the various conventional arsenic removal methods, in addition to small / household scale treatment processes. Finally, a detailed

description of the SORAS process is reported, including factors affecting its efficiency and issues pertaining to the continuous flow aspect of the process.

Laboratory methods are outlined, and then the experiments to investigate the different parameters involved (namely arsenic, iron and citrate) at batch and small-scale continuous flow systems under an artificial UV lamp are detailed. Then different water quality parameters (phosphate, silicate, dissolved oxygen, pH and temperature) are investigated in order to determine their effects on the arsenic removal efficiency. Large scale experiments are then conducted under natural sunlight to establish the parameters involved in upscaling to a full scale treatment system.

The removal of arsenic-iron precipitate is then examined by conducting settling velocity experiments on the discharged water from the SORAS reactor. A review of coagulant aids is also carried out, leading to coagulation-flocculation experiments to compare natural and industrial coagulants, and their effect of the settling velocity of the SORAS treated particles.

Then an investigation of an appropriate technology to achieve the iron requirement for the SORAS reaction is undertaken. Laboratory experiments are conducted using a column filled with corroded iron metal with water pumped through the column to obtain iron dissolution from the hydrous ferric oxide surface. The development of a numerical model calibrated to these experiments is then described.

The information from all the experiments is then synthesised to produce a design of a continuous flow system for a hypothetical village in an arsenic affected region.

Finally, a set of conclusions is drawn from the experimental results and observations, and recommendations for future research are given.

CHAPTER 2: LITERATURE REVIEW

2.1 Arsenic in the environment

2.1.1 Arsenic chemistry

Arsenic (As) is a toxic chemical element of the metalloid group, which occurs naturally in the rocks, minerals, sediments and soils of the earth's crust, with a crustal abundance of 1.5mg/kg (Sherwood Lollar, 2005). It is mainly associated with minerals of iron (Fe) and sulphur (S), the most abundant ores being arsenopyrite (FeAsS), and arsenianpyrite ($Fe(SAs)_2$) (Nordstrom, 2000). They are formed in the earth's crust at high temperatures. Arsenic is also associated with elements (amongst others) copper (Cu), nickel (Ni), cobalt (Co), silicon (Si), aluminium (Al), and manganese (Mn). It is released to the environment by geochemical and geophysical processes, such as erosion and volcanic activity, thereby making its way into both ground and surface waters. As bedrock composition and weathering conditions can vary greatly, a wide range of arsenic concentrations are found in groundwater.

Arsenic located in solution in water is usually in its inorganic form, either arsenite As(III), typically found in anaerobic groundwaters, or arsenate As (V), normally observed in aerobic surface waters. The structure of both are illustrated in Figure 2.1. It is an oxyanion-forming element which can be mobilised at a wide pH range under both reducing and oxidising conditions, and can be found in concentrations up to levels of mg/l, whereas most other metals are generally only found in µg/l (Smedley and Kinniburgh, 2002). Many cases of high arsenic concentrations also correlate to high concentrations of boron (B), molybdenum (Mo), selenium (Se), and uranium (U), amongst others. As in

Bangladesh/West Bengal, a number of other affected areas are low-lying river basins where arsenic can accumulate in the groundwater. Many arsenic affected regions also display large seasonal variations in As concentration, due to different pumping rates, microbiological activity, precipitation, etc. (Frankenberger, 2001).

Figure 2.1 *Structure of (a) arsenite and (b) arsenate*

Due to the complex nature of arsenic speciation in aquatic environments, ie. being stable in a number of oxidation states (+5, +3, 0, -3), Figure 2.2 illustrates the predominance of the main species (arsenate and arsenite) as a function of pH. Gupta and Chen (1978) observed As(V) is predominantly found as H_2As0_4- in waters with pH between 3 and 6.5, and As(III) is primarily found as H_3As0_3 in waters with a pH range of 0 to 9.

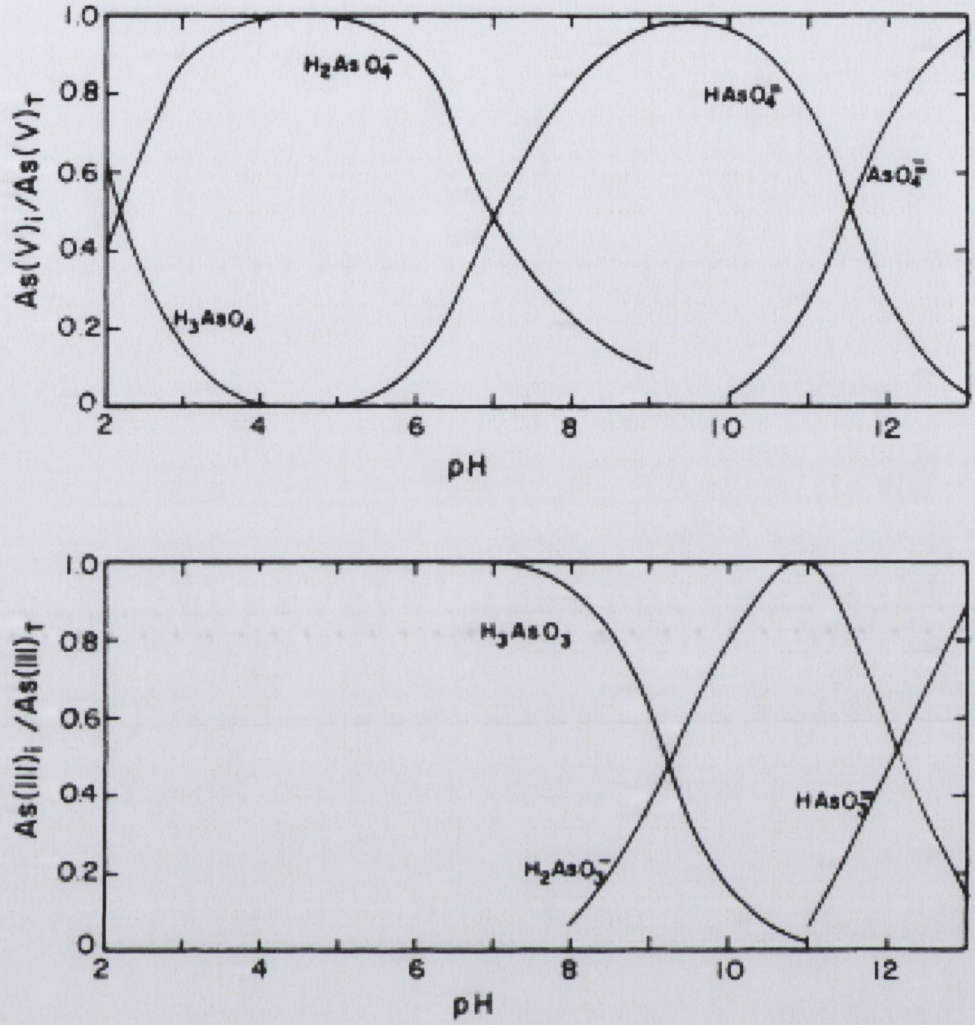

Figure 2.2 *Predominance diagram for As(V) (above) and As(III) (below)as a function of pH (Gupta and Chen, 1978)*

Figure 2.3 (World Bank 2005) shows a world map indicating arsenic affected regions and their respective sources. The general extent of the problem of arsenic in drinking water is illustrated, however many other cases of arsenic have been documented throughout the globe (some of which are discussed in the subsequent sections), and new instances are found regularly.

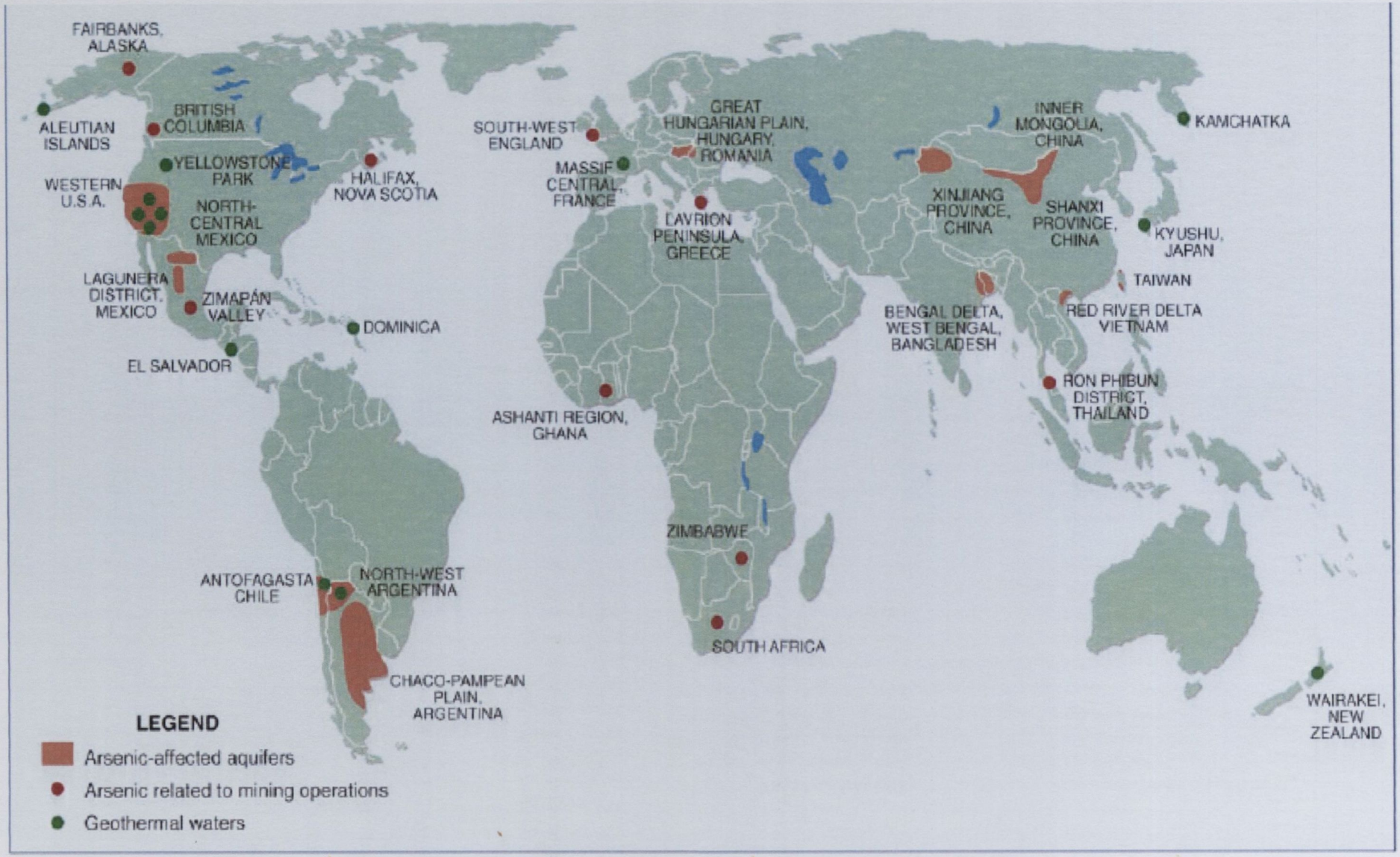

Figure 2.3 *Global arsenic occurrence (World Bank, 2005)*

2.1.2 Groundwater contamination from reducing conditions

2.1.2.1 Bangladesh and India

Since the 1970s, over 10 million boreholes (shallow tube wells) have been dug and drilled in Bangladesh and West Bengal, India in order to provide an alternative water source for the local populations to surface waters which have a high risk of contamination from pathogenic microorganisms. Unfortunately a large amount of groundwater in the region has recently been found to have arsenic concentrations of up to over 3000 μg/l, (Kinniburgh and Smedley, 2001; Das, 1995). As a result up to 77 million people there are at risk of consuming high amounts of arsenic, and it is believed that arsenic poisoning (see Section 2.2.) will become the principal cause of death in Bangladesh/Bengal in the near future. After an in-depth study of arsenic affected waters in Bangladesh, the British Geological Survey (Kinniburgh and Smedley, 2001) concluded that large scale aquifer contamination arises in the region due to anerobic conditions which leads to strongly reducing conditions in the water. This causes reductive dissolution of Fe-oxides and arsenic particles become either desorbed from their Fe-minerals, or the arsenic particles themselves are reduced and dissolution also takes place. The rates of these chemical reactions are influenced by the pH and Eh (redox potential) of the water, the rate of diffusion of gases through the water, and microbiological activity in the aquifer. Arsenic contaminated groundwater has been found to be only in shallow tubewells (less than 100-150 m deep), where the aquifer is made up of sediments of the Holocene age deposited by the Ganges, Brahmaputra and Meghna rivers. The sediments are made up of sand, silt and clay, and are generally unconsolidated (Mukherjee *et al.*, 2009). These sediments are covered by a layer of clay which limits air penetration to the aquifer thereby promoting

anaerobic conditions, (Kinniburgh and Smedley, 1999). Arsenic in this area is associated with high Fe concentrations and alkalinity and generally has a neutral or near-neutral pH. The accumulation of arsenic is a result of low flows in the groundwater due to the flat, low-lying land and the recent rise in global sea levels. Hence, the aquifer is not flushed out and high arsenic concentrations have accumulated. Figure 2.4 is a map showing general arsenic concentrations in groundwater in the Bengal Basin region. The red areas highlight regions with As of over 50 μg/l, and the orange show places with mixed high and low concentrations. The green areas indicate As of less than 50 μg/l – the Bangladesh and India MCL, but this is still up to 5 times greater than the 10 μg/l drinking water limit specified by the World Health Organisation (2006).

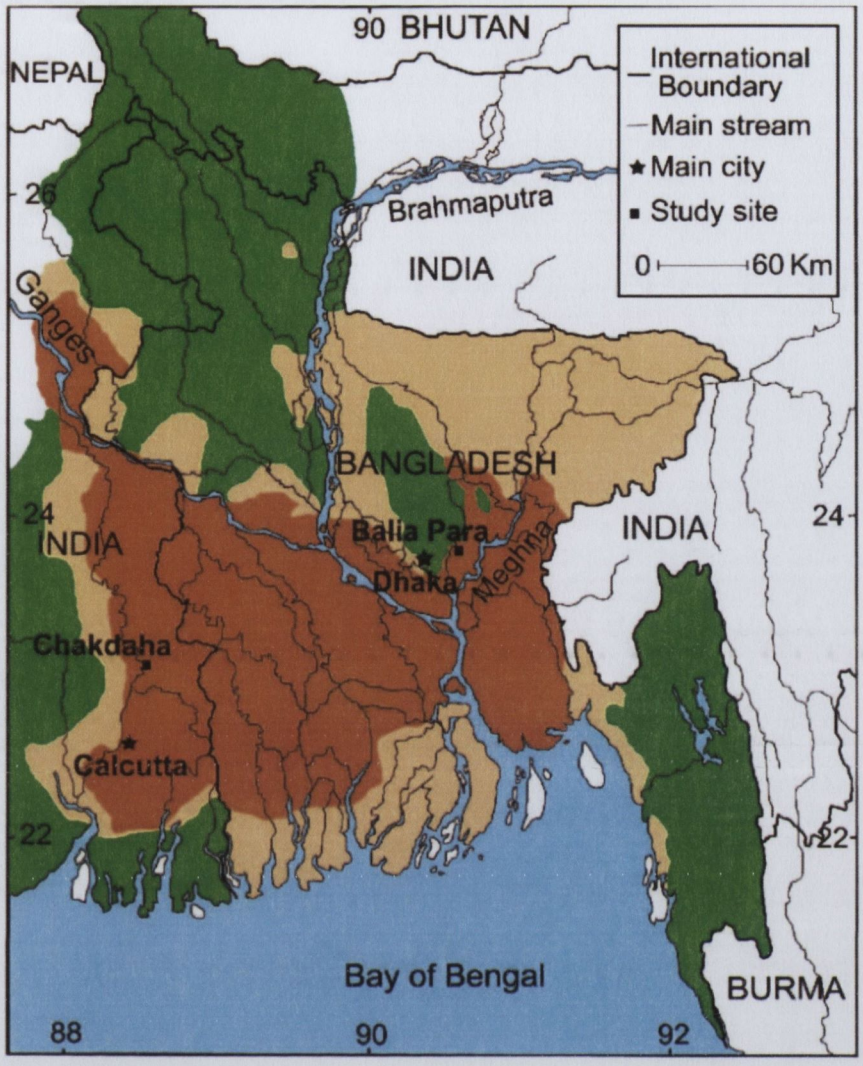

Figure 2.4 *Arsenic distribution in the Ganges-Brahmaputra Basin. The red area indicates tubewells containing >50 µg/l, green <50 µg/l, and orange shows wells with mixed distribution of high-low As concentrations (Metral et al., 2008)*

2.1.2.2 East and South East Asia

The situation in China is comparable to that of Bangladesh/Bengal, although the affected aquifers are much more widespread throughout the country and were discovered much earlier. Kuo (1968) investigated artesian well water contaminated with arsenic in Taiwan, finding highly reducing conditions with neutral pH similar to Bangladesh/Bengal, but derived from black shale sediments. Also studied were areas in Inner Mongolia (Luo *et al.*, 1997) and Xinjiang (Wang *et al.*, 1994), again with similar conditions (strongly reducing,

neutral pH, high alkalinity, Holocene sediments), but in addition many were found to contain humic acid. The Mekong Delta in Cambodia and Red River Delta in Vietnam have also been shown to have Holocene sediment aquifers with water of neutral pH and reducing conditions, releasing arsenic to groundwater of up to 1610 µg/l and 3050 µg/l in Cambodia and Vietnam respectively (Berg *et al.,* 2007). Polya *et al.* (2005) also studied aquifer contamination in Cambodia, concluding that well depths greater than 16m in Holocene sediments and/or proximity to Mekong river channels were key indicators of high arsenic concentrations.

2.1.2.3 Other areas

Reducing conditions leading to arsenic release were also observed in Hungary (Varsanyi *et al.,* 1991), in Quaternary sediment aquifers, and in Nevada, USA (Welch and Lico, 1998), in aquifers of mixed Holocene, alluvial and volcanic sediments.

2.1.3 Arsenic in groundwater from oxidizing conditions

As mentioned previously arsenic can also enter the groundwater environment under oxidising conditions. Vast aquifers in the US and South America are contaminated due to aerobic conditions with pH increasing to over 8.5, resulting in As(V) becoming rapidly desorbed from its minerals. These oxidising aquifers have been investigated in: Argentina (Nicolli *et al.,* 1989), finding Holocene and volcanic sediments and high alkalinity and salinity; Chile (Caceres *et al.,* 1992), having probably Quaternary volcanic sediments, also with high salinity; Mexico (Del Razo *et al.,* 1990), with volcanic sediment aquifers; and Arizona, US, (Robertson 1989), involving alluvial sediments. In the case of South

America, despite occurrence being well documented, the scale of the problem has only recently been brought to the forefront of global arsenic research. In 2010, a special session of the Third International Congress on Arsenic in the Environment held in Taiwan was entitled "Arsenic in Latin America: A Forgotten Continent?", where many prominent researchers presented on the issues in the region. Figure 2.5 is a map showing nearly 100 different arsenic occurrences from across the region that has been compiled by 14 authors (Bundschuh, *et al.*, 2011). Another case in the US is that of the San Joaquin Valley, California, (Fujii and Swain, 1995). This is unusual due to the fact that aquifer has a mixture of both oxidising and reducing conditions, the speciation of arsenic differing, ie. As(V) predominating in oxidising states and As(III) in reducing. The aquifer is made up of Holocene and other sediments, and also shows high salinity in places.

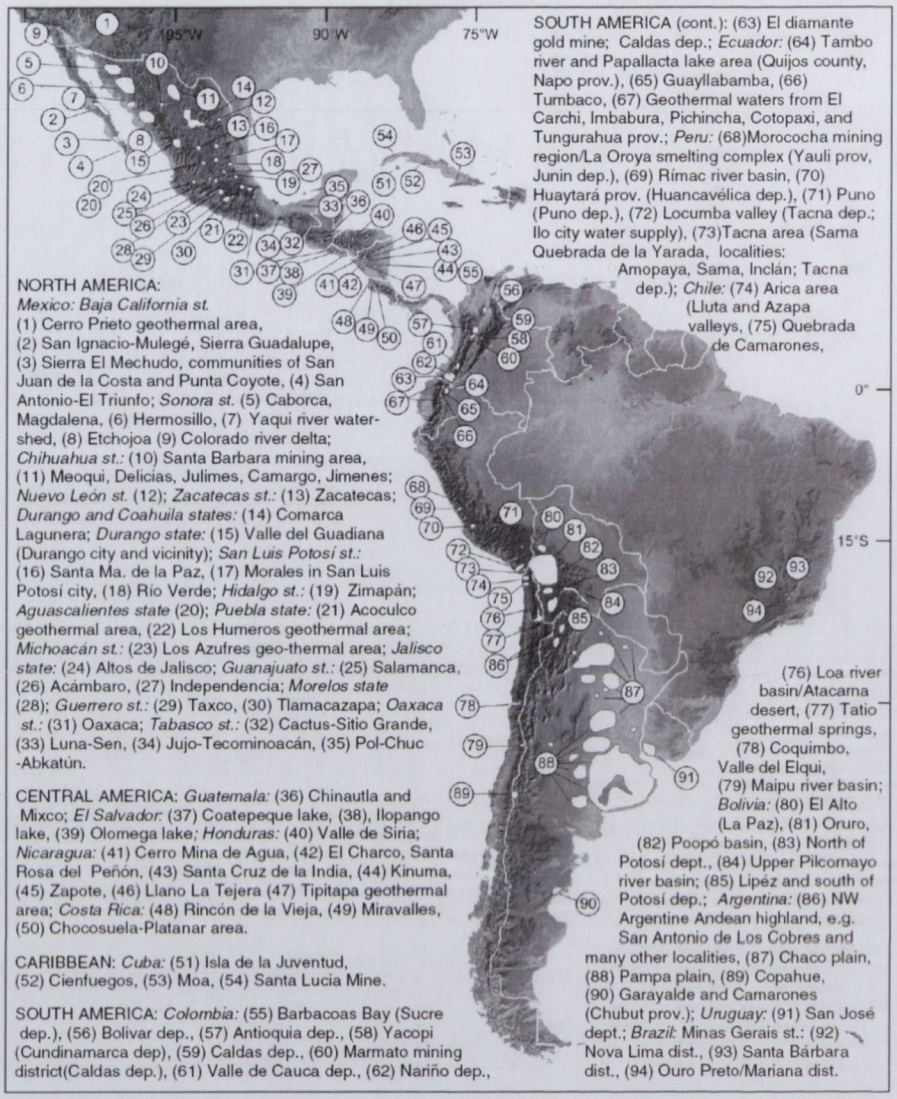

Figure 2.5 *Arsenic occurrences in North, Central and South America (Bundschuh et al., 2011)*

2.1.4 Geothermal sources

Arsenic has also been found in high concentrations in water affected by geothermal activity. As warm geothermal water ascends to the surface, it reacts with the wall rocks causing mineral dissolution (Tyrovola *et al.* 2006). Arsenic can be naturally present in solution, and is usually associated with high salinity in geothermal waters, (White *et al.*, 1963). Cases have been reported worldwide, (Criaud and Fouillac, 1989), but especially in

the south-western states of California and Nevada in the US, (Benson and Spencer, 1983).

2.1.5 Anthropogenic sources

Arsenic also reaches water from anthropogenic sources, such as mining activities, smelting operations, combustion of fossil-fuels, agriculture and industry. Contamination from mining, especially those associated with gold and copper mining, have been documented in Ghana (Smedley, 1996), Thailand (Williams *et al.,* 1996), the US (Plumlee *et al.,* 1999), and Spain (Garcia-Sanchez and Alvarez-Ayuso, 2003), to name but a few. The extraction process which leaches out precious metals uses liquids which are selective to certain ores, but the dissolution of these ores during leaching also enables the release of arsenic. The untreated waste mine tailings that are usually dumped locally can pollute both surface and groundwater sources. In addition, serious arsenic pollution of water sources for the local populations are associated with the cassiterite mining in eastern Democratic Republic of Congo (Gill, 2006). Industrial activity can also create an air pollution problem. For example, Crecelius (1975) reported average arsenic content of rainwater effected by a smelting plant in Seattle, USA of 16 μg/l, far in excess of average values reported to be 0.013-0.032 μg/l, (Andreae 1980). Arsenic is still used, but to a lesser extent than in the past, in agricultural pesticides and herbicides, and their leaching has been shown to contaminate groundwater (Korte and Fernando, 1991). Some wood preservation methods use pressure treating with chromated copper arsenate (CCA) or ammonical zinc-copper arsenate (AZCA) and the incineration of this timber leads to air pollution (Bhattacharya *et al*, 2002).

2.1.6 Food

Arsenic also occurs naturally in foods, especially seafood, but is in organic form and is easily metabolised by the body and therefore non-toxic. However, a study from Bangladesh suggests crops irrigated with arsenic contaminated water were a source of human poisoning, (Delowar *et al.,* 2005; Chappell *et al.,* 2003) also found that crops irrigated with groundwater in Bangladesh had increased levels of arsenic incorporated within the plants. Vegetables were found to have higher concentrations than that of rice.

2.2 Health:

The effects of ingesting arsenic on human health are extremely serious. 150-300 mg arsenic can be deadly, while daily intake above the recommended limits leads to chronic arsenic poisoning or arsenicosis. Drinking water is the primary exposure pathway for arsenic, as it cannot penetrate skin. The symptoms of arsenicosis are numerous and can affect all parts of the body. There is no treatment for arsenicosis, only the individual illnesses can be cared for. Even the age-old practice of taking small amounts of poisonous substances to develop a resistance to its effects does not work in the case of arsenic. Smith et al. (2000) reported arsenic related diseases in the Atacameño tribe of Chile, despite generations of exposure to low amounts in their drinking water. Argos *et al.* (2011) carried out an in-depth all-cause mortality study over 9 years of 11746 people in Araihazar, Bangladesh consuming water with up to 864µg/l arsenic. The findings showed an increase in mortality rate with increased arsenic exposure. UNICEF (2011) estimates that the

arsenic exposure from drinking water is leading to 68,000 deaths per year in Bangladesh, with an economic cost of between 6-20 billion US dollars over the next 20 years.

2.2.1 Skin

Diseases associated with arsenic include skin disorders such as lesions caused by dermatosis, keratosis (Figure 2.6), peripheral vascular disorder - blackfoot disease (Figure 2.7), melanosis, hyperpigmentation (black rain) and hypopigmentation. Such diseases have been documented in various arsenic affected regions, for example, Bangladesh (Tondel *et al,* 1999), West Bengal (Mazumder, 1998), Chile (Smith *et al.,* 2000), and Taiwan (Tseng, 1977). Studies have shown that these disorders are most likely due to the arsenic inducing overstimulation of keratinocyte growth factors such as TGF-alpha, which is a known cause of skin tumours (Germolec *et al*, 1997, 1998).

Figure 2.6 *Hyperkeratosis on the palms of a villager in Bangladesh resulting from arsenic contaminated water (http://earthday.ning.com/photo/arsenichands-1?context=latest)*

Figure 2.7 *Blackfoot disease of patient in Taiwan (http://www.watchwater.de/en/products/watch-envirosorbR-filter-medias/arsensorb.html)*

2.2.2 Cancers

Arsenic has been widely recognised as a known carcinogen, (International Agency for Research on Cancer, 2004). The estimated cancer risk involved in drinking water over a lifetime containing 10 μg/l arsenic, is 1 in every 500 people, a figure that increases linearly with dose at a gradient of 1:1.65, (National Research Council USA, 2001). Skin, lung, bladder, kidney, liver and uterus are the main locations of cancer caused by chronic arsenic exposure, and have been documented worldwide, (Bates *et al.,* 1995; Hopenhayn-Rich *et al.,* 1996, 1998; Tseng *et al.,* 1968; Chen *et al.,* 1992; Tsuda *et al.,* 1995). Many modes of action of arsenic induced cancer are considered. Skin cancer can occur when cell carcinomas develop from the various types of keratoses mentioned previously. Oxidative stress caused by reactive oxygen species (ROS) can damage DNA, proteins, enzymes, etc. and cause apoptosis (disintegration of cells), which allow cancerous cells to develop from this damage. Studies show that arsenic gives rise to elevated levels of ROS as a result of the many reactions arsenic is involved in when it enters the body, (Kitchin and Ahmad,

2003, Kessel *et al.,* 2002). Arsenic also interrupts the pathways of cellular signalling, causing uncontrolled cell growth and transformation, (Bode and Dong, 2002, Qian *et al.,* 2003). Reichard *et al.,* (2007), and others, suggested that arsenic can induce DNA methylation loss and this in turn reduces the ability to prevent cell carcinomas. Chromosomal mutagenic effects have also been seen in arsenic exposed subjects, (Mahata *et al.,* 2003), this is also known as a cancer inducing condition.

2.2.3 Heart problems

Other health effects noticed are hypertension (high blood pressure) (Chen *et al.,* 1995) and cardiovascular problems (Pi *et al.,* 2000; Ahmad *et al.,* 2006). Arsenic is believed to cause mutations in ion channels that carry impulses in the heart, in turn causing longer QT intervals, (time between contraction of ventricles and end of recovery of the ventricles). This abnormal electrical activity results in arrhythmia, ventricular fibrillation and even cardiac arrest, and has been mainly studied in leukemia patients who receive arsenic trioxide as part of their treatment (Ficker *et al.,* 2004; Soignet *et al.,* 2001; Zhang *et al.,* 2001).

2.2.4 Other health effects

Mazumder *et al.,* (2000) and Milton *and Rahman,*(2002) have both researched the relationship between arsenic ingestion and respiratory effects such as chronic cough, bronchitis and shortness of breath. Neurological effects were also documented by Dannan *et al.,* (1984) and Morton and Caron, (1989) in workers exposed to arsenic, stating symptoms like anxiety, lethargy, mental confusion, panic attacks, seizures and persistent

headache. Campbell and Alvarez (1989), amongst others, reported gastrointestinal effects of arsenic, such as pain, nausea and vomiting. Diabetes associated with arsenic poisoning has been reported (Tseng, 2004; Rahman *et al.,* 2002; Lai *et al.,* 1994), and is thought to be brought about by a number of mechanisms. Ogihara *et al.,* (2004) suggested that the arsenic reactions produce ROS and this oxidative stress induces insulin resistance, whereby the amounts of insulin produced are inadequate. The signalling cytokine TNF-alpha has been shown to be upregulated by arsenic, also causing insulin resistance (Yu *et al.,* 2002), and the hormone receptor PPAR-gamma, responsible for activating insulin action, is thought to be inhibited by arsenic (Wauson *et al.,* 2002).

2.2.5 Pregnancy

Trends have shown that arsenic consumption can bring about complications in pregnancies, for example low birth weight, congenital malformations, still and premature births, and neonatal death, (Chakraborti *et al,* 2003, Milton *et al.,* 2005, Yang *et al.,* 2003, von Ehrenstein *et al.,* 2006). Arsenic has also been reported to disrupt the endocrine system, which is essential for gene regulation and embryonic development, amongst other important functions (Davey *et al.,* 2007, 2008). All of the above health effects are influenced by enzyme actions in the body, and arsenic has also been shown to affect many important enzyme functions, aggravating these symptoms (Squibb and Fowler, 1983).

2.2.6 Nutrition

Research has also indicated that malnutrition and vitamin and mineral deficiencies increase susceptibility to poisoning and exacerbates the symptoms, (Hsueh *et al,* 1995, Mazumder

et al, 1998, Mitra *et al.,* 2004 and Milton *et al*, 2004).

2.3 Removal:

There are many different methods of arsenic removal, and they vary greatly with cost, efficiency and complexity. There are four broad categories of removal, namely precipitative processes, adsorptive processes, ion exchange, and membrane processes. It has been found in many techniques, that the oxidation of arsenite (As(III)) to arsenate (As(V)) is required to attain efficient removal (Scott *et al*, 1995, Hering *et al*, 1996), as As(III) only weakly adsorbs to coagulants and adsorbents. Several oxidation methods currently used by water treatment facilities, including chlorination, permanganate addition and ozonation, are effective (Ghurye and Clifford, 2001), however involve handling hazardous chemicals and can generate harmful byproducts such as trihalomethanes. The U.S. Environmental Protection Agency has numerous publications on the subject, and according to 'Technologies and costs for removal of arsenic from drinking water 2000' (EPA, 2000), and other sources (referenced where applicable), the following is an overview of the foremost arsenic removal processes.

2.3.1 Oxidation/Coagulation/Filtration

As stated above, oxidation of As(III) is usually needed. Simple oxidation is followed by mixing with a coagulant such as iron or alum, which allows the As(III) to attach to the

suspended particles. The particles are then removed by filtration through various media. The oxidation plants are basically iron removal plants, with no chemical addition, simple aeration occurs by cascading of the water and then filtration is used to remove the resulting iron and arsenic precipitate. Actual removal rates varied considerably due to differences in inlet water parameters and improved with higher iron concentrations. Average removal efficiency was about 67% (Johnston and Heijen, 2001). A recent oxidation technique involves re-pumping well water back into the ground creating an oxidation zone, supplying arsenic free water in six plants in West Bengal (Gupta *et al.* 2009)

During coagulation, a chemical coagulant is added, usually in the form of either alum or ferric sulphate, or ferric chloride (Hering *et al*, 1996). This is combined with mechanical flocculation by mixing, which allows dissolved and suspended solids floc or agglomerate. Then the resulting mixture is filtered (1μm filter) for up to over 90% arsenic removal. Removal efficiency increases with increase in coagulant dosage, and the process is only effective in the pH range of 4-9. Ferric & alum coagulants have been shown to have roughly the same removal at pH < 7.6, but ferric coagulants perform much better at pH > 7.6, (Hering *et al*, 1997). Upstream controlling of the pH can help reduce the coagulant dose (Sancha, 2006). In coagulation plants in Chile, arsenic was reduced from 400 μg/l to 10 μg/l at a rate of 500 l/sec using 40-56 mg/l ferric chloride (after pre-oxidation with Cl_2 (Sancha, 2006)). Wickramasinghe *et al.* (2004) compared coagulation (and subsequent microfiltration) on well water from Colorado, USA to Bangladesh, finding removal efficiency was highly dependent on the raw water quality and increased with iron dose. A study carried out by the University of Houston (Clifford *et al.*, 2007), including pilot studies at Albuquerque NM, used direct filtration (microfiltration system) as a means of removing the arsenic following an initial treatment of the contaminated water by iron

addition and coagulation. They found that As(V) concentrations were consistently reduced to below 2 μg/l. The critical factors in the treatment process were found to be coagulant dose, mixing energy, detention time and pH.

Sand filters have been used successfully as a means of removing arsenic from water. Selecky *et al.* (2005), carried out a review of many small scale arsenic treatment units, finding a number of different filter media may be used, including sand, greensand, solid manganese dioxide such as pyrolucite, and manganese dioxide coated sand such as BIRM™. A study carried out by Berg *et al.* (2006) tested sand filters in a field study conducted in the Red River delta, Vietnam. The removal efficiency of the sand filters was examined in 43 households whose pumped groundwater contained high arsenic levels. The sand filters comprised of two large concrete containers. One container was placed on top of the other, with the upper filled with locally sourced sand; occasionally gravel, manganese dioxide or charcoal was added. It was recommended that the sand be allowed to run dry between subsequent filtration periods so as to inhibit microbial activity. The residence time in the sand filter was approx 3 mins and a through flow of 0.1-1 L/min. The lower container stored the treated water. An average removal rate of 80% was achieved.

The oxidation/coagulation/filtration processes have the added advantage of removing many other dissolved and suspended particles from the water along with arsenic. These can include turbidity, phosphates, fluoride, and improvements in the colour and odour.

2.3.2 Adsorption

Feed water is passed through a packed bed of specific adsorbents, which are highly adsorptive to As. The surface sites on these are filled with arsenic particles. Removal efficiency can be over 90%, but is controlled by the pH and arsenic concentration of the incoming water (Lin and Wu, 2001). The pH range from 5.5 to 6.0 optimises removal, however the pH must be below 8.2. The number of bed volumes that can be treated is dependent on the arsenic content, after the bed is exhausted the adsorbent needs regeneration, usually with a rinse of NaOH and then H_2SO_4. Gupta and Chen (1978) compared the use of activated alumina, carbon and bauxite on various arsenic contaminated waters in California, USA. Results showed activated alumina (2 g/l dose) outperformed the other tested adsorbents at a range of initial As(III) and As(V) concentrations and pHs. Dikshit *et al.* (2000) investigated arsenic adsorption from groundwater in West Bengal onto kimberlite tailings. In column studies, the performance of a fixed-bed reactor was studied and the adsorption capacity was found to be 0.27 mg/g of adsorbent with up to 94% removal. The capacity of kimberlite was only one quarter that of alumina, but these tailings are a mining waste product and are free of charge.

2.3.3 Adsorption onto Iron Media

The surface sites of iron in various forms are used like activated alumina, etc., to adsorb arsenic. Most of this type of removal process use zero valent iron (ZVI) filings and/or their corrosion products, or scrap iron to adsorb arsenic in both batch and column tests. Sorption of As(V) onto HFO (hydrous ferric oxide) and goethite is more favorable than that of

As(III) below pH 5–6, whereas, above pH 7–8, As(III) has a higher affinity for the solids (Dixit and Hering, 2003). Ferric hydroxide particles attract the arsenic which can be settled or filtered, and efficiencies of up to 99% have been seen in laboratory studies, (Biterna, 2007, Manning, 2002). Biterna (2007) demonstrated arsenic concentrations below 10 µg/l for up to 1900 bed volumes without regeneration in column tests. This has also been demonstrated in household filter systems in Bangladesh, with considerable success, (Hussam, 2007; Ngai, 2006). Vaishya and Gupta (2003) compared the performance of iron impregnated sand (IIS) with iron oxide coated sand (IOCS), with both removing 1000 µg/l As(III) to 50 µg/l. The adsorptive capacity of IIS was 52% greater than IOCS, due to the higher proportion of Fe coating on this media. However, the household column flow rate and the number of bed volumes treated compared badly to other filter systems (2 l/hr and <100 bed volumes respectively).

2.3.4 Lime Softening

Lime is usually used to reduce hardness in water. Different forms of lime (usually $Ca(OH)_2$) can be added to increase the pH, so bicarbonate converts to carbonate and calcium and magnesium precipitate as calcium carbonates and magnesium hydroxides (Harper and Kingham, 1992). As in the coagulation process mentioned in Section 2.3.1, arsenic is removed by agglomeration into these larger particles. The process gives up to 100% removal at an optimal pH of ~10.5. McNeill and Edwards (1995) carried out a study on a full scale lime softening plant, finding up to 90% arsenic removal at pH 11. It is recommended that a plant for arsenic removal only be used if hardness is also an issue.

2.3.5 Ion Exchange

This is a chemical process whereby arsenic is adsorbed onto a solid polymer resin bed comprised of sand grain sized, spherical beads. Water is passed through the resin bed and ions are released into the water from the bed, being replaced with the arsenic ions in the water. Removal can be over 90%, in the pH range of 6.5-9 (Ficklin, 1983). The resin must be regenerated when the majority of ions have been lost, and this is achieved by flushing the bed with a highly concentrated solution of these original ions. The US EPA (EPA, 2000) reported on the efficiency of two different ion exchange plants, both treating groundwater containing As(V). One plant showed 97% removal efficiency with regeneration every 6 days, while the other showed breakthrough after 1 month (3000 bed volumes.

2.3.6 Nanofiltration (NF)

Filtration occurs through a semipermeable membrane of tiny pores (<2nm) that can reject arsenic particles effectively. Both dissolved As(III) and As(V) can be removed by this process, with up to over 90% efficiency (Nguyen *et al.*, 2009). Pressure on the membrane ranges from 0.345 to 1 N/mm^2. Sato et al. (2002) reported As(III) and As(V) removal of 75 and 95% respectively using NF with a membrane pressure of less than 1.1 MPa at a water treatment plant in Japan.

2.3.7 Reverse Osmosis (RO)

This process is typically used in desalination of sea water, but has also been implemented for arsenic removal of up to 99% (Geucke *et al.*, 2009) It is a physical process by which particles are removed by applying pressure (0.69 – 1 N/mm^2) on the influent water to pass it through a semipermeable membrane (pore size <2 nm), this overcomes the natural osmotic pressure of the water, and arsenic ions are rejected based on size and electrical charge. Ning (2002) investigated the use of RO and found it was more effective for As(V) removal, while Schneiter and Middlebrooks (1983) reported 60-90% arsenic removal with RO.

It is worth noting that membrane processes (NF and RO) use high energy and the membranes themselves are prone to fouling due to small pore sizes, but there is usually no need for any added chemicals.

2.3.8 Electrodialysis Reversal / Electrocoagulation

This is an electrochemical process whereby cations or anions are selectively allowed to pass through a stack of electrically charged semipermeable membranes. Ions are selected based on their attraction to charged electrodes and the charge on membranes can be altered to reject arsenic ions for effective removal. Ribiero *et al.* (2000) obtained 99% arsenic

removal from chromate copper-arsenate treated timber waste using electrodialysis. Electro coagulation has been shown to efficiently remove arsenic on a small scale in Bangladesh (Addy, *et al.* 2011). An iron electrode is electrochemically dissolved in arsenic contaminated water, with the dissolved iron quickly forming a sludge with a high affinity for arsenic.

Table 2.1 gives an overview of the common arsenic removal processes, along with advantages and disadvantages associated with each.

Technique	Household	Community level	Removal	Efficiency	Working pH	Interferences	Operator skill	Relative cost	Advantages	Disadvantages	Remarks
			As(III)	As(V)							
Oxidation/Precipitation											
Air oxidation	X	X	–	–					relatively simple, low cost	partial removal of arsenic slow process	
Chemical oxidation	X	X	–	+					relatively simple and rapid process oxidises other impurities and kills microbes		
Coagulation/Co-precipitation			–	+++		little		low	no monitoring of breakthrough is required low costs and simple chemicals	toxic sludge is produced operation requires training	most effective process the regulation standard wide range of influent arsenic concentrations
Alum coagulation	X	X	–	+++	6.0-8.0		medium	low	chemicals normally available low capital costs	pre-oxidation is a must (low removal of As(III)) produces toxic sludge	proven at central level piloted at community and household level phosphate and silica may reduce As removal
Iron coagulation	X	X		+++	<8		medium	low	efficient at low costs simple operation, common chemicals	medium removal of As(III) pre-oxidation may be required	well proven at all three levels phosphate and silica may reduce As removal
Lime softening	X	X	+	+++	>11.5		medium	low-medium	common chemicals also reduces hardness	re-adjustment of pH is required large waste volume	proven in lab and pilot scale
Enhanced coagulation	X	X	++	+++	5.0-9.0		medium	low-medium	high removal efficiency of As also removal of organic matter and metal hydroxides	emerging technique, not proven on practical scale	
Sedimentation	X	X	–	–			low	low	simple	low reduction	relies on passive coagulation with iron
Oxidation/Filtration			–	++	5.5-8.5		medium	medium			
Adsorption			+	+++		average			no daily sludge problem	requires monitoring breakthrough requires periodical regeneration or medium shift	
Activated Alumina	X	X	++	+++	5.5-6.0		low	medium	well known, commercially available very efficient removal low maintenance, no daily sludge	re-adjustment of pH required toxic solid waste monitoring is difficult	pilot scale in community and household level in industrial countries arsenite removal is poorly understood
Iron Based Sorbents (IBS)	X	X	+	+++	6.0-8.5		low	low-medium	plenty of possibilities well defined technique no regeneration	requires pH control requires replacement of media after exhausting requires regular testing to provide safe operation	
Ion exchange											
Anion resin	X	X	-	+++	6.5-9.0	many	high	medium	well defined medium on pH correction	only As(V) removed interference from sulfate, nitrate and TDS adding of salt monitoring is difficult high costs	pilot scale in central and household systems, mostly in industrial countries
Membrane/Reverse osmosis								high	high removal efficiency no solid waste capable of removal of other contaminants	high running costs high tech operation and maintenance re-adjustment of water quality is required	shown effective at lab scale in industrial countries pretreatment required research needed on removal of arsenite
Reverse osmosis	X	X	++	++			medium	high	easily monitored no chemicals required no toxic wastes	removal of As(III) lower than As(V) removal high investment costs high tech operation and maintenance	
Electrodialysis		X	++	+++			medium	high	removal of other contaminants	interference by oxidizing agents toxic waste water	
Nanofiltration			++	++			medium	high	well defined, high removal efficiency	very high capital and running costs	
CAMP (Coagulation Assisted Membrane Process)		X	+++	+++				high		pretreatment required high costs	
Other											
In-situ oxidation/immobilisation		X	++	+++				medium	no arsenic-rich wastes	possibility of aquifer clogging	very limited experience

+++ = > 90% removal
++ = 60-90% removal
+ = 30-60% removal
- = <30% removal

Table 2.1 *Comparison of main arsenic removal methods (Feenstra et al., 2007)*

2.3.9 Bioremediation

Another not so mainstream process involves using natural/modified organisms discovered to be proficient in metabolizing As. *Marinomonas communis* is one of a number of non-engineered marine bacteria, found to be capable of accumulating arsenic within its cells, (Takeuchi *et al*, 2007). Kostal *et al*, (2004) showed *E. coli* can be engineered to increase removal of As(III) and As(V) by genetic modification, involving the overexpression of metalloregulatory protein ArsR. Phyto remediation has also been used in arsenic removal, involving altering plant/fungal biomass so that arsenic is adsorbed. Pokhrel and Viraraghavan (2006) modified *Asperigillus niger* with an iron oxide coating to achieve up to 95% removal from water. Arsenic has also been found to accumulate into living plant bodies, for example *Pteris vittata,* (Singh *et al.*, 2006).

2.3.10 Costs

Nearly all of the above processes have the distinct disadvantages of high costs, problems with sludge disposal, and complicated maintenance and/or regeneration. Table 2.2 shows cost comparisons for different removal technologies based on a population of 1000, (National Research Council (US), 2001). Despite the figures being a few years old, coagulation-filtration is by far the most cost effective system. However, what this illustrates is that there is a necessity for simple, cheap and efficient ways of removing arsenic, especially for those arsenic contaminated regions in developing countries, where both the lack of capital and decentralised population are problematic.

Processes	Treatment cost (US$)
Coagulation–filtration	11325
Lime softening (LS)	19681
Reverse osmosis (RO)	143199
Ion exchange (IX)	169273
Activated alumina (AA)	83871

Table 2.2 *Comparison of treatment costs (National Research Council (US), 2001)*

2.3.11 Small-scale treatment in developing countries

The previous sections focused on treatment technologies suitable for large-scale applications, those in operation and those still in pilot phase. In many developing countries, large-scale treatment is next to impossible, especially in rural areas where funding and logistics are major issues. The ideal solution would be to have a system whereby each household, or small village, would treat their own water. This has been attempted with considerable success in Bangladesh, and the following are some examples of smaller scale treatment systems that are currently being implemented (World Bank, 2005).

- Bucket treatment

The bucket treatment system is for an individual household and uses oxidation and coagulation followed by settling. This unit comprises of two 20 litre buckets, one set on top of the other. First, coagulants are mixed with contaminated water by hand in the upper bucket by stirring briskly and then flocculated by slow stirring for a minute and a half. The water is allowed to settle and then runs into the second bucket. This bucket contains sand which filters out any arsenic sediments. Household field trials were carried out by Meng *et*

al. (2001) on water with up to 600 µg/l arsenic. 2 g of combined ferric and hypochlorite salts were needed to treat 20 litres of water, to between 0.7 and 45 µg/l. The initial flow rate of 1.5 l/min reduced to 0.4 l/min after 10 bed volumes due to clogging. The rinsing of the sand bucket however only needed 2 bed volumes of well water with no chemicals added.

- Tubewell filter

The tubewell filter uses oxidation and adsorption, and has been shown to remove over 90% of the arsenic for a village, (200-300 households). This compact arsenic removal unit is attached to the well head at the hand-pump and contains 100 litres of activated alumina. It comprises of two separate cylindrical chambers, the first to aerate the pumped water to promote oxidation of dissolved iron, and the second containing the alumina for sorption on top of gravels as basic filtration. It has been found to be capable of treating 10000 bed volumes of water at 8-10 l/min with arsenic concentrations of over 500 µg/l (removal to below 50 µg/l) in West Bengal (Sarkar *et al.*, 2005).

- 3-pitcher filter

The 3-pitcher filter system (SONO) is for household use and involves adsorption of arsenic by iron chips and sand. It is comprised of three clay pitchers, each on top of the next. The top pitcher contains 2 kg of sand laid on top of 3 kg of zero valent cast-iron filings. The second pitcher contains 2 kg brick chips, 1 kg charcoal and 2 kg sand. Contaminated water is poured into the uppermost pitcher and the clean, filtered water is taken from the last pitcher. Hussam *et al.* (2007) reported no breakthrough after 5 years use (approximately 120 l/day), and consistently removing a range of arsenic concentrations to below the MCL.

2.4 Solar Oxidation and Removal of Arsenic (SORAS):

2.4.1 Background

Photo-oxidation as a process to remove arsenic is also mentioned in 'Technologies and costs for removal of arsenic from drinking water 2000' (EPA, 2000), which was first investigated by Khoe *et al.*, (1997) as a means for treating mining effluent (see also Emett and Khoe, (2001)). In 1999, a presentation on the arsenic crisis in Bangladesh (Murcott, 1999) described and evaluated different removal methods according to their appropriateness- namely performance and cost. Photochemical oxidation was listed in the presentation, but as no experimental data existed at that time, only the potential of the method is stated. Hug *et al.,* (2001) and others at EAWAG, researched this potential extensively in relation to groundwater in Bangladesh conducting laboratory and field studies, both with considerable success (discussed below). The solar oxidation and removal of arsenic (SORAS) process they describe is extremely simple, but involves complicated chemical reactions.

2.4.2 Mechanism

Since arsenic usually exists as arsenite As(III) in groundwater (see Section 2.1.1), this removal method entails oxidizing this to arsenate As(V). As mentioned in Section 2.3, As(III) only weakly adsorbs to coagulants and so this oxidation step is important. The rate of oxidation of As(III) by dissolved oxygen is very slow (Eary and Schramke, 1990), and so this method accelerates the oxidation by subjecting the water to sunlight, which photochemically oxidises As(III) in the presence of Fe. A Fenton-like reaction takes place whereby instead of hydrogen peroxide (H_2O_2) oxidizing the Fe, photons from the UV light

are absorbed by the iron (Figure 2.8), producing highly reactive hydroxyl radicals. These free radicals are involved in the oxidation and reduction of Fe(II) to Fe(III), and vice versa, producing more reactive oxygen species that convert As(III) to As(V) via the As(IV) intermediate. Co-precipitation then occurs as the As(V) can then adsorb to positively charged Fe(III)(hydr)oxide particles and the flocs can settle out by gravity. Given the wavelength range for absorption of photons by Fe of 350-400 nm, the UV-A portion of light (see Figure 2.9) is the most relevant part of the solar spectrum for this process. The reactive oxygen species (ROS) generated in these reactions have been studied closely by Hug *et al.* (2001) and Hug and Leupin (2003). It was concluded by using 2-propanol (an $^{\bullet}OH$ scavenger) that the $^{\bullet}OH$-radicals had no influence on As(III) oxidation at circumneutral pH as no change was seen in the rate of conversion of As(III) to As(V). However, in the lower pH range (<5) 2-propanol actually quenched oxidation completely. These findings indicate that As oxidation mechanisms are very much pH dependent. H_2O_2 and O_2 did not oxidise As(III) in the dark, and $O_2^{\bullet-}$ is omitted from consideration as the rate constant required is inconsistent with experimental data. It is postulated that $CO_3^{\bullet-}$ and higher valence iron (Fe(IV) for example) are the species responsible for As oxidation (Hug *et al.*, 2001).

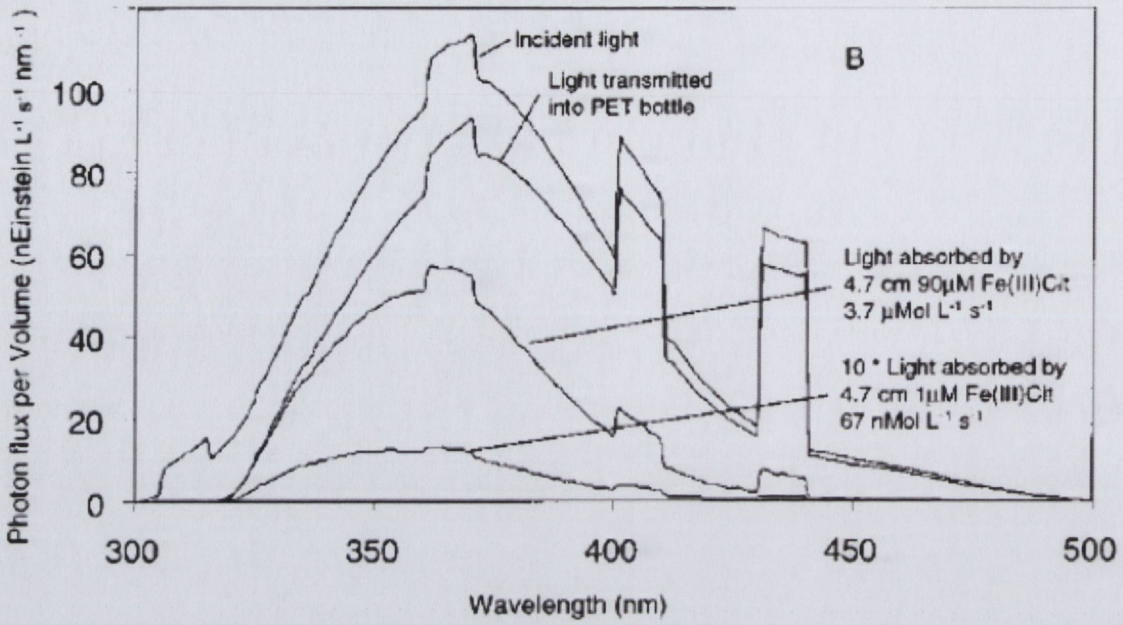

Figure 2.8 *Photon flux absorbed per volume by 1 and 90 µM Fe(III)/l (Hug et al. 2001)*

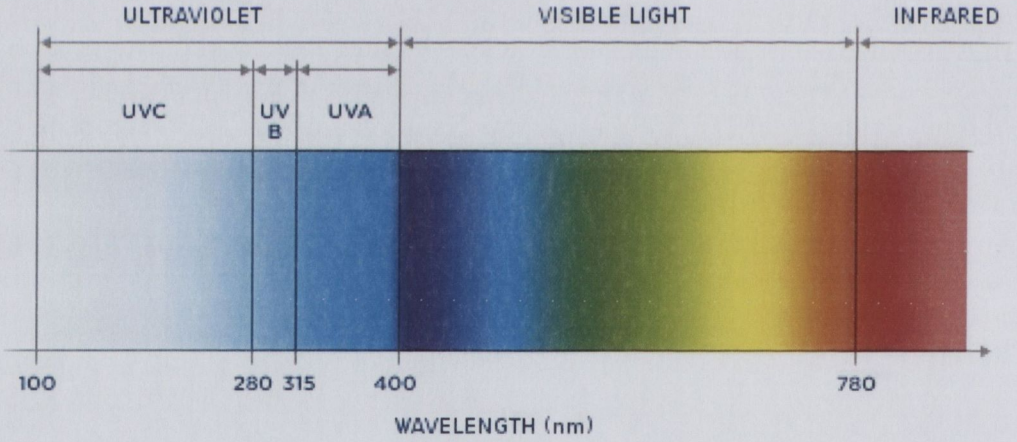

Figure 2.9 *Light spectrum* (http://www.jnjvisioncare.com/en_US/uv-damage-cnt1.jsp)

It was also found that if a chelating agent was added before irradiation, the rate of oxidation of As(III) was greatly increased. Citrate was added as this complexant, forming intermediate compounds with the iron (e.g. $Fe(III)CitOH^-$), which, when involved in photolysis, produces even more oxidants for the As(III). This iron-citrate reaction cycle occurs again and again as the photooxidation keeps taking place and the iron is reduced

and re-oxidized as above. The final pH decreased marginally, (around 0.05 units), due to the addition of citrate (Hug *et al.*, 2001; Garcia *et al.*, 2004). Table 2.3 gives a detailed list of the pertinent chemical reactions taking place in the SORAS process (adapted from Hug *et al.*, 2001). It was concluded that photochemical oxidation of As(III) can occur immediately after Fe(II) and citrate addition, when Fe(II) and forming Fe(III) are in solution, or when predominantly Fe(III) is present.

TABLE List of Reactions with Known, Estimated, and Adjustable Rate Constants[a]

	Arsenic Oxidations		
R1a	$As^{III} + O_2^{\bullet-} \rightarrow As^{IV} + H_2O_2$	**3e6**	adjustable
R1b	$As^{III} + CO_3^{\bullet-} \rightarrow As^{IV} + HCO_3^-$	1.1e8	(Klaning, et al. 1989)
R1c	$As^{III} \bullet OH \rightarrow As^{IV}$	8e9	(Klaning, et al. 1989)
R1d	$As^{IV} + O_2 \rightarrow As^{V} + O_2^{\bullet-}$	1.1e9	(Klaning, et al. 1989)
	Fe^{III} Photolysis		
R2a	$Fe^{III}CitOH^- \rightarrow Fe^{II} + 3HGA^{\bullet 2-}$	**0.013**	adjustable
R2b	$Fe^{III}OH^{2+} \rightarrow Fe^{II} + \bullet OH$	**0.00004**	adjustable
	Photolysis Follow-up Reactions		
R3a	$3\text{-}HGA^{\bullet 2-} + O_2 \rightarrow 3\text{-}OGA^{2-} + O_2^{\bullet-}$	1e6	fast, estimated
R3b	$3\text{-}HGA^{\bullet 2-} + Fe^{III}OH^{2+} \rightarrow 3\text{-}OGA^{2-} + Fe^{II}$	1e6	fast, estimated
R3c	$3\text{-}HGA^{\bullet 2-} + Fe^{III}CitOH^- = 3\text{-}OGA^{2-} + Fe^{II}Cit$	1e6	fast, estimated
R3d	$Fe^{II}Cit \rightarrow Fe^{II} + Cit$	1e6	fast, estimated
R3e	$HO_2^{\bullet} + O_2^{\bullet-} \rightarrow H_2O_2$	9.7e7	(Rush and Bielski, 1985)
	$\bullet OH$ Reactions		
R4a	$Fe^{II} + \bullet OH \rightarrow Fe^{III}$	3.2e8	(Stuglik and Zagorski, 1981)
R4b	$Cit^{3-} + \bullet OH \rightarrow 3HGA^{\bullet 2-}$	1.5e8	(Zepp, et al. 1992)
R4c	$H_2O_2 + \bullet OH = HO_2^{\bullet}$	3e7	(Buxton, et al. 1988)
R4d	$\bullet OH + isoprop \rightarrow O_2^{\bullet-}$	1.9e9	(Buxton, et al. 1988)
R4e	$HCO_3^- + \bullet OH \rightarrow CO_3^{\bullet-}$	8.5e6	(Buxton, et al. 1988)
	Fe^{II}-Oxidations		
R5a	$Fe^{II} + O_2 \rightarrow O_2^{\bullet-} + Fe^{III}OH_2^+$	60	(Stumm and Lee, 1961) at pH 7.5
R5b	$Fe^{II} + O_2^{\bullet-} \rightarrow Fe^{III} + H_2O_2$	1e7	(Rush and Bielski, 1985)
R5c	$Fe^{II} + CO_3^{\bullet-} \rightarrow Fe^{III} + HCO_3^-$	3.6e8	assumed same as $Fe(CN)_4^{4-}$ (Huie, et al. 1991)
	Fenton Reaction		
R6a	$Fe^{II} + H_2O_2 \rightarrow Fe^{III} + \bullet OH$	1.1e6	pH 7.5 (Millero and Sotolongo, 1989)
	Fe^{III}-Reductions		
R7a	$Fe^{III}OH^{2+} + O_2^{\bullet-} \rightarrow Fe^{II} + O_2$	1.5e8	(Rush and Bielski, 1985)
R7b	$Fe^{III}(OH)_2^+ + O_2^{\bullet-} \rightarrow Fe^{II} + O_2$	1.5e8	(Rush and Bielski, 1985)
R7c	$Fe^{III}CitOH^- + O_2^{\bullet-} \rightarrow Fe^{II} + Cit$	0	(Sedlak and Hoigne, 1993)
	Fe^{III} Equilibria		
E1	$Fe^{III} + Cit^{3-} \leftrightarrow Fe^{III}CitOH^-$	1e12/6	adjustable
E2	$Fe^{III} \leftrightarrow Fe^{III}OH^{2+} + H^+$	4.57e7/1e10	$pK1$: 2.3 (Smith and Martell, 1979)
E3	$Fe^{III}OH^{2+} \leftrightarrow Fe^{III}(OH)_2^+ + H^+$	2.51e6/1e10	$pK2$: 3.6 (Smith and Martell, 1979)
E4	$Fe^{III}(OH)_2^+ \leftrightarrow Fe^{III}(OH)_3 + H^+$	1.17e2/1e10	$pK2$: 7.9 (Smith and Martell, 1979)
E5	$Fe^{III}(OH)_3 + Fe^{III}(OH)_3 \leftrightarrow Precip$	1e12/3e4	formation of Fe(III) precipitates, adjustable
	Superoxide Equilibria		
E6	$O_2^{\bullet-} + H^+ \leftrightarrow HO_2^{\bullet}$	1e10/1.58e5	pK: 4.8 (Rush and Bielski, 1985)
E7	$air \leftrightarrow O_2$	1e10/1e16	constant $[O_2]$ (250 M air reservoir)

[a] Equations are balanced for reactive species. Unreactive products and educts such as H_2O, CO_2, and acetone are omitted. $[O_2]$ and $[H^+]$ are constant. Equilibrium reactions (indicated with $\leftrightarrow$) have to be written as separate forward reactions and back reactions (with k_f/k_b) for the modeling with the ACUCHEM program.

Table 2.3 *List of reactions in the SORAS process (adapted from Hug et al., 2001)*

2.4.3 SORAS testing

Emett and Khoe (2001) tested the SORAS process on acid mine water (pH ranging from 0.5-2.5) in Montana, USA, which had arsenic concentrations of up to 150 mg/l, finding that they needed an Fe(III) to As(III) molar ratio of 1:2 with no citrate added for effective arsenic removal. However, as explained above, the acidic conditions of mine tailings promote different oxidation mechanisms and therefore it is difficult to draw comparisons with experiments conducted at circumneutral pH. In other field tests iron did not need to be added to the water as it occurred naturally in Bangladesh (up to > 5 mg/l), and citrate was added in the form of citric acid namely 6-8 drops of lemon juice per litre. Transparent PET bottles were filled to 60-70% capacity (leaving room for air) and shaken vigorously to saturate the water with dissolved oxygen, samples were then irradiated for up to 6 hours- the laboratory tests used a UV lamp, whereas in the field, the bottles were left to lie on roofs in the sunlight. They were then allowed to stand vertically overnight, while the Fe-As precipitates descended to the bottom. The chemistry involved in the process is given in simplified form in Figure 2.10. The resulting water was decanted or filtered through a cloth and showed up to 90% arsenic removal in the laboratory, although the field tests only achieved up to 78%. The effects of varying initial iron content, along with other trace elements like phosphates, silicates, manganese, DOC, sulphates and other unknowns in the field water were thought to be behind the difference in removal efficiencies. Note, a more concise presentation of this research is also available in, Wegelin *et al.*, (2001). As PO_4 is a known competing ion for oxygen, Mukherjee *et al.*, (2007) investigated the process at a household level in West Bengal which involved testing with phosphate concentrations of up to 2.5 mg/l. Results confirmed that the arsenic removal efficiency decreased with increases in PO_4 levels. Alkalinity has been shown to have the opposite effect, Garcia *et al.* (2004) determining the greatest arsenic removal efficiency at the highest bicarbonate

concentration - most likely due to enhanced co-precipitation of the ironoxide-arsenic particles.

These tests were also conducted by Garcia *et al,* (2004) and Lara *et al,* (2006), in studies to treat water in Argentina and Chile respectively. In both cases, Fe needed to be added as the water composition was quite different from that in Bangladesh, but removal was found to be roughly the same. Lara *et al* (2006) concluded that a molar ratio (citrate:arsenic:iron) of 1:4.5:18.7 was the situation for optimal removal. However, Garcia *et al.* (2004) disputes the use of citrate at higher amounts, as these concentrations were found to have adverse effects on removal. Mukherjee *et al.* (2007) also examined the effect of various chelating agents (including citrate) in batch tests, finding EDTA (ethylenediaminetetraacetic) to give the most significant increase in efficiency, (over 98%).

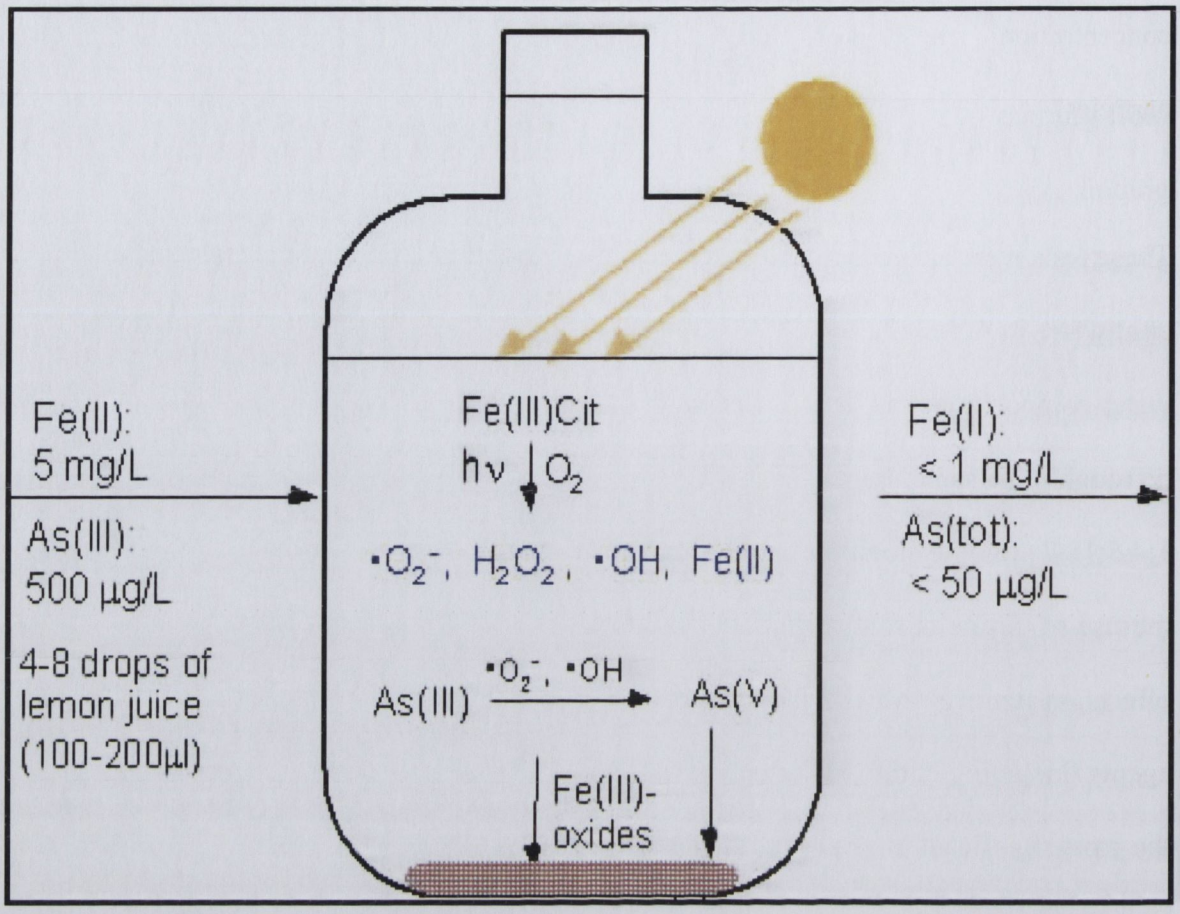

Figure 2.10 *Photochemical formation of the reactive oxidants and settlement of Fe-As particles*

2.4.4 Factors affecting efficiency of SORAS

- Initial arsenic concentration: as inlet arsenic concentrations can vary widely (Section 2.1), and previous studies have shown molar As:Cit:Fe ratios of 1:4.5:18.7 (Section 2.4.3), the amount of iron required for the process greatly depends on the initial arsenic content.
- Irradiation time and intensity: batch tests in the field were conducted in good sunshine, and as the photon flux to the water is the basis of the chemical reactions, the intensity of the sunlight and time subjected to it is of paramount importance. Studies have shown greater efficiency over longer irradiation time (Hug *et al*, 2001). The suitability of regions for solar applications was investigated by Acra *et*

al. (1984). Bands around the earth from latitude 15-35° north and south of the equator were found to be most favourable for the amount and intensity of irradiation received (Figure 2.11).

- Turbidity: turbidity causes dispersion of light received by the water, reducing the UV flux and so can adversely affect the removal efficiency. As turbidity is made up of suspended solids, these solids may be competing ions for O_2, OH^- or Fe.
- Dissolved oxygen: DO is crucial to the reactions in the SORAS process, so sufficient DO must be ensured throughout the system
- pH: as pH changes can influence the speciation of arsenic (Section 2.1) and Fe, variance in pH can affect the efficiency positively or negatively.
- Temperature: although it seems that no studies have been carried out on differences in temperature on the SORAS method, it is known that higher temperatures imply lower DO concentrations as the oxygen saturation concentration reduces with increased temperature.
- Water quality parameters: as seen in Section 2.4.3, competing inorganics such as phosphate and silicate have adverse effects on removal efficiency. It should be noted that no studies have been reported on microorganisms competing for oxidative species, which could influence the process.

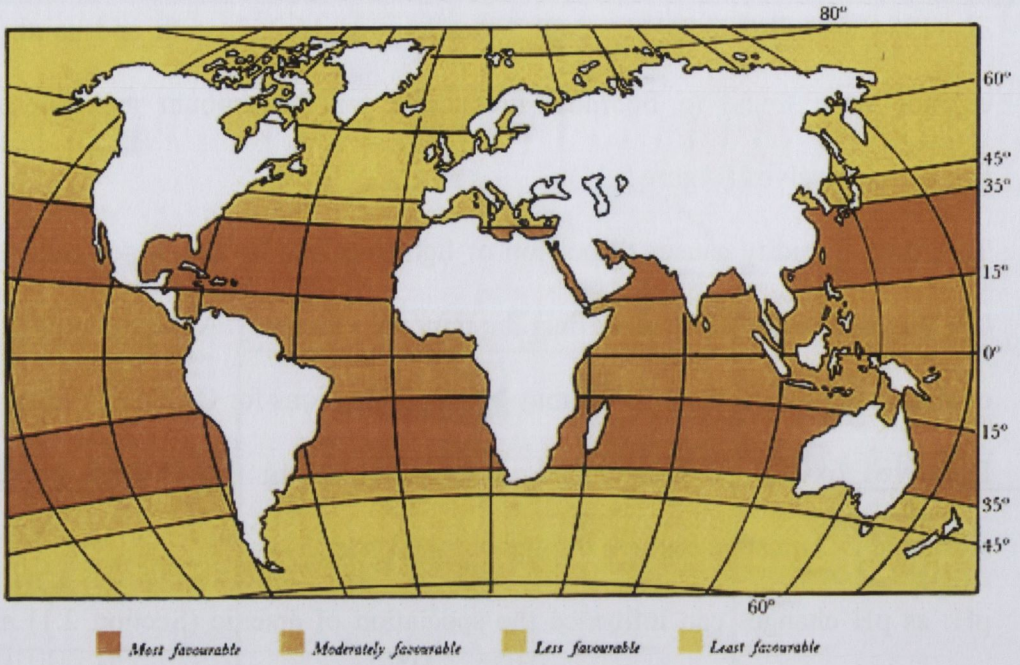

Figure 2.11 *World distribution of solar radiation indicating suitability of areas for solar applications (Acra et al., 1984b)*

2.4.5 Use of photocatalysis with SORAS

Photocatalysts are used in many water/wastewater treatments as advanced oxidation processes (AOPs) to remove organic and inorganic contaminants (Matthews, 1992, Guillard, 2003), and have also been used to oxidize As(III) to As(V) more rapidly. Bissen (2001) studied batch experiments with arsenic concentrations up to 10 mg/l under UV light, adding suspensions of titanium dioxide TiO_2 as the photocatalyst. Complete oxidation of As(III) was found to occur in just 200 seconds with 10 mg/l TiO_2, the only disadvantage being the necessity for its subsequent removal along with the As(V). A further development in the SORAS process can be achieved by using an immobilized coating of TiO_2 on the inside of the PET bottles (Fostier, 2008). TiO_2 was fixed on the

plastic to give concentrations from 2-20% w/v, achieving over 99% removal, (from an initial As(III) concentration of 500 μg/l) after 120 minutes illumination time (optimal TiO_2 10% w/v). Ferguson (2008) also used fixed TiO_2, but on glass beads in a fixed bed upflow reactor. Samples were irradiated from above but counterintuitive efficiencies were seen, most likely due to unsuitable design of reactor geometry.

Using the SORAS process in closed containers such as PET bottles has the advantage of protecting the water from dust and pathogens, and these bottles are readily available. However, the technique has some disadvantages. The volume of water treated is limited to the number of containers that are used, and larger bottles (greater than 10 cm diameter) are not recommended for solar disinfection, (a process which is comparable on the issue of light transmission) in order to minimise water depth and allow sufficient irradiance of the water (EAWAG, 2002). More importantly, the process is completely dependent on the dedication of each individual user, and as collecting water is often a necessary daily task, having to then treat the water as well could prove a tiresome undertaking (discussed again in Section 2.6.2). It could be therefore more beneficial to have a community based treatment system, which requires little maintenance and technical difficulty. As far as can be determined from the international; literature no attempts have been made at adapting the SORAS method to a continuous flow process, with or without the use of photocatalysts.

2.5 Continuous Flow Solar Reactors:

Continuous flow solar reactors for water treatment have been based on the designs of traditional solar thermal collectors which absorb solar energy from the sun, to either heat fluids or generate electricity. Solar reactors were first employed for solar photocatalytic detoxification of wastewater (Pacheco, 1990). Usually TiO_2 is used as the photocatalyst in suspended or fixed form, which degrades organic and inorganic pollutants by the production of ROS. Collectors are capable of efficiently gathering solar photons and transferring them into the absorber component of the reactor.

2.5.1 Types of solar collectors

The two types of collector are concentrating and non-concentrating. Concentrating collectors converge light onto a focal point or linear focus, the main types being parabolic trough collectors (PTC) and parabolic dishes. PTCs consist of a parabolic reflecting surface which concentrates light onto a tube located at the focus of the parabola. The trough then follows the path of the sun, remaining perpendicular to its rays at all times. The light reflected into the absorber tube is used with the photocatalyst in the detoxification of flowing water.

Non-concentrating collectors do not have solar tracking and usually consist of either a flat plate tilted toward the sun or multiple small tubes connected in parallel. As sunlight hits the flat plate, water to be treated flows over the plate (or between two plates) and absorbs

radiation. The advantages of non-concentrating collectors are that they are able to collect both direct and diffuse radiation, (concentrating only collecting direct radiation), and they are much simpler and cheaper to build and maintain, as they have less components and no moving parts. Non-concentrating collectors are therefore the choice for photocatalytic applications (Ajona, 2000) due to their higher efficiencies of collecting solar radiation.

2.5.2 Compound parabolic collectors

The compound parabolic collector (CPC) is a low concentrating static collector with a curved reflective surface which follows an involute around the circumference of the reactor tube. As will be discussed in Chapter 4, the CPC was found to be the most efficient design for the SORAS method, so it will be covered in more detail here. It is similar to the PTC but has no solar tracking. It has high energy efficiency, collecting both direct and diffuse solar rays (nearly 100% of the UV radiation arriving at the reactor). Figure 2.12 shows the profile of the CPC, the rays being reflected to illuminate the circumference of the reactor tube. High levels of dissolved oxygen can be achieved in CPCs as turbulent flow regimes are employed. Due to its extremely efficient design, CPCs are considered to be the optimal system for the photocatalytic detoxification of wastewaters, (Blanco, 1999, Robert, 2002). A pilot study on the treatment of greenhouse wastewater using CPCs showed effective photocatalytic degradation of 4 different pesticides (Malato *et al.*, 2002).

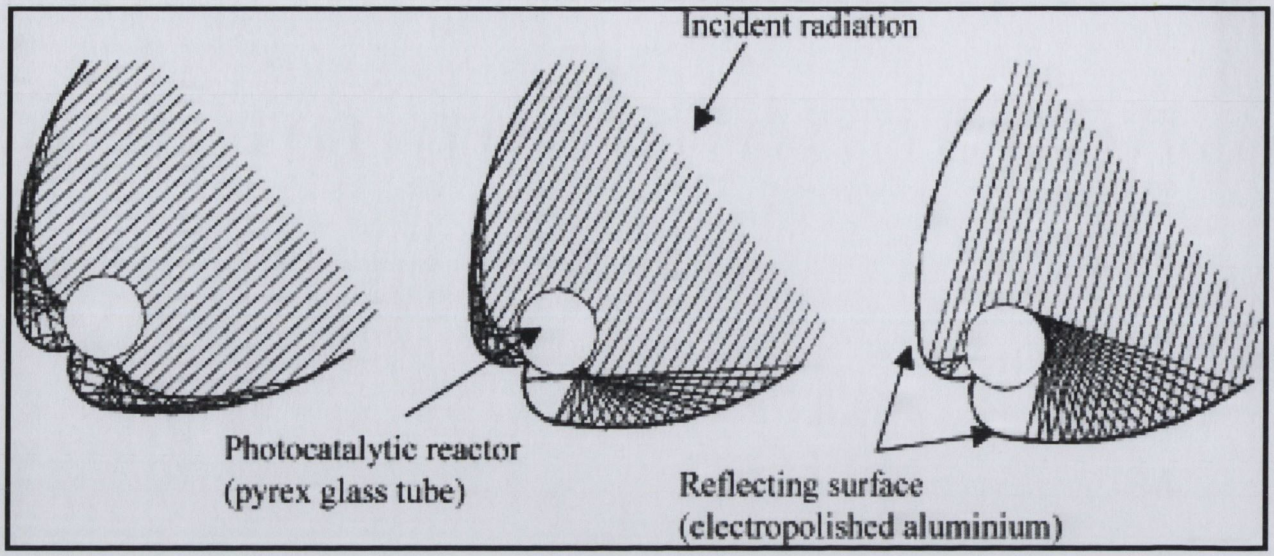

Figure 2.12 *Profile of CPC reactor (McLoughlin et al., 2004)*

Equally, solar disinfection (SODIS) is now also being performed in continuous flow reactors. McLoughlin *et al.* (2004) compared three different small scale reactors in natural sunlight, compound parabolic (CPC), parabolic (P), and v-groove (V), for water disinfection, using *E. coli* as the representative microorganism. Results showed the CPC efficiency to be greater than both the P and V, and depended on illumination time and flow conditions.

2.5.3 Design of CPCs

The absorber tube material needs to be durable, weather resistant and sufficiently transmissive to UV light, without being damaged by it or allowing migration of particles from the material into the water by UV action. As a result, low-iron content glass like borosilicate glass is used for these reactor tubes. Glass can also withstand the force of the system being pressurised.

The collector surface needs to reflect light (between 300-400 nm) efficiently to be absorbed by the reactor, and so highly polished surfaces which are specular (keeps each ray intact as it hits the surface), are considered most effective (Malato Rodriguez *et al.*, 2004). Polished aluminium and copper are used, although need a protective layer to resist degradation by weather conditions which reduces reflectivity.

The tube thickness and diameter must be considered in the design of the system. The thinner the tube the more transmissive it is, but it needs have sufficient thickness to be able to withstand the pressure of the water. The diameter chosen must be such that it ensures an even UV dose to each particle passing through it. Malato Rodriguez *et al.* (2004) suggested a minimum tube diameter of 20 mm and an ideal of 25-50 mm for use in photocatalytic CPCs.

The flow rate through the reactor should be turbulent to ensure sufficient mixing, and turbulence also allows for higher dissolved oxygen levels. Mixing will aid in the transmission of uniform radiation.

2.6 Solar Disinfection:

2.6.1 Mechanism

Since the late 19th Century, sunlight has been known to have an inhibiting effect on microorganisms, (Hockberger, 2000). Solar light/energy is used in the treatment of contaminated water by two synergetic mechanisms, namely radiation and increased water temperature. Light in the spectrum of UVA (wavelength 320-400 nm), is able to inactivate microorganisms by the absorption of photons which penetrate the cell wall. Energy can then react with molecules inside the cell, altering components such as nucleic acid, which control the cell functions. These are crucial for growth and reproduction, hence cells are damaged or totally destroyed. Bacteria, viruses and protazoa can all be eliminated by irradiation with sunlight.

2.6.2 SODIS

The solar water disinfection (SODIS) process was, like SORAS developed extensively by EAWAG from previous studies as a simple, low cost method to improve the quality of drinking water in developing countries, (EAWAG, 2002). SODIS uses solar radiation in batch form to kill the pathogenic microorganisms that are known to cause water borne diseases like cholera, typhoid, diarrhoea, dysentry, cryptosporidiosis, parasitic worms, etc. SODIS is perfect for treating small amounts of water for individual use at household level. Contaminated water is filled into transparent PET bottles (500 ml or 1.5 litre) and sealed, and shaken for 20 seconds to ensure sufficient dissolved oxygen, which assists the process. The bottles are then exposed to full sunlight for six hours in clear, bright weather, but if cloud cover is high, the bottles need to be subjected to light for up to two days. Again, the

regions of superior solar radiation levels are located between 15 and 35° North and South of the equator, where cloud and rain are limited. Turbidity of the water to be treated also affects the efficiency of the process, as suspended solids interfere by absorbing the light, (turbidity must be below 30 NTU). The bottles are left to lie in the sunlight on roofs, preferably those made of corrugated iron sheets, as this reflects light back into the bottle for maximum radiation intensity and higher temperatures. As the physical process of heating also destroys microorganisms, water temperatures above 50°C increase the efficiency of the disinfection process by threefold, (Wegelin, 1994). After the bottles are illuminated, the water is safe to drink.

The method has been put into practice in many developing countries by EAWAG and other agencies including NGOs. The outcome has been very successful due to the simplicity of the process and the readily available inexpensive materials needed. Conroy (1996) studied an area in Kenya which implemented a SODIS project, finding a great reduction in water borne diseases in children, (for example children under the age of six being eight times less likely to contract cholera.) Others have observed up to 73% reduction in diarrhoea cases when using solar disinfected water. However, the user acceptability of the system has been called into question by du Preez *et al.* (2010) and Mäusezahl *et al.* (2009) due to ineffective implementation. In a study in South Africa du Preez *et al.* (2010) found no significant reduction in dysentery in children in 75% of cases where SODIS was implemented, suggesting that strong participant motivation was the determinant in effective treatment. A similar study in Bolivia (Mäusezahl *et al.*, 2009) found that despite an extensive promotional campaign, mean SODIS compliance was only 32%, and diarrheal incidences in children were 3.6/year compared to 4.3/year for those not informed of

SODIS. These studies indicate that individual/household water treatment systems need to be thoroughly evaluated in field trials. Hence the option of community level systems could be more effective.

2.6.3 Photocatalytic disinfection

Further investigation into the process has been carried out using photocatalysts, mainly TiO_2. The catalyst can absorb UV light of broader wavelengths than microorganisms, and generates reactive oxygen species (ROS) which attack living cells further. Fixed and suspended TiO_2 has been researched in batch solar disinfection experiments, both resulting in improved efficiency. Salih, (2002) and Rincon, (2003) found TiO_2 in suspension to perform better than the immobilized form. Again, suspensions would have to be removed before consumption.

2.6.4 Continuous flow solar disinfection

Solar collecting reactors have been studied with a view to implementing solar and solar photocatalytic disinfection on a large scale. As discussed above research on small-scale reactors showed that compound parabolic was the most efficient profile (McLoughlin *et al.*, 2004). TiO_2 was also fixed on 2 mm diameter rods and placed inside the absorber tubes, enhancing the efficiency of the CPC even further. This type of disinfection experiment was also conducted by Fernandez (2005), using only the CPC reactor. These studies confirmed the complete deactivation of *E. coli* within 60 minutes.

Several large scale applications have recently been put into practice, such as SOLWATER (Navntoft *et al.*, 2007) and AQUACAT (Chapelon and Herrmann, 2004) and the first full-scale field application in sub-Saharan Africa has recently been installed at a village in Kenya (Gill and Price, 2010).

CHAPTER 3: MATERIALS AND METHODS

3.1 Materials

3.1.1 Chemicals

The following is a list of chemicals used to simulate conditions that are found in contaminated groundwater, and other possible compounds that could affect arsenic removal, positively or negatively, in order to investigate the continuous flow removal process. As this research focused on contaminated groundwater in developing countries, which was not available for testing, As(III) was the preferred form of arsenic as this is most common in groundwater. As iron is a requirement in the SORAS technique, iron was dissolved from laboratory grade chemical powder. Citrate was shown to aid arsenic removal in SORAS batch tests, so both natural citrate and sodium citrate were used in experiments. As phosphate and silicate were shown to be competing ions, these were also added to samples from chemical powders.

3.1.1.1 Arsenic

To obtain a stock solution of 1 g/l As, 1.32 g Fluka Arsenic trioxide (As_2O_3) was weighed on an electronic microbalance (Mettler H33 4-place balance), and was dissolved in 1 litre of distilled water using a Pyrex beaker, magnetic stirrer and hotplate. The stock solution was kept in a sealed Pyrex flask, and tested periodically with ICP-AES to ensure consistency (see Section 3.2.4.1).

3.1.1.2 Iron

4.84 g or 19.36 g BHD Iron(III)chloride 6-hydrate ($FeCl_36H_2O$) was weighed on an electronic balance (Adventurer Pro, OHAUS) and dissolved in 1 litre of distilled water to give a stock solution of 1 g/l and 4 g/l Fe respectively. The stock solutions were kept in sealed Pyrex flasks, and tested periodically with ICP-AES to ensure consistency (see Section 3.2.4.2).

3.1.1.3 Citric acid

14.7 g Fisher Sodium citrate ($Na_3C_6H_5O_7$-$2H_2O$) was weighed on an electronic balance and dissolved in 500 ml of distilled water to give a stock solution of 100 mM sodium citrate. For the experiments which used natural citrate, lemons (Spain) were squeezed using a kitchen juicing utensil, and then passed through a 0.6 mm sieve to remove any pulp which may interfere with UV absorption. The clear juice was then frozen in batches of 5 ml in universal plastic containers, and defrosted overnight before use. These were then kept in the fridge for up to 3 days to ensure the juice was fresh. Lemon juice contains 5-10% citric acid, and it was established from an earlier study using a simple titration with NaOH, that 79.65g/l (7.2%) was contained in these lemons. This compares adequately with the value quoted by Hug *et al.*, (2001) of 76.85g/l, and corresponds to 0.415 M citrate as the molar mass of $C_3H_5O(COOH)_3$ is 192.12 g/mol, so 200 µl lemon juice is approximately 80 µM.

3.1.1.4 Phosphate

A stock solution of 1000 mg/l, was made up with 2.06 g Sigma-Aldrich Potassium phosphate (KH_2PO_4) dissolved in 1 litre of distilled water.

3.1.1.5 Silicate

2.788 g Sigma-Aldrich Sodium metasilicate (Na_2SiO_3) was dissolved in 1 litre of distilled water to give a stock solution of 1000 mg/l.

3.1.1.6 Sodium sulphite

To obtain a 1% stock solution, 1g Sigma-Aldrich (Na_2SO_3) was dissolved in 100 millilitres of distilled water. This was used to remove dissolved oxygen from sample solutions by the following reaction:

$$2Na_2SO_3 + O_2 = 2Na_2SO_4$$

3.1.1.7 Titanium dioxide

Titanium dioxide was used as the photocatalyst in all of the experiments. The TiO_2 was supplied by the Degussa company and was of the type P25 Aeroxide (80:20 anatase:rutile). For batch experiments, the appropriate mass of TiO_2 was measured out using a four-figure microbalance (Cahn C-33) and mixed with 1 L of distilled water in an autoclave bottle (Figure 3.1). The contents of the bottle were then sterilised by autoclaving [HiClave HV-25 autoclave (HMC, Japan)] for 40 minutes at 121 °C. For other experiments, the appropriate mass of photocatalyst was added to the reservoir and allowed to mix before the experiment was started.

3.1.1.8 Other Chemicals

The following chemicals were used in the acidification and analysis of samples (see Section 3.2). Sigma-Aldrich Nitric acid, Sigma-Aldrich Hydrochloric acid, Sigma-Aldrich Potassium iodide, Fisher Scientific Sodium borohydride, BDH Sodium hydroxide, and all were reagent grade.

3.1.2 Bacteria

Escherichia coli K-12 (ATCC 10798) was used as the bacteria for all experiments and was stored in freeze dried form at -80 °C before being prepared to give an *E. coli* concentration of approximately 1 x 10^9 CFU/mL, as outlined in Section 3.2.1.

3.1.3 Growth media

Luria Agar and Luria Broth (Sigma Aldrich, USA) were used as the growth media for the *Escherichia coli*. The agar was prepared by adding 40 g of powdered agar to 1 L of sterile water in an autoclave bottle. The bottle was autoclaved for 40 min at 121 °C. When the bottle had cooled to about 50 °C, the agar was poured into Petri dishes and the plates were allowed to dry.

3.1.4 Water

Tap water from the Civil Engineering Laboratories was used in all SORAS experiments (excluding combined SORAS-SODIS tested on the large scale reactor, which used distilled water as discussed in Section 3.2.3.1). Table 3.1 details the average tap water composition

which was analysed by a number of methods. Data was obtained from Dublin City Council's Water Services Department. This data was verified in the laboratory by ICP analysis (Section 3.2.4), chemical test kits supplied by Merck, and by data received from the Centre for Environmental Studies, TCD. pH was measured with a pH 330 (WTW, Germany) and O2 was measured with a Cyberscan DO5000 (Eutech).

Parameter	Value	Unit
Temperature	10.5 - 14	°C
pH	6.89 - 7.94	-
Ca	15 - 23	mg/l
Cl	22 - 28	mg/l
Free Chlorine	0 - 0.2	mg/l
Cu	0 - 0.15	mg/l
Fe	0.014 - 0.0596	mg/l
F	0.6 - 1	mg/l
O_2	8.96 - 11.1	mg/l
Mg	13 - 19	mg/l
Al	0.05 - 0.12	mg/l
P	0.013 - 0.027	mg/l
Alkalinity (as $CaCO_3$)	70 - 150	mg/l
Na	3.7 - 5.9	mg/l
ρ	1000	kg/m3

Table 3.1 *Tap water composition*

3.1.5 Reactors

Two compound parabolic collectors (CPCs) were used in the majority of experiments, one laboratory scale (Figure 3.2) and one full-scale (Figure 3.3). Their characteristics are summarised in Table 3.2. As the SORAS process has not before been tested in a continuous flow system, experiments were carried out on a number of different reactor designs at laboratory scale before more extensive testing on the most efficient design.

3.1.5.1 Laboratory scale reactors

The four laboratory scale reactors were manufactured in the Department and consisted of six parallel Pyrex tubes (9.6 mm internal diameter), each 250 mm long, connected by opaque plastic tubing (which was covered during experiments to ensure that only the Pyrex tubes were illuminated). The reflector itself was cut out from lightweight aluminium and polished (Figure 3.2). Four reflector designs were tested, each reactor having a different reflector profile: compound parabolic (CPC), parabolic, V-groove and flat plate (Figure 3.1). The CPC had been used in other solar applications, however as none have been reported as being used in SORAS, all four were tested upon to examine their performance. In the V-groove (45° angle) the centre of the tube was placed 14mm above the base, and in the flat plate, the centre of the tube was positioned 10 mm above the base. The half acceptance angle of the compound parabolic reflector was 90^0 and the concentration ratio was approximately 1. The closed loop reactors were connected in series to a submersible pump (2.8 L/min, giving a fluid velocity of 0.64 m/s) pumping from a 1 L reservoir which was located in the dark. The Reynolds number for the flow rate was calculated to be 5450 meaning that the flow regime was in the smooth

turbulent zone. The water undergoing treatment was continuously recirculated throughout the experiment.

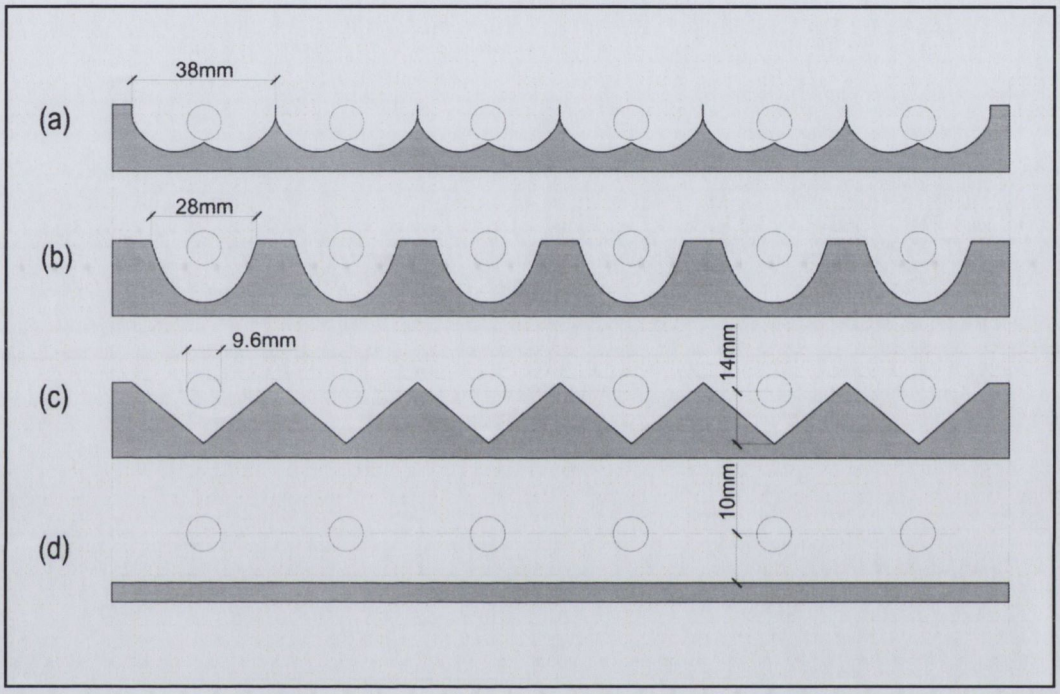

Figure 3.1 *Cross-section through reactors: (a) compound parabolic; (b) parabolic; (c) V-groove and (d) flat plate*

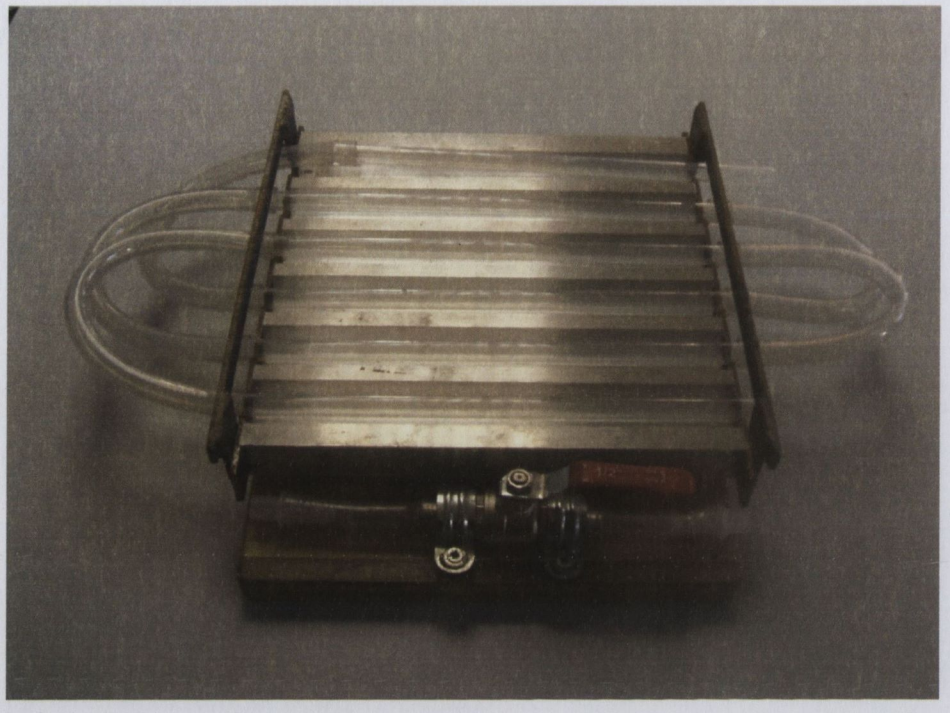

Figure 3.2 *Laboratory scale CPC*

3.1.5.2 Full-scale CPC

As will be discussed in Chapter 4, the CPC reactor was found to be the most efficient design in laboratory scale experiments, therefore the same design was used in the large scale testing. The full-scale CPC (Figure 3.3), obtained from AO SOL (Portugal), consisted of ten parallel glass tubes (47 mm internal diameter), each 1504 mm long, connected by opaque plastic joints, which were 549 mm (left-hand side of CPC) and 389 mm long (right-hand side). The half acceptance angle of the aluminium reflector was 90^0 and the concentration ratio was 1 (see Figure 3.4). The reactor was gravity fed and was connected to two reservoirs, one above the top tube and one on the ground. A peristaltic pump (Watson Marlow, USA) was used to transfer water from the lower reservoir to the upper. The flow rate through the reactor was

measured at 9-11 l/min. The characteristics of the two CPCs used are summarized in Table 3.2.

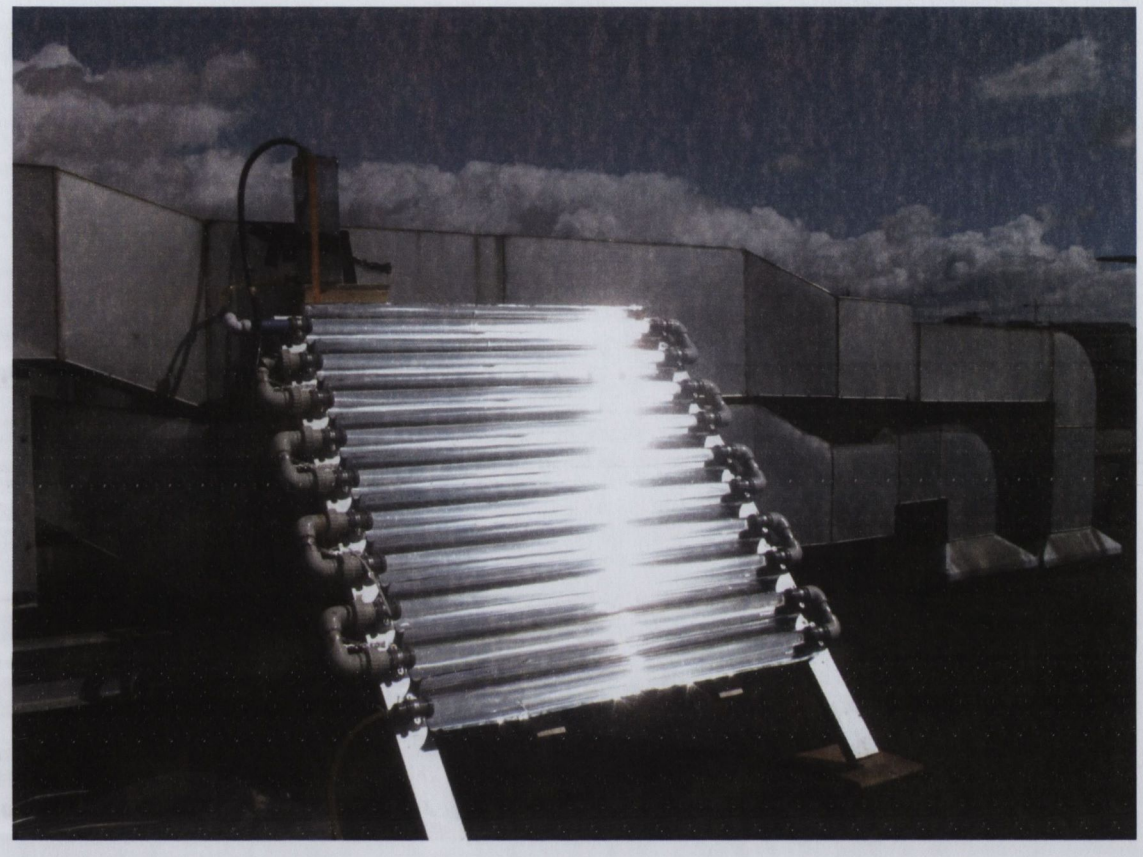

Figure 3.3 *Full scale CPC*

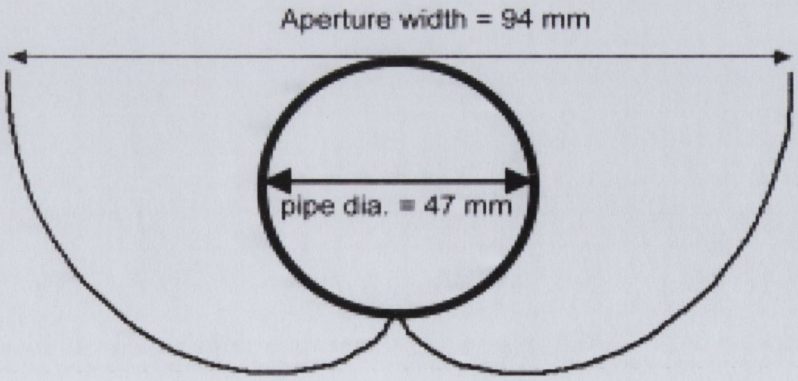

Figure 3.4 *Cross section through large scale CPC*

	Bench-scale	Full-scale
Profile	Compound parabolic	Compound parabolic
Half acceptance angle	90 °	90 °
Concentration ratio	~ 1	~ 1
Number of tubes	6	10
Tube length (mm)	250	1504
Internal diameter of tube (mm)	9.6	46
Total irradiated area (m^2)	0.057	2.31
Total circulating volume (L)	1	40
Total irradiated volume (L)	0.108	22.5
Reynolds number of flow	5450	4480

Table 3.2 *Reactor characteristics*

3.1.6 UV Lamp

The lamp used in small scale experiments was a 75 W Philips HB175 facial solarium, consisting of four parallel UVA tubes (Figure 3.5). It was mounted 30 cm above the CPC, giving an intensity of 15 W/m^2 UV-A at all parts of the collector (as measured by the UV

radiometer during experiments). Emission spectrum data were obtained from the manufacturer and are displayed in Figure 3.5.

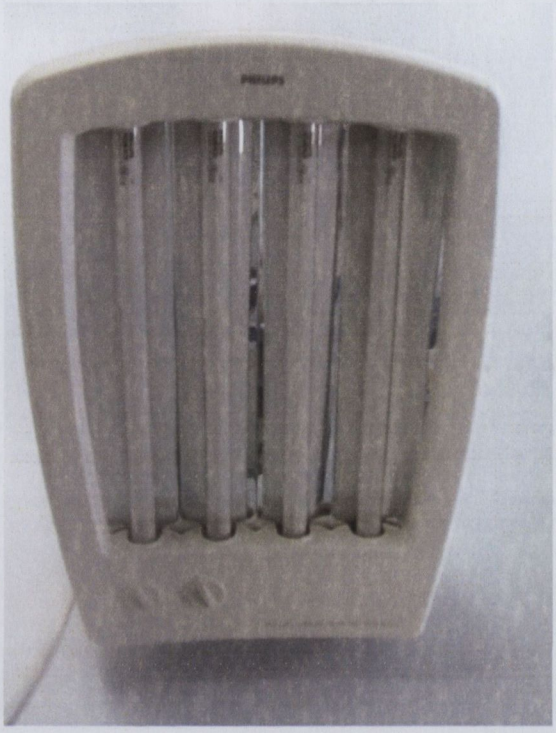

Figure 3.5 *Small scale UV lamp*

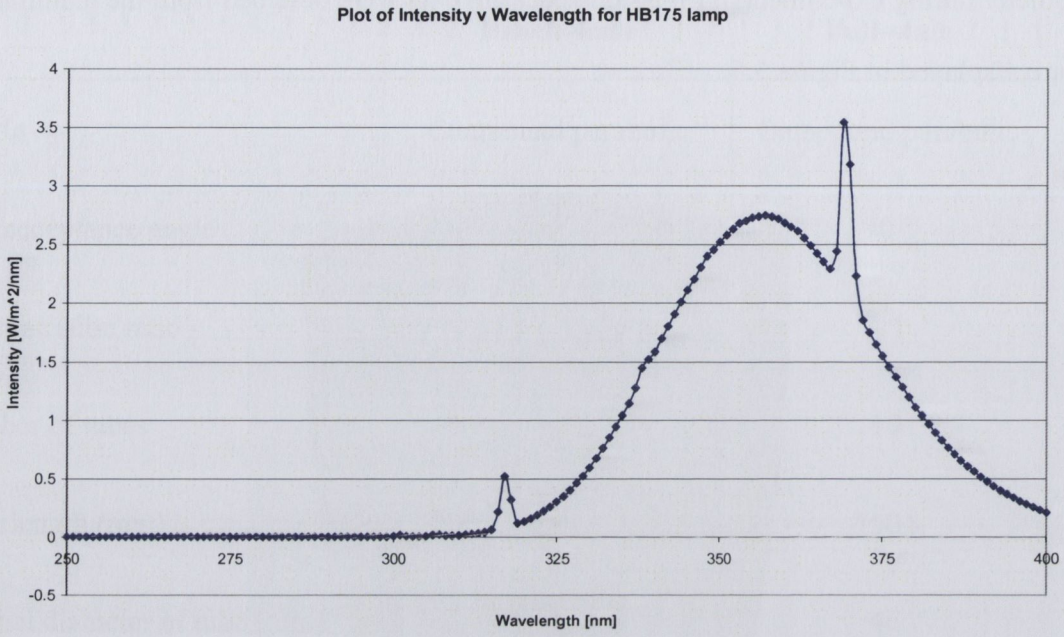

Figure 3.6 *Emission spectrum of lamp, plotted with information obtained from Philips.*

3.1.7 UV Radiometer

Light intensity levels were measured using a PMA2100 radiometer (Solarlight, USA), with UVA and UVB sensors (Figure 3.7). The radiometer could be set to record the UVA and UVB intensity in W/m^2 at varying time intervals. The radiometer was calibrated once yearly by the manufacturers.

Figure 3.7 *Solar radiometer*

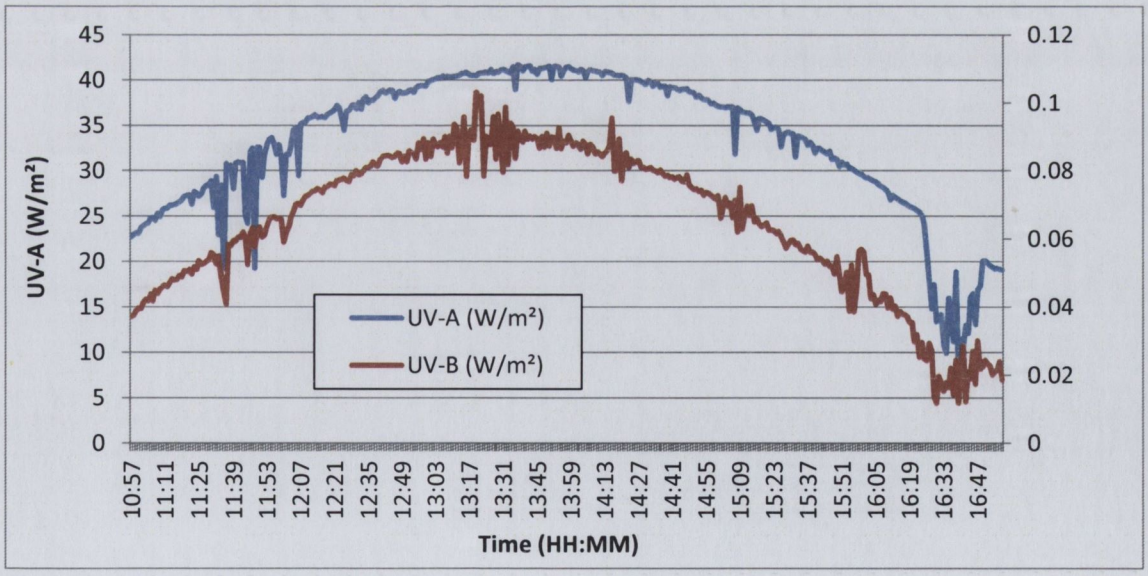

Figure 3.8 *Example output from PMA2100 giving UV data for summer day*

3.1.8 Direct and diffuse solar radiation

For the full-scale experiments outside, direct and diffuse radiation were also monitored by two Kipp and Zonen CMP6 pyranometers (one with a shadow ring) next to the reactor. The meters were aligned level to the ground and the shadow ring adjusted once every week to ensure the pyranometer was always in shade throughout the day. Data was logged at 3 second intervals onto a SQ2010 Data Logger (Omni Instruments, UK).

Figure 3.9 *Example of pyranometers (shadow ring on left) used in measuring global radiation*

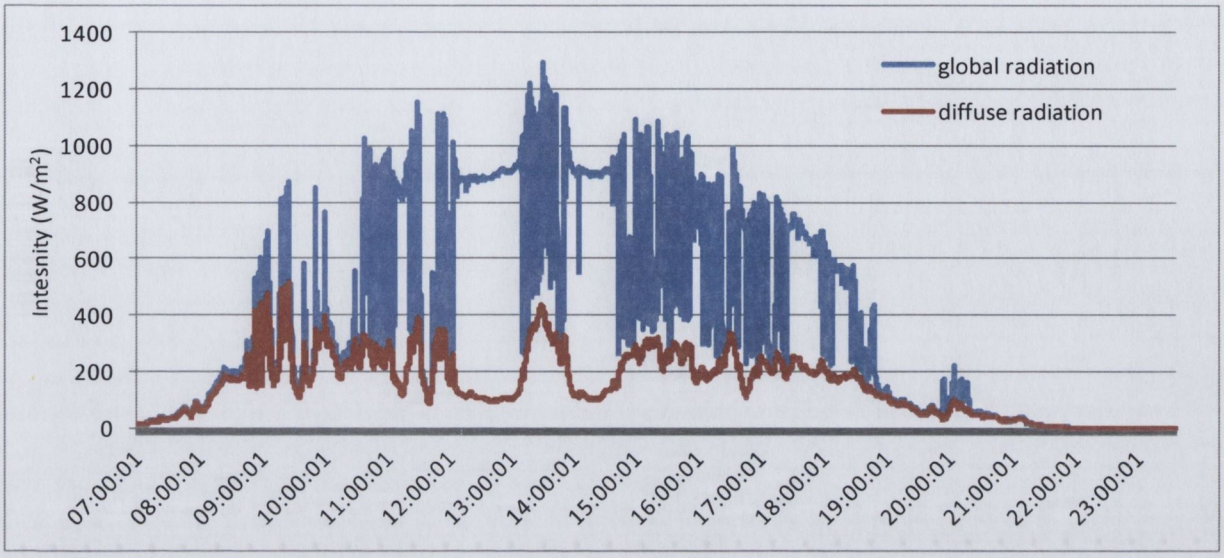

Figure 3.10 *Example output from pyranometers giving global radiation data for summer day*

3.2 Methods

3.2.1 Batch studies

For initial batch studies, a total of 700 ml of sample was poured into a 1 litre Duran bottle. This was prepared by pipetting As stock solution to give 150 µg/l, and different amounts of the iron solution to give 3.5, 5.25, 7 and 14 mg/l. This was then topped up to 700 ml with tap water, and approximately 200 µl (≈ 6 drops) of lemon juice were added. The bottle was closed securely and shaken for 60 seconds. Each test was carried out using two identical samples, being placed a blacked-out box with reflective base. This ensured all of the light was

concentrated solely on the bottles. The halogen lamp (as mentioned above) was placed on top of the box.

The sample bottles were placed in the centre of the box, parallel to the bulbs. The bottles were left under the light for up to 4 hours, with the lamp completely covering the top of the box, and then they were allowed to stand upright for at least 48 hours in the dark for any precipitate to settle to the bottom. The clear water was then decanted into a 30 ml universal container and acidified with 1% nitric acid and refrigerated to be used in the analysis. This procedure was carried out twice for each iron concentration. Sets of samples were also tested without citric acid addition, at the optimum found iron dosage to examine its effect on the process.

3.2.2 Small scale continuous flow experiments

3.2.2.1 Reflector profile experiments

Samples were prepared as in the batch tests, this time each sample being 1 litre total and initial As concentration of 500 µg/l, Fe of 5, 10, 15 and 20 mg/l and 200 µl/l lemon juice. Each reactor type was placed in the blacked-out box, covered with the UV lamp and connected to the pump and 1 litre reservoir (Figure 3.8). As the illuminated tube volume was 200ml, the sample was recirculated for a total of 20 hours, giving the equivalent 4 hour actual irradiation time. Each test was carried out in triplicate. At the beginning of each experiment, the pump circulated the sample for 1 minute to ensure it was fully mixed before subjecting it to the UV light. As in batch tests, they were again allowed to stand for at least 48 hours in the dark for

any precipitate to settle out, and the clear treated sample was decanted and acidified and stored in a refrigerator for up to 4 weeks awaiting analysis.

In between experiments, the tubing was cleaned by circulating a 5% nitric acid solution through the reactor for several minutes, followed by circulating at least 4 flushes distilled water.

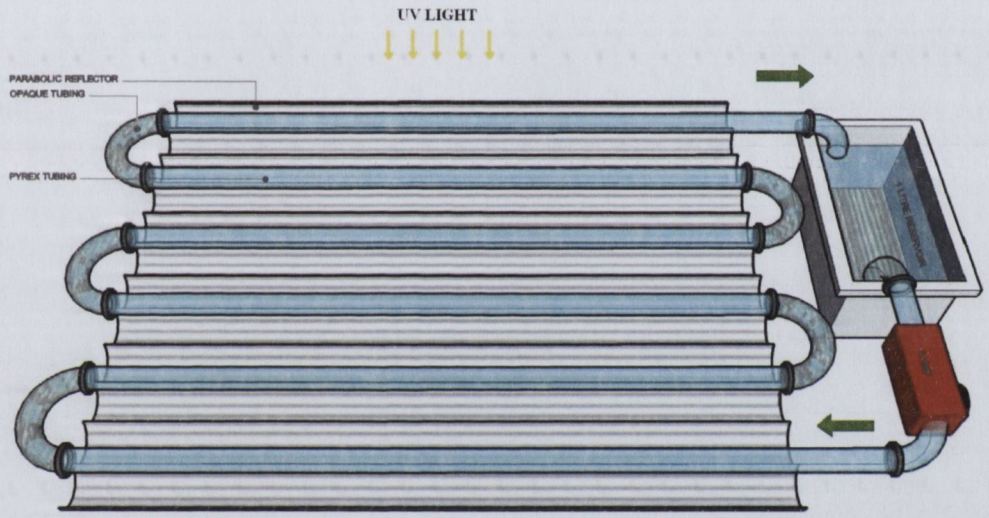

Figure 3.11 *Schematic of reactor set-up*

3.2.2.2 Effects of varying initial As and Fe concentrations on the SORAS process

As the CPC reflector was found to be the most effective design (see results in Chapter 4), it was used in a series of continuous flow experiments with varying arsenic and iron concentrations. To get the overall reaction kinetics for the process, 3 initial As concentrations

were chosen based on actual values found in naturally contaminated water. 'Low' As was 100 µg/l, and was tested with initial Fe concentrations of 2 – 6 mg/l. 'Medium' As was 500 µg/l, and was tested with initial Fe values of 5 – 10 mg/l. 'High' As was 1000 µg/l, and was tested with initial Fe concentrations of 5 – 15 mg/l. Samples were prepared and tests carried out as in the reflector profile experiments, using the aforementioned initial As and Fe concentrations, and 200 µl/l lemon juice. As the arsenic removal rate kinetics were being investigated in these experiments, irradiation time was looked at in more detail. In each experiment, 30 ml aliquots were taken from the outlet of the reactor after 15, 30, 60, 120 and 240 minutes actual irradiation time, and were immediately replaced with 30 ml of tap water to maintain the same reactor volume (this dilution factor was subsequently taken into account after sample analysis). These 30 ml samples were allowed to settle as before, decanted, acidified and refrigerated until analysis.

3.2.2.3 Effect of citric acid addition on the SORAS process

Garcia *et al* (2004) found in batch tests that citrate at higher concentrations had a negative effect on the removal efficiency, and concluded that it was most likely due to interference in the formation of the solid. Therefore, to examine the effect of citric acid addition on the process, varying amounts were added to experiments, conducted as before, at the optimal found iron dosages. 0, 200, 500 and 1000 µl/l lemon juice were added (0-400 µM), and tested as in the previous continuous flow experiments. The same experiments were then repeated using sodium citrate solution (again final solutions of 0-400 µM).

3.2.2.4 Effects of pH, DO, temperature, phosphates, silicates on the SORAS process

As inlet water quality will undoubtedly vary in different locations due to the nature of the bedrock and sediments contained in the groundwater source, experiments to examine the effect of other water parameters on efficiency were conducted. These were all carried out in the small scale CPC reactor at the optimal iron concentration. A range of values (as reported in the literature for ground and surface waters in affected regions) for pH, DO, temperature, phosphates and silicates were investigated. For the pH experiments, small amounts of hydrochloric acid or sodium hydroxide were added at the beginning to alter the initial pH (between 4 and 10), and the pH recorded using a pH meter (pH 330, WTW, Germany) at each sample time. It was calibrated periodically using a three point calibration against standard pH 4, 7 and 10 solutions. For the DO experiments, different amounts of sodium sulphite (see Section 3.1.1.6) were used to decrease the initial DO, or a triple-stone aeration diffuser was used to increase the DO. The tests were carried out at different DO concentrations, being measured using a DO probe (Cyberscan DO5000, Eutech) throughout the run. The temperature experiments were conducted by placing the 1 litre reservoir in a water bath, the temperature being measured with a thermometer at regular intervals. Phosphate and silicate (see Sections 3.1.1.4 and 3.1.1.5) were also added separately in different concentrations, as these have been reported to affect efficiency (Mukherjee *et al.* (2007), Hug *et al.* (2001)).

3.2.3 Large Scale experiments

3.2.3.1 Outdoor testing

During summer months, experiments were performed in the full-scale CPC reactor under natural sunlight. The CPC reactor, as described in Section 3.1.4.2, was tilted due south at 53°21' to the horizontal (as shown in Figure 3.3), which corresponds to the angle of latitude of the location at which the experiments were undertaken (i.e. Dublin, Ireland). The water was allowed to flow by gravity from a covered elevated reservoir through the CPC reactor to a second covered reservoir situated at ground level. The water was pumped back to the higher reservoir using a peristaltic pump (Watson Marlow 624S, USA) and the pump flow rate was adjusted to ensure a constant head was achieved. The UV-A and UV-B detectors were attached to the frame of the reactor, which meant they were also inclined at an angle corresponding to the angle of latitude. The large scale reactor was rinsed between experiments as in the small scale tests, and the reactor was covered at the beginning of each experiment for 5 minutes to ensure the sample was fully mixed before subjecting it to sunlight, as proved using a Rhodamine WT tracer study in earlier research (Misstear, 2010).

Samples were made up as in the small scale experiments, this time having a total volume of 40 litres. Arsenic and Fe stock solutions were used to give initial concentrations of 100-1000 µg/l and 3-15 mg/l respectively. Experiments ran during daylight hours from 9.30am for up to 8 hours in total, with 30 ml aliquots being taken at regular intervals as in small scale tests. These were allowed to settle as before, decanted, acidified and refrigerated. The radiometer recorded UV intensities at 10 minute intervals throughout the test, and two thermocouples were

installed, one in the outlet tube from the reactor and one in the upper reservoir, to record the water temperature into and out of the reactor at 1 minute intervals during the experiment.

For the microbiological tests, the reactor was first disinfected by pumping 0.1 M ethanol around it for 20 minutes. This was then followed by rinsing with four flushes of sterile water to ensure that no ethanol would remain in the system and lead to unwanted bacteria kill-off during the experimental periods. This rinsing procedure was proven to remove all traces of ethanol in a previous study on the same system (McLoughlin, 2005). Distilled water was required for these experiments as any levels of chlorine from tap water could distort bacterial degradation results due to some disinfection occurring during the tests. The reactor was covered while *E. coli* (as prepared in 3.1.1) was spiked into the lower reservoir. After five minutes, when complete mixing of the microorganism had occurred, the first sample was taken. 1 mL samples were then taken using a sterile transfer pipette at the following times: 15, 30, 45, 60, 90, 120, 180, 240, 300 and 360 minutes.

3.2.4 Analysis

3.2.4.1 Arsenic analysis

Arsenic analysis was carried out in the Environmental Engineering Laboratory of Trinity College Dublin on a Varian Liberty AX Series II ICP-AES with hydride generation (Varian VGA). 10 ml of sample/standard was pipetted to a 50 ml universal container and 12.5 ml hydrochloric acid was added. 0.5 ml of 10.0% w/v potassium iodide was then added and allowed to stand for 1 hour to reduce all As to As(III) oxidation state. This was then made up

to 50 ml with distilled water. For the hydride generation, the acid was 50% hydrochloric acid (diluted with distilled water in a 500 ml container), and the reductant was made up of 2.5 g of sodium hydroxide dissolved in 500 ml distilled water, then 3 g of sodium borohydride was dissolved in this solution. A certified reference standard solution (AccuTrace 1002 µg/ml) was supplied by Accustandard (Connecticut, USA). Calibration was carried out with a maximum percentage error of 10%. Samples were also chosen at random to be sent for analysis to a fully accredited laboratory by City Analysts Ltd., Dublin, as a quality control measure. The samples showed a maximum difference of ±8.5% (average 6.4%) between these results and the ICP results from the present study.

3.2.4.2 Iron analysis

Iron concentrations were also analysed on the abovementioned ICP-AES. In the case of iron, no hydride generation was required, and so liquid sample was acidified with 10% nitric acid and tested. Again, the analysis used a certified reference standard solution by Accustandard.

3.2.4.3 Microbiological propagation and enumeration

In order to propagate the bacteria, a single colony of *E. coli* was transferred from a streaked plate to 50 ml of Luria broth (Sigma-Aldrich). This was incubated for 18 hours at 37 °C and then centrifuged at 3,000 rpm for 12 minutes. The broth was poured off and replaced with 50 mL of sterile water and the sample was centrifuged again. This water was poured off and again replaced with 50 mL of sterile water and centrifuged. When this water was poured off, a

pellet of *E. coli* was left at the bottom of the vial. 5 mL of sterile water was added to this to give an *E. coli* concentration of approximately 1 x 10^9 CFU/mL.

Serial dilutions of the experimental samples were made by adding 100 µL of sample to 900 µL of sterile water. The number of viable cells in the water samples was determined by plating 20 µL (or 200 µL if a low count was expected) of an appropriate dilution on Luria Agar (Sigma-Aldrich, St. Louis, MO) and counting colonies after incubation at 37°C for 18 hours, using the spread plate method. Quality control and assurance guidelines described in the Standard Methods (APHA, 1999) were strictly followed, while all samples were plated in duplicate. The method detectable limit (MDL) was 50 CFU/mL, as the minimum cell count for statistical methods was 10.

In order to calculate the concentration of *E. coli* at time t (N_t) in CFU/mL (colony forming units/ml), the following equation was used:

$$N_t = (\text{number of colonies on plate}) \times (\text{dilution factor}) \times 50 \qquad \text{(Eq. 3.1)}$$

If 200 µL of sample had been plated without dilution, the concentration was obtained by:

$$N_t = (\text{number of colonies on plate}) \times 5 \qquad \text{(Eq. 3.2)}$$

For a sample taken at time t, the phage concentration (N_t) was divided by the initial concentration (N_0) and the log of this value was plotted against cumulative UV dose (see Chapter 4).

CHAPTER 4: SORAS RESULTS

4.1 Introduction

This chapter details the results of the SORAS experiments carried out as described in Chapter 3. Initially batch tests were carried out in order to obtain an indication of the optimum iron dosage for use in the extensive experiments using the continuous flow reactor. These results also provided an interesting comparison to similar experiments carried out by previous authors (Hug *et al.*, 2001, Garcia *et al.,* 2004, Lara *et al.,* 2006 and Mukherjee *et al.*, 2007). Then laboratory and full scale continuous flow tests were completed for a range of different parameters, in order to understand the process kinetics of the different variables from which a an optimum design can be derived for a full-scale SORAS treatment system at village level.

4.2 Batch scale tests

4.2.1 SORAS batch studies

Batch tests, as described in Section 3.2, were carried out using tap water spiked with arsenic in 1 litre glass bottles. The bottles were placed in a blacked-out box, the top of which was completely covered by a Phillips fluorescent lamp. The lamp gives majority UVA (315-400nm), with 355-385nm being optimal for photon absorption by iron (Hug, *et al.,* 2001). Figure 4.1 shows final arsenic concentration against iron dosage for the average of 3 repeat tests using initial arsenic of 150 µg/l and 4 hours irradiation time at 15 W/m^2 UVA. All tests included 200 µl/l lemon juice. The results show that the optimum iron concentration was 7 mg/l, which reduced the As concentration to below the WHO MCL of 10 µg/l. No further decrease was seen when the iron dosage was increased, as the plot

levels off and remains reasonably steady despite the additional iron. Removal at the highest iron dose of 14 mg/l decreases slightly, however this may be due to higher turbidity at this concentration affecting light transmission into the bottle. Arsenic removal against irradiation time experiments were then carried out to in order to investigate the rate of As degradation. These results showed (Figure 4.2) that at the optimal iron dosage of 7 mg/l, removal to below 10 µg/l could be obtained after just 3 hours illumination. This optimum iron dosage is significantly higher than that found by most previous authors, but is difficult to compare to these studies for a number of reasons outlined below.

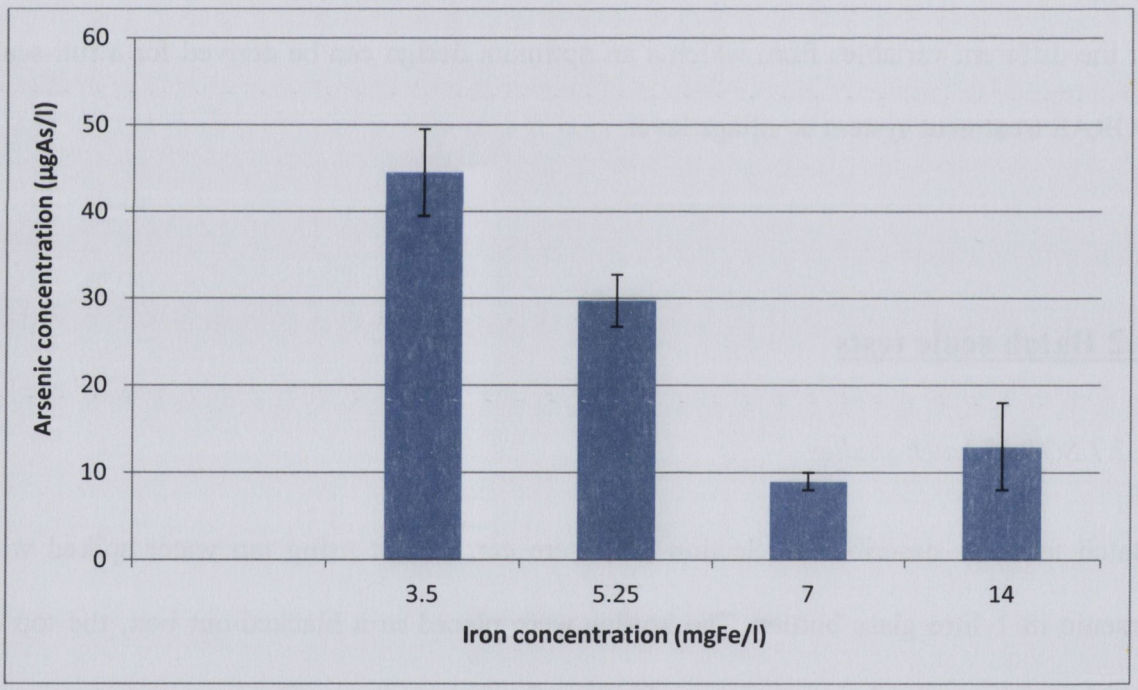

Figure 4.1 *Plot of As remaining against initial iron dosage after 4 hours irradiation at 15 W/m^2 UVA*

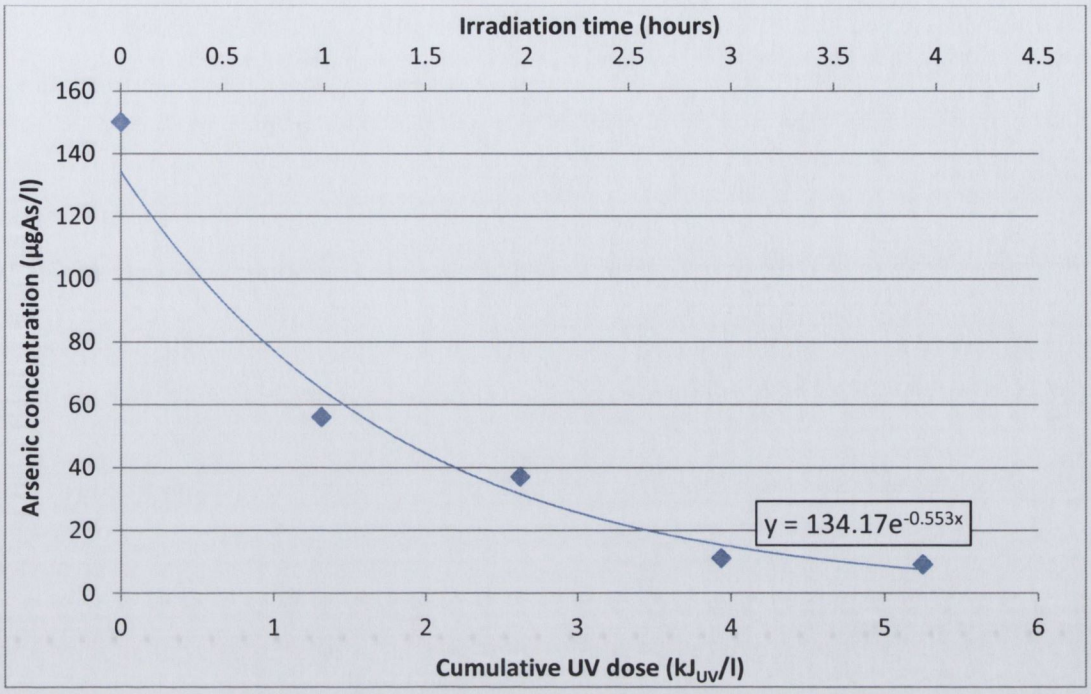

Figure 4.2 Plot of *As removal against cumulative UV dose and irradiation time (initial As: 150 µg/l, Fe: 7 mg/l, lemon juice 200 µl/l)*

The initial arsenic and iron concentrations used by other researchers has varied greatly, as has the form of iron used. As stated previously, this study used 150 µg/l As initially with varying Fe(III) in the form of ferric chloride, and aimed to obtain final arsenic concentrations of below the WHO MCL of 10 µg/l, whereas other studies, detailed below, have had the aim of removing As down to below the Bangladeshi standard of 50 µg/l. Khoe and Emett (2001) used Fe(III) and Fe(II) to remove 150 mg/l As (a far greater amount of arsenic than attempted in this or other related research), and found Fe(III) to be more efficient, with twice the amount of iron needed per mole of initial arsenic. But as stated in Section 3.4, at the low pH of mine tailings, As oxidation mechanisms differ. Garcia *et al.* (2004) used Fe(III), ($Fe(NO_3)_3$), in natural and synthetic samples to remove As from 297 µg/l to 22 µg/l, needing 3 mg/l Fe and up to 6 hours irradiation time. Lara *et al.* (2006) removed As to below 10 µg/l from 500 µg/l initially with 7 mg/l Fe(II) in the form of ferrous sulphate and 4 hours irradiation time. The optimum iron dose found by

Mukherjee *et al.* (2007) was 5.26-6.12 mg/l (total iron, ferrous sulphate added when necessary) for the removal to below 10 µg/l from 200-300 µg/l initially after 4 hours irradiation time.

The lamps used for irradiation also delivered different UV intensities, or experiments were conducted in natural light. In all but one of these articles, the irradiated area was not reported, (hence a rigorous comparison of cumulative UV dose between experiments, which would be vital in this type of study, was not possible). However, one study, Hug *et al.* (2001) did give the details of irradiance, using a lamp giving 90 W/m^2 over a 48 cm^2 area compared to the lamp used in this study giving 15 W/m^2 over 170 cm^2. Fe(II) (in the form of ferrous sulphate) was used for the initial iron concentration in laboratory studies and naturally present iron from groundwater in Bangladesh in field trials. It was found that 5mg/l Fe(III) would be required to remove As from 500 µg/l initially to 50 µg/l after 5 hours irradiation time. Hence, the lower required Fe dose to remove over 3 times the amount of initial As compared to the results in this research, could be due to the increased UV dose (over twice as high). In general Fe(II) outperformed Fe(III), however Roberts *et al.*, (2004) reported longer settling times were needed for suspensions obtained using Fe(II) after a passive co-precipitation process in the dark. This would also have significant implications for design of a full scale system.

Differences between the spiked tap water used in this study and the water used in the other research could also be a factor in the variation in results. Table 3.1 (Section 3.1) gives the tap water composition used, and the following details the most likely causes of variation. (Note: as natural groundwater samples typically have larger ranges of component concentrations, only the synthetic waters used (when reported) have been investigated for comparative purposes (Hug *et al.*, 2001; Garcia *et al.,* 2004; Mukherjee *et al.*, 2007)). Calcium, which is usually naturally present in high amounts in groundwater, was on

average, 3 times higher in these others studies. Magnesium concentrations were comparable, but alkalinity was also significantly lower in Dublin tap water. As lime can also be used as a coagulant for arsenic (Section 2.3.4), there is a possibility of the higher natural alkalinity concentrations found in the other studies were significant in that the calcium could agglomerate into the precipitate and promoting sedimentation, hence promoting higher arsenic removal efficiencies than were obtained in this study. Chlorides were also higher in these previous studies, which could benefit arsenic adsorption onto iron as reported by Zhang et al. (2004). All other reported values were comparable.

To examine the effect of citrate addition, a number of experiments were performed using 200 µl/l citrate in the form of lemon juice as had been used previously, and were compared to samples tested without the addition of citrate. Figure 4.3 shows the final As concentrations after 4 hours irradiation time of samples containing 150 µg/l arsenic and 7 mg/l iron initially. It is very evident that the citrate has a major effect on As removal, with over 93.3% being removed, compared to only 63.3% when no citrate was included in the initial sample solution. As discussed in Section 2.4.3, previous studies also showed the positive effects of citrate on the removal process (Hug *et al.*, 2001; Garcia *et al.,* 2004; Lara *et al.,* 2006; Mukherjee *et al.*, 2007).

As described previously, samples were allowed to stand in the dark overnight for sedimentation of the As-Fe precipitate to occur, and the supernatant was then analysed for total arsenic concentration. Figure 4.4 shows an example of a sample solution before irradiation and post UV treatment and settlement. As this settlement is slow due to the size of the particles, the possible enhancement of the process was investigated and is discussed in Chapter 5.

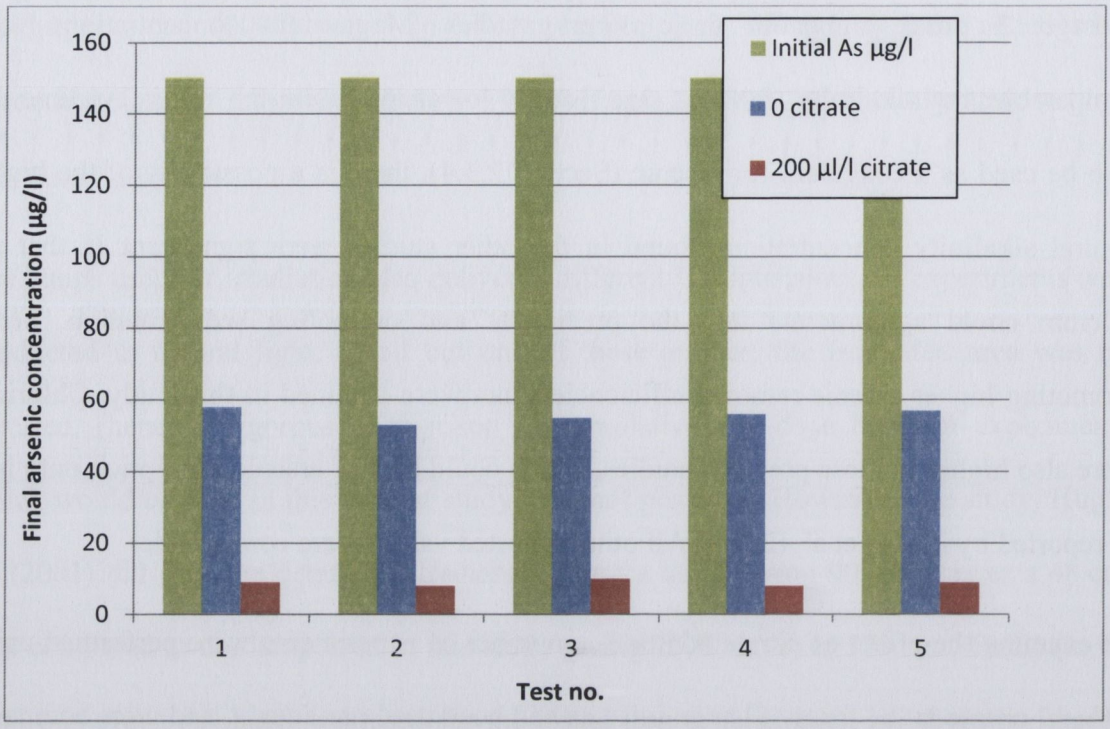

Figure 4.3 *Final As concentrations with and without citrate addition*

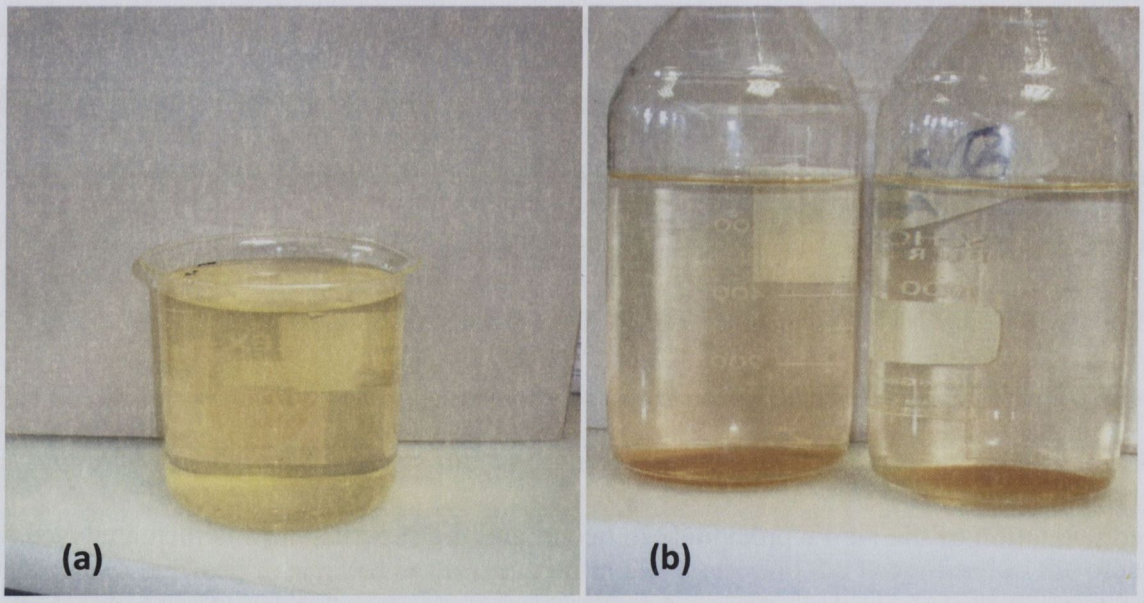

Figure 4.4 *Sample solution* ***(a)*** *before irradiation and* ***(b)*** *after irradiation and settlement*

4.2.1 SORAS batch studies using TiO_2

As discussed in Section 2.4.5, photocatalysts are used in many water/wastewater treatments as advanced oxidation processes (AOPs) to remove contaminants. In this set of

batch scale tests, suspensions of titanium dioxide (TiO_2) of between 1 and 20 mg/l were added to arsenic spiked tap water, and tested at a range of iron dosages. These were carried out with the same procedure as the initial SORAS batch tests, and as TiO_2 also requires UVA fraction of light, the same lamp was used. Figure 4.5 shows the percentage arsenic removal for each TiO_2 and iron concentration for initial arsenic concentration of 500 µg/l after 4 hours irradiation time (at 15 W/m^2). The optimum dosages found were 9 and 10 mg/l Fe and TiO_2 respectively. As a more effective removal rate was expected, a higher initial As concentration was used, however this makes it difficult to compare to the batch studies conducted without TiO_2. Generally greater removal was seen with increased iron and photocatalyst dose, however a slight decrease in removal occurred at the 10 mg/l iron and 10 and 20 mg/l titanium dioxide doses. This is most likely due to the higher turbidity of the sample from the combination of these 2 additives. Misstear *et al.* (2010) observed a similar phenomenon in photocatalytic disinfection experiments, which was attributed to particle shading by the TiO_2 at higher concentrations. Arsenic removal profile experiments were then carried out at the optimum iron dosage to obtain the removal kinetic, with the results shown in Figure 4.6. The results indicate that after 3 hours, sufficient irradiation of the sample has occurred to obtain a final concentration below 10 µg/l. Again, as the previous batch tests had a lower initial arsenic concentration, a meaningful comparison is difficult, however for the same irradiation time and a small increase in iron dose, the same final removal was obtained. Further experiments were carried out using 9 and 10 mg/l Fe and TiO_2, this time with 1000 µg/l initial arsenic. The removal against time plot is shown in Figure 4.7. The results indicate a significant decrease in removal efficiency, with less than 80% arsenic removed after 3 hours irradiation time, and needing 9 hours to obtain a final arsenic concentration below the MCL. This would obviously not be practical in a field situation, with a limited time frame available for sufficient natural sunlight for the

process. An increase in iron and/or photocatalyst dose would be needed to achieve more effective removal. These results indicate the potential benefit from using photocatalysts, however the problem of removing TiO_2 after treatment is a definite drawback. As Fostier (2008) conducted SORAS tests using immobilised TiO_2 and showed successful removal, the application of fixed photocatalysts for continuous flow reactors could solve this problem, but requires a lot more research.

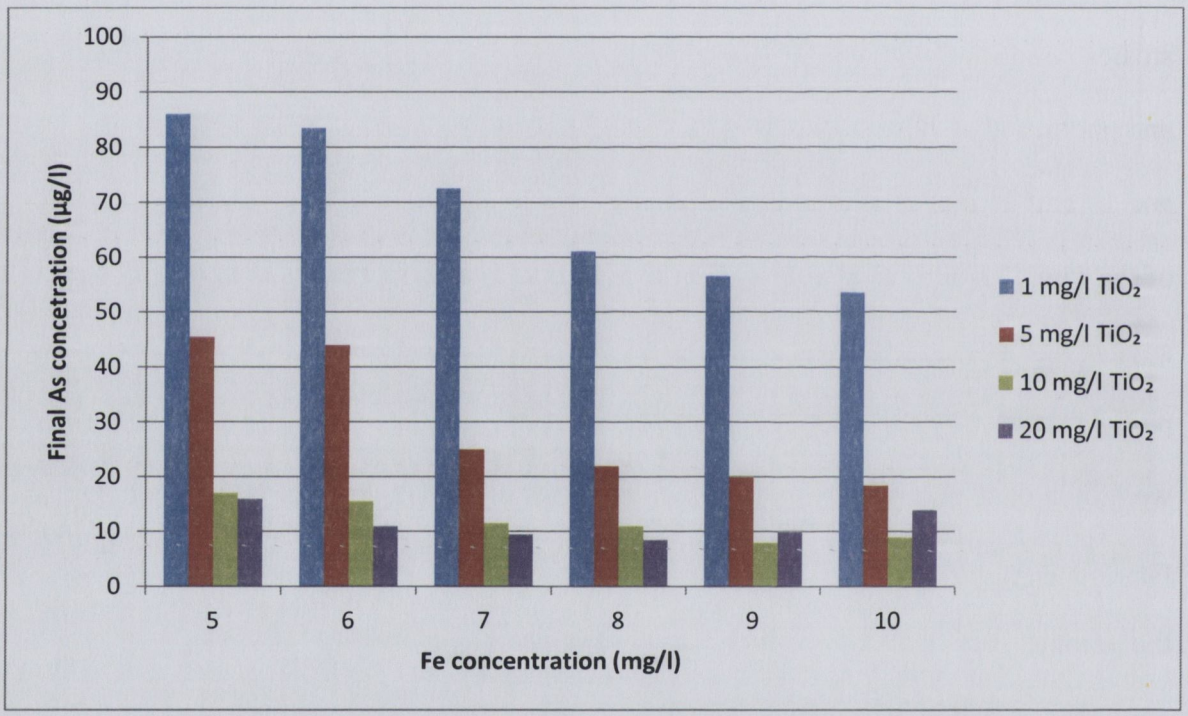

Figure 4.5 *Plot of final As concentration from 500 µg/l against initial iron dosage for each photocatalyst dose after 4 hours irradiation at 15 W/m^2 UVA (5.25kJ$_{UV}$/l cumulative)*

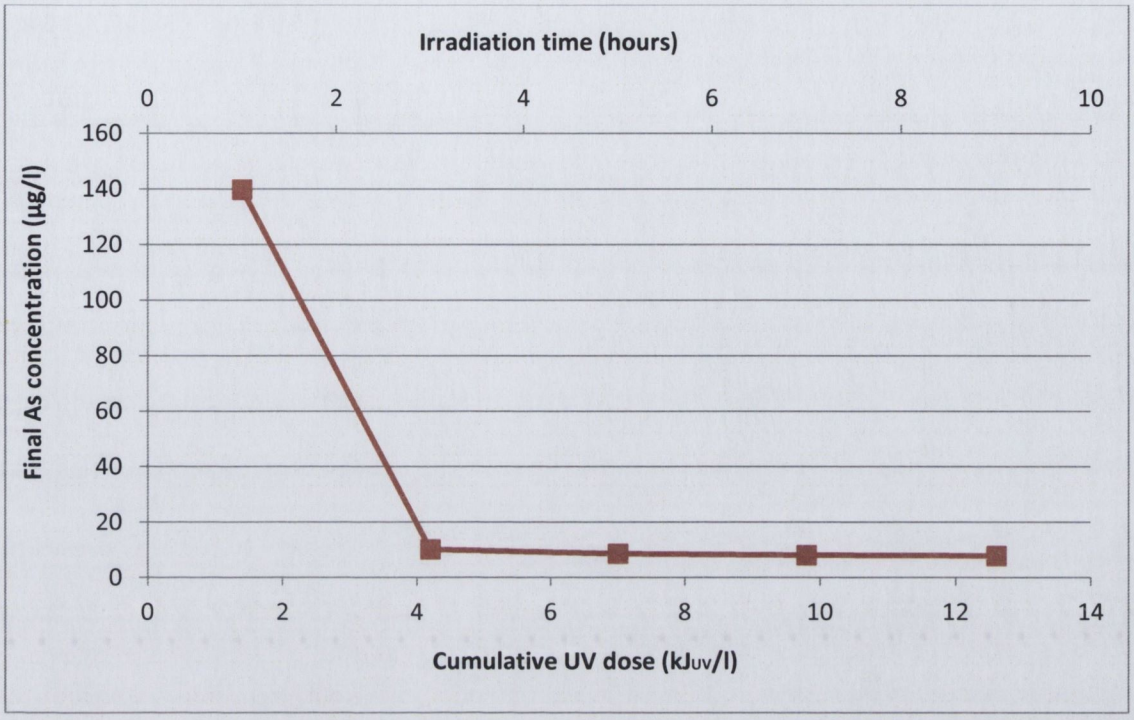

Figure 4.6 Plot of final *As concentration against cumulative UV dose and illumination time (initial As: 500 µg/l, Fe: 9 mg/l, TiO_2: 10 mg/l)*

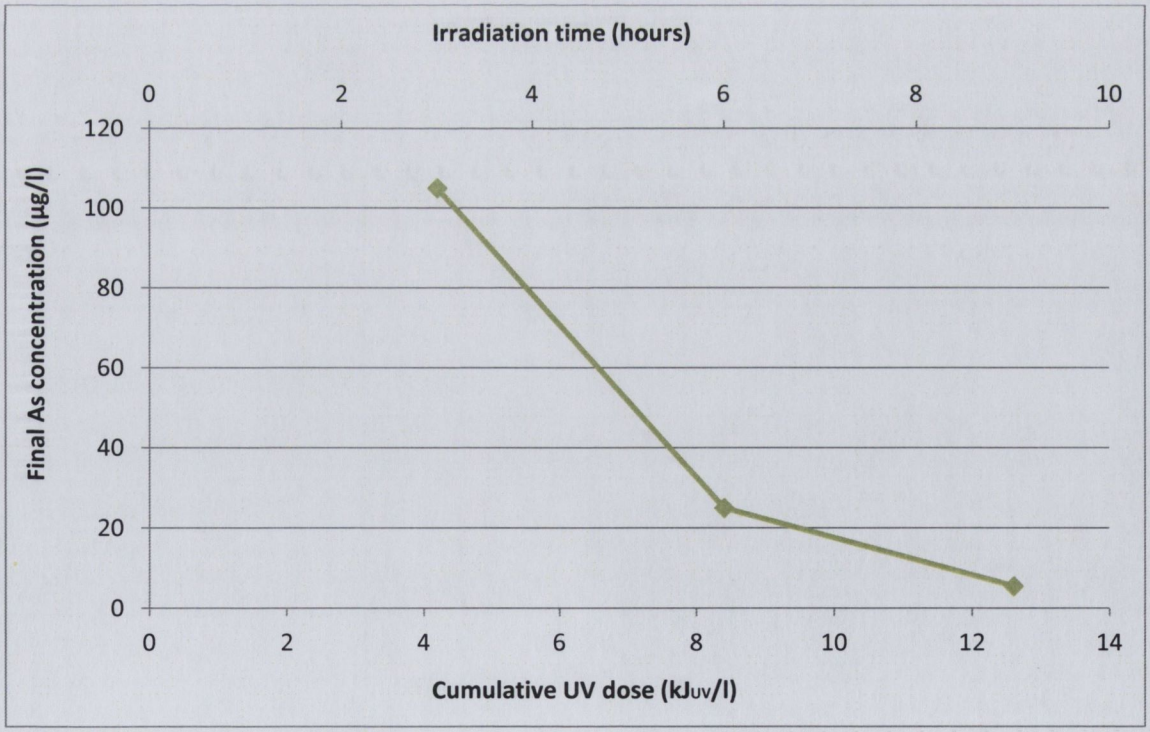

Figure 4.7 Plot of final *As concentration against cumulative UV dose and illumination time (initial As: 1000 µg/l, Fe: 9 mg/l, TiO_2: 10 mg/l)*

No studies appear to have been reported on the effect of citrate on the SORAS process when using photocatalysts. Figure 4.8 shows the results of batch experiments using 5, 7 and 9 mg/l iron, 1 and 10 mg/l TiO_2, and 1000 µg/l initial arsenic, with and without 200 µl/l citrate in the form of lemon juice. Unexpectedly, the lower TiO_2 dose gave better removal at this higher initial arsenic concentration, for which a rational explanation is still being investigated. The results also clearly show the adverse effect of citrate in all cases, indicating that citrate is not essential to this process when using a photocatalyst. It may be the case that the citrate is actually competing for ROS in this set-up, or that it is preventing adsorption of As to Fe. Tzou *et al.* (2005) used TiO_2 and Fe-citrate complexes in the reduction of Cr(IV) to Cr(III), indicating that indeed it promotes reducing condition and the aim in the present study is to promote oxidizing conditions for As(III).

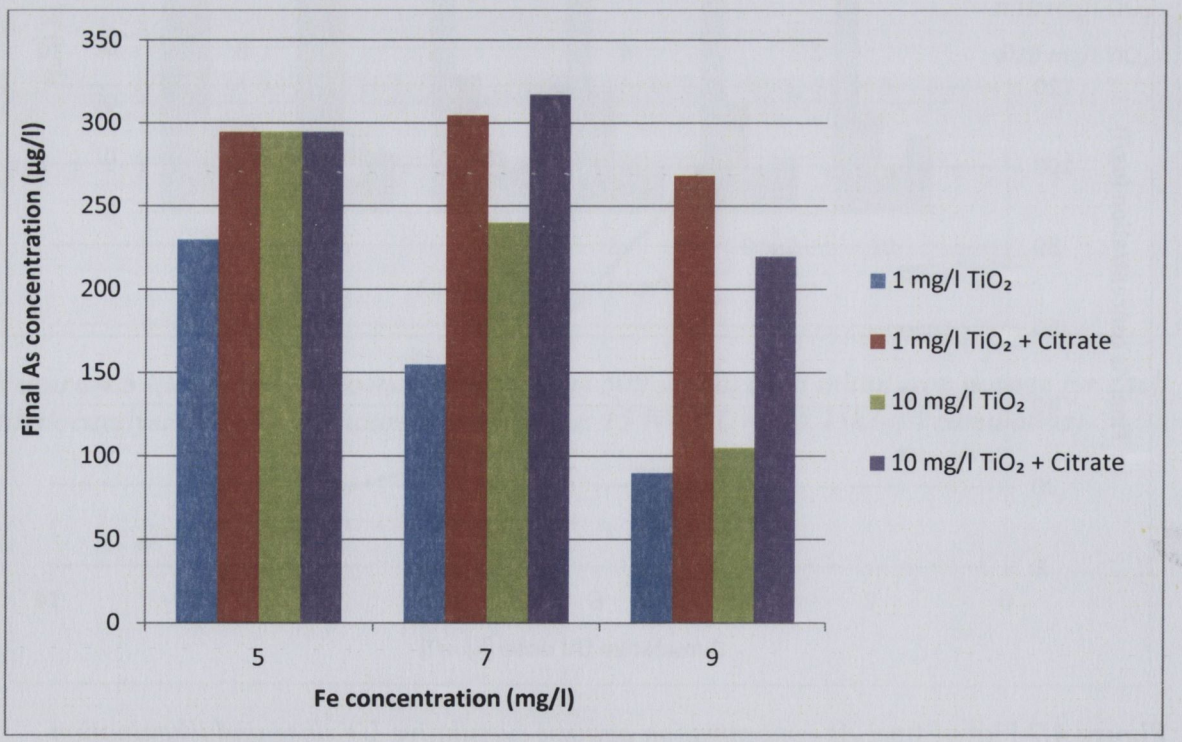

Figure 4.8 *Plot of final As concentration from 1000 µg/l against initial iron dosage for 1 and 10 mg/l TiO_2, with and without citrate after 4 hours irradiation at 15 W/m^2 UVA (5.25kJ$_{UV}$/l cumulative)*

4.3 Continuous flow reactor profile experiments

The continuous flow experiments were carried out as detailed in Section 3.2. The reactors were placed in the blacked out box and subjected to UVA light at 15 W/m^2 as used in the batch tests. Samples spiked with arsenic were re-circulated through the reactor to a 1 litre capacity reservoir kept in the dark. Tests ran for 20 hours, an equivalent of 4 hours actual irradiation time due to the proportion of illuminated volume to total volume (as any particle was in darkness for 80% of the experimental time), samples were collected for settlement and analysis at the end of the experimental run. To investigate the most effective reflector type, four different reflector profiles were tested (compound parabolic (CPC), parabolic, V-notch and flat plate) with an initial arsenic concentration of 500 µg/l, varying iron, and 200 µl/l lemon juice as detailed in Section 3.2.2.1. As seen in Figure 4.9 the CPC reactor showed the greatest efficiency, consistent in removing arsenic to below 10 µg/l in small scale experiments, with the optimum iron dosage of 10 mg/l. The CPC reactor gave a 2.2% increase in overall arsenic removal efficiency at the optimum iron dose on the next best reactor with the parabolic reflector. This may seem only a slight increase, however, this was the only reactor to was to remove As to below the drinking water MCL at reasonable iron concentrations (which is the ultimate aim in this study); for example, the recator with the parabolic reflector needed twice the amount of initial iron to succeed in attaining that goal. It must be noted however, that no iron dosages between 15 and 20 mg/l were tested, and this result would require further testing. These results conform with reflector theory whereby the CPC reactor was expected to give greater light capture (concentration ratio of 1) than the other profiles. They also agree with results reported in a similar study on solar disinfection by McLoughlin *et al.* (2004), with the reactor with CPC reflectors outperforming the reactors with parabolic and V-notch profile reflectors (flat plate not used in this paper). Although the CPC reactor did perform better

than the others tested, the overall arsenic removal was similar, indicating that the main pathway of UV transmission was likely to be directly onto the reactor tubes, rather than being reflected. The one anomaly from these tests was the 20 mg/l iron dose used with the flat plate profile, as the final arsenic concentration actually increased on the 15 mg/l dosage despite several repeats. One hypothesis is that the decrease in removal efficiency is linked to the higher turbidity of the sample due to the increased iron content. The refective capability of the flat plate is lower than the other profiles but only at this dosage was it extremely evident. If the light transmitted to the sample was lowered because of turbidity, the iron could precipitate more readily before the arsenic was fully oxidised and able to adsorb to these Fe(hydr)oxides. Radiation intensity is reduced by increasing turbidity (e.g. 85% reduction at 40 NTU and a 10 cm depth (EAWAG, 1998), thus raw water of low turbidity (< 30 NTU) is reccommended for use in solar disinfection systems (EAWAG, 1998). The mean depth of water for the light to be transmitted through in this case was less than 0.5 cm, but turbidity was estimated at over 20 NTU, hence there is reasonable cause for the hypothesis.

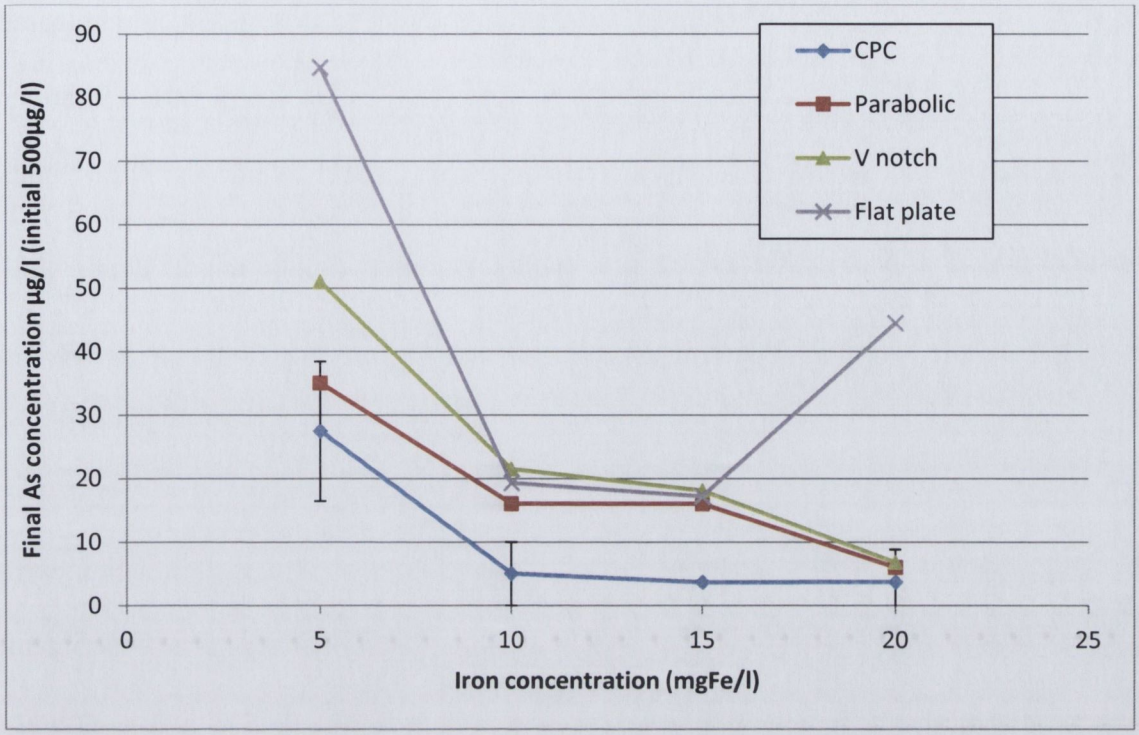

Figure 4.9 *As concentration (initial 500 µg/l) after 4 hours irradiation time in the continuous flow set-up (at 15W/m^2 or 12.3kJ$_{UV}$/l cumulative) against iron dosage for the four reactor profiles (Note: error bars only shown on one plot to avoid confusion)*

4.4 Optimum iron dose experiments

As it was concluded that the CPC reactor was the most efficient in removing arsenic in the SORAS process, it was then used in further a series of continuous flow tests as discussed above (see also Section 3.2.2.2). As the reactor profile tests only gave the final arsenic concentration after 4 hours irradiation, this set of experiments investigated the rate of arsenic removal in relation to irradiation time, using varying initial arsenic and iron concentrations. As discussed previously, arsenic concentrations present in natural groundwater fluctuate greatly, both spatially and seasonally. As the batch testing only concentrated on limited initial values to give a general idea of what would be required for more extensive testing in the reactors, these experiments chose a range of As concentrations that represent actual values (Smedley and Kinniburgh, 2002): 'high' being 1000 µg/l; 'medium' being 500 µg/l; and 'low' being 100 µg/l (it should be noted however,

that considerably higher concentrations (over 3000 µg/l) have been found in contaminated aquifers, and 'low' is still 10 times the WHO MCL). These initial arsenic concentrations were tested with 200 µl/l lemon juice and the range of iron concentrations with results shown in Figure 4.10.

It is seen from the plots that at the upper end of initial As concentrations, the lower iron concentrations (5 and 7 mg/l) removed arsenic much more rapidly (up to 79% improvement on the higher iron levels) during the first half hour irradiation time. However, subsequent enhancement on this value was not achieved despite further illumination, with these plots continuing to be moderately steady throughout the remainder of the experiment, and never reaching the required 10 µg/l level. This may be due to the higher turbidity incurred by increased iron concentrations as discussed above, and as seen in batch tests and in previous literature, the required molar ratio of arsenic to iron must be met for effective removal due to the limited number of adsorption sites on the Fe(hydr)oxides at lower concentrations.

The gradient of the removal curves, i.e. the rate of oxidation and co-precipitation of arsenic, decreases with decreasing initial arsenic concentrations. This indicates similarity with many other removal processes, such as degradation of pathogens, whereby it becomes more difficult to eliminate undesirable contaminants at lower levels. This is most likely due to the ROS being scavenged by other compounds present in the water as their proportion becomes greater when the arsenic concentration is decreased. Hence, the chances of As(III) oxidation and co-precipitation of As(V) with Fe become less and less. Consequently, the required iron dose at decreasing arsenic concentrations becomes proportionally higher.

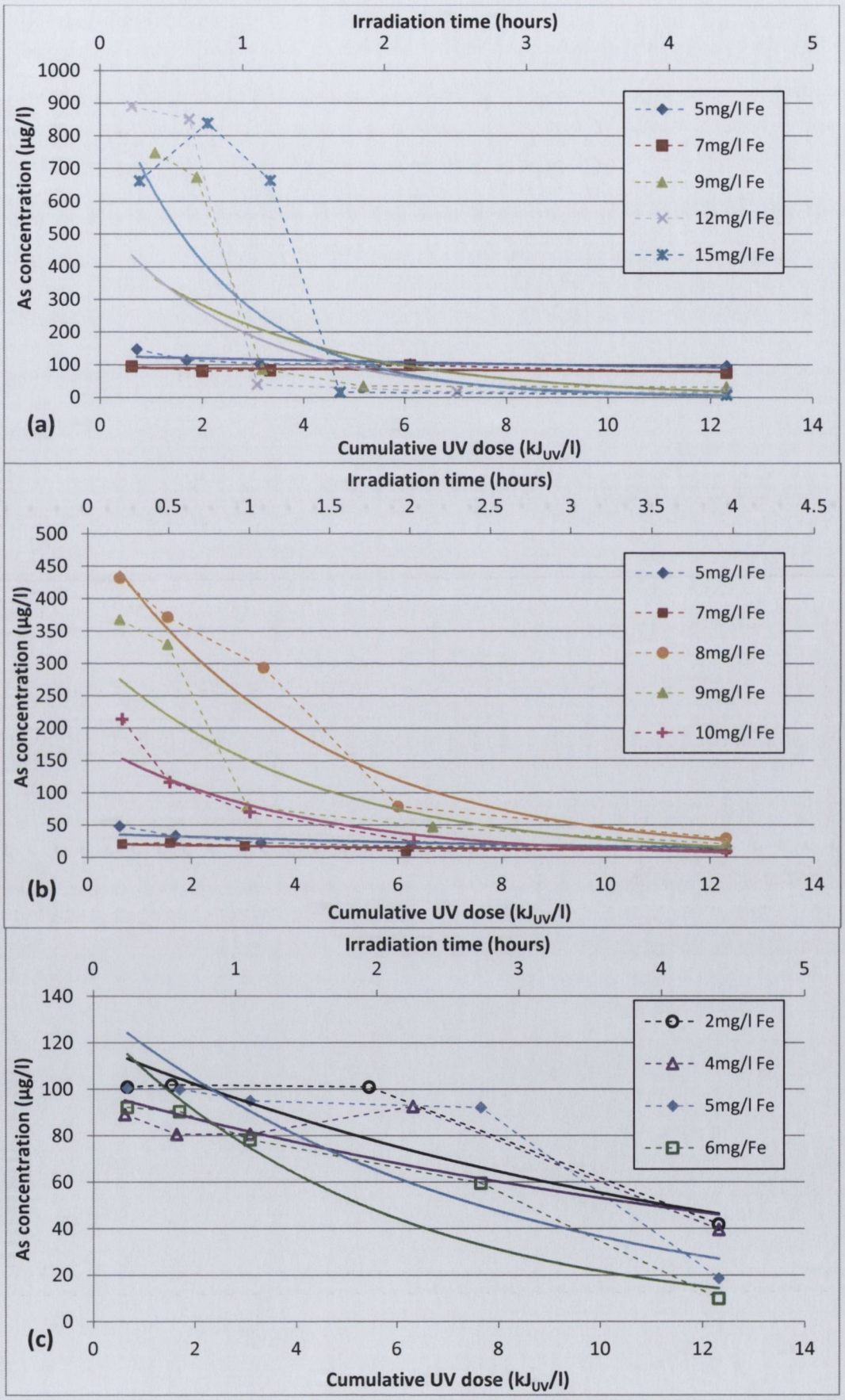

Figure 4.10 *As concentration vs cumulative UV dose and irradiation time under artificial lamp (initial As* ***(a)****1000 µg/l* ***(b)****500 µg/l* ***(c)****100 µg/l)*

The optimum dosages found in this set of experiments for 1000 µg/l, 500 µg/l and 100 µg/l initial arsenic over 4 hours irradiation time were 15 mg/l, 10 mg/l and 6 mg/l iron respectively. As expected, greater overall removal efficiency is seen with increased iron dosage and this is evident in all 3 plots. It is also apparent from these graphs however, that slightly lower iron doses may be needed if more irradiation time was allowed. This theory was not investigated further here, as given the nature of continuous flow systems, the time required in the reactor must be kept to a minimum to ensure the smallest and most cost effective set up. However, this issue will be addressed later in the large scale experiments (see Section 4.9).

4.5 Optimum natural citrate dose experiments

As the preceding experiments all used 200 µl/l citrate as recommended by most previously published research, experiments with a view to possibly optimise this citrate dose were conducted. However, as mentioned previously, Garcia *et al.* (2004) did dispute the addition of citrate based on laboratory and field trials, but this was mainly regarding higher concentrations of citrate (above 750 µl/l) and when alkalinity was not taken into account as acid complexants may have a negative effect. The results of the tests carried out are shown in Figure 4.11 which clearly show that citrate (in the form of lemon juice) had a significant negative effect on the rate of arsenic removal, and to a lesser extent, the final concentration after 4 hours irradiation time. Figure 4.11 shows the rate of arsenic removal of the 3 different initial arsenic concentrations with the optimum iron doses found in Section 4.4, using 0-1000 µl/l lemon juice. The difference between tests using any of these amounts of citrate and the tests without citrate is very evident in the plots below.

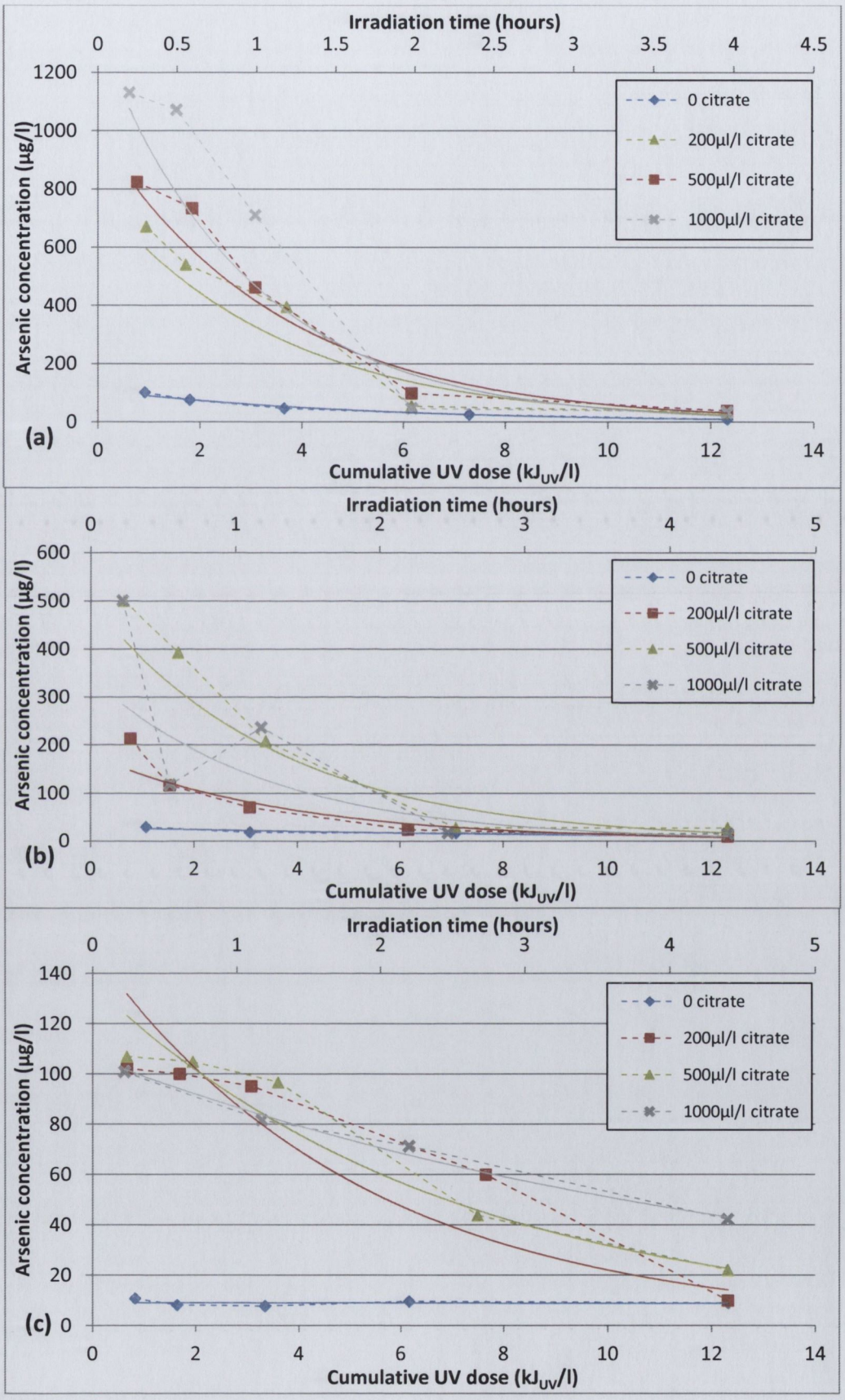

Figure 4.11 Plot of *As concentration vs cumulative UV dose and irradiation time – the effect of natural citrate (initial As, Fe* ***(a)****1000 µg/l, 15 mg/l* ***(b)****500 µg/l, 10 mg/l* ***(c)****100 µg/l, 6 mg/l)*

When no citrate was used, an improvement of between 20 and 90% in overall removal on the next most efficient citrate dose was seen in the first half hour irradiation. This percentage enhancement decreased with respect to irradiation time for all citrate levels until the end of the experiment. As the majority of previous research (using any As concentration or Fe form or concentration), including the batch studies carried out as part of this research (Section 4.2), showed the positive effect of citrate on the process, these results imply the negative effect may be attributed to the continuous flow aspect of the experiments. As the sample is continuously mixing, the Fe-citrate complexes may not have time to form given the constant movement, or the turbulence may cause the added citrate to interfere with the formation of the solid precipitate rather than enhance it. This possible impedance could be due to nature of the natural citrate, i.e. any pulp or other organic matter in the lemon juice could cause interference (despite the juice being sieved before use). It may also be caused by the citrate masking either the iron or arsenic during photooxidation. The higher levels of citrate could also be a sink for ROS, actively competing with As and Fe. Although the general trend showed that citrate had a negative effect on removal, at the highest citrate dose tested (1000 µl/l) (using 'medium' (500 µg/l) and 'high' (1000 µg/l) initial arsenic concentrations), the difference in final arsenic concentration (compared to using no citrate) was lowest (however this was not the case for 'low' initial arsenic). These observations suggest that in a continuous flow system, the citrate required to enhance the removal process may be significantly higher than in the batch method. This was not investigated further, as any amount of citrate needed greater than 1ml/l would not be considered practical at a large scale level, given the average volume of juice from 1 lemon being approximately 50ml. The most likely reason for the adverse effect of citrate on the continuous flow process is the higher levels of reaeration that occurs in the recirculating system. During the Fenton cycle Fe(II) is oxidized to Fe(III)

with UV and produce ROS, then Fe(III) is reduced back to Fe(II) by producing O_2. When citrate is added, the Fe(III) formation is accelerated by forming the stable Fe(III)CitOH- complex. Consequently the reduction of Fe(III) is accelerated which leads to As removal (the citrate complex can also be more reactive because of its conformation). With the continuous flow reactor, the opposite effect occurs because the dissolved oxygen concentrations are higher, less Fe(III) is reduced to Fe(II) because this reaction is producing O_2, and consequently the rate of the reaction decreases, leading to a decrease in As removal. This negative effect is aggravated by increasing the citrate dose, occurring due to the higher ratio of citrate to iron, as non-reactive $Fe(III)Cit_2$ forms. This was also observed in batch experiments (as mentioned above) by Garcia *et al.* (2004).

4.6 Optimum sodium citrate dose experiments

To eliminate the possibility of natural organic matter in lemon juice being the cause of reduction in arsenic removal efficiency, the same experiments as detailed above in Section 4.5 were carried out, this time replacing lemon juice with sodium citrate solution prepared in the laboratory (see Section 3.1.1.3). Overall, similar results to the lemon juice experiments were seen using sodium citrate, with an increasingly negative effect on removal efficiencies with increasing citrate dose (Figure 4.12). This occurred in all cases apart from the 'high' initial arsenic tests, where, after 1 hours irradiation time, the plots all tended to similar values and the citrate dose became negligible until the final samples were taken; only the highest citrate dose (along with no citrate) achieved less than 10 µg/l. When testing 'medium' or 'low' initial arsenic concentrations, 80µM citrate (equivalent to 200 µl/l lemon juice as recommended by Hug *et al.*, 2001) performed best (with a near exact match to using no citrate with 'medium' initial arsenic, and better with 'low' initial

arsenic after 2 hours irradiation time). However, these results imply that citrate may not required for a continuous flow SORAS process, and that the use of natural or sodium citrate in a dynamic system does affect either the oxidation-reduction reactions involved with the photolysis of iron, or the oxidation of arsenic and subsequent co-precipitation of As(V) with Fe(hydr)oxides. That said however, by comparing Figure 4.10 (c) with Figure 4.2 (the most comparable set of experiments from batch scale to continuous flow), it can be seen that the actual final As concentration after 4 hours is the same, but the rate of removal is very different. This may indicate lower concentrations of citrate which were not tested, therefore could be optimal in a continuous flow system.

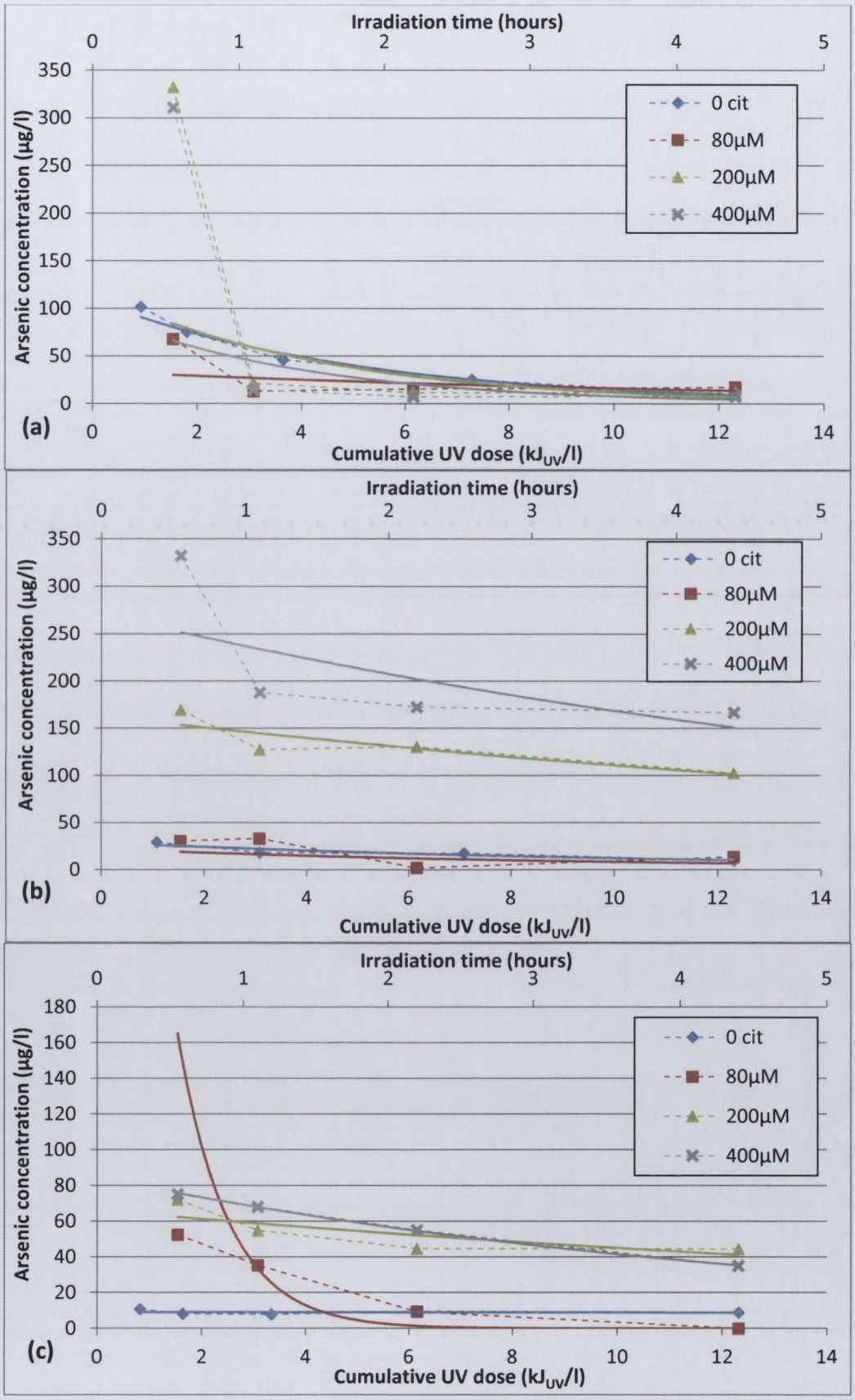

Figure 4.12 *As concentration vs cumulative UV dose and irradiation time – the effect of sodium citrate (initial As, Fe* ***(a)****1000 µg/l, 15 mg/l* ***(b)****500 µg/l, 10 mg/l* ***(c)****100 µg/l, 6 mg/l)*

4.7 Optimum iron dose experiments (repeated without citrate)

Given that the addition of citrate negatively affected arsenic removal efficiency, the optimum iron dose experiments were repeated, this time without using citrate. Figure 4.13 illustrates the significant difference in the arsenic removal pattern compared to the experiments using citrate (Figure 4.10). The arsenic concentrations fell by 90% in the first half hour irradiation, indicating rapid As oxidation in the presence of Fe(III). As originally expected, there was an increase in As removal with increasing iron dosage, which contradicts the theory that higher turbidity (due to increased dissolved iron content) affects the transmission of UV to the sample. It is suspected that, given the results on citrate dose, this occurrence was due to citrate interference with oxidation/co-precipitation. The results also show that 92% of iron dosages tested removed arsenic to below the Bangladesh MCL of 50 µg/l. However, even if the final concentrations did not get down to the MCL, as arsenic related disease risk factors increase with dose, any significant decrease in concentration is clearly beneficial. Only a slight change to the optimum iron dose was observed compared to results using 200 µl/l or 80 µM natural/sodium citrate, but even such a small reduction in required iron is clearly an advantage with respect to the design and feasibility of a full-scale system. The optimum dosages found in this set of experiments for 1000, 500 and 100µg/l initial arsenic over 4 hours irradiation time were 12, 10 and 5 mg/l iron respectively. A similar trend to the experiments using citrate was observed in that the gradient of the removal curves decreased (but to a lesser extent in this case) with decreasing initial As concentration.

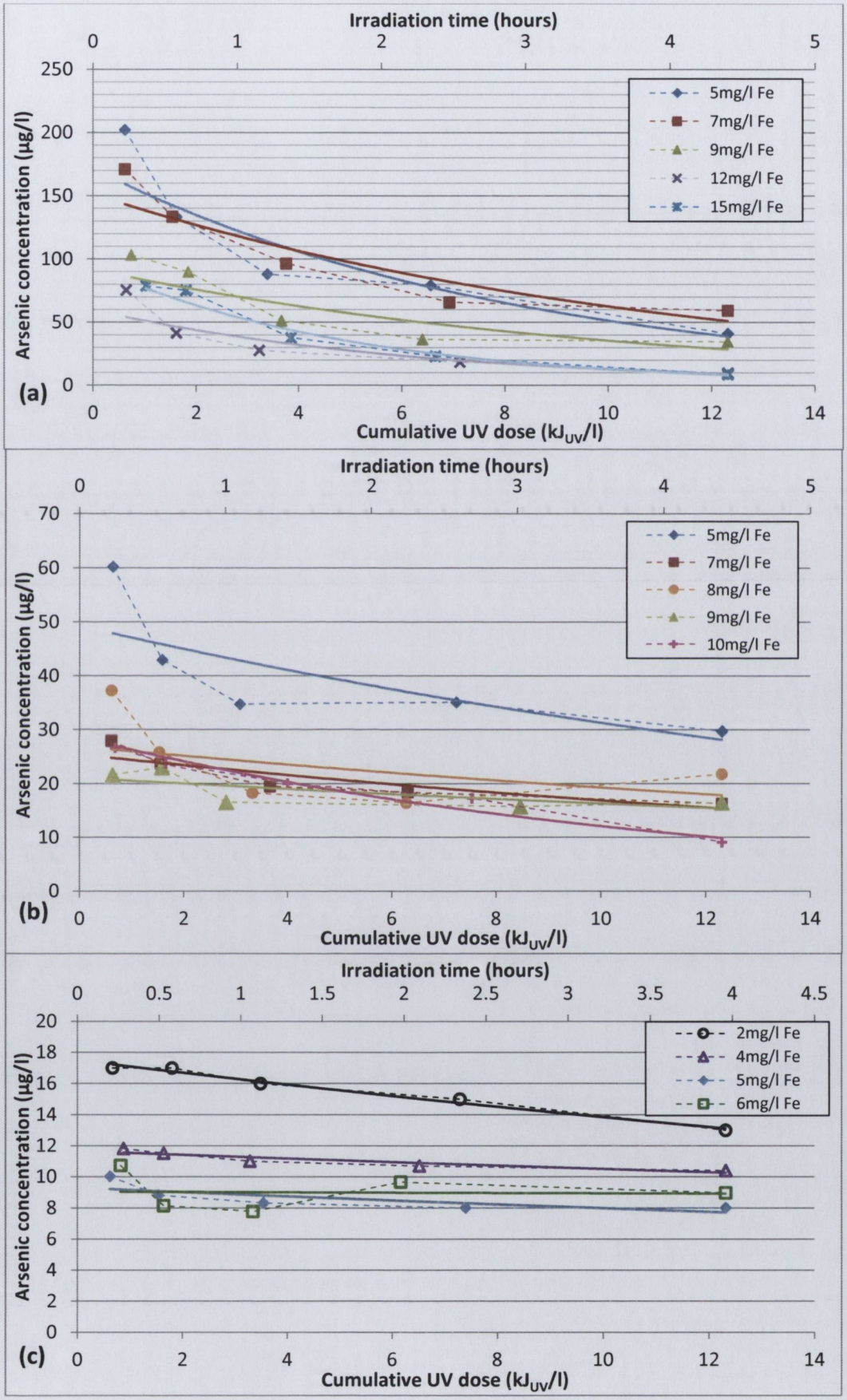

Figure 4.13 *As concentration vs cumulative UV dose and irradiation time without citrate (initial As* ***(a)****1000 µg/l* ***(b)****500 µg/l* ***(c)****100 µg/l)*

An analysis of the system kinetics has been made by comparing the molar ratio of arsenic to iron against the arsenic removal kinetic is shown on the following Figures 4.14 and 4.15. As shown in Figure 4.13, the arsenic removal kinetic exhibit a diphasic process with a initial fast (almost instantaneous) removal of arsenic within the first 0.2 hours irradiation time (defined as the k_1 kinetic) and then a more gentle reduction with respect to irradiation time or UV dose (defined as the k_2 kinetic) as detailed in Table 4.1 .

During the first initial reaction period, the molar ratio vs kinetic graphs (Figure 4.14) show that there is a general positive correlation; i.e. proportionally higher iron will produce faster arsenic removal, no matter what the starting concentration arsenic. However, during the second slower removal period, the graphs for the higher starting As concentrations of 500 and 1000 µg/l show an interesting hysteresis, whereby the same removal kinetic can be achieved at a low and high Fe:As molar, up to a point. Hence, this indicates that it might be worth designing a full scale process to operate at the lower Fe:As molar ratio to attain a reasonable removal kinetic (although this dose will also have to be balanced against the removal in the first k_1 period). The result for the lowest dose of 100 µg/l does not show the same hysteresis pattern however, this is probably due to the fact that, at such small k values, slight experimental differences have a disproportionally high impact. The 6 mg/l line (which appears to be out of synch with the other results) has the lowest k_2 kinetic due to the fact that the system performed so well in the initial period (i.e. a high k_1).

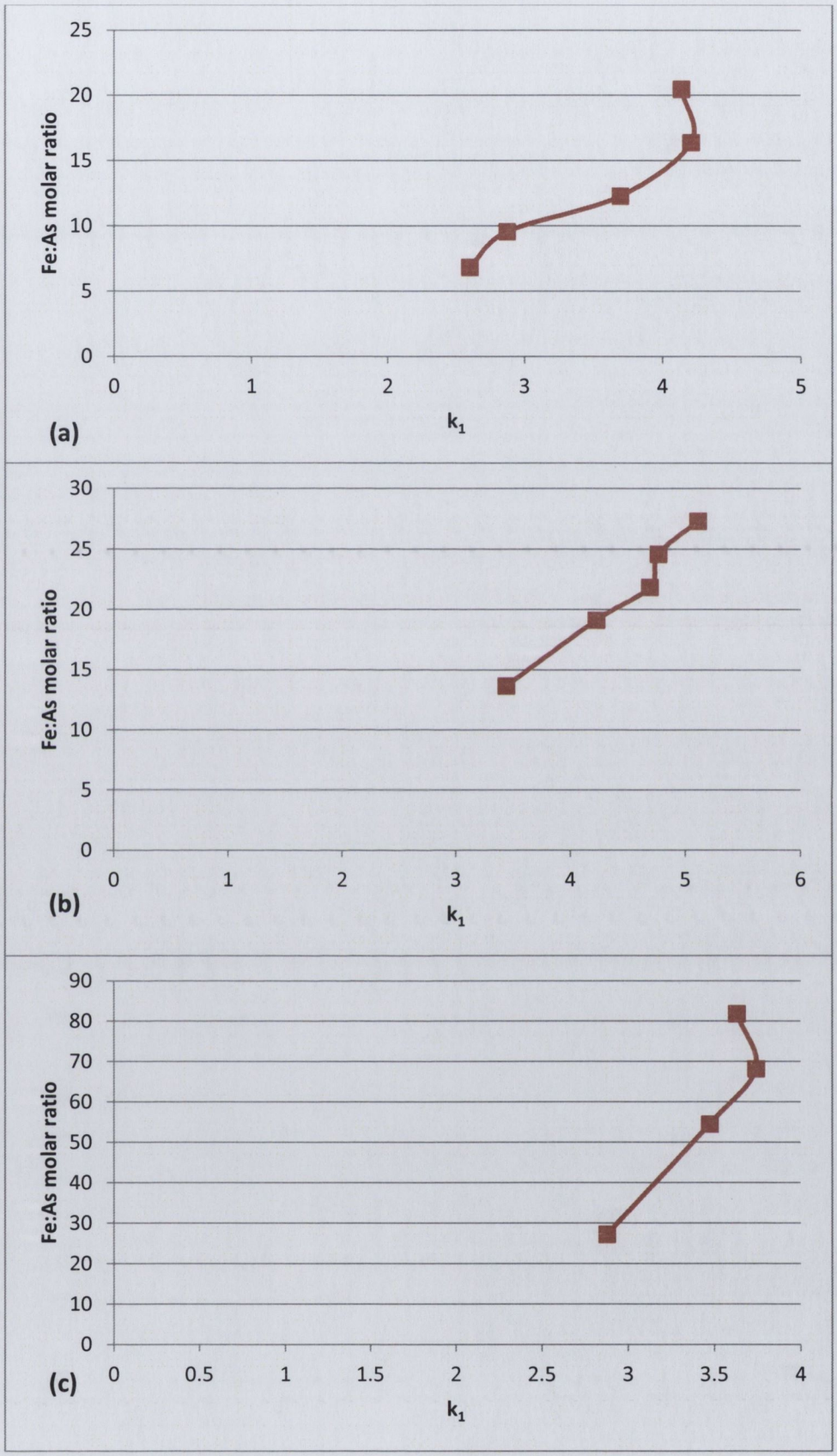

Figure 4.14 *Molar ratio against k_1 for initial As of (a) 1000 (b) 500 (c) 100 µg/l*

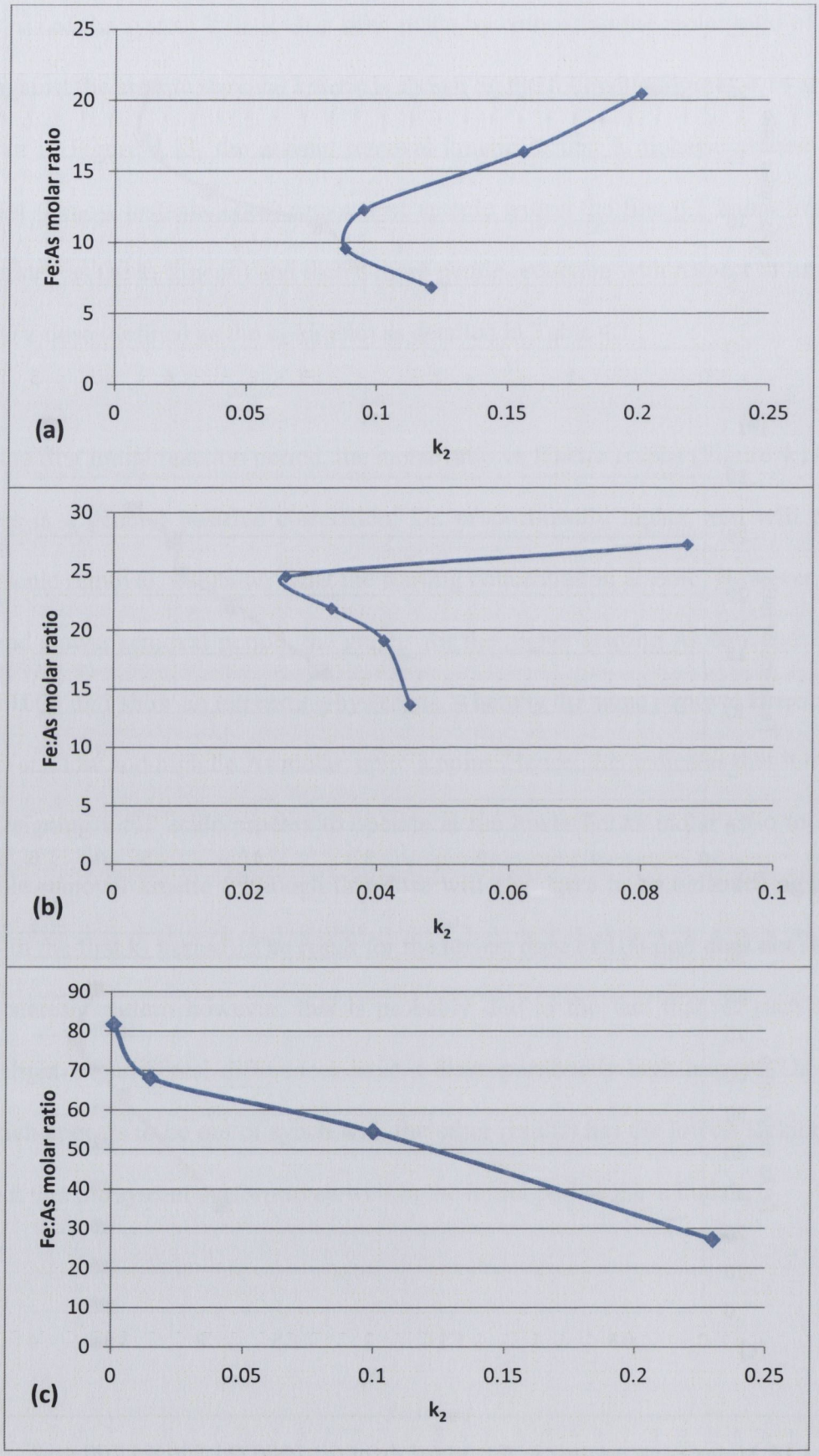

Figure 4.15 *Molar ratio against k_2 for initial As of (a) 1000 (b) 500 (c) 100 µg/l*

Initial As (µg/l)	k_1	k_2	Fe:As
1000	2.598	0.121	6.82
	2.872	0.088	9.55
	3.694	0.095	12.27
	4.206	0.156	16.36
	4.136	0.201	20.45
500	3.44	0.045	13.64
	4.224	0.041	19.09
	4.689	0.033	21.82
	4.763	0.026	24.55
	5.108	0.087	27.27
100	2.878	0.23	27.27
	3.472	0.1	54.55
	3.74	0.015	68.18
	3.629	0.001	81.82

Table 4.1 *Comparison of k_1 and k_2 values for tested molar Fe:As ratios*

Figures 4.16 and 4.17 below show arsenic removal on a logarithmic scale against cumulative UV dose, giving values for the k_1 and k_2 kinetics respectively. If the initial rapid degradation is taken as instantaneous, a number of factors could play a role in this phase of removal. Firstly, despite As(III) only weakly adsorbing to iron, it is still possible when concentrations of arsenic and iron are present, for sorption of some As(III) on to the Fe present in the sample. Roberts *et al.* (2004) showed passive adsorption of up to 500 µg/l As(III) and As(V) onto Fe(II) and Fe(III) in dark experiments, albeit at significantly higher iron concentrations (30-40 mg/l). Secondly, no account is taken of the possible As adsorption during the dark phase in these experiments. Samples were allowed settle for 48 hours in the dark before filtration and analysis. As mentioned above, Roberts *et al.* (2004) found adsorption of both As(III) and (V) onto iron in tests carried out in darkness. This was over a 4 hour time period, reducing arsenic to below the Bangladeshi MCL of 50 µg/l.

Again, the Fe concentrations were far greater in these experiments, however this indicates that some of the initial rapid removal could be attributed to immediate As(III) adsorption, and adsorption continuing in the dark phase. Finally, some As(III) oxidation could also be put down to the presence of free chlorine in the sample water – despite levels being quite low, and the tap water being left out for a time before making up the sample to allow the free chlorine to degrade. Dodd *et al.* (2006) found that 0.1 mg/l Cl_2 was sufficient to oxidise 98% of 50 µg/l As(III) within 10 seconds of addition, so it is possible, given there was residual chlorine in the tap water, for some oxidation to take place. However, the free chlorine tested during random spot checks was up to 0.2 mg/l, and degraded whilst standing for 10 minutes to 0 mg/l, so it is assumed that this would not cause significant oxidation of As(III) during the initial phase.

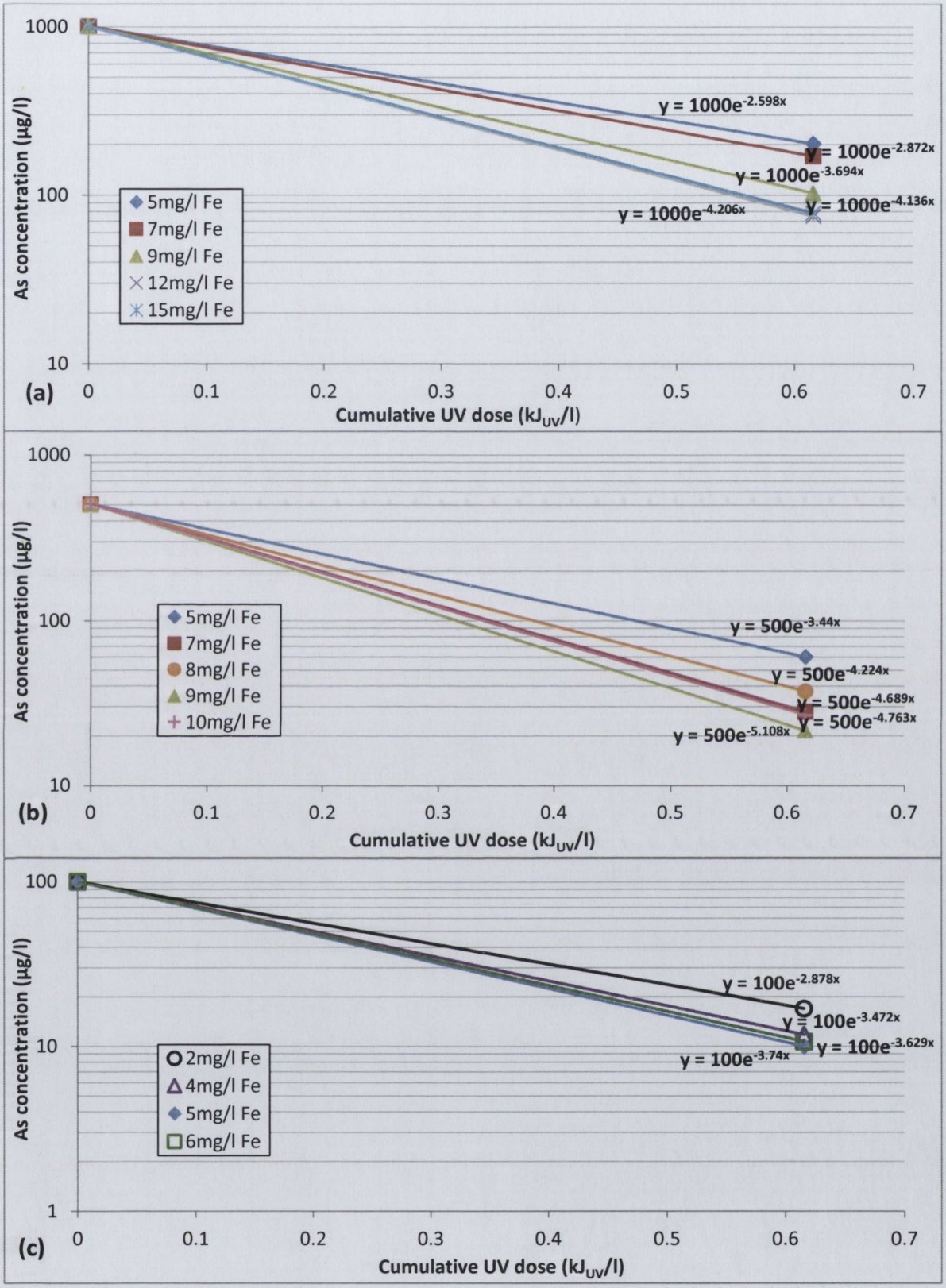

Figure 4.16 *As concentration vs cumulative UV dose (without citrate) on a log scale showing k_1 values (initial As* ***(a)****1000 µg/l* ***(b)****500 µg/l* ***(c)****100 µg/l)*

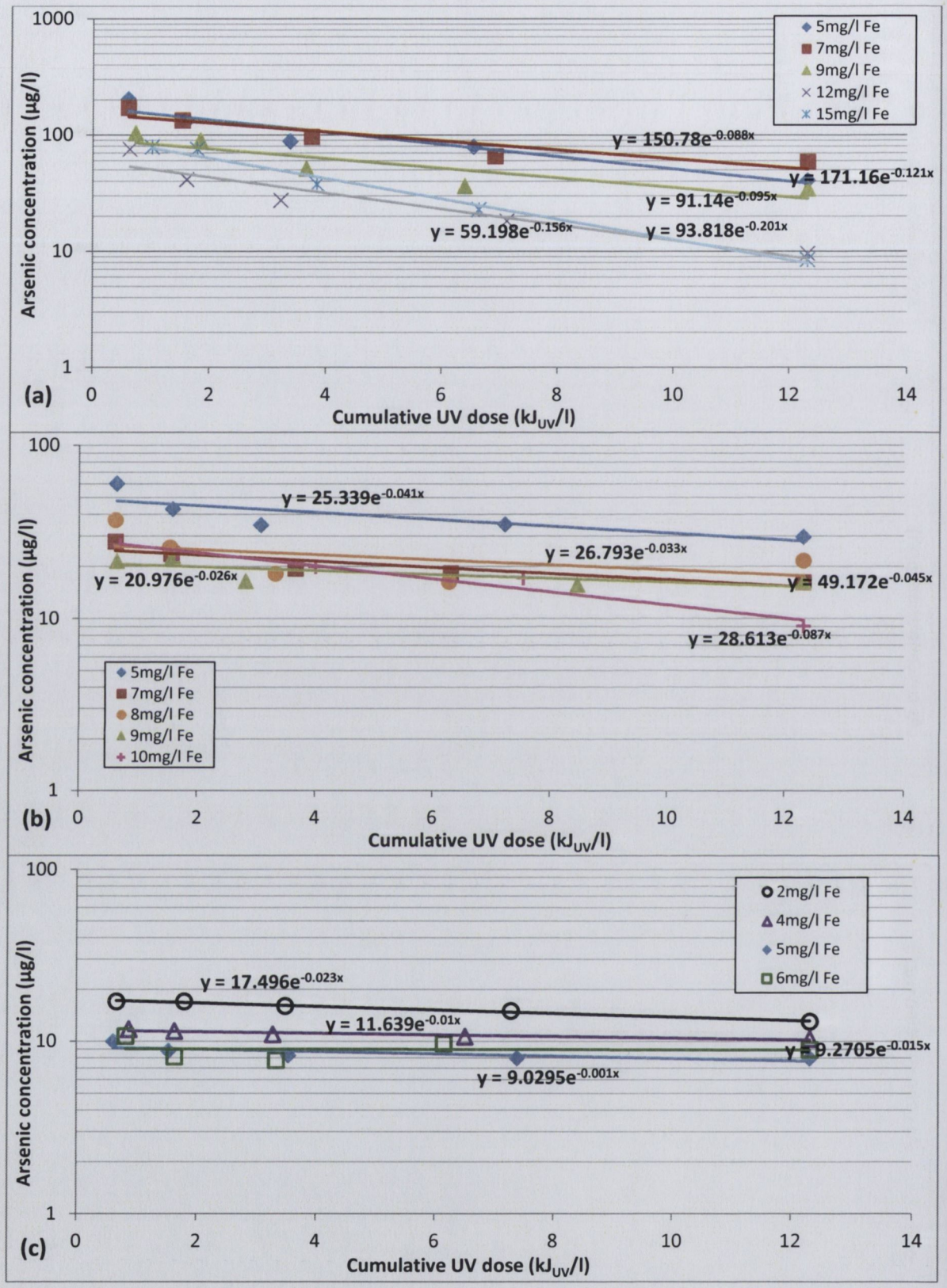

Figure 4.17 *As concentration vs cumulative UV dose (without citrate) on a log scale showing k_2 values (initial As* ***(a)****1000 µg/l* ***(b)****500 µg/l* ***(c)****100 µg/l)*

The optimum iron dose of 5 mg/l for initial arsenic of 100 µg/l in these tests is the closest in operating conditions for comparative purposes to the batch studies where, given initial arsenic of 150 µg/l, 7 mg/l iron was needed. Although the initial arsenic was slightly higher, the decrease in the iron requirement is attributed to the increased solar flux of the continuous flow reactor, whereby the irradiated area per unit volume was increased. While the cross sectional area of the Pyrex tubes is considerably smaller than that of the 1 litre bottle, the irradiated area taken is that of the whole compound parabolic collector as it reflects light with a concentration ratio of 1. The experiments between the 1 litre batch and continuous flow systems revealed only a minor increase in removal efficiency, however real design kinetics to be used at full-scale were tested in the large scale reactor with the results detailed in Section 4.9. Figure 4.18 shows the cumulative UV dose corresponding to irradiation time (with a lamp delivering 15 W/m^2) for the batch and small scale continuous flow experiments, illustrating a 57% increase in UV dose when using the CPC reactor compared to batch tests.

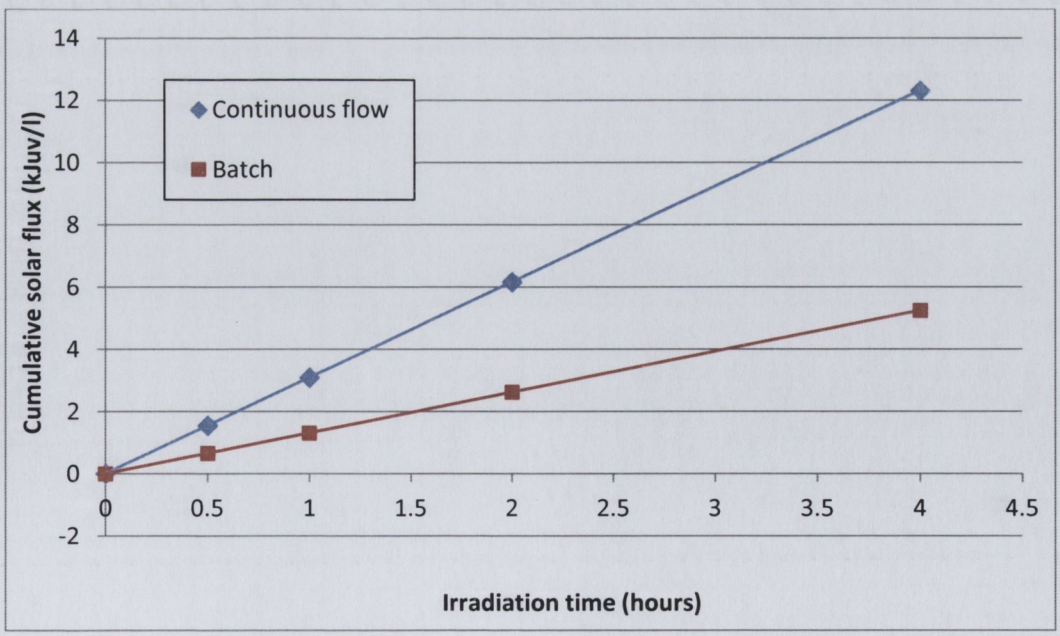

Figure 4.18 *Comparison of cumulative UV dose per litre in batch and continuous flow reactors*

4.8 Effect of other water quality parameters

As discussed previously, the raw water quality can have a major effect of arsenic removal. Due to the nature of the earth's sediments, the components of groundwater can vary widely, hence the following experiments were conducted in the small scale reactor (under the UV lamp) to examine the effect of other water parameters on efficiency.

4.8.1 Effect of phosphate and silicate

Figure 4.19 illustrates the effect on arsenic removal efficiency of 0.5-10 mg-PO_4/l (Section 3.1.1.4) during continuous flow experiments (using optimum iron dosage for each arsenic concentration and without citrate). As expected, the results clearly show that increasing PO_4 concentrations generally had a negative effect on removal. At higher initial arsenic concentrations there is an insignificant difference to the overall removal efficiency between 0.5 and 1 mg-PO_4/l, as can be seen clearly in Figure 4.19(a) and (b), with both sets of data points matching for most of the duration of the experiment. One concern that these experiments raise is that the final As concentration did not drop below 10 µg/l for any level of phosphate, which would imply that more iron is needed for adsorption sites when PO_4 is present. Although the general pattern for each arsenic concentration is very similar, a much higher percentage removal is seen for higher arsenic concentrations. For example, for 5 mg/l added PO_4, 85% removal was achieved with initial arsenic of 1000 µg/l, while only 50% removal was obtained with 100 µg/l initial arsenic. This is explained by the higher iron doses present for higher initial arsenic, due to the increased number of adsorption sites.

Due to time constraints, less extensive tests on the effect of silicate were carried out. It was decided that an initial arsenic concentration of 500 µg/l with its optimum iron dosage of 10 mg/l was to be used in experiments with 10 and 30 mg/l silicate (Section 3.1.1.5), and 30 mg/l silicate and 10 mg/l phosphate to examine their combined effect on the process. Figure 4.20 shows the results of these experiments and, as expected, silicate clearly shows a negative effect on arsenic removal. There was no significant difference in arsenic removal efficiency between using 10 and 30 mg/l SiO_3, indicating considerable increases in silicate concentration will not have the same effect as increased phosphate concentration, though this would need to be investigated further. Interestingly, the effect of using both 30 mg/l SiO_3 and the highest dose of PO_4 tested 10 mg/l was negligible to that of using 10 mg-PO_4/l alone. This implies that phosphate is the more competitive ion (also shown by Meng *et al.*, 2002), and that although silicate alone does have an effect on arsenic removal, As(V) competes comparably with it in the presence of PO_4.

These results match the findings of other research reported in international literature. Meng *et al.* (2002) studied adsorption constants of phosphate and silicate in the co-precipitation of arsenic with iron with their results indicating that both had a high affinity for iron hydroxide sites as they are negative ion species. Phosphate also competes with arsenic for the photooxidation products of iron, obstructing As(III) oxidation in the solar oxidation process. In batch scale experiments, Mukherjee *et al.* (2007) added concentrations of phosphate (PO_4) from 0-2.5 mg/l to SORAS samples (initial As: 500 µg/l, Fe: 6 mg/l, irradiation time: 4 hours) in order to determine its effect on arsenic removal. The results showed a decrease in efficiency of approximately 10% with each increment of 0.5 mg-PO_4/l.

Phosphate concentrations in groundwater can vary spatially and seasonally, but the highest levels tested here would not appear to be normally found in the groundwaters of the Bengal

Basin region. For example, Mukherjee *et al.* (2007) reported an average concentration of 2.48 mg-PO_4/l in wells surveyed in the Nadia district of West Bengal, whilst Kinniburgh and Smedley (2001) showed high variation in their survey of Bangladesh, with a median total phosphorous value of 0.3 mg-P/l). However, the negative effect of phosphate on the SORAS process must be taken into account when designing a full scale system, and as mentioned above could be prevented with increasing the iron dosage.

Equally, silica is a major component of groundwater in Bangladesh, resulting from the intense chemical weathering of silicate minerals. Stollenwerk *et al.* (2007) reported silica concentrations in groundwater surveyed outside Dhaka, Bangladesh of 9-25 mg/l, while McArthur *et al.* (2001) found concentrations up to 131 mg/l also in Bangladesh. Again, the negative effect of such anions on As removal efficiency must be taken into account in the design of any full-scale SORAS system.

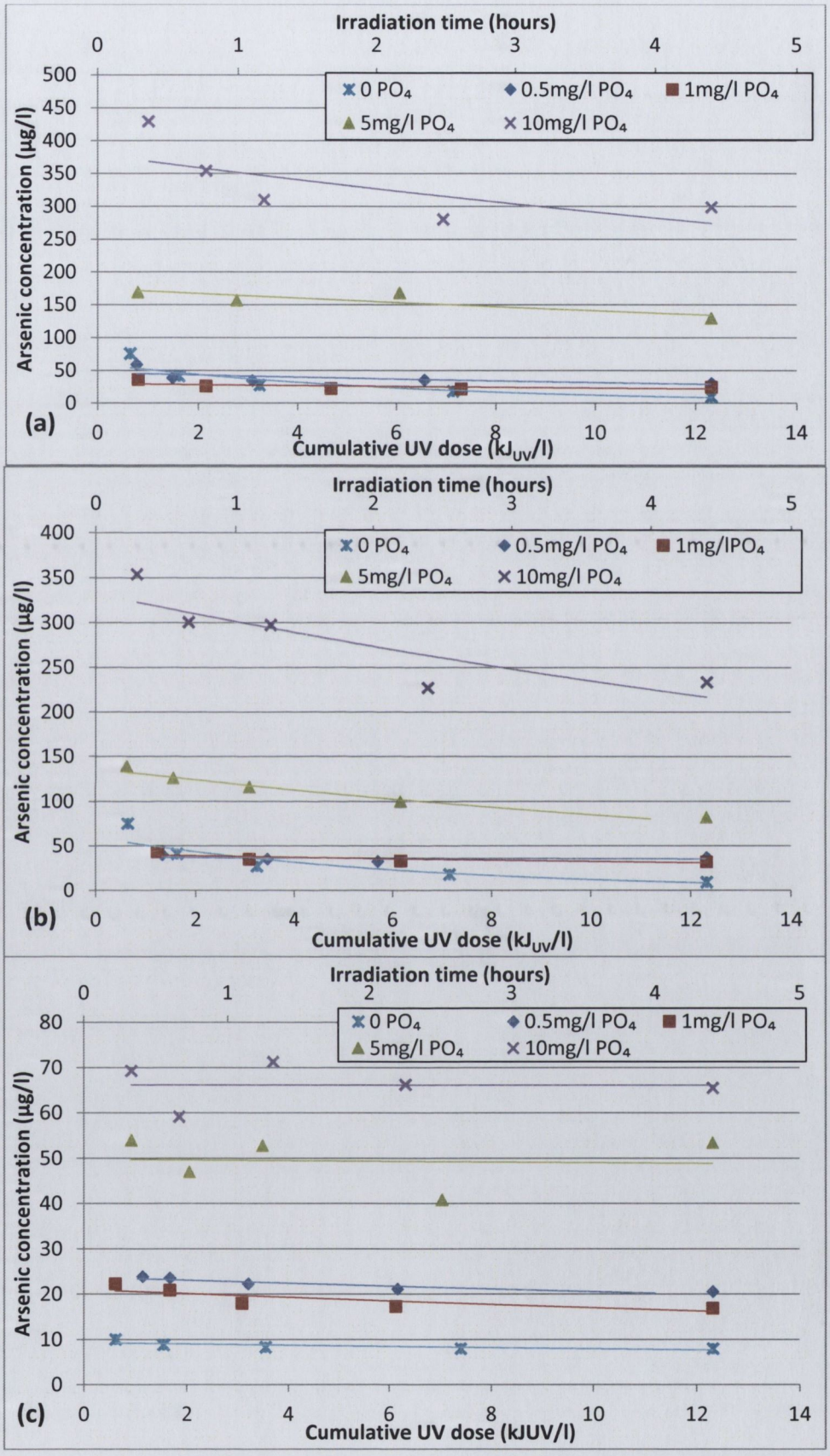

Figure 4.19 *As concentration vs cumulative UV dose and irradiation time – the effect of phosphate (initial As, Fe* ***(a)****1000 µg/l, 12 mg/l* ***(b)****500 µg/l, 10 mg/l* ***(c)****100 µg/l, 5 mg/l)*

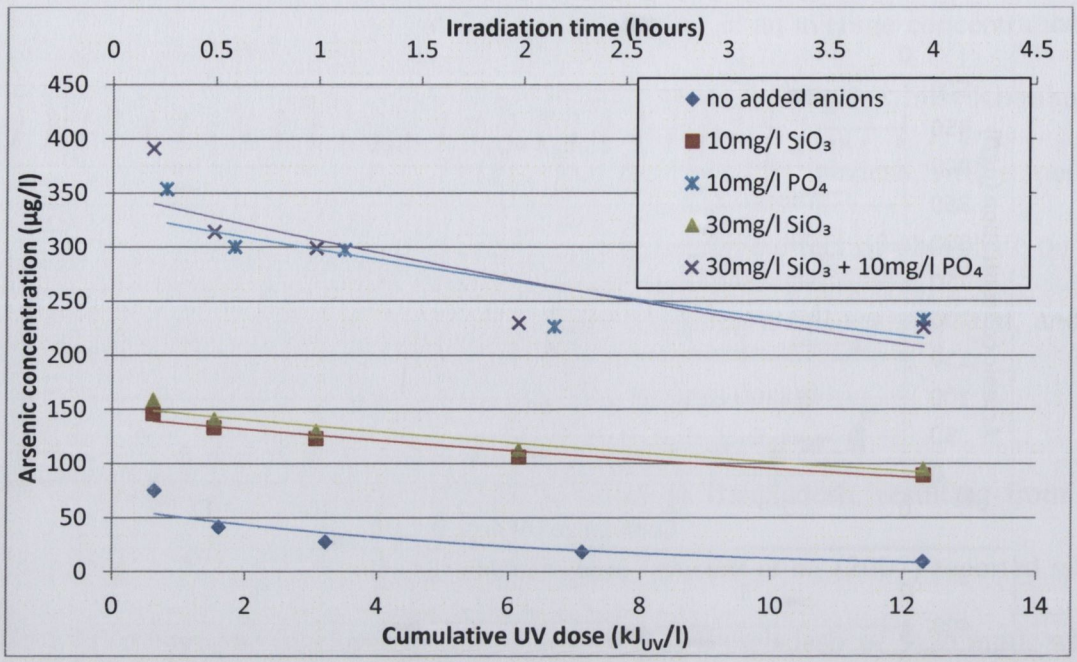

Figure 4.20 *As concentration vs cumulative UV dose and irradiation time – the effect of silicate (and phosphate) (initial As: 500 µg/l, Fe: 10 mg/l)*

4.8.2 Effect of pH

As pH has been shown to affect the SORAS process (Khoe and Emett, 2001) a series of experiments were conducted using 500 µg/l arsenic, 10 mg/l iron, and varying the initial pH using nitric acid or sodium hydroxide solutions (see Section 3.1.1.6). The pH was first monitored throughout experiments using no acid/alkali additions to obtain a baseline pH level (Figure 4.21). As stated previously, the pH of the tap water used ranged from 6.89 to 7.94, and upon addition of Fe the pH dropped (~0.5 units) due to the acidic nature of iron salts. The baseline pH plot shows a steady increase in pH with irradiation time (up to almost 3 hours), and despite an initial decrease, exceeds the initial value by approximately 1 unit. After it reaches this maximum, the pH then drops until the end of the experiment, though still remains higher than the original pH level at the beginning of the experiment. A similar trend was observed by Garcia *et al.* (2004) and Hug *et al.* (2001) in batch SORAS

tests, however full datasets are not reported. This has been explained by CO_2 loss during removal of aliquots for analysis, and protonation of the forming iron complexes. For the varying pH experiments, nitric acid or sodium hydroxide was added dropwise to the sample to give initial pH values of 4.5, 5.75, 8.25 and 9.5. PH readings were taken throughout the experiment which revealed a significant change in pH after 1 hour in the reactor (0.2 hours irradiation time). Therefore the pH was subsequently measured every minute for the first hour to obtain more data points for this critical period, as greatest removal was achieved in this time frame. Figure 4.22 shows the change in pH with respect to time for the first hour of the experiments. The plots clearly show a fast progression to equilibrium irrespective of initial pH, with the acidic samples neutralising more quickly than alkali solutions, probably due to the natural presence of bicarbonate acting as a buffer and converting the acid to CO_2 and H_2O.

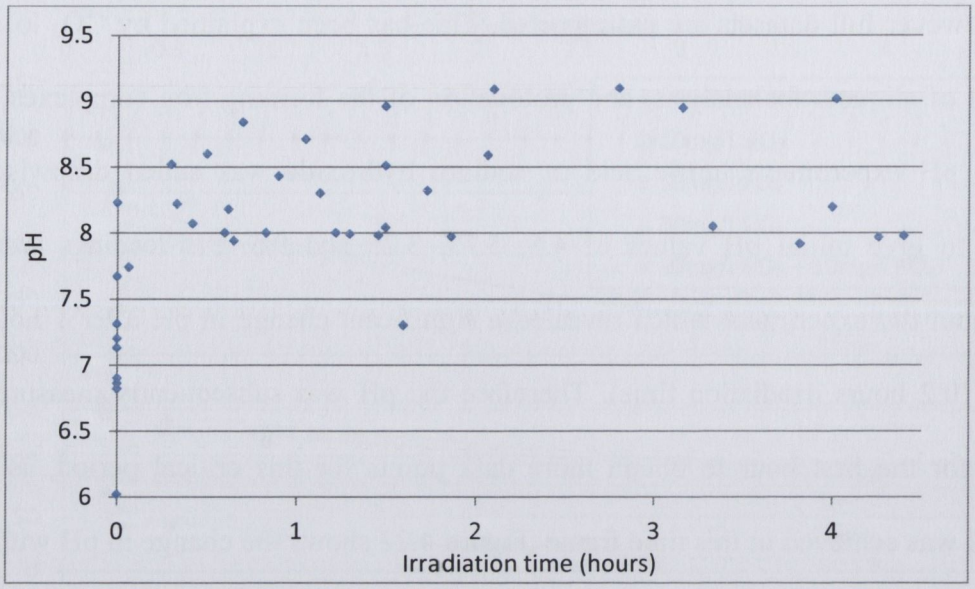

Figure 4.21 *Change in pH against irradiation time*

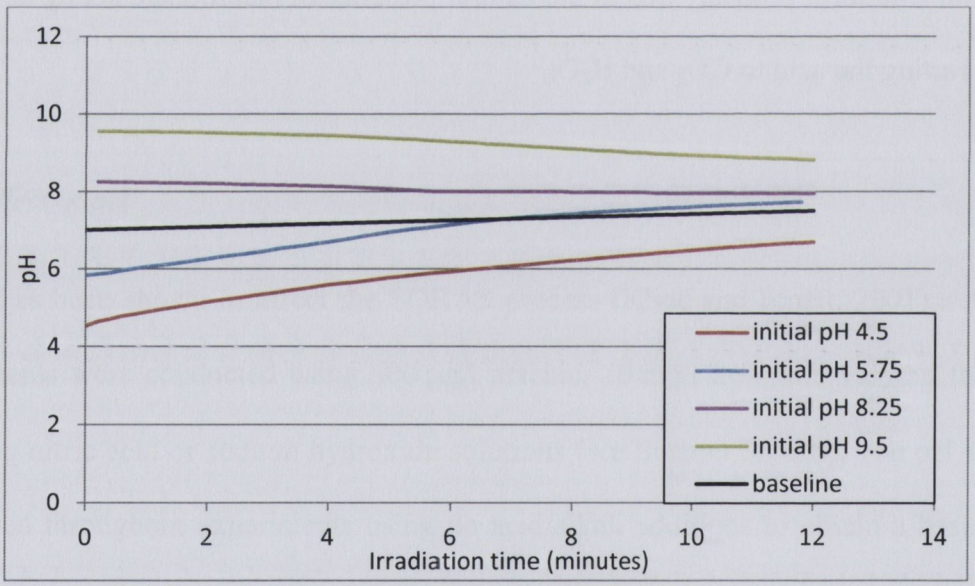

Figure 4.22 *Change in pH over first 0.2 hours irradiation time for varying initial pH*

Overall arsenic removal efficiency increased with decreasing pH, although there was only a minor improvement on the baseline pH at low pH values. However, a considerable decrease in removal (with respect to the baseline performance) was observed at the higher initial pH values (Figure 4.23). Although the different initial pH values tended to the same

equilibrium, the decrease in efficiency at higher pH levels was probably due to the change in the rate of Fe oxidation, and more importantly the change in the oxidative species that As(III) will accept at different values of pH (as discussed in Section 2.4.2). Nickson *et al.* (2000) reported that pH values of groundwater in a study in Bangladesh and West Bengal were between 5.51 and 7.4, averaging 6.5. Based on those values, these results indicate that there should be no significant negative interference from the effect of pH on the SORAS process.

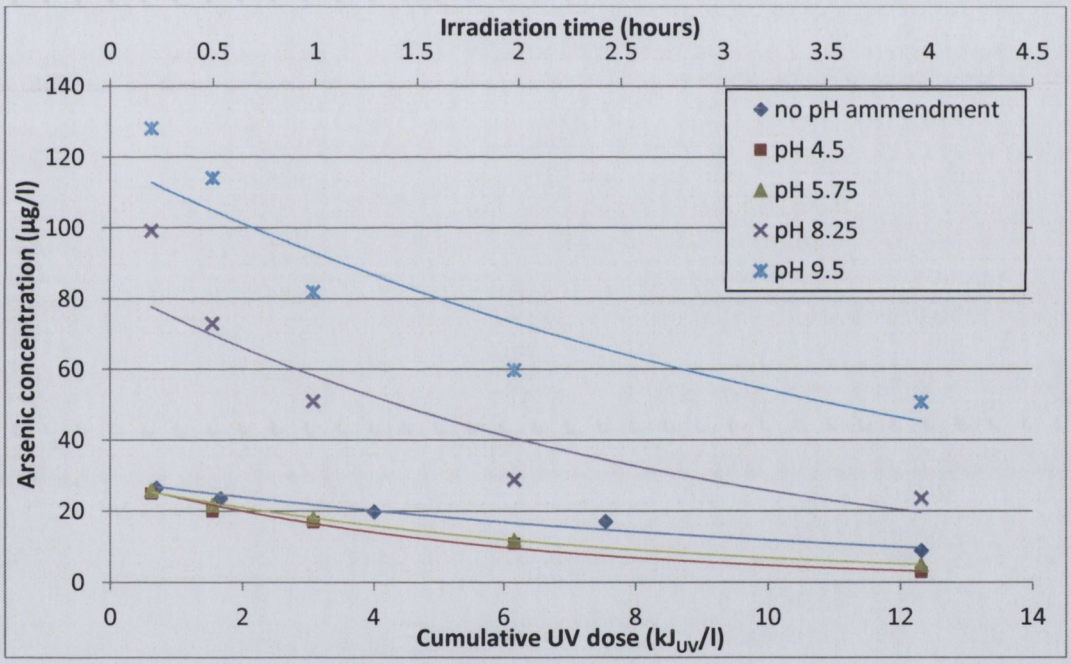

Figure 4.23 *As removal vs cumulative UV dose and irradiation time – effect of initial pH*

4.8.3 Effect of temperature

As the oxygen saturation concentration of water reduces with increased temperature (Chapra, 1997), higher temperatures could have an effect on SORAS efficiency. The rates

of chemical reactions are also subject to change with differences in temperature, therefore Fe and As oxidation could be affected.

Figure 4.24 shows the variation in temperature with time in standard experiments. The temperature increase in the first hour's irradiation time was due to the heat generated by the UV lamp, and it remained steady (28-29°C) until the last hour when it dropped, most likely caused by the decrease in ambient temperature in the laboratory at night. Hug *et al.* (2001) reported similar changes in temperature in SORAS batch tests, increasing from 24-32°C.

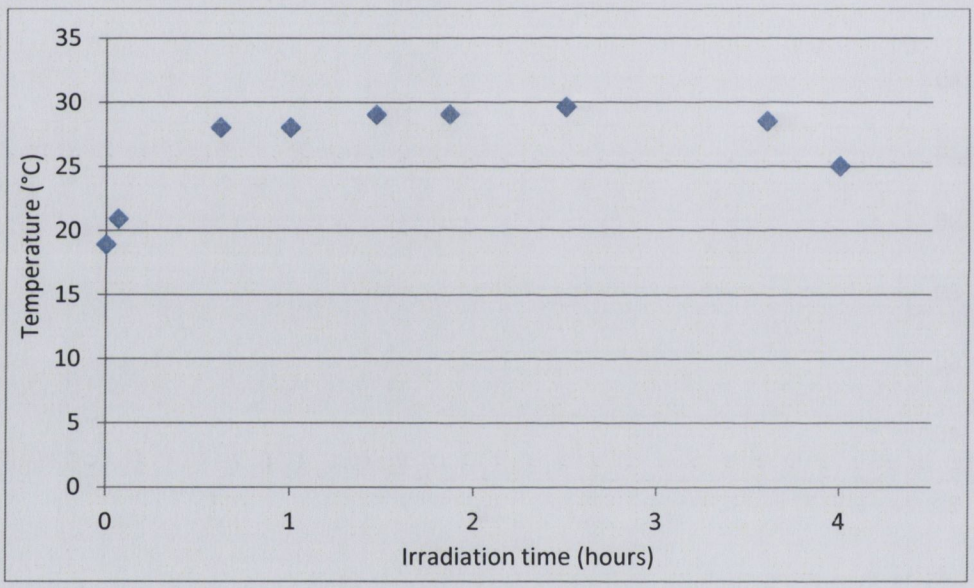

Figure 4.24 *Change in temperature vs irradiation time*

Again experiments using 500 µg/l arsenic and 10 mg/l iron in the CPC reactor were conducted, this time placing the 1 litre reservoir in a water bath to maintain temperatures of 10-60°C. Ice packs were used for the cold experiments, and to sustain warmer temperatures, a hot-plate was used. As there is heat generated by the lamp, the colder temperatures were more difficult to maintain at a constant level, so the removal profile reported here is for the range of temperatures from 10 to 15°C. Figure 4.25 illustrates

arsenic removal efficiency at these different temperatures, with a clear pattern of increased efficiency at higher temperatures. The rate of removal at 40 and 60°C improves on the baseline (~30°C), with the MCL being reached after 2 hours irradiation time in both cases. Although experiments at lower temperatures eventually reached this target value of 10 µg/l, it occured at a significantly lower rate.

A review of the international literature indicated that the effect of temperature on the SORAS process does not seem to have been explicitly investigated, although Tyrovola *et al.* (2006) did examine arsenic removal by adsorption onto zero valent iron at varying temperatures. Significant increases in removal efficiency were observed with increasing temperature, indicating that the adsorption process favours higher temperatures. For example, after 2 hours in a batch reactor, the average As(III) removal increased from 30% at 20-30°C to 60% at 40°C, and As(V) removal increased from 15% at 20°C to 50% at 30°C, and 82% at 40°C. Although this process is different from the SORAS method, the adsorption of arsenic onto iron is very similar, hence higher temperatures may improve removal efficiency. Nishimura et al. (1996) also found the As(III) oxidation reaction was appreciably enhanced by a rise in temperature in experiments with Fe(II), S(IV) and dissolved oxygen. Again this research was not using SORAS, however the oxidation of As(III) is comparable, signifying higher temperatures being favourable.

These results (along with those of the literature cited above) indicate that there is a possibility of using a lower iron dosage at higher temperatures, or indeed a smaller reactor due to the decrease in required irradiation time. Since most arsenic affected areas have tropical climates, and hence hotter ambient temperatures, this could improve the SORAS method further a topic that is discussed again later in Section 4.10.

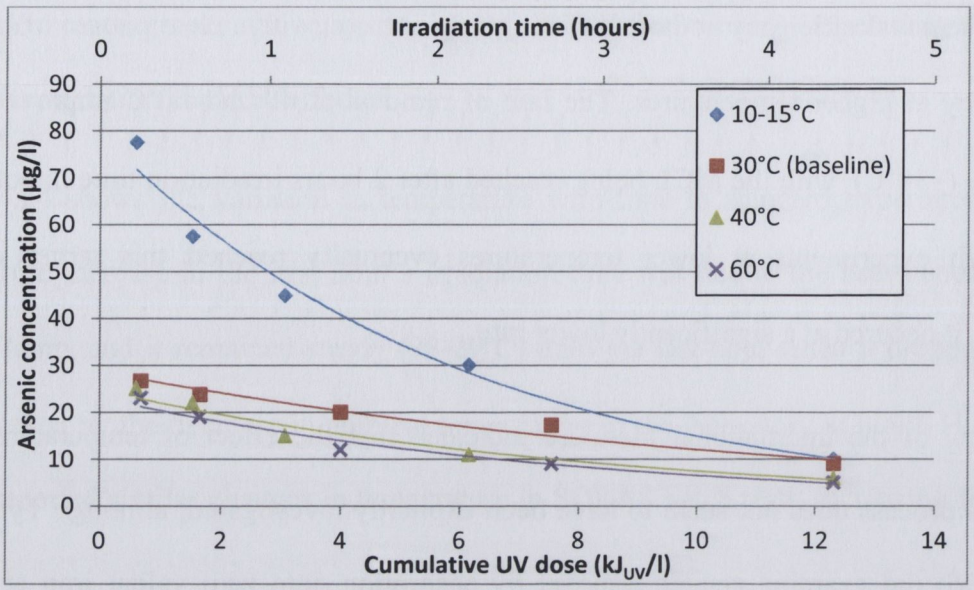

Figure 4.25 *As removal vs cumulative UV dose and irradiation time – effect of temperature*

4.8.4 Effect of dissolved oxygen

Dissolved oxygen (DO) present in SORAS samples is vital for the redox reactions involved with arsenic and iron (see Table 2.3 in Chapter 2) and so an investigation into high and low DO levels was conducted. For the high DO experiments, samples were kept fully aerated using a triple stone diffuser placed in the 1 litre reservoir, pumping air at a rate of 1 litre per minute (this relatively low air flow rate was used in order to prevent air bubbles getting into the reactor.). For the low DO experiments, small amounts of sodium sulphite solution was added to remove (practically) all the DO present, and a rubber membrane was placed over the reservoir to minimise any reaeration through the water surface. Figure 4.26 shows the removal efficiency of fully aerated samples and samples deoxygenated before subjecting them to UV light (initial 500 µg/l arsenic and 10 mg/l iron). During the first half hour irradiation time the fully aerated sample removed 96% of the initial arsenic, whereas the deoxygenated removed only 74%. Although there was a

considerable change in the rate of removal between the 2 sets of samples, there was only a minor difference in the final arsenic concentration achieved after 4 hours (both <10 μg/l). When trying to optimise a SORAS system however, it is evident that having higher levels of dissolved oxygen is beneficial, The action of pumping tubewells does help to promote groundwater aeration and this process could be enhaced by dischraging the water over an artficial cascade before entering such a SORAS system. DO measurements were taken over the course of these experiments and the results shown in Figure 4.27. As with the pH observations, both experiments tended to an equilibrium DO concentration regardless of initial DO concentration. Dissolved oxygen was used up in the redox reactions of the SORAS process as expected, with a linear decrease in DO observed in the aerated experiments. Interestingly, the results show that the DO levels in the deoxygenated experiments rose quickly before to stabilizing in the final few hours of the experiment. It was believed unlikley that the increase in DO attributed to turbulence and mixing in the system and surface reaeration is minimal, would have accounted for this rate or level of DO increase. However, when a control experiment was carried out with no arsenic or iron in the system, it showed a rapid increase in dissolved oxygen, despite every effort to seal the reservoir. Therefore, the difference in removal rates is most likely due to the short period of low DO concentration, with the photoxidation products generated throughout the experimental run being minor constituents of this DO.

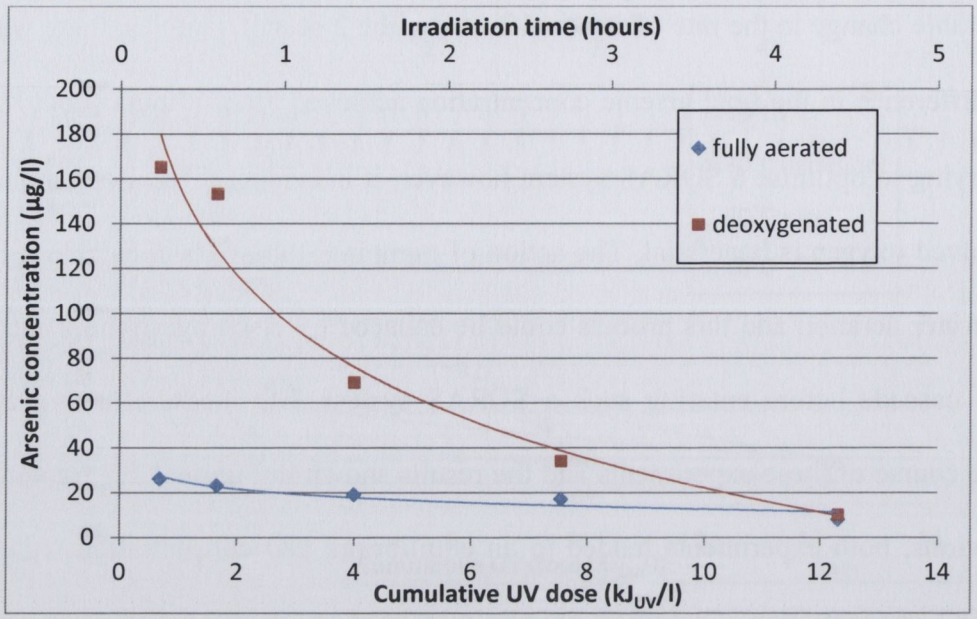

Figure 4.26 *As removal vs cumulative UV dose and irradiation time – effect of dissolved oxygen*

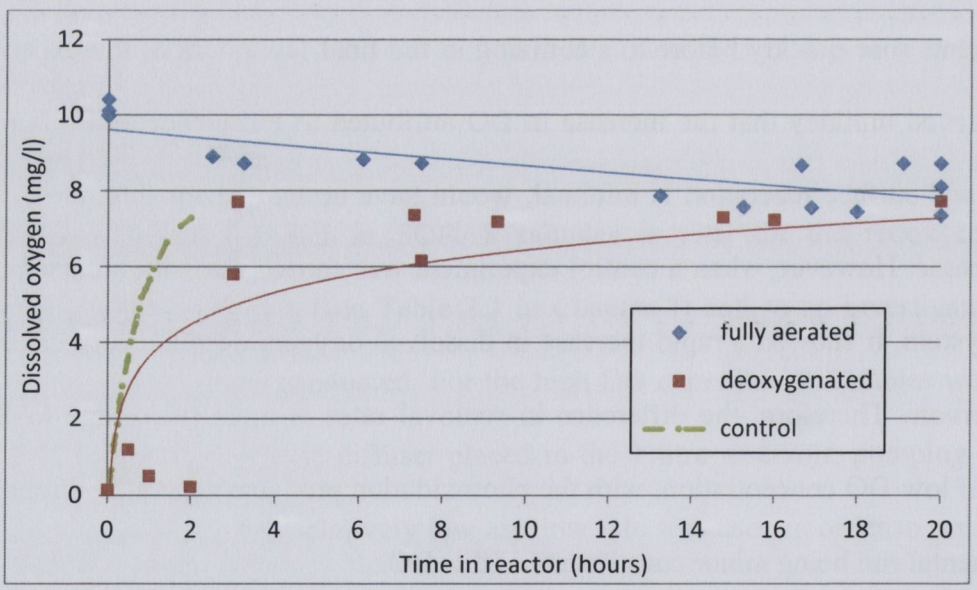

Figure 4.27 *Change in DO vs time (note: irradiation time = 0.2 times total time in reactor)*

4.9 Effect of titanium dioxide photocatalysts

Further to the batch scale studies on the use of TiO_2, continuous flow experiments were carried out to investigate the potential benefit from using the reactor system. Samples made

up as in the batch scale tests were used in the small scale reactor as in the previous sections. Figure 4.28 shows the percentage arsenic removal from an initial concentration of 1000 µg/l, using 9 and 10 mg/l Fe and TiO_2 respectively. These results indicated a significant increase in removal efficiency on the batch scale experiments, needing only 3 hours irradiation time (compared to 9 hours in batch tests). Again, it should be noted that the suspended TiO_2 particles used must be removed after UV treatment. However, research has been carried out on the development of TiO_2 immobilised on an insert of efficient geometry for maximum particle hits for solar disinfection applications (Misstear, 2010) which could prove to have an equal promise for such a continuous flow SORAS system. The subject of immobilsed photcatalysts still requires further research however.

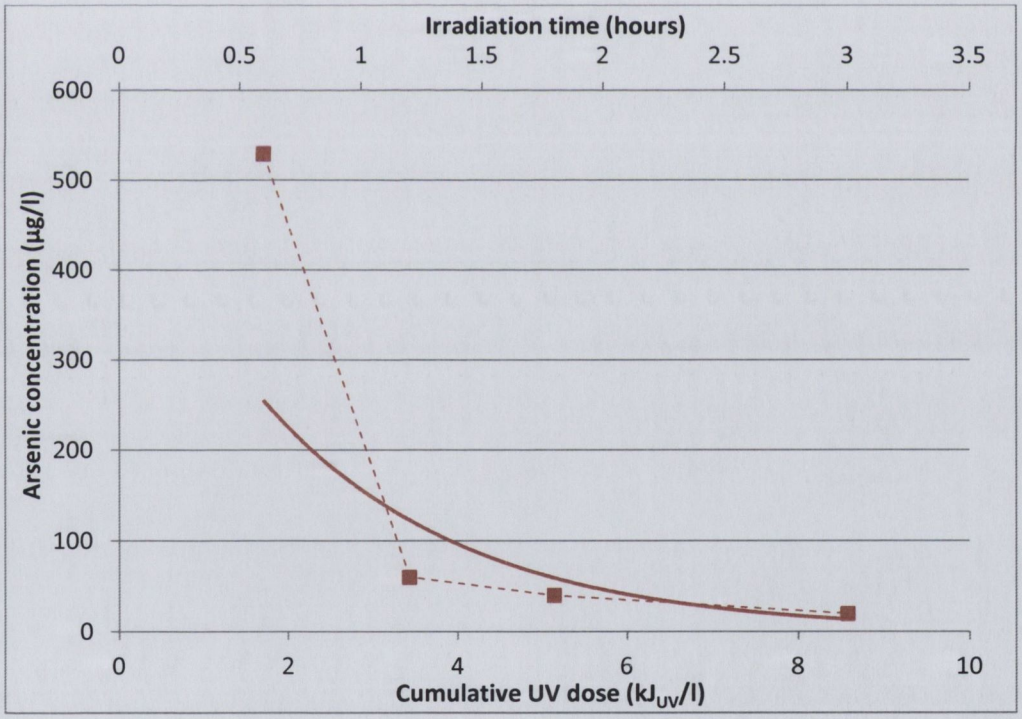

Figure 4.28 *Plot of As removal against cumulative UV dose and irradiation time (initial As: 1000 µg/l, Fe 9 mg/l, TiO_2 10 mg/l)*

4.10 Large scale testing

Experiments using the large scale reactor (Section 3.1.5.2) were carried out as detailed in Section 3.2.3.1. All of these experiments took place outside in natural sunlight in Dublin, Ireland, using the same starting concentrations of arsenic as the small scale tests and a range of iron dosages.

4.10.1 Light intensity

As the intensity of UV-A light and the irradiation time are critical factors in the SORAS process, this section will detail some aspects of light intensity encountered in the experiments under natural light. Diurnal UV-A patterns follow those of global radiation closely, and recordings from both radiometers concur with this. Figures 4.29 and 4.30 show intensities for a sunny and overcast day respectively. UV-A was found to average 6% of total global radiation, generally agreeing with previous studies (Kudish *et al.* (2005) reported averages of 4-5% in studies conducted in Israel). For the most part, higher proportions of UV-A seen during dips in total global radiation, which would seem to be due to proportionally more scattering of longer wavelength light by clouds. As UV-A has been shown to be by far the dominant spectrum in adsorption of photons by Fe (Hug *et al.*, 2001), UV-B readings are not recounted here (though they imitated the UV-A activity closely at much lower intensities – by a factor of 2.3×10^{-3} on average).

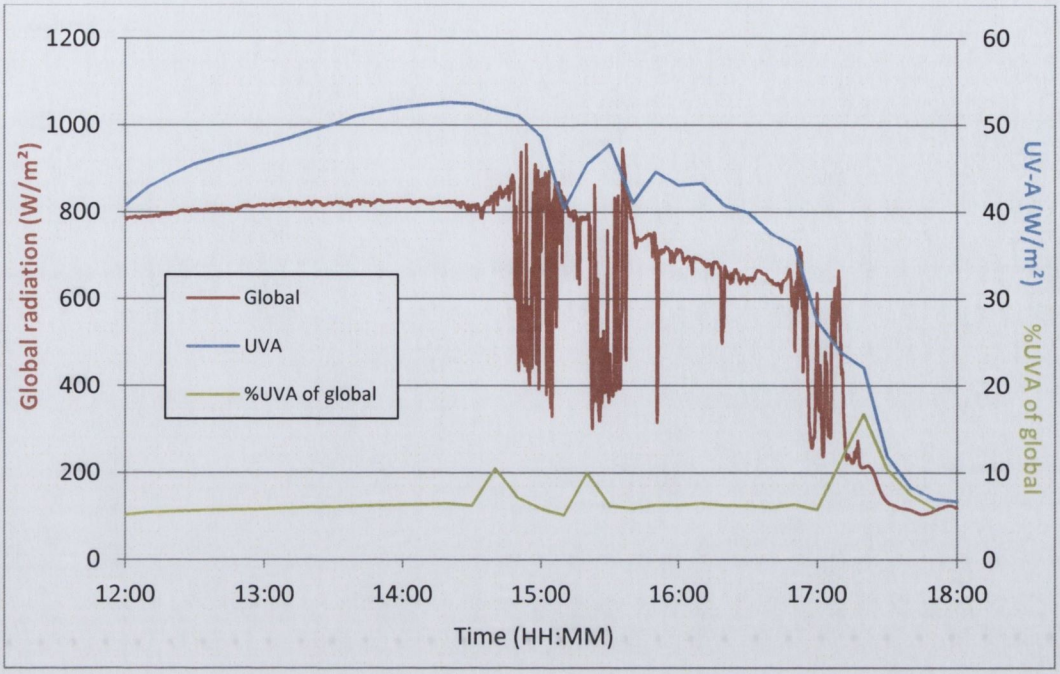

Figure 4.29 *Light intensity data for 27th July 2011 (sunny day)*

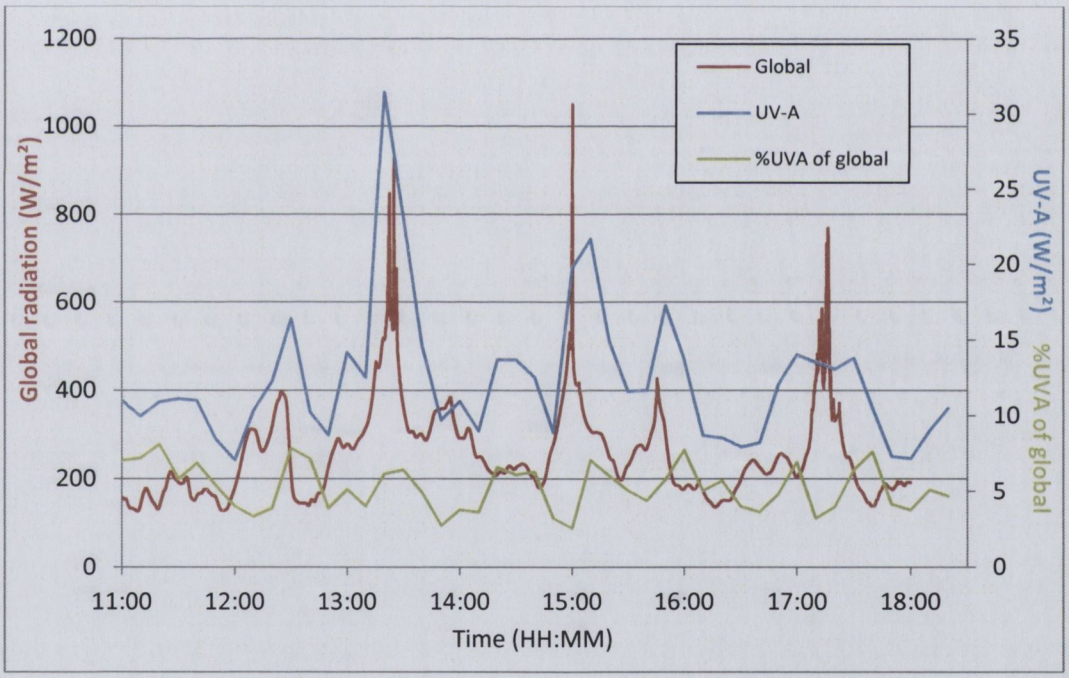

Figure 4.30 *Light intensity data for 19th July 2011 (overcast day, intermittent clouds)*

Figure 4.31 displays average diurnal UV-A readings from Coimbatore (southern India) for different months of the year (Balasaraswathy *et al.*, 2002). The measurements clearly show a significant increase in UV-A compared to the readings taken in our study as expected

(note: the units for UV-A are in mW/cm^2 - to convert to W/m^2 for comparison with the values given in Figure 4.29, the Coimbatore readings need to be multiplied by 10).

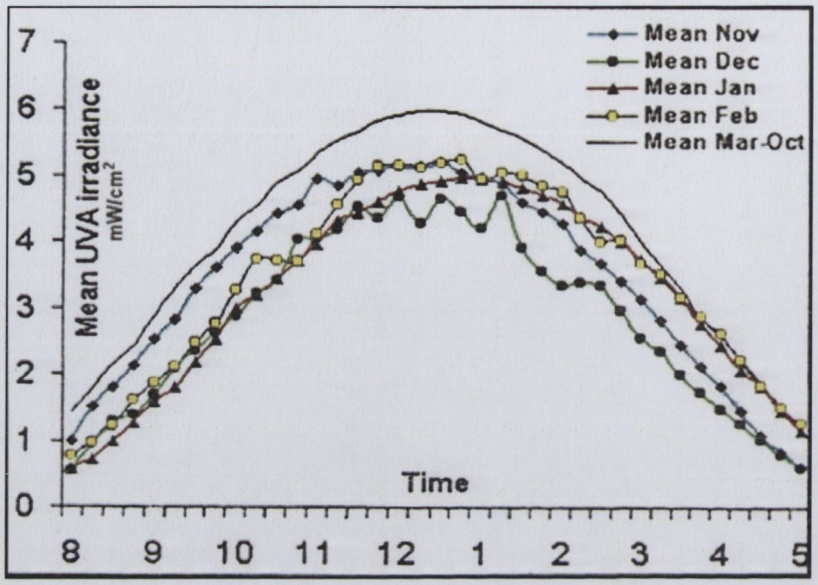

Figure 4.31 *Light intensity data for southern India* (Balasaraswathy *et al.*, 2002)

The cumulative UV dose (cumulative solar flux) was calculated using the following formula:

$$Q_{uv,n} = Q_{uv,n-1} + \frac{\Delta t_n UV_{G,n} A}{V_T} \qquad \text{(Eq. 4.1)}$$

where Q_{UVn} and Q_{UVn-1} are the cumulative irradiated UV energy received per litre of sample at times n and n-1; Δt_n is the time interval between sampling times; $UV_{G,n}$ is the average incident radiation on the irradiated area; A is the irradiated area; and V_T is the total circulating volume.

4.10.2 Optimum iron dosage

Three different initial arsenic concentrations were tested in the large scale reactor (Section 3.2.3) with varying amounts of iron, as in the small scale experiments (As: 1000, 500 and 100 µg/l). For all initial arsenic concentrations, the large scale reactor performed better than the small scale, needing smaller iron dosages for removal below the target MCL. This is most likely due to the more effective transmission of light through the larger diameter tubes, with a greater surface area for direct sunlight. Each combination of initial arsenic and iron concentrations were tested on at least 3 different days during the summer months, with varying weather conditions. Figures 4.32-4.34 show the results from all the large scale tests, with the remaining arsenic concentration this time plotted against cumulative UV dose (kJ_{UV}/l), as the UV intensity was constantly changing throughout the day (Section 4.9.1). As the data points generally match extremely well, irrespective of the particular day the test was carried out, we can conclude that arsenic removal is directly proportional to UV dose. The 'low' initial arsenic concentration results had the most variation, and this could be attributed to the difficulties mentioned earlier in removing smaller amounts of arsenic. The optimum dosages found in this set of experiments for 1000, 500 and 100 µg/l initial arsenic (over 4 hours actual irradiation time) were 10, 8 and 5 mg/l iron respectively. (These optimum iron dosages could even be slightly less depending on the cumulative solar flux, but would require further testing.) As in the small scale tests, the lower iron dosages removed arsenic at high percentages (e.g. 90, 88 and 75% removal at the lowest tested iron dose for 1000 µg/l, 500 µg/l and 100 µg/l initial arsenic respectively (and at the same cumulative UV dose as the most effective iron dose)), These results indicate great potential for the system in the field, where even more sunlight would be available (Section 4.9.1)

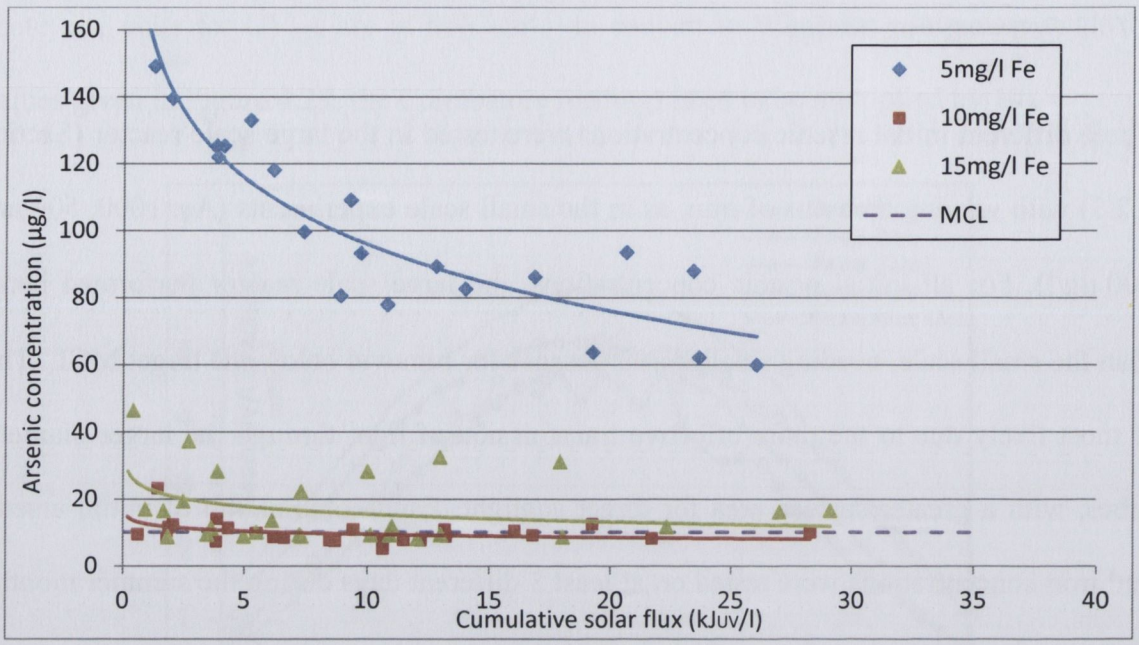

Figure 4.32 *As concentration against cumulative UV-A flux (initial As 1000 µg/l)*

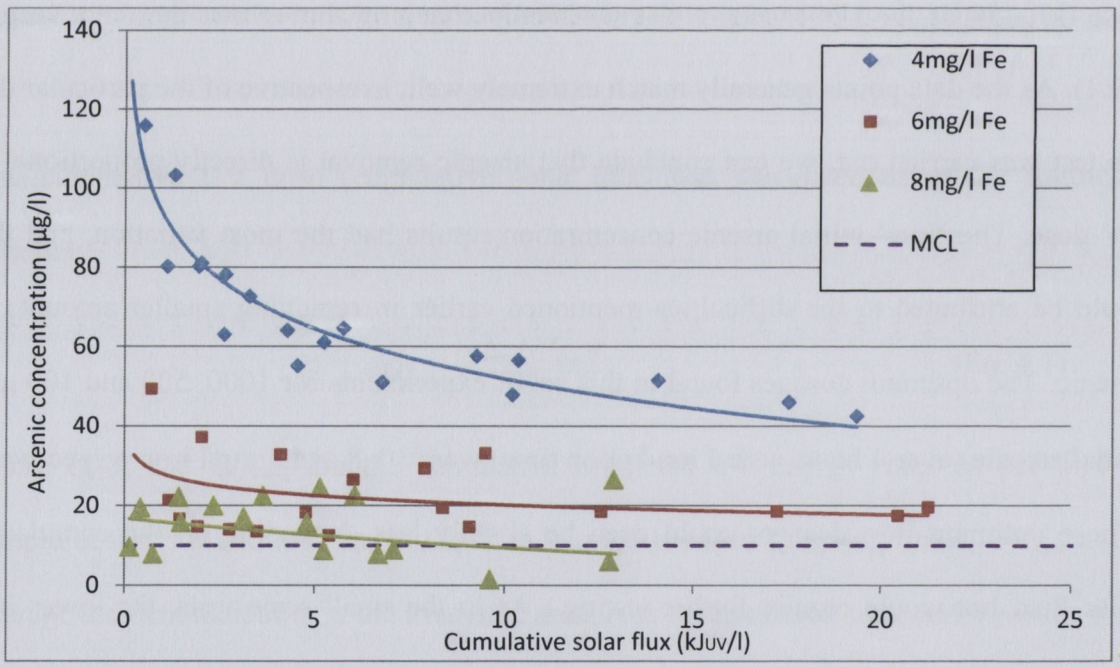

Figure 4.33 *As concentration against cumulative UV-A flux (initial As 500 µg/l)*

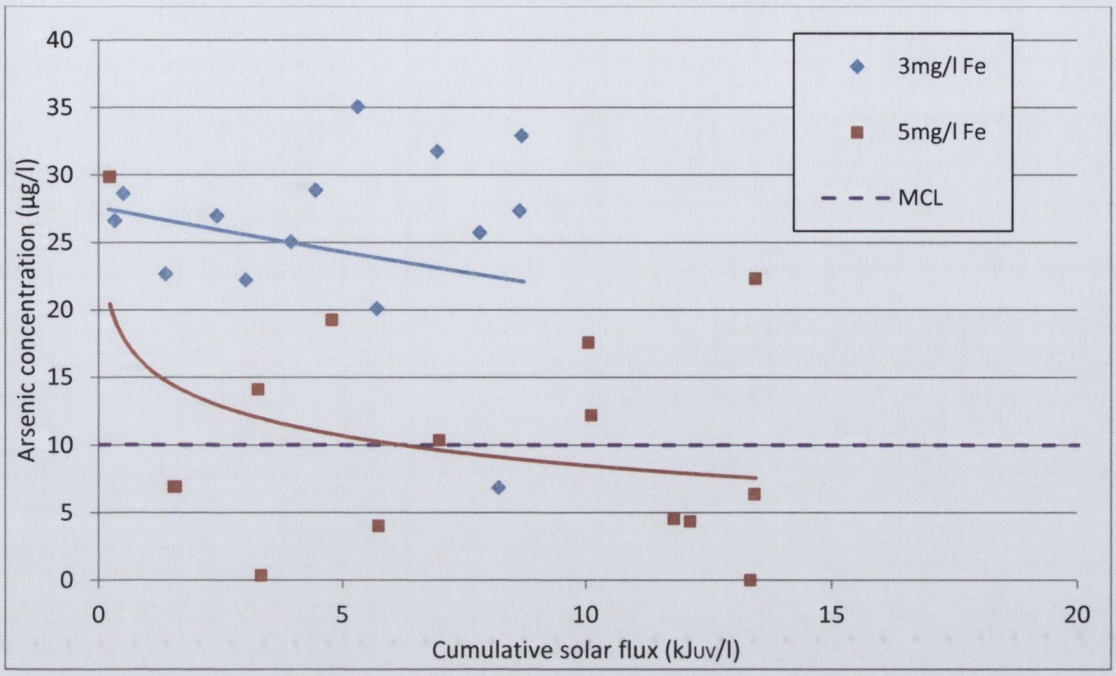

Figure 4.34 *As concentration against cumulative UV-A flux (initial As 100 µg/l)*

To compare the removal performance of the continuous flow system between the large and small scale experiments, the removal rates at the optimum iron dosages were plotted against cumulative solar flux (Figure 4.35). Using the large scale reactor (irrespective of initial concentration), removal to below 10 µg/l was achieved between 5 and 7.5 kJ_{UV}/l, thus indicating the threshold required for effective arsenic removal. The removal pattern using the small scale reactor was considerably different, with the 'high' and 'medium' arsenic doses needing 10 to 12.5 kJ_{UV}/l, and 'low' requiring less than 2.5 kJ_{UV}/l. Again, this could be attributed to the more effective transmission of light in the large scale reactor. Figure 4.36 shows the requisite iron concentration for different initial values of arsenic for both the small and large scale (given the necessary cumulative UV dose has been reached). These curves display a similar pattern with an offset from the more efficient removal capabilities of the large reactor. Interestingly, at the 'low' initial arsenic concentration (100 µg/l), both systems needed 5 mg/l for effective removal, reiterating the evidence that it becomes more challenging to remove contaminants at lower concentrations.

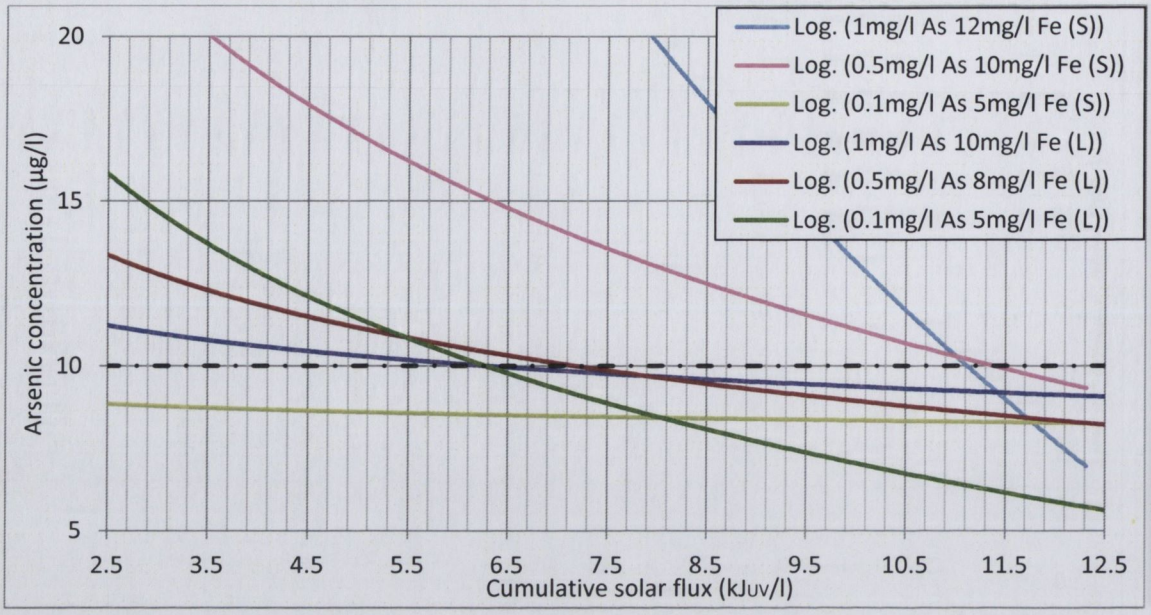

Figure 4.35 *As concentration against cumulative UV-A flux (S=small scale, L=large scale)*

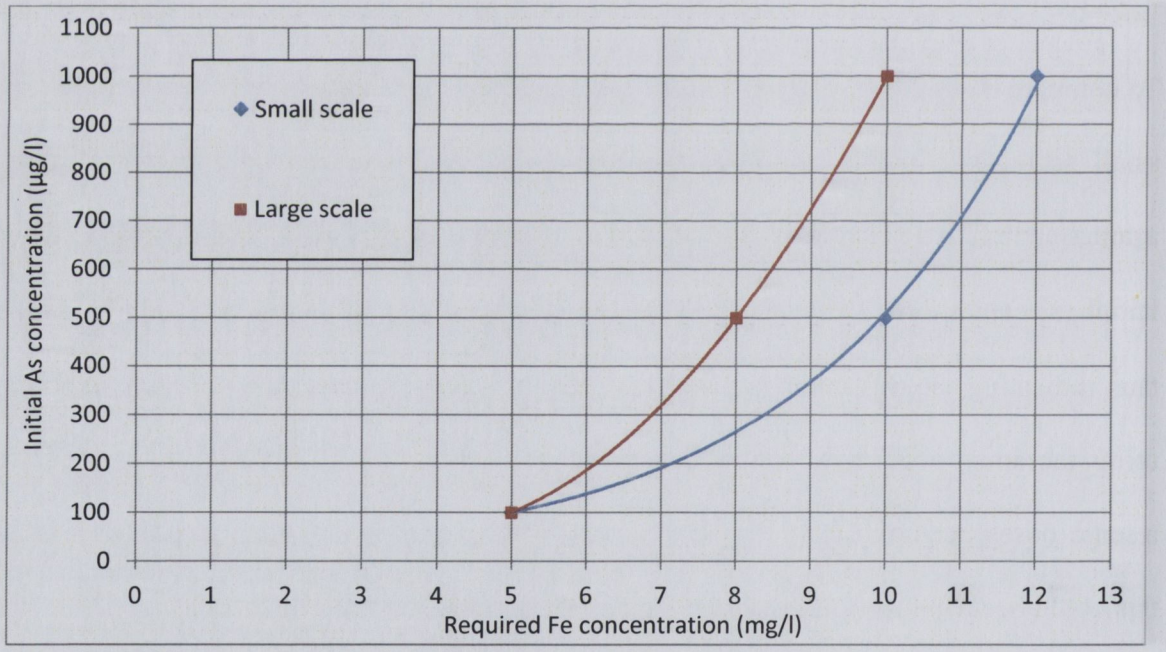

Figure 4.36 *The iron requirement for varying arsenic starting concentrations to reduce the As concentration to 10 ug/l (once there has been the threshold cumulative dose of UVA)*

The driving factors behind arsenic removal in the SORAS process are the iron requirement and the cumulative UV dose. Despite having a much greater UV dose, a lower initial iron content did not result in arsenic concentrations of below the required MCL of 10 µg/l. This

indicates that iron is the limiting factor, as stated previously its capacity is bound in terms of adsorption sites. However, even with the necessary iron concentration, the UV threshold of 7.5 kJ_{UV}/l must also be met.

4.10.3 Effect of temperature

As discussed previously, higher temperatures had a positive impact on arsenic removal rates in the small scale tests. Temperature readings during the large scale reactor experiments were taken at the outlet from the reactor from the bottom pipe, and at the upper reservoir (inlet) (see Figure 4.37), every minute during the course of the experiments. There was an average difference in temperature of 0.04°C between upper reservoir and outlet from bottom tube of reactor (the slightly higher temperature recorded at the outlet), indicating the mean increase in heat generated over time in the illuminated tubes. When this data was analysed along with the arsenic removal data, no difference was seen with any change in temperature. The evidence is not conclusive however, as the average difference in temperature that occurred was never greater than 15°C. Figure 4.38 gives an example of temperatures in the reactor and ambient outdoor temperatures from a 'hot' (red lines) and 'cold' (blue lines) day. The reactor temperatures averaged 33.1 and 19.1°C, and the mean outside temperatures were 21.3 and 16.2°C for the hot and cold days respectively. The change in overall arsenic removal efficiency between these two days (shown in Figure 4.39) was only ±0.5%, hence the effect of temperature in large scale experiments within this temperature range would appear to be minimal. The actual time in the reactor was also comparable. However, this issue could certainly undergo further investigation which would involve either field testing in the appropriate climatic conditions, or indoor experiments carried out in a temperature controlled environment.

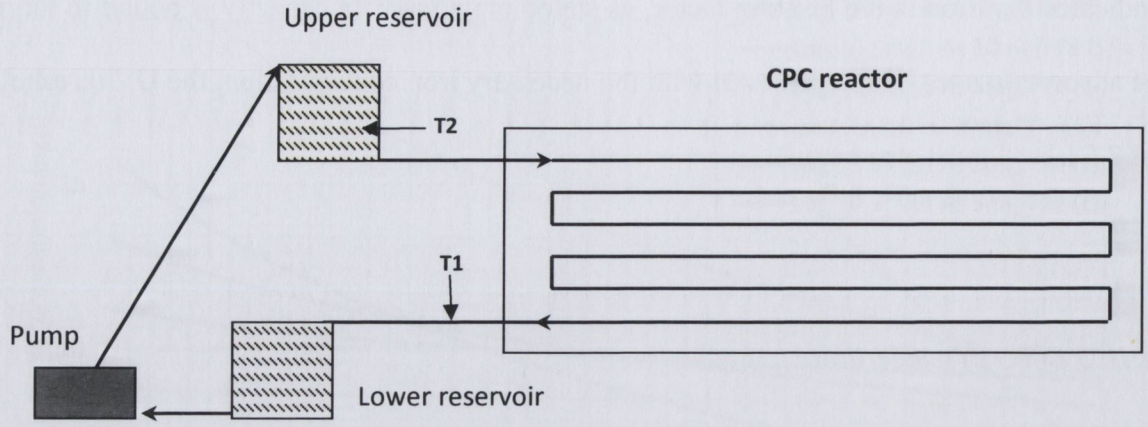

Figure 4.37 *Large scale reactor set up indicating locations of temperature probes*

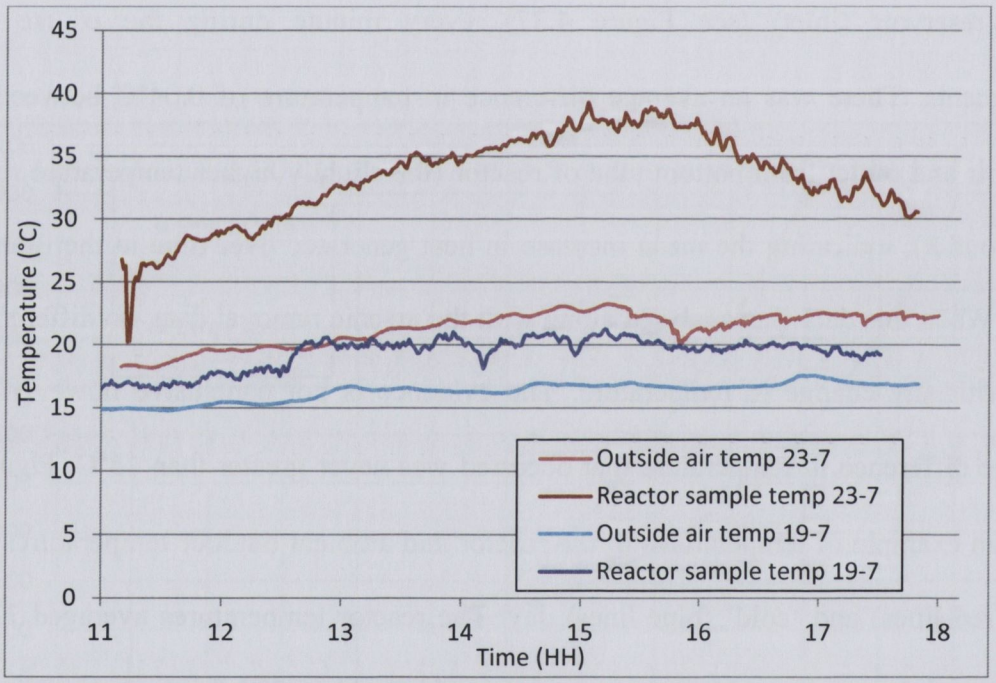

Figure 4.38 Temperature variation with time of day (reactor and ambient)

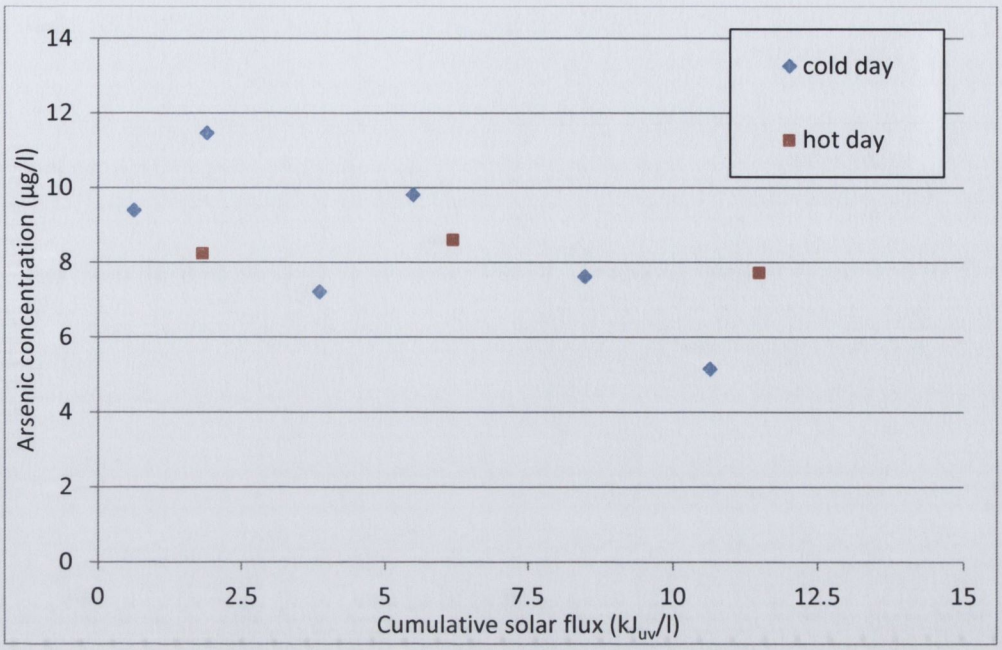

Figure 4.39 *Arsenic removal during hot and cold day (initial As:1000 µg/l, Fe: 10 mg/l)*

4.11 Combined SORAS-SODIS experiments

As described in Section 3.2.3, microbiological experiments were carried out on the large scale reactor in parallel to the As removal experiments to investigate the potential for combined solar disinfection and As removal in such a continuous flow process. A review of international literature to date indicates that it appears that no SORAS testing has been conducted to examine the possible effects of SORAS on SODIS or vice-versa. Although, in general, groundwater has very little pathogenic contamination, many areas with surface water arsenic problems (mainly due to mining) could also present a water source which is also prone to such microbiological contaminants. An initial arsenic concentration of 1000 µg/l was chosen with 5, 10 and 15 mg/l iron, and initial *E. coli* concentrations of $5x10^3$ to $2x10^6$ CFU/ml were added as an indicator organism for enteric bacterial contamination. It must be stressed that these experiments were not directly comparable to the previous data due to differing experimental conditions, namely the use of distilled

water. Figures 4.40-4.42 show the arsenic removal alongside bacterial degradation for these experiments. The most important value for comparative purposes from the microbiological aspect is the inactivation rate of the bacteria. The inactivation rate constants k_{UV} (l/kJ) were derived from Chick's Law:

$$\frac{dN}{dt} = -kN \rightarrow N_t = N_0 e^{-k_t t} \qquad \text{(Eq. 4.2)}$$

$$\frac{dN}{dQ_{UV}} = -kN \rightarrow N_t = N_0 e^{-k_{UV} t Q_{UV}} \qquad \text{(Eq. 4.3)}$$

The results show very similar *E. coli* inactivation rates between tests carried out with comparable initial concentrations. The difference in k values vary from 0.03 to 0.17 l/kJ. The plots clearly show a large reduction in arsenic removal efficiency compared to the tests conducted without microbiological addition (Section 4.9). Removal ranged from 20-45% in these tests compared to 90-99% previously (depending on iron concentration) at the required UV dose found above. Interestingly, the kinetics of As removal also differed from the previous experiments, as a linear decrease was seen in the microbiological tests, compared to a exponential increase when no bacteria were present. This indicates that any microorganisms (and possibly other organic matter) present in the water to be treated can have a severely adverse effect on arsenic removal, and so must be taken into account in the design of any full-scale system. Arsenic removal improved with increasing *E. coli* concentrations and interestingly, decreasing iron content. Conversely *E. coli* removal reduced with decreasing iron concentrations and increasing starting concentrations of bacteria. Thus, it is postulated that a significant amount of the reactive oxygen species (ROS) generated by the iron photolysis were used up in the degradation of the bacteria, hence the smaller amounts of iron present creates less ROS for the disinfection process to

exploit, and more opportunity is given to As species to react. Arsenic could also be having an effect on the bacterial inactivation, whereby arsenic can inhibit DNA repair mechanisms (as has been reported by Rossman *et al.* (1975)) and leave the bacteria more vulnerable to disinfection. The higher concentrations of *E. coli* may also be generating ROS and hence improving arsenic removal.

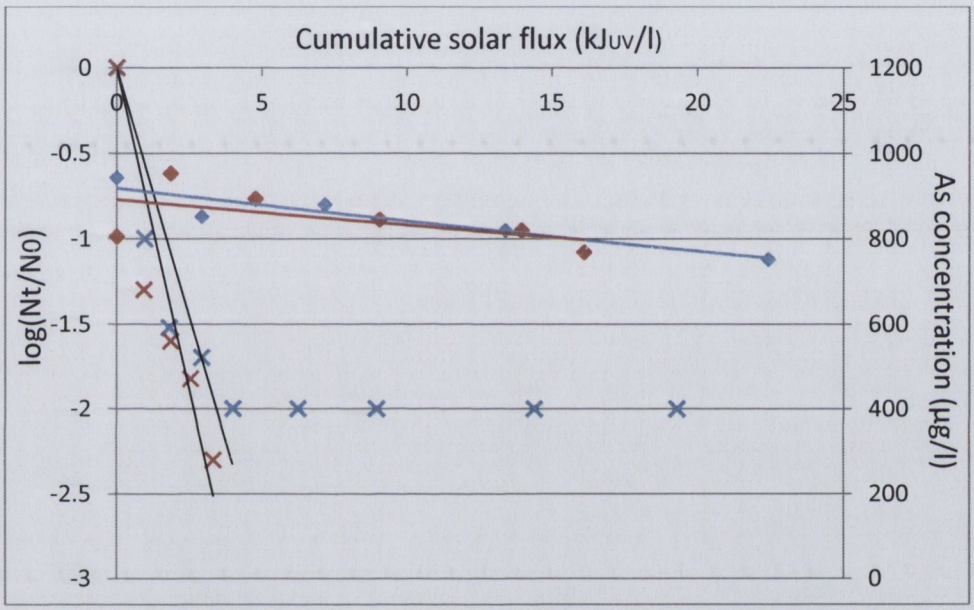

Figure 4.40 Plot of log decay in bacteria and remaining arsenic concentration against cumulative solar flux. Initial conditions: As 1000 µg/l, Fe 15 mg/l, *E. coli* 5-10 x 10^3 CFU/ml. Test 1: ◆As, x *E. coli*; Test 2: ◆As, x *E. coli (The inactivation rate constants for test 1 and 2 were k_1=0.754 and k_2=0.581 respectively)*

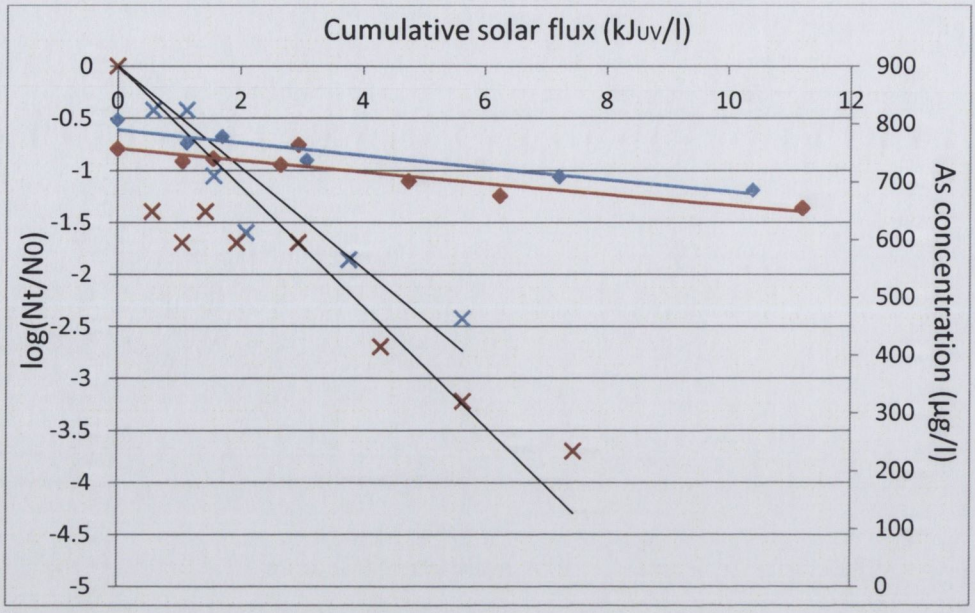

Figure 4.41 Plot of log decay in bacteria and remaining arsenic concentration against cumulative solar flux. Initial conditions: As 1000 µg/l, Fe 10 mg/l, *E. coli* 4-25 x 10^4 CFU/ml. Test 1: ◆As, x *E. coli*; Test 2:◆ As, x *E. coli (The inactivation rate constants for test 1 and 2 were k_1=0.485 and k_2=0.576 respectively)*

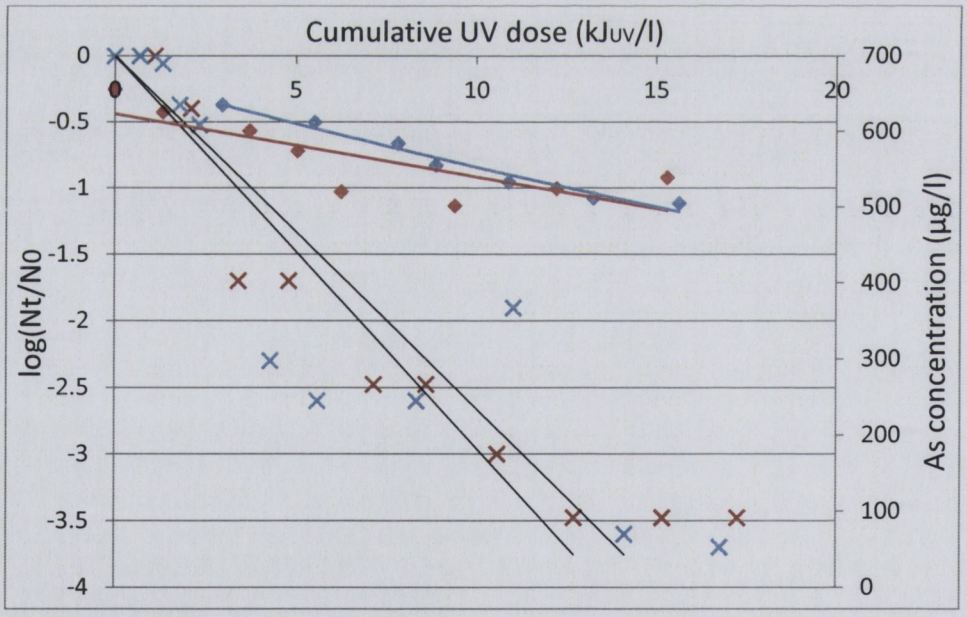

Figure 4.42 Plot of log decay in bacteria and remaining arsenic concentration against cumulative solar flux. Initial conditions: As 1000 µg/l, Fe 5 mg/l, *E. coli* 1.5-2 x 10^6 CFU/ml. Test 1: ◆As, x *E. coli*; Test 2:◆ As, x *E. coli (The inactivation rate constants for test 1 and 2 were k_1=0.295 and k_2=0.266 respectively)*

Comparing the bacterial decay reaction kinetic values found here with Misstear (2010), who carried out solar disinfection experiments using distilled water on the same large scale reactor used in this study, reveals a marked difference in removal rates of bacteria. The k values found in that study ranged from 0.67 to 1.19, whereas the present experimental results give values of 0.27 to 0.75 (see Table 4.2 for summary). This suggests the parallel arsenic removal process is also having a negative effect on bacterial removal, as could be expected due to the increased competition for the ROS.

Experimental values	Test 1	Test 2	Test 3
C_0 As µg/l	1000	1000	1000
C_0 *E. coli* CFU/ml	5-10e^3	4-24e^4	1.5-2e^6
C_0 Fe mg/l	15	10	5
Mean k_1 (As)	0.075	0.227	0.321
Mean k_2 (As)	0.008	0.014	0.014
Mean k_{1b} (As)	1.8	3.4	0.83
Mean k_{2b} (As)	0.008	0.006	0.03
Mean k (*E. coli*)	0.67	0.53	0.28
Mean k_c (*E. coli*)	0.93	0.93	0.93

Table 4.2 *Comparison of removal coefficients (Note: k1b and k2b from study without bacteria addition – Section 4.9.2; kc is average value found by Misstear (2010) (without using As or Fe))*

It should also be noted that stresses caused by the absence of nutrients and ions in distilled water can make bacteria prone to disinfection and less capable of repair mechanisms in the dark (Malato *et al.*, 2009; Wist *et al.*, 2002).

4.12 Other testing issues

The following is a discussion of other issues that arose during testing that cannot be dealt with in the sections above.

4.12.1 Particulate conglomeration in the reactors

One important design and maintenance issue of a full scale SORAS treatment system is the periodic cleaning that would have to be carried out due to the phenomenon of Fe-As particles sticking to the inner walls of the reactor tubing that was noticed during the experimental tests. Figure 4.43 shows this particulate build up in the small scale reactor tubes (after approximately 30 days consecutive testing). More extensive adhesion was observed in the plastic tubing as opposed to glass, and at the joints of connecting tubes. If the precipitate was allowed to build, the UV transmission would be reduced and the reactor would become less efficient. A greater amount of particle adhesion was noticed in the small scale tubing than in the large scale. The cleaning procedure used in the experiments, i.e. rinsing with a dilute acid, would be the easiest method of cleaning as minimal manual labour would be required, however the chemicals needed would add to the cost. To avoid the expense incurred by chemicals, and the logistical problems in transporting them to rural areas, the reactor tubing could simply be cleaned with pipe cleaners and water, which was also carried out on both reactors and proved successful.

Figure 4.43 *Precipitate adhesion to reactor tubing*

4.12.2 Arsenic concentration and speciation

It must be noted that the reaction rate coefficient k_1, is increased significantly from the initial rapid precipitation of arsenic and iron. Despite arsenic being added as As(III), initial samples taken prior to irradiation were up to 50% less than that added initially. Hug *et al.* (2001) reported an average As(III) reduction of 20% after iron addition and before illumination, despite arsenic being added as As_2O_3. This phenomenon was also observed by Garcia *et al.* (2004), whereby up to 40% removal occurred before irradiation. This is most likely caused by high dissolved oxygen levels promoting quick As oxidation, and the almost instantaneous co-precipitation with iron from mixing in the reactor (or vigorous shaking of bottles in batch tests), and as discussed in Section 4.7, As(III) adsorption onto iron.

Due to time and financial constraints, no speciation studies were carried out; hence the arsenic oxidation states cannot be reported. Based on the literature however, it has been assumed that any arsenic remaining after SORAS treatment was in its trivalent or pentavalent form.

4.12.3 Remaining iron concentrations

Iron is not deemed a health hazard in drinking water, as concerns over higher amounts are considered an aesthetic issue only - namely taste and colour (WHO, 2006), so the drinking water guidelines quote 0.3 mg/l as the maximum allowed. Not every SORAS sample was tested for iron, but all that were complied with this regulation, ranging from 0.04 to 0.19 mg/l. (Note: Garcia et al. (2004) reported final iron concentrations of below 0.3 mg/l in batch tests in over 52% of samples, the remainder averaged 1.79 mg/l).

CHAPTER 5: PRECIPITATE REMOVAL

5.1 Introduction

As described previously, effluent from the continuous flow reactor contains arsenic-iron precipitates that need to be removed from the water before it is safe for consumption. Samples taken from the laboratory and natural sunlight tests in this study have been left in darkness for the precipitate to settle by gravity for up to 48 hours, and in field trials, they have been left to stand overnight (Hug *et al.*, 2001). This may be suitable in a household scale scenario with relatively small water volumes, but in a full scale treatment system would be impractical. Hence, this chapter will investigate the nature of the precipitating particles, the settlement process and the possible methods for the enhancement of the continuous flow process. It is important to note again that appropriate technology methods are preferred for this research owing to the ultimate aim of implementing these systems at community level in rural areas in developing countries.

5.2 Background

5.2.1 Coagulation-Flocculation

As settlement of colloidal particles from solutions is usually very slow, chemicals (coagulants) are added in water/wastewater treatment processes to increase removal efficiency. The particles, or colloids, usually carry a negative electrical charge with diameter ranging between 10^{-4} and 10^{-6} mm. This negative charge inhibits agglomeration and the lack of agglomeration

combined with their low specific gravity results in a resistance to settlement. Coagulants are typically positively charged compounds that destabilise the particles enabling them to get close enough to allow the attractive van der Waals forces to take over (Bratby, 2006). Rapid, or flash mixing is vital upon introduction of the coagulant to ensure uniform dispersion and increased opportunity for inter-particle contact, and much research has been conducted in this area (Rossini *et al.*, 1999; Dharmappa *et al.*, 1993; Mhaisalkar *et al.*, 1991). Once the charges have changed, they adhere partly by this electrical attraction and partly by cohesion between the interlocking spaces on the surface. The charges are somewhat neutralised as the particles stay in contact with each other and the floc takes on a common charge. Cohesion is then the predominant force holding the floc together. The main factors affecting coagulation are listed in Table 5.1.

Coagulant Characteristics	**Physical Characteristics**	**Raw Water Characteristics**
• Coagulant type • Coagulant dose • Proper solution makeup and dilution • Proper coagulant age	• Settling time • Mixing intensity • Mixing time • Coagulant addition point • Proper coagulant feed	• Suspended solids • Temperature • pH • Alkalinity • Presence of microorganisms and other colloidal species • Ionic constituents (sulfate, fluoride, sodium, etc.)

Table 5.1 *Factors affecting coagulation (Murcott et al., 1996)*

The most commonly used coagulant chemicals are salts of aluminium and iron, as they are 3^+ charged ions and are also cheap, efficient, and easy to use and store. The majority of these chemicals are acid salts, and therefore lower the pH of the solution. The particle surface charge and floc precipitation are affected by pH during coagulation, so an alkali may also

needed to be added when they are used. Both alum and ferric based coagulants destabilize the particles in water through hydrolysis. Lime is also a commonly used coagulant but works differently to alum and iron, as it increases the pH of the solution, and the resulting carbonate ions, namely $CaCO_3$ conglomerate with the particles that need to be removed. Table 5.2 details the advantages and disadvantages of conventional coagulants used in water/wastewater treatment.

Name	*Advantages*	*Disadvantages*
Aluminum Sulfate (Alum) $Al2(SO_4)_3.18H_2O$	Easy to handle and apply; most commonly used; produces less sludge than lime; most effective between pH 6.5 and 7.5	Adds dissolved solids (salts) to water; effective over a limited pH range.
Sodium Aluminate $Na_2Al_2O_4$	Effective in hard waters; small dosages usually needed	Often used with alum; high cost; ineffective in soft waters
Polyaluminum Chloride (PAC) $Al_{13}(OH)_{20}(SO_4)_2.Cl_{15}$	In some applications, floc formed is more dense and faster settling than alum	Not commonly used; little full scale data compared to other aluminum derivatives
Ferric Sulfate $Fe_2(SO_4)_3$	Effective between pH 4–6 and 8.8–9.2	Adds dissolved solids (salts) to water; usually need to add alkalinity
Ferric Chloride $FeCl_3.6H_2O$	Effective between pH 4 and 11	Adds dissolved solids (salts) to water; consumes twice as much alkalinity as alum
Ferrous Sulfate (Copperas) $FeSO_4.7H_2O$	Not as pH sensitive as lime	Adds dissolved solids (salts) to water; usually need to add alkalinity
Lime $Ca(OH)_2$	Commonly used; very effective; may not add salts to effluent	Very pH dependent; produces large quantities of sludge; overdose can result in poor effluent quality

Table 5.2 *Advantages and disadvantages of inorganic coagulants (US Army, 2001)*

Natural coagulants of plant and soil origin have been used for centuries in developing countries for water treatment (Schulz and Okun, 1984). *Moringa oleifera* is a non-toxic tropical plant belonging to the *Moringacae* family and is found throughout India, Asia, sub-Saharan Africa and Latin America. Laboratory studies have shown that *Moringa oleifera*

seeds possess effective coagulant properties (Ndabigengesere *et al.,* 1995, 1998a; Babu and Chaudhuri, 2005). It has also been traditionally used in water purification in Sudan (Jahn, 1981, 1986). Dhekane *et al.,* (1970) showed success in using the seeds of the *Strychnos potatorum* or Nirmali tree (found in India) as a natural coagulant. Two plant materials, *Cactus latifaria* and the seeds of *Prosopis juliflora* (mesquite bean), were investigated to remove turbidity in drinking water in Venezuela by Diaz *et al.*, 1999. Both materials' performance was comparable to that of *Moringa oleifera*, and were needed at lower dosages than aluminium sulphate for the same purpose.

The process of coagulation is often enhanced through the use of coagulant aids. In cases where even large doses of primary coagulant will not produce a satisfactory floc, polymeric coagulant aids can be added after the coagulant to hasten reactions and produce denser floc (Bratby, 2006). Polyelectrolytes can be anionic, cationic or non-ionic, depending on their application. They have relatively high molecular weights (up to 20,000,000) and function primarily through inter-particle bridging. Advantages of using polyelectrolytes include the fact that they do not affect pH or add to the total dissolved solids concentration and produce less sludge (EPA Ireland, 2002). They can also be used to reduce the dosage or eliminate the need for the inorganic coagulants discussed above. Activated silica has been used for many years as a coagulant aid in conjunction with aluminium and iron coagulants (EPA Ireland, 2002). Currently, many synthetic polyelectrolytes, usually polyacrylamides are used in water treatment plants. The charge density and molecular weights of these polyelectrolytes are the most important characteristics to enhance coagulation. Starch extracted from potatoes or corn is recognised as a negatively charged phosphate, bearing natural polyelectrolyte. It has also

been shown to produce excellent flocculation of negatively charged particles (La Mer, 1966 and Campos *et al.*, 1984). Various forms of clay such as bentonite or fuller's earth have also been used as an aid to coagulation.

Flocculation provides the conditions for collisions between particles for them to gather into flocs. The amount of floc formation depends on the rate of the collisions between particles and the effectiveness of the collision in promoting the particles to attach. Flocculation requires gentle agitation of the water to increase contact time between particles and therefore slow speed paddles, turbines, etc. are used in both vertical and horizontal flow systems. The flocs become larger as they continue to agglomerate and due to their size they readily settle by gravity. These larger flocs however, break up easily (due to turbulence for example) more so than smaller, stronger flocs, and if they do separate, they will not coagulate again as the surface charges have been partially equalised. Therefore careful handling of flocs is extremely important in gaining efficient particulate removal (Parker *et al.*, 1972). The factors affecting the rate of flocculation include the velocity gradient, the retention time of the tank, the mixing intensity and the tank shape. The velocity gradient G (s^{-1}) is a measure of the degree of mixing, and is a function of the power input to the water. Flocculation chamber design is based on the dimensionless parameter Gt, which is the velocity gradient times the residence time t (seconds).

$$G = \sqrt{\frac{P}{(\mu V)}}$$

Where, G = velocity gradient (s^{-1})

P = power transmitted to the water (W)

V = volume of water to which the power is applied (m^3)

μ = dynamic viscosity of water ($kgm^{-1}s^{-1}$)

Power transmitted in a batch reactor i.e. jar test, can be obtained from the reactor geometry:

$$P = \rho \cdot \pi^3 \cdot (1\text{-}k)^3 \cdot N^3 \cdot \sum(C_d \cdot L_b \cdot (r_u^4 - r_i^4))$$

Where, P = power transmitted to the water

ρ = density of water = $1000kgm^{-3}$

π = pi (constant = 3.14)

k = constant $\approx$ 0.25

N = rotational speed of blade(s) (revolutions per minute)

C_d = drag constant $\approx$ 1.5

L_b = length of mixer blade (m)

r_u = distance from exterior of mixing blade to axis (m)

r_i = distance from interior of mixing blade to axis (m)

When using alum and iron coagulants during flocculation, G values usually range from 20 to $100s^{-1}$, with residence times from 10 to 40 minutes. Increasing these values beyond floc formation can lead to shearing in particles and floc break up, while below these values flocculation may not occur. Gt depends on the incoming raw water quality and the size of floc required. Table 5.3 gives typical G and Gt values for varying water quality.

Type	$G(s^{-1})$	Gt
Low turbidity, colour removal coagulation	20-70	60,000-200,000
High turbidity, solids removal coagulation	50-150	90,000-180,000
Softening, 10% solids	130-200	200,000-250,000
Softening, 30% solids		300,000-400,000

Table 5.3 *Typical G and Gt values for flocculation (Wang et al., 2004)*

The most effective flocculation systems have been found to be ones that use separate basins in which the turbulence is reduced in succeeding basins by decreased mixing speeds (Metcalf and Eddy, 2003). Table 5.3 gives the experimental conditions used by various authors in jar-test coagulation studies. These were used as the basis of the experimental methods in Section 5.3.3.1.

Contaminant	Coagulant aids	Coagulation	Flocculation	Settlement	References
DOM	Ferric chloride	2 minutes 100 rpm	20 minutes 25 rpm	60 minutes	Dennett *et al.* (1996)
As(III), As(V)	Ferric chloride	1 minute 100 rpm	30 minutes 45 rpm	15 minutes	Hering *et al.* (1996)
Colour, NOM	Alum, Ferric chloride	1 minute 400 rpm	10 minutes 30 rpm	Not reported	Ratnaweera *et al.* (1999)
Turbidity, NOM	Ferric sulphate	1 minute 100 rpm	20 minutes 30 rpm	30 minutes	Khan and Thiem (2008)

Table 5.3 *Experimental conditions of the process of coagulation-flocculation-settlement chosen by various authors*

As mentioned above, mechanical paddles, turbines and impellers are employed to gently mix the water for flocculation. Paddle flocculators (Figure 5.1) comprise of a number of paddles attached to a shaft which rotates slowly and can be vertical or horizontal systems. The size and shape of the paddles, as well as the rotational speed are adjusted to enhance the process. Turbine and propeller flocculators consist of blades attached to a shaft which rotates to mix the water. Usually these are horizontal systems, comprising of a number of compartments, each propeller reducing speed as the water moves downstream. The blade shape is adjusted to limit the amount of floc break-up. The advantages of mechanical flocculators include: no head loss in the system, reliability and flexibility of method, and generally they produce large flocs. The disadvantages are: maintenance of moving parts, energy requirement, higher costs, and complete shutdown of the system with one component failure or for maintenance.

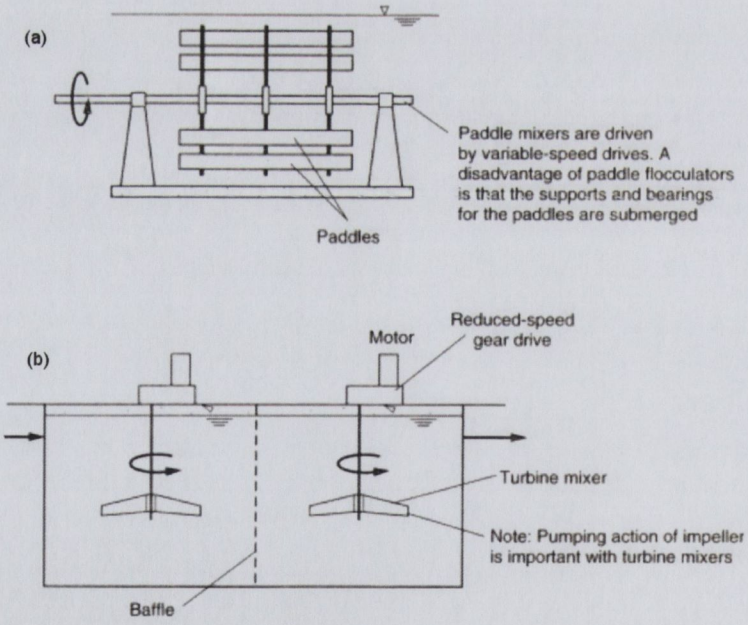

Figure 5.1 *Mechanical flocculators (a) paddle mixed and (b) turbine mixed (Metcalf and Eddy, 2003)*

Hydraulic flocculators utilize the energy dissipation achieved by the change in direction of the flow of water, usually using channels. Mixing occurs by the flow being directed either around or over and under a series of baffles. Figure 5.2 shows both scenarios, whereas Figure 5.3 demonstrates the use of forming a hydraulic jump by narrowing of the channel for flash mixing. Baffled channels are the most common type of hydraulic flocculator, with horizontal systems being preferred over vertical ones as they encounter less build-up of precipitate on the upstream side of the baffles. The channel width and length, and spaces between baffles and baffle and channel wall, are designed for appropriate velocity gradient through the system. The advantages of baffled channels include: low cost, simplicity, no moving parts and so no energy requirement and little maintenance, and effective in producing large flocs. Their disadvantages are: large head losses in the system and little flexibility once geometries are chosen. This type of flocculator design would be an appropriate technology for a small scale system in a developing country. Coarse grained media are also used as hydraulic flocculators, but are less popular than baffled channels. They use various sized and shaped media to promote mixing.

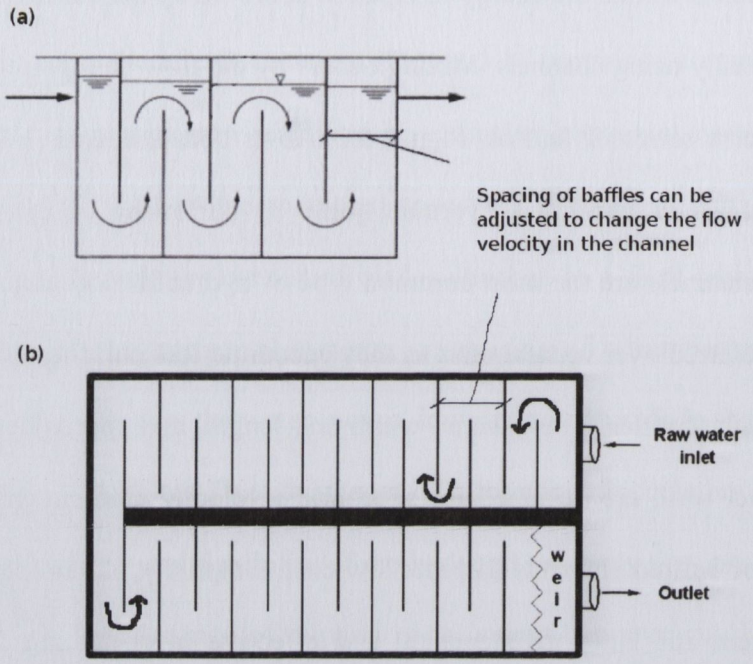

Figure 5.2 *(a) Vertical (over and under) baffled channel in cross section (b) Plan view of horizontal (around the end) baffled channel*

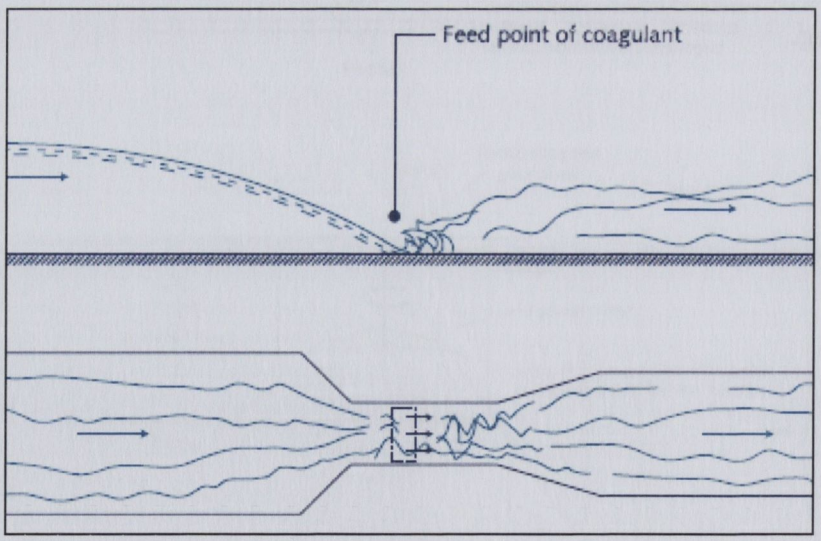

Figure 5.3 *Hydraulic jump (Smet, 2002)*

5.2.2 Clarification

Clarification/sedimentation in water treatment is the removal of suspended solids. With little or no movement, solids can settle by their own weight. The objective is to efficiently separate the clear supernatant water from the flocs, this sludge being disposed of and the clean water going to further treatment or distribution. This is usually achieved by forcing a change in velocity to allow the flocs to settle. Again as little turbulence as possible is required so as not to break up the flocs and enable the natural falling velocity of the flocs to occur. Sedimentation tanks/basins are employed to achieve particle settling. Various types of tank are used, each with their own inlet, settling zone, sludge zone and outlet set-up. The inlet ensures an even distribution of flow, the settling zone is where sedimentation occurs and the flocs accumulate, the sludge zone is where the settled material is deposited for removal, and the outlet directs the supernatant water out of the basin. The settling zone depends greatly on the settling characteristics of the flocs, the surface loading rate – flow rate divided by surface area of the tank, and the tank depth. The particle size and density are needed to calculate the settling velocity.

As the viscosity of the water containing the particles is important in sedimentation, temperature changes can affect performance, therefore settlement is adversely affected by cold. Settling velocities for colloidal particles such as the flocculated 'light' particles, which result from the SORAS process, must be obtained by means of a settling column test in order to design a full scale system.

The sedimentation tank is then designed according to the settling velocity and the flow rate:

$$Q = Av_p$$

where Q = flow rate (m^3/s)

A = surface area of tank (m^2)

v_p = settling velocity of particle

Figure 5.4 shows the four main types of sedimentation basins. The horizontal flow tank is a basic early design still in use today. The velocity is decreased by the large surface area of the tank and the settling zone occurs in the middle of the tank. The base is usually sloped to aid sludge scraping from the sludge zone. In the radial flow system, the inlet is located in the middle of the circular tank. The flow from the centre is baffled to flow outward to the perimeter, hence the horizontal flow is decreasing as it moves to the outlet, enabling the flocs to settle. Again sludge is scraped from the base. The most common type of sedimentation tank is the upflow clarifier. This consists of an inverted pyramid or cone, with the water discharged downwards, turning 180° and flowing back upwards. The velocity decreases as the cross sectional area increases up the tank. As the velocity continues to decrease, the downward weight of the flocs counterbalance the upward force of the rising water causing the flocs to be suspended in a sludge blanket and the supernatant rises to the outlet.

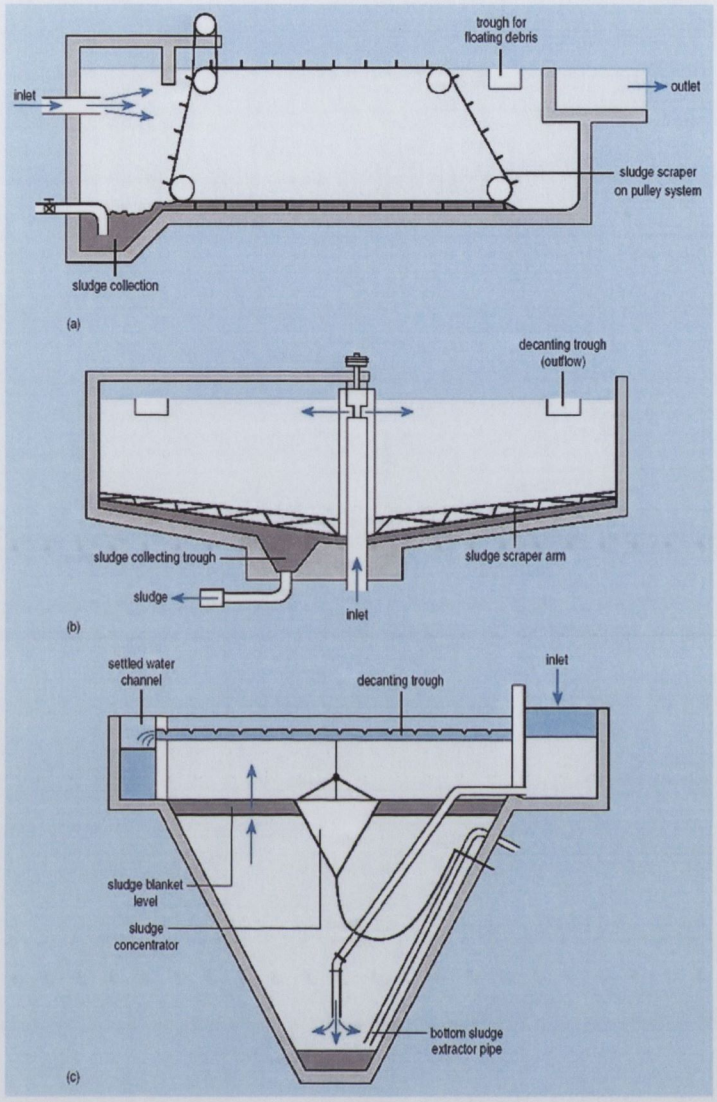

Figure 5.4 *Typical sedimentation tanks (a) horizontal flow rectangular tank (b) radial flow circular tank (c) hopper-bottomed upward flow clarifier (*http://openlearn.open.ac.uk/mod/resource/view.php?id=185898*)*

5.3 Materials and methods

5.3.1 Chemicals

5.3.1.1 Aluminium sulphate

A 1% (10mg/mL) stock solution was prepared by dissolving 2 g of aluminium sulphate powder (Merck $Al_2 (S0_4)_3 .18 H_20$) in distilled water. Approximately 100 mL of distilled water was added initially and the mixture was shaken vigorously to dissolve the alum. Further distilled water was added to make the solution up to 200 mL.

5.3.1.2 Moringa oleifera

The *Moringa oleifera* seed kernels (Figure 5.5) used as a coagulant in this study were obtained from a company based in India called Mother Herbs and Agro Products, and the extract was prepared as follows according to Jahn (1986). The seeds were crushed and ground to a medium fine powder using a pestle and mortar and then stored in dry conditions at room temperature until required. 5 g of the powder was placed in a beaker containing 200 ml of distilled water. This suspension was then mixed thoroughly for approximately 4 minutes in order to extract the active ingredient of Moringa Oleifera. Next, the suspension was passed through a muslin cloth and the filtrate captured in a beaker. Distilled water was again added to the filtrate to bring the solution up to a volume of 500 ml; thus creating a stock solution of 10 g/l.

Figure 5.5 *Moringa oleifera seeds*

5.3.1.3 Potato Starch

Potato starch (Figure 5.6) was produced by first grating approximately 100 g of clean potato. The grated potato was then placed in the mortar and 100 ml of distilled water added. The potato was ground with the pestle carefully and the liquid decanted off through a tea strainer into a beaker, leaving the potato behind. Another 100 ml of water was added to the mortar, the potato was ground and the effluent strained and finally this was repeated for a third time. The mixture was then allowed settle for five minutes before the water was decanted from the beaker, leaving behind the white starch which had settled to the bottom. 100 ml of distilled was added to the starch and the mixture stirred gently, again it was left to settle and the water decanted off, leaving the starch behind. The starch was then made up into a 1% stock solution, 2 g of the powder being dissolved in 200 ml of distilled water.

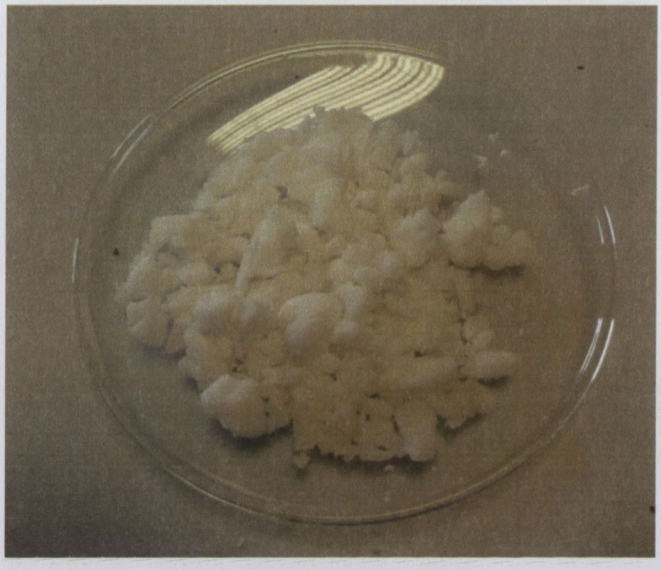

Figure 5.6 *Potato starch*

5.3.1.4 Magnafloc LT22S

Magnafloc(R)LT22S is a high molecular weight cationic polyacrylamide with a particle size of less than 1500 μm and a density of 0.7 g/cm^2. It is supplied as a free-flowing white granular powder, and was chosen as it is an approved coagulation aid commonly used in industry. The stock was made up to 0.01% solution. 0.1 g of Magnafloc(R)LT22S (Ciba) was added to a dry beaker together with 3ml of methanol in order to thoroughly wet out the product. Next, 97 ml of distilled water was added, the beaker closed and the contents shaken periodically over a 45 minute period to complete the process.

5.3.2 Apparatus

5.3.2.1 Flocculation Unit

The flocculation test unit (Armfield, UK) used in the coagulant/polyelectrolyte dose experiments is shown in Figure 5.7. It consisted of an illuminated stand capable of holding

four 1 litre beakers, each having a separate variable speed (25-240 rpm) mechanical paddle mixer, 50 mm in length and 15 mm in depth..

Figure 5.7 *Flocculation unit*

5.3.2.2 Fall Velocity Test Apparatus

The modified bottom withdrawal tube (mBWT) method (5.2.4) was used to calculate the settling velocity of the precipitate. The apparatus consisted of a Perspex tube with a diameter of 50 mm and a volume of approximately 3.5 litres (an example of which is given in Figure 5.8). The base of the open-topped tube was fitted with a funnel and a short rubber tube to collect the samples. The withdrawals were controlled by the positioning of a pinch clam to the rubber tube which acts as a valve for quick withdrawals. The instrument was held in a vertical position during the procedure by a retort stand.

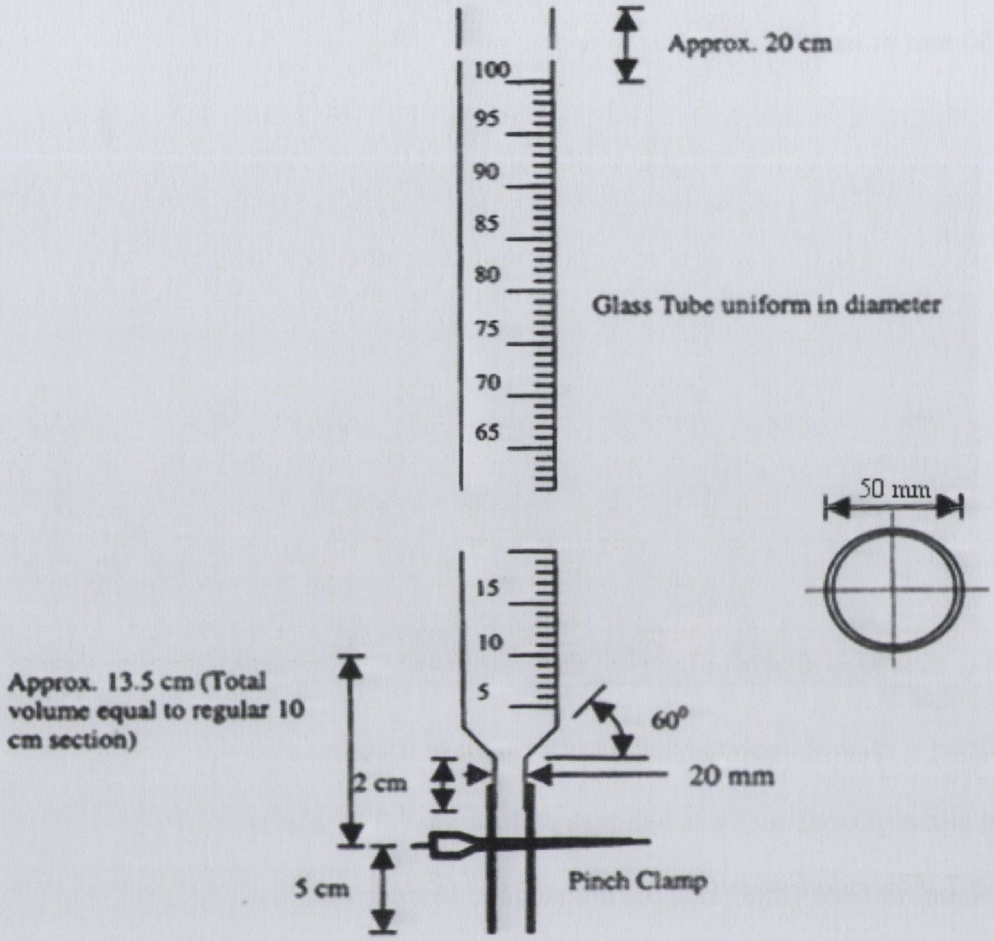

Figure 5.8 *Modified bottom withdrawal tube*

5.3.3 Methodology

5.3.3.1 Flocculation-Coagulation tests

The test was carried out in accordance with the procedure set out by ASTM D2035-08 (ASTM, 2008). Four Pyrex beakers of the test sample were placed on the flocculation unit, the stirrers were switched on, their operation was checked to ensure they were working properly and samples were mixed gently for 1 minute. (All test samples, each 1 litre, were taken

directly from the outflow of the large-scale reactor after an experimental run in natural sunlight (see Section 3.4.1.). Initial concentrations of As and Fe were 1000 μg/l and 10 mg/l respectively.) Dosages of the relevant coagulant were added to three of the beakers. The remaining beaker was used as a control. At the instant of coagulant addition, a 1-minute rapid flash mix (120 rpm) began. At the end of the 1-minute flash mix, a slow mix (30 rpm) was performed for 20 minutes. The velocity gradient G was $300s^{-1}$ for the flash mix and $45s^{-1}$ for slow mixing (information from manufacturer). (Note, the mixing times and rates used in all experiments were based on a previous set of experiments carried out to determine the optimum hydraulic conditions for these tests). The time taken for the formation of visible floc was recorded. Once the flocculation process has occurred, the paddles were removed and the samples were left to settle for 20 minutes (or transferred immediately to the fall velocity test apparatus). These experimental times were based on the literature mentioned in Section 5.3.2. The time taken to the formation of the first visible floc was recorded, as was the size of the flocs formed, the colour and turbidity of the supernatant between the samples and the amount of sedimentation which occurred.

5.3.3.2 Fall velocity tests

A stopwatch was set to zero and the pinch clamp was closed. 3.5 litre samples (either directly from the reactor or from the flocculation unit) were poured into the mBWT (5.3.2.2), and care was taken when transferring the effluent in order to ensure that the flocs formed remained intact in the tube. A rubber bung was placed in the open top of the tube once it had been filled and it was then inverted slowly a number of times to ensure an even distribution of the floc throughout the length of the apparatus. The mBWT was placed in the vertical position in the

retort stand and the timer started (corresponding to time, t = 0). Following this, samples were withdrawn, using the pinch clamp, at time intervals of 2, 10, 20, 40, 60, 80, 100, 120, 150 and 180 minutes to best define the settling characteristics of the sediment. The mBWT was calibrated with markings from top to bottom, corresponding to 5 cm intervals for the first 4 readings and 10 cm intervals for the remainder of the readings. These were necessary only as guideline indicators of the volumes to be withdrawn in each sample. A rapid opening was necessary at the start of the withdrawal to ensure that any deposited settlement was cleared from the cone above the nozzle. Two experiments were carried out for each sample.

The effluent withdrawn in each sample was weighed (determined by subtracting the mass of the (pre-weighed) aliquot from the total mass of the effluent and aliquot). Then, representative samples of each individual aliquot were made by suspending all the sediment in the sample (mixing thoroughly) and pouring a small proportion of this into a graduated cylinder. The volume contained in the graduated cylinder was recorded, and the contents then passed through the suction filter apparatus using (pre-weighed) 0.45 μm 47 mm cellulose membrane filters (Millipore). Two representative filtrations were carried out for each sample. These filter papers containing the sediment (Figure 5.9) from each sample were then placed in an oven at 105°C for 1 hour in accordance with BS1377-s 1990 (BSI, 1990). The mass of the dried sediments and filter paper was then measured. The mass of the samples was measured to an accuracy of 0.1g on a balance (OHAUS Adventurer Pro), and the mass of the filter paper was measured to an accuracy of 0.0001 g on a balance (Mettler H33).

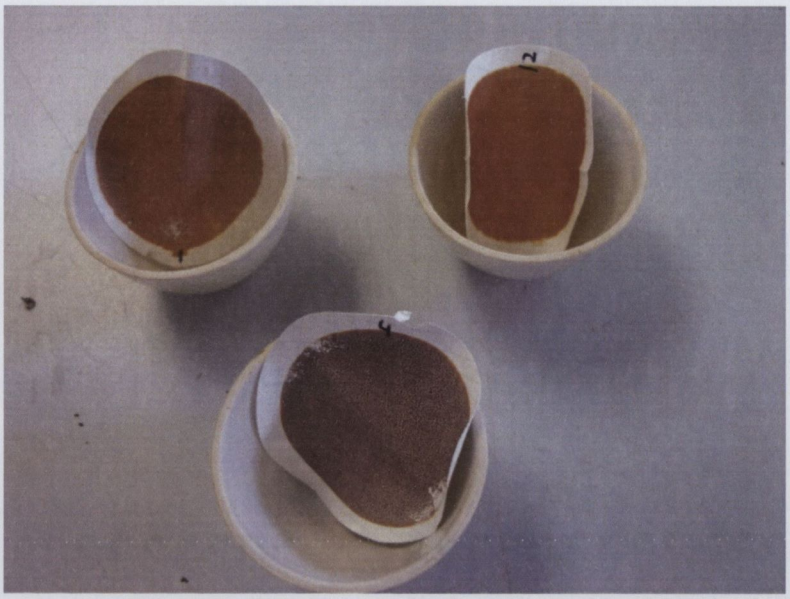

Figure 5.9 *Filter papers containing As-Fe sediment*

5.4 Results and discussion

5.4.1 Flocculation tests

The coagulants and polyelectrolytes (5.3.1) were added to the sample effluent from the large scale reactor and tested as discussed in Section 5.3.3.2 above. The dosages and corresponding observations are detailed in Table 5.4. Efficiency was rated visually, a limitation of jar tests performed in this manner, as observations are subject to variation in the operator's interpretation. The fall velocity tests were carried out not only to determine the settling velocity of particles, but to confirm these visual results by more detailed calculations. As expected, alum, and alum used with Magnafloc LT22S performed best, with relatively small dosages needed (20 mg/l and 0.1 mg/l respectively) for large flocs to be formed in a short flocculation time. *Moringa oleifera* (MO) did perform well, with the results in general

Jar	Aluminium Sulphate mg/l	Moringa Oleifera mg/l	LT22S mg/l	Potato Starch mg/l	Observations
1	20	-	-	-	Visible flocs formed in jar 1 after 15 minutes flocculation. Floc size was small and greatest settlement of precipitate occurred in jar 1. Optimum aluminium sulphate dosage found to be 20mg/l.
2	80	-	-	-	
3	160	-	-	-	
4	0	-	-	-	
1	20	-	0.1	-	Flocs were visible in all jars after 7 minutes flocculation. Largest flocs and greatest settlement occurred in jar 1. Optimum LT22S dosage deemed to be 0.1mg/l.
2	20	-	0.4	-	
3	20	-	0.9	-	
4	20	-	0	-	
1	20	-	-	20	After 15 minutes flocculation, visible flocs formed in all jars. Flocs were smaller than those with LT22S addition. Optimum potato starch doasge 20mg/l, with greatest settlement in jar 1.
2	20	-	-	80	
3	20	-	-	160	
4	20	-	-	0	
1	-	20	-	-	Flocs visible after 15 minutes flocculation, and greatest settlement in jar 1 but no substantial difference between jars. Optimum Moringa dose found to be 20mg/l. Performed more efficiently than iron sulphate, not as well as alum.
2	-	80	-	-	
3	-	160	-	-	
4	-	0	-	-	
1	-	20	0.1	-	Larger flocs visible in all jars after 15 minutes flocculation, with largest seen in jar 1. Greatest settlement also seen in jar 1. Optimum LT22S dosage found to be 0.1mg/l
2	-	20	0.4	-	
3	-	20	0.9	-	
4	-	20	0	-	
1	-	20	-	20	After 15 minutes flocculation, jars 1 and 2 had visible flocs, with greatest settlement and supernatant in jar 1. Optimum potato starch dose deemed to be 20mg/l
2	-	20	-	80	
3	-	20	-	160	
4	-	20	-	0	

Table 5.4 *Flocculation test results giving coagulant/polyelectrolyte dosages and observations*

agreement with previous literature (although these earlier studies were primarily aimed at turbidity removal, so direct comparisons cannot be drawn.) Ndabigengesere *et al.,* (1998a) achieved turbidity reduction of 105 NTU to 10 NTU after jar tests and 30 minutes sedimentation using the same doses of either MO or alum – 50 mg/l. It was also found that the sludge generated was innocuous and 4-5 times less volume than that of alum. Babu and Chaudhuri (2005) found that a much higher dose of *Moringa oleifera* was required (200 mg/l) to reduce turbidity from 25 NTU to 0.3 NTU. As mentioned in the paper, this is most likely due to the non-filtered MO used in suspension. It is also interesting that 280-500 CFU/ml heterotrophic bacteria and 280-500 MPN/100ml fecal coliforms were also reduced to 5-20 CFU/ml and 5-10 MPN/100ml respectively at this dosage (although it should be noted that this study used filtration with a sand filter post-coagulation). The use of potato starch as a polyelectrolyte did make a difference to using alum or MO alone, but did not work as well as LT22S. Figure 5.10 shows an example of two different samples during jar tests, with the flocs forming clearly visible in the picture on the right. The optimum dosage of each coagulant and polyelectrolyte found (Table 5.5) were then used in further jar tests for use in the fall velocity tests detailed below.

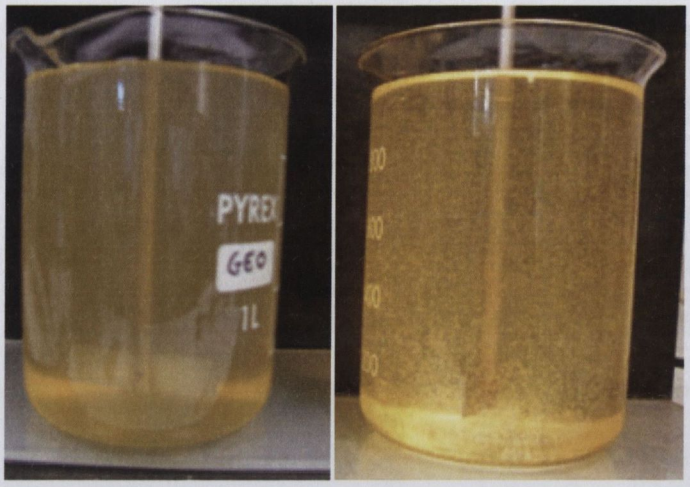

Figure 5.10 *Standard effluent (left) and effluent with MO addition (right) during flocculation*

5.4.2 Fall velocity tests

Fall velocity tests (5.3.3.2) were carried out on standard effluent straight from the outflow of the large scale CPC reactor, and on flocculated effluent, with and without coagulant/polyelectrolyte addition. Optimum doses were used as found in the flocculation tests as discussed in 5.4.1. and Table 5.5 details these dosages. Tests were then carried out to make a comparison between the effectiveness of the natural coagulant *Moringa oleifera* and the industrial coagulant alum. During the next tests polyelectrolytes were introduced, in order to evaluate the efficiency of using natural aids (MO and potato starch) and compare them to the conventional aids (alum & LT22S).

Test	Sample	Coagulant added	Polyelectrolyte added
1	Standard effluent	-	-
2	Flocculated effluent	-	-
3	Flocculated effluent	Alum 20 mg/l	-
4	Flocculated effluent	Alum 20 mg/l	LT22S 0.1 mg/l
5	Flocculated effluent	MO 20 mg/l	-
6	Flocculated effluent	MO 20 mg/l	LT22S 0.1 mg/l
7	Flocculated effluent	MO 20 mg/l	Potato starch 20 mg/l

Table 5.5 *Fall velocity test parameters (MO = Moringa oleifera)*

In order to calculate actual settling velocities, a depth factor is introduced to equate the actual observed settling times to a constant depth of 100 cm. This depth factor is obtained by dividing the volume remaining after each withdrawal by the total volume. This depth factor is then multiplied by the cumulative mass of the sediment taken off in each withdrawal, reducing it to the mass of sediment in suspension which would be present in a 100 cm depth at the same average density. The percentage of sediment in suspension was also obtained - the ratio of the sediment in suspension to the total sediment weight of the sample. The time for the sediment in each sample to fall through a distance of 100 cm is found by multiplying the actual withdrawal time by the depth factor. Thus, the calculations reduce the observed times of settling and mass of sediment in suspension to a constant depth of 100 cm. The value for the settling velocity is calculated by dividing 100 cm by the time taken to fall through 100 cm.

To determine the average settling velocity V_{50} for 50% removal of precipitate, a semi-logarithmic plot (Figure 5.11) was used. From this graph it is clear that the coagulant aids

make a significant difference to the settling velocity, and to the percentage of precipitate left at the end (180 minutes) of the fall velocity tests.

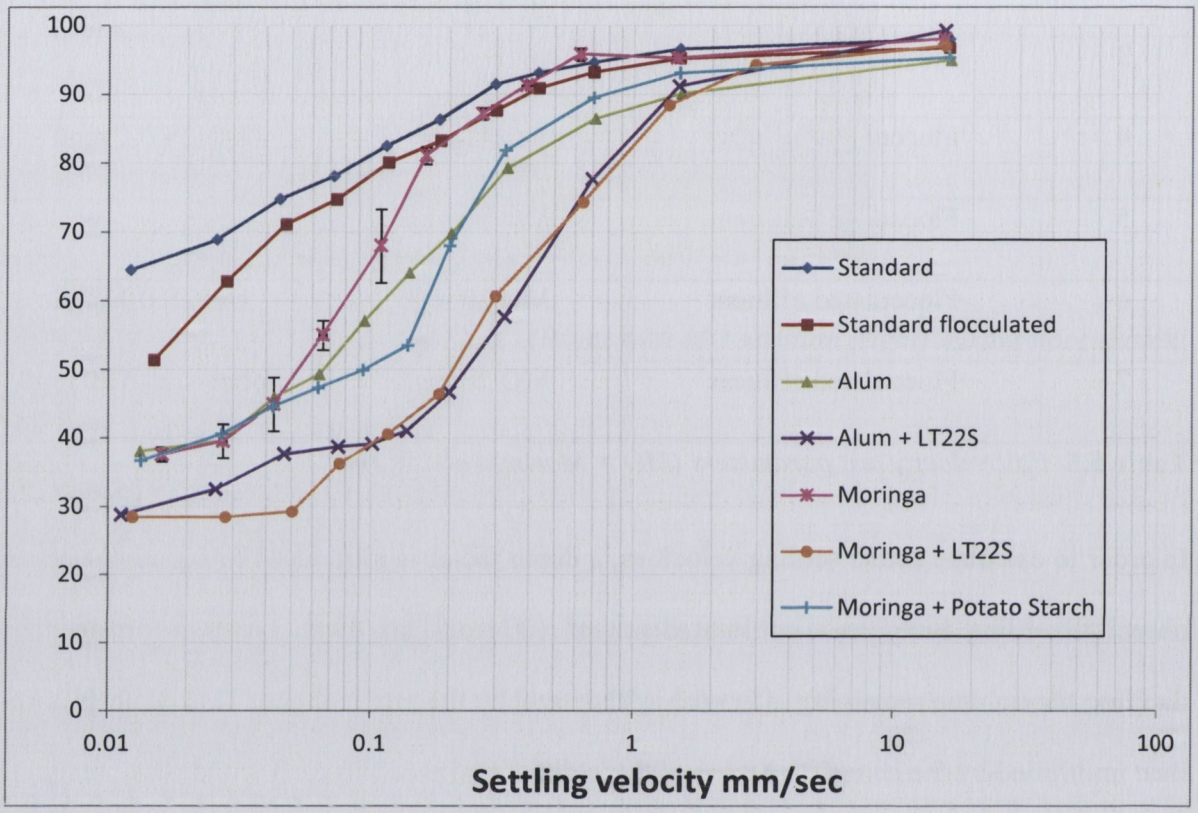

Figure 5.11 *S-curves showing % slower than against settling velocity for the seven different fall velocity tests with and without flocculation and coagulants/polyelectrolytes (Note: error bars only shown on one line to avoid confusion)*

The portion of precipitate remaining in suspension after the 180 minute test on the standard effluent was 64.4%, and an improvement of just over 20% was seen with flocculation alone (51.3% remaining). The residual fractions in the alum and *Moringa oleifera* tests were equivalent, 37.5 and 37.6% respectively. This showed another good improvement on the purely flocculated sample of nearly 27%. The use of potato starch with MO gave only a 1% enhancement of the precipitate remaining (36.6%) compared to when *Moringa* was used

alone. The best results were seen when using both alum and MO with Magnafloc LT22S. Again, final residuals were very similar, with less than 0.5% difference between the two (alum and LT22S 28.7%, MO and LT22S 28.4%), giving over 44% improvement on unaided flocculation.

Table 5.6 lists the average settling velocities, V_{50}, for 50% precipitate removal and their respective standard deviations, found in the S-curves above. As the velocity has a direct correlation with the percentage remaining at the end of the test, similar variations in the V_{50} values are seen. Very little difference is noted between the standard effluent and the flocculated. When using *Moringa oleifera*, a 3.6 fold increase in settling velocity is observed on that of flocculated only. This compares extremely well to that of alum, with a 4.4 fold increase. Potato starch addition nearly doubles the settling velocity on using only MO, but when using LT22S, the value is more than doubled again (either with MO or alum, which are again comparable). The alum-LT22S combination was used in order to illustrate the maximum achievable precipitate removal using conventional treatment methods, while the MO-starch arrangement was used to illustrate the potential gains to be achieved by using completely natural amendments. Although no measurements were taken of sludge volume in this research, Ndabigengesere *et al.,* (1998b) found sludge remaining from coagulation using alum was 4-5 times more voluminous than that using *Moringa oleifera*, during turbidity removal experiments. This is due to the formation of aluminium hydroxide as a precipitate, and it is expected that the SORAS process have a similar ratio of sludge volume. The use of these natural alternatives did show encouraging improvements to the settling characteristics and hence promise for use in full scale treatment in the field.

Sample	V_{50} mm/sec	Standard deviation
Standard effluent	<0.01	-
Flocculated effluent	0.015	-
Alum addition	0.066	0.0033
Alum and LT22S addition	0.238	0.0409
Moringa addition	0.054	0.0044
Moringa and LT22S addition	0.212	0.0447
Moringa and potato starch addition	0.096	0.0049

Table 5.6 *Settling velocities (V_{50}) for 50% removal of precipitates*

As discussed in Section 2.3, coagulation with alum and ferric salts is already a commonly used technique for arsenic removal from drinking water. By using a coagulation step after the SORAS process to accelerate sedimentation, further arsenic could also be removed, resulting in a possible reduction the size of the solar reactor itself. Although arsenic concentrations were not measured after coagulation-flocculation-sedimentation in this study as naturally settled samples from the reactor were already below the MCL of 10 µg/l, it has been shown that As(V) (and to a lesser extent As(III)) can be effectively removed from aqueous solutions by alum (Kartinen and Martin, 1995) and *Moringa oleifera* (Kumari, *et al.*, 2006). The As concentrations and coagulant dosages used in these experiments differed to the present study, with 30 mg/l alum used to reduce 300 µg/l As(V) by 90%, and 10 g/l *Moringa oleifera* to remove up to 85.6% of 25 mg/l As(V). Any arsenic remaining after the SORAS process could

be further reduced with this coagulation as it is needed at this stage for the treatment system to supply clean water at an efficient rate.

5.5 Precipitate-sludge disposal

As seen in this chapter and in previous sections, many techniques of arsenic removal from drinking water are available, however liquid and/or solid sludge is generated from nearly all of these methods. This sludge is likely to have very high As concentrations and so is potentially hazardous to its receiving environment.

5.5.1 Leaching of arsenic residuals

Hamel and Zinia (2001) investigated sludge disposal methods from 15 different treatment units in Bangladesh, including the three examples described previously (Section 2.3.11). The standard EPA Toxicity Characteristic Leaching Procedure (TCLP) was carried out on samples taken from the field, (see WWW document 2 for procedure). This test estimates the amount of mobilization of possible hazardous substances, by using acidic extraction fluid mixed with a solid sludge sample for up to 20 hours. The limit for As in the resulting leachate is 5 mg/l, and results from all 15 treatment units showed leachate concentrations well below the limit, (the highest being 0.043 mg/l). A similar study in Bangladesh (Badruzzaman, 2003), used a modified, more suitable TCLP, as using acidic extraction fluid on wastes where the As was adsorbed by hydrous ferric oxy-hydroxides would not be as effective as using a more alkaline leaching fluid. These results also showed leachate containing minimal arsenic concentrations,

and as such can be considered nonhazardous and can be disposed of through stream discharge, land application, landfill, etc., (Treatment of arsenic residuals from drinking water removal processes, EPA 2001). In addition, Chappell *et al.* (2003) carried out TCLP tests on fresh and aged (2 and 6 months) arsenic residuals from 6 different treatment plants in the US. These also found concentrations of leachate below the allowable limit (the maximum found was 0.162 mg/l). However, CaWET (California Waste Extraction Test) were also carried out. This method of extraction is more rigorous (a legal requirement in the state of California only), and results showed higher concentrations of arsenic in the leachate than in TCLP tests. All fresh samples were below 5 mg/l, but 66% of aged samples had As concentrations over the maximum permitted, ranging from 5.38-15.24 mg/l, with the remainder conforming to the limit. Zaw and Emett (2002) conducted TCLP on sludge from using SORAS on acid mine water and also found that the leachate met EPA requirements.

5.5.2 Possible uses of arsenic sludge

Another disposal method is stabilization/solidification, where the waste is chemically altered to a less soluble form and encapsulated into a solid material. Stabilized/solidified arsenic sludge has been incorporated with ordinary Portland cement, and other additives including lime, fly ash, iron and silicates, to make concrete blocks for pavements or roadbeds, (Zaw and Emett, 2002, Akhter *et al.*, 1990, Dutre and Vandecasteele, 1998, and Chu *et al.*, 1991). TCLP was also carried out on the blocks, and again the leachate could be classed as nonhazardous. This is therefore a viable disposal option with potential economic benefits.

Although no TCLP tests were performed on SORAS sludge during this project, it is assumed that results would be similar to that found above. This implies that sludge could be applied to land (soil, cow dung, etc.) in any region as it is in Bangladesh (Hamel and Zinia, 2001), with only a minimal threat of recontamination. It should also be noted that Hug *et al.*, (2001) stated that SORAS sludge stored or buried close to the surface should remain largely immobilised due to the presence of oxygen.

CHAPTER 6: IRON DISSOLUTION

6.1 Introduction

In areas where arsenic laced water does not have sufficient dissolved iron for the SORAS process, methods of achieving the correct level were explored. The easiest way would be to dissolve iron in powdered form (ferric chloride or sulphate for example) as has been used in the literature for laboratory experiments - although this method would obviously not always be a practical solution for the types of rural village scenario in developing countries for which this process is being developed. Hence, a more sustainable idea was investigated whereby water is passed through scraps of rusted iron to see whether this could get the requisite dose of iron into solution. A review of the literature showed that no investigation seemed to have been carried out with the aim specifically to optimise iron release into solution from pieces of corroded scrap metal. This suggestion was made by Roberts *et al.* (2004) however, in relation to achieving the required iron for their passive co-precipitation process, where concentrations of 35-55mg/l Fe(II) or 3-80mg/l Fe(III) were needed to remove arsenic from 500µg/l to below 50µg/l.

Scrap iron has been used however, in water and wastewater treatment systems as a reactive barrier, for removal of nitrate (Hao, 2005), toxins (Sharma, 2004), chlorinated methanes and benzenes (Matheson, 1994; Lu, 2004), phosphorous (Fytianos, 1998), chromium (Abdo, 1998) and even arsenic reduction (as discussed in Section 2.3.3).

6.2 Background

6.2.1 Iron oxides – rust

Corrosion of metals is the disintegration of the material due to its environment. The corrosion of iron and steel is commonly referred to as *rusting*. This form of corrosion is electrochemical oxidation of the solid metal. It involves the iron, an anode (negative charge) releasing electrons by oxidation:

$$Fe \rightarrow Fe^{++} + 2e \qquad (Eq.\ 1)$$

and water, a cathode (positive charge) consuming electrons by reduction, oxygen in this case:

$$O_2 + 2H_2O + 4e \rightarrow 4OH^- \qquad (Eq.\ 2)$$

The iron and hydroxide ions then react:

$$Fe^{2+} + 2OH^- \rightarrow Fe(OH)_2 \qquad (Eq.\ 3)$$

The ferrous hydroxide ($Fe(OH)_2$), in the presence of oxygen and water, will then either oxidize:

$$4Fe(OH)_2 + O_2 + 2H_2O \rightarrow 4Fe(OH)_3 \qquad (Eq.\ 4)$$

or convert to hydrated ferric oxide – i.e. rust:

$$4Fe(OH)_2 + O_2 \rightarrow 2Fe_2O_3 \cdot H_2O + H_2O \qquad (Eq.\ 5)$$

Ferrous ions on the surface are soluble and therefore can dissolve in water for iron release, but

the ferric ions already in solution are oxidized to form insoluble rust. Figure 6.1 shows the rusting process of iron on the left hand side, and the incurring iron release on the right. A water droplet (shown in blue) on the surface of the metal initiates the chemical reactions described in Equations 1-5 above.

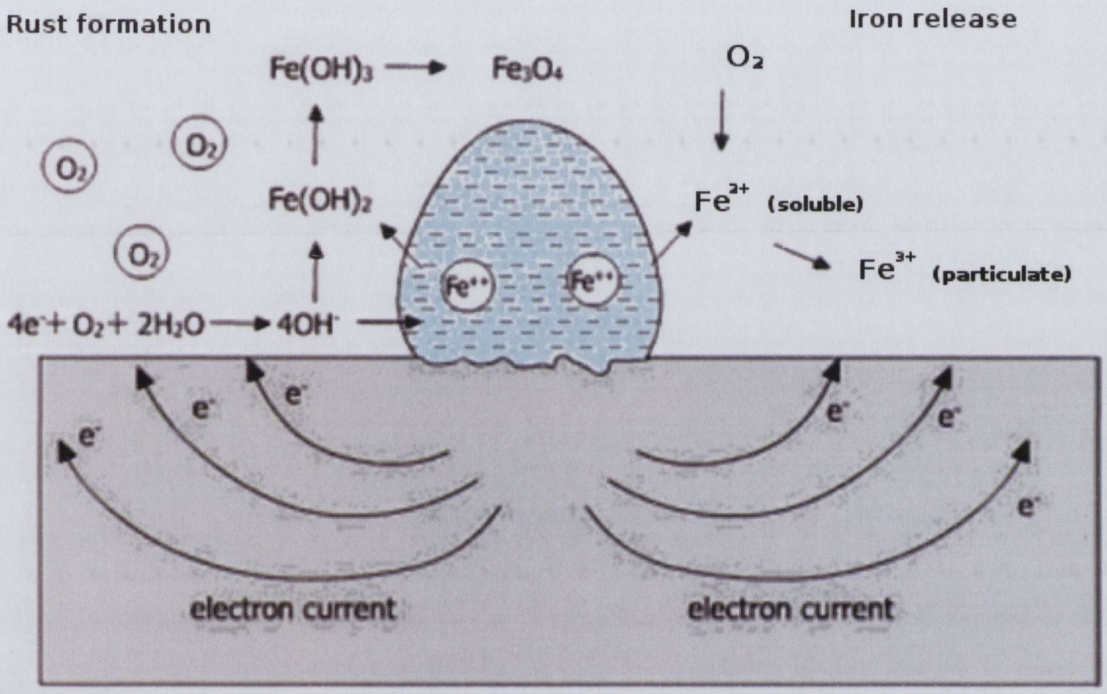

Figure 6.1 *Diagram of iron oxide occurring and iron release (adapted from Ahmad, 2006)*

6.2.2 Factors affecting corrosion

The rate and extent of corrosion are dependent on the surrounding environment. In the case of iron corrosion in an aqueous setting (e.g. a water distribution network), the following are the main factors affecting corrosion (Mays, 1999):

- Velocity: higher flow rates can increase the rate of transfer of dissolved oxygen to the surface, hence increasing corrosion
- Temperature: generally rates of chemical reactions increase with higher temperatures
- pH: as pH is defined as the minus log of the concentration of H^+ ions, lower pH increases corrosion due to H^+ being the electron acceptor during corrosion
- Alkalinity: bicarbonate ions act as a pH buffer in water and so can help to minimise corrosion
- Dissolved oxygen (DO): oxygen is a vital component of corrosion, reacting to form ferrous and ferric ions and so increasing corrosion and iron dissolution
- Total dissolved solids (TDS): a high level of dissolved solids in water indicates a high ionic concentration and therefore greater conductivity, meaning greater flow of electrons and increased corrosion
- Microbial activity: microorganisms generate reactions which can alter the pH, DO concentration, etc. hence can increase or decrease corrosion

6.2.3 Iron dissolution

The main bulk of relevant research has been focused on iron release from corroded pipes in water distribution networks, (Sarin *et al.*, 2001, 2004a and b; Tang *et al.,* 2006). This causes 'red water' or 'coloured water', giving rise to water quality problems such as turbidity, taste, etc., and is one of the main causes of consumer complaint (Mutoti *et al.,* 2007a). As discussed, iron is released by corrosion of the metal, dissolution of ferrous components from the corrosion scales, and hydraulic scouring action of the flowing water. The relationship between

the rate of corrosion and rate of iron release is not a simple one, (Benjamin, 1996). Corrosion is the electrochemical process described above, and results in the direct release of predominantly iron(II) into the water. Dissolution of the corrosion scales is widely accepted as the primary mechanism of iron release. Release from these passive layers is dependent of the solubility of the layer. It is the water contained in the inner porous layers that act as electrolyte transport for Fe ions (Sarin *et al.*, 2004a). McNeill and Edwards (2001) showed scouring of the corrosion scales at excessively high velocities, giving rise to higher suspended solids concentrations, i.e. particulate iron. These studies have given good indications of the parameters involved the dissolution of iron from rusted metal, namely: dissolved oxygen (DO), pH, chloride concentration, sulphate concentration, alkalinity, buffer intensity, temperature, and water flow characteristics. Tang *et al.* (2006) observed that total iron release increased as both pH and alkalinity decreased, and Sarin *et al.* (2004b) noted higher iron release with the lowest DO concentrations and stagnation, and the vast increase in iron release under longterm exposure to anoxic conditions. Water quality modelling in water distribution systems involve the principles of mass conservation, complete mixing of water entering junctions, and application of the suitable generation and decay kinetics (Clark and Grayman, 1998). The following is the advection-dispersion equation provided by Clark and Grayman (1998) amongst others:

$$\frac{\delta C(t,x)ij}{\delta t} = -u_{ij}\frac{\partial C_{(t,x)ij}}{\delta x} + k_{ij}C_{(t,x)ij} \qquad (Eq.\ 6)$$

in which $C_{(t,x)ij}$ is the concentration, x is the location along the pipe length, t is the time at location x, ij is the link between nodes i and j; u_{ij} is the link's flow velocity, and k_{ij} is the first-

order rate constant within the link. Recent iron release models for water distribution systems have been developed mathematically and empirically by Mutoti *et al.* (2007a), based on pipe material and geometry, flow characteristics, and water quality. It was found that using the above advection-dispersion equation, substituting the generation term with $K_m(SA/V)$:

$$\frac{\partial C_{(t,x)}}{\partial t} = -\left(\frac{Q}{A}\right)\frac{\partial C_{(t,x)}}{\partial x} + K_m\left(\frac{SA}{V}\right) \qquad (Eq.\ 7)$$

where K_m is the surface-release flux term (mgFe/m^2/day), SA is the surface area of the pipe (m^2), V is the pipe volume (m^3), Q is the flow rate (m^3/s) and A is the cross sectional area (m^2). For known initial conditions and steady-state flow:

$$\frac{\partial C_{(t,x)}}{\partial t} = 0 \; and \; \frac{\partial C_{(t,x)}}{\partial x} = \frac{dC}{dx} \qquad (Eq.\ 8)$$

$$\therefore 0 = -\frac{QdC}{Adx} + K_m\left(\frac{SA}{V}\right) \leftrightarrow u\frac{dC}{dx} = K_m\frac{SA}{V} \qquad (Eq.\ 9)$$

As:

$$\frac{Q}{A} = u \qquad (Eq.\ 10)$$

with u being the velocity of the water (m/s)

Now: (*Eq. 11*)

$$\frac{SA}{V} = \frac{\pi DL}{\pi D^2 L/4} = \frac{4}{D}$$

And:

$$dx = udt \qquad (Eq.\ 12)$$

where D is the pipe diameter (m)

So: (*Eq. 13*)

$$\frac{dC}{dt} = \frac{4K_m}{D}$$

And finally by integrating both sides:

$$\Delta[Fe] = 4K_m(HRT)/D \qquad (Eq.\ 14)$$

where HRT is the hydraulic retention time (days)

and:

$$K_m = \beta_o + \beta_1(Re - 2000) \qquad (Eq.\ 15)$$

where: β_o and β_1 are parameter estimates established for each pipe material and water quality, and Re is the Reynolds number of flow. As expected, the flux value for unlined cast iron pipes was over twice that of galvanized iron. Subsequent pilot scale testing of this iron release model on a functioning drinking water distribution system verified the developed model (Mutoti *et al.,* 2007b).

These modelling aspects are very different from the current study however, as pipeflow equations cannot realistically be used in water flowing through corroded iron objects with a

varying size distribution. It may be possible though, for other models to be adapted in some way to suit new experimental conditions, which is investigated later in Section 6.5.

6.3 Materials and Methods

6.3.1 Materials

6.3.1.1 Iron metal

Iron metal to fill the reactor was obtained from Bisset Engineering Ltd., a steel engineering and fabricators based in Dublin. The swarf - turnings, chips, or filings - are shavings and chippings of metal, and are the debris resulting from metalworking operations including milling and grinding. These were all of varied size distribution and were sourced from the steel production area only. Larger pieces of steel – nails, bolts and off-cuts of beams, rods, etc., were taken from the Structural Engineering Laboratory (TCD). All of the metal was washed with a degreasing agent (Swarfega Jizer - DEB Group, UK), and then cleaned with several rinses of tap water. The metal was then spread out on trays to dry and corrode. To speed up the corrosion process, the metal was doused in tap water daily and allowed to dry. Once the metal had been completely covered in rust, the swarf was sorted by passing it through a 10mm sieve. Anything that passed through the sieve was termed 'small', anything that did not was classed as 'medium', and all of the larger pieces combined were called 'large'. An example of the rusted iron used in the experiments can be seen in Figure 6.2.

Figure 6.2 *Example of corroded iron pieces*

6.3.1.2 Reactor

The upflow reactor consisted of a 15 cm diameter PVC pipe that tapered into a valve at the base (Figure 6.3). The schematic shows and example of two holes drilled for drain tubing and sample collection, positioned at the appropriate height (just above the level reached by each set of iron pieces).

Figure 6.3 *Schematic of the experimental rig*

6.3.2 Methods

To make a comparison between the different sizes of corroded iron, all experiments were carried out with the iron packed to achieve the same void space. To obtain equivalent void spaces in the reactor for the 3 different size categories, a section of 15cm diameter pipe was cut and attached to a flat base. A sample of 600g of each size of iron pieces was then placed in the section, with water being added to fill it. The volume of water was recorded, and the volume required to fill the empty section was also recorded. The base of the reactor was filled with stones (which were washed and dried beforehand) to where the pipe had a uniform diameter and then a permeable geo-membrane on top of the stones so any sediment would not

clog or damage the valve. The mass of iron (of each size) required to displace 4 litres of water was placed in the reactor for separate experiments, with the pipe contents being shaken to compact the material as much as possible. Holes were drilled into the side of the reactor at the appropriate height for each size grading as shown on Figure 6.3, with a discharge tube fitted going to a drain. A peristaltic pump (Watson Marlow 220S) was then used to pump tap water from a 100 litre capacity tank up through the iron filled reactor at 3 different flow rates (0.3, 0.6 and 1.2 l/min). 30ml samples were taken from the discharge tube after each HRT of clean water flow through the reactor for up to 8 HRTs. The samples were then filtered through a 0.45μm filter paper, acidified with 1% nitric acid (BDH) and refrigerated until analysis. Each experiment was repeated twice, with the iron being allowed to dry completely and fully rust again between tests. This process took up to 3 days on average. (As mentioned in Section 6.2.3, iron release can occur from hydraulic scouring of the metal, so the corrosion scales are essentially washed off the metal during the experimental run).

Long term experiments were then carried out, using all sizes of metal packed into the reactor to minimise the void space. This time 2 different flow rates were used, 0.125 and 0.6 l/min, and ran constantly for up to 3 weeks. During these tests, air was pumped into the reactor instead of water for time periods ranging from 6 minutes to 24 minutes. Arbitrary sample times were chosen throughout the experiments, and samples were taken and treated as above.

For the purposes of providing a data set with definable physical properties against which to calibrate the geochemical model PHREEQC (as described later in Section 6.5), another set of experimental runs were carried out using only rusted nails of the same size from the 'large'

portion of iron materials. 319 six inch nails were placed in the reactor standing up so as to fill the reactor with one layer evenly. Again tap water was pumped through the reactor, this time at a rate of 0.6 l/min, and samples were taken as before. There were also periods when air was introduced to the reactor for these tests, with the reactor being drained and material allowed to dry.

The total iron content of all samples was measured by ICP-AES as described in Section 3.9.

6.4 Results and discussion

6.4.1 Sized iron experiments

Figure 6.4 shows the results from ICP analysis of samples taken from the experiments involving the 3 different size categories of iron and at the 3 flow rates. The plot shows a clear trend of decreasing iron dissolution with increasing water flow through. This conforms with the theory that corrosion scales are washed off with flowing water, especially since very little air (only already dissolved oxygen and aeration of the water through its surface) is available and able to penetrate the iron pack when submerged. As the dissolution of hydrous ferric oxides progresses over time, and a lack of oxygen is available for further iron oxides to form on the metal surface, the rate of dissolution slows and eventually the resulting concentration drops significantly, and in the case of the 'large' pieces, to an almost negligible level.

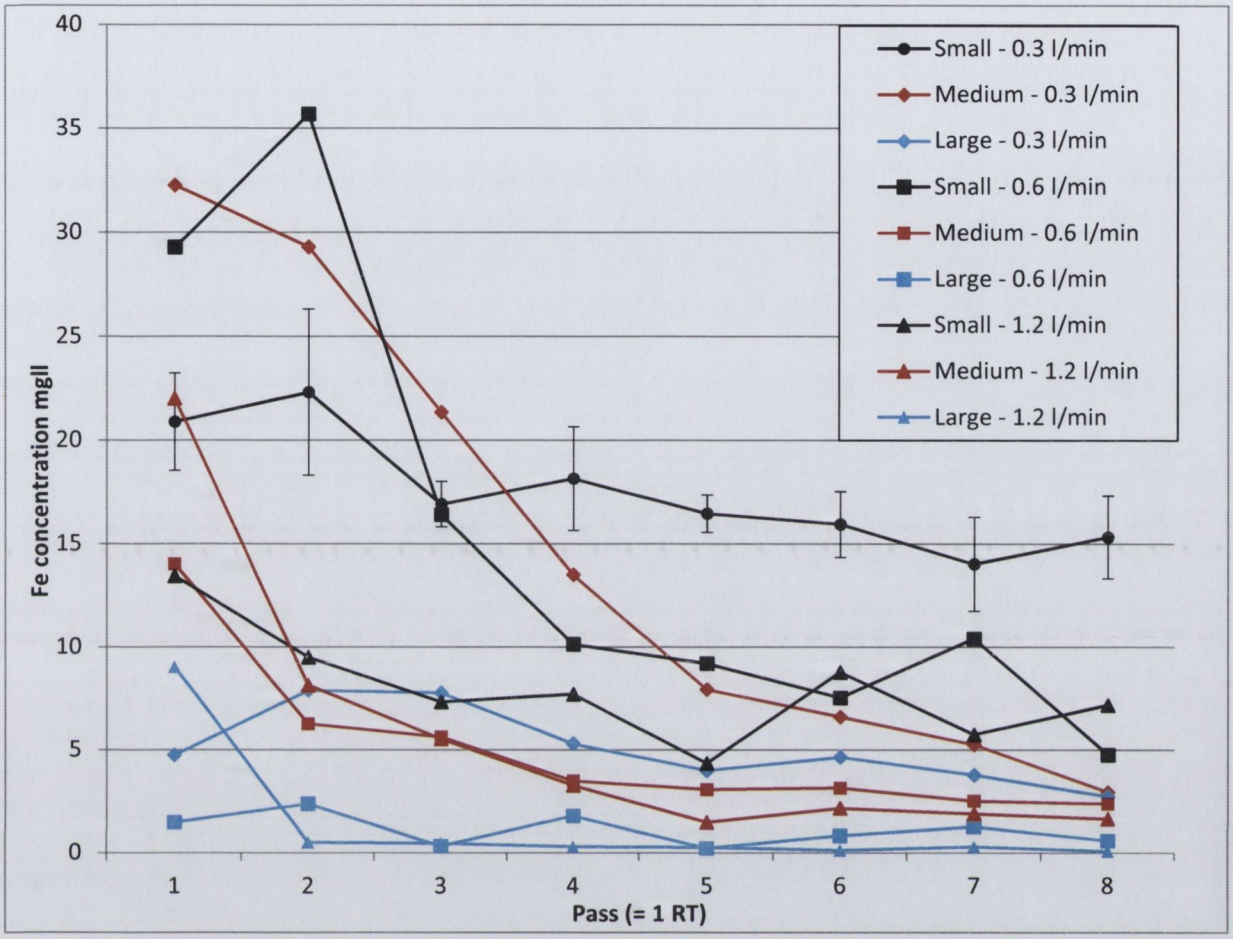

Figure 6.4 *Plot of iron dissolution against each flow through of clean water (defined as 1 hydraulic retention time) for different sized material and flow rates (Note: error bars only shown on one line to avoid confusion)*

Due to the difference in surface area to mass ratio of the 3 size category packs, a considerable decrease in iron dissolution is noted with increasing iron size. This is as expected, with the 'small' size having the greatest surface area for the water to come into contact with, and hence generally most dissolution. This trend continues with the 'medium' size having next best dissolution efficiency, and 'large' performing worst. The trend is also by and large consistent across the 3 different flow rates.

Also, as expected was the higher level of iron dissolution with decreasing flow rate. The

slower the water movement through the reactor, the greater contact time with the iron material, and so the water has more time to react with the hydrous ferric oxides on the metal surface. Again, this trend was noticed across the 3 size categories.

The actual amount of iron dissolution is very high given a relatively small mass of iron was used in the experiments (1.544 - 5.58 kg), in fact up to 5 times the concentration required for use in the SORAS process (depending on initial As concentration). Hence, these initial tests have shown promising results for possible full-scale use of such a process in the field.

6.4.2 Long term experiments

To investigate the sustainability of such a system, long term experiments as described in Section 6.3.2 were carried out and the results are presented in Figure 6.4. As the reactor was fully packed with all sizes of iron material, a significant increase in iron dissolution was seen during the first 3 passes of clean water compared to those in the sized iron tests. Again a large difference is noted between the 2 flow rates, the slower (0.12 l/min) rate giving a four-fold increase in resulting Fe concentration over the faster (0.6 l/min) rate after the first HRT of flow. For both flow rates, iron dissolution dropped quickly (after the first 3-5 HRT of flow), but continued to be sufficient for the SORAS process (~10 mg/l) for over 100 reactor volumes for the slower flow rate (until air was introduced) and 300 reactor volumes for the fast rate (again until air was introduced), which is 650 litres and 1950 litres respectively.

When air was introduced to the system (shown by arrows on the plot), a sharp increase in iron concentration was seen in the samples taken. Each time, air was pumped through the reactor that was already filled with water. The green arrow indicates the point during the 0.12 l/min

run when air (pumped at the same rate) was introduced to the system for a 26 minute duration (0.5HRT). Almost immediately, a spike in concentration of 13.8 times the previous sample is noticed. As with the previous tests, the concentration then declines to when it eventually reaches – after 8 days – a constant low level (1-3 mg/l). A similar trend was observed during the 0.6 l/min run. The pink arrow shows when air was pumped through the reactor instead of water for 6 minutes (0.5HRT) at 0.6 l/min. This time, a 7.4-fold increase in iron concentration was recorded, with it subsequently dropping only to over half that value after almost 150 more HRTs. Air was introduced once again (yellow arrow), for 24 minutes (2 HRTs) at this point and a second spike is seen. This peaked at over 200mg/l after 150 HRTs, and subsided again, this time over a longer period, with the concentration still remaining high (>90mg/l) even after 500 more HRTs.

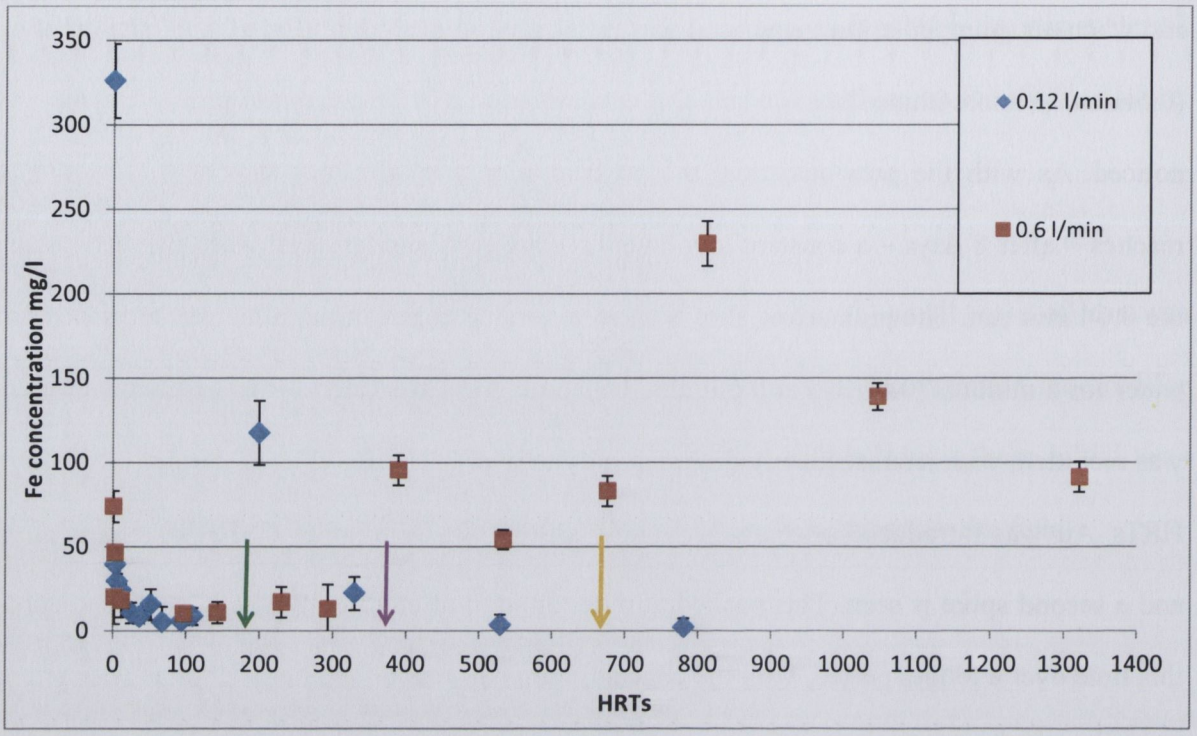

Figure 6.5 *Plot of iron dissoultion against hydraulic retention times at 0.12 l/min and 0.6 l/min for long term tests.* ↓ *Indicates point at which air was pumped through the reactor at 0.12 l/min for 26 minutes.* ↓ *Air was pumped into the reactor at 0.6 l/min for 6 minutes at this point.* ↓ *At this point, air was pumped (again at 0.6 l/min) through the reactor, this time for 24 minutes.*

As discussed for the sized iron experiments, iron dissolution decreased after each subsequent water pass, with corrosion scales being washed away. This long term study showed the same tendency, but the decline was reversed when air sparging was initiated. The oxygen introduced by sparging recommences the corrosion process by the activity described in Section 6.2.1, and the soluble ferrous ions on the surface dissolve for further iron release. This has major implications on the long term sustainability of using this method for the required iron content in the SORAS procedure, whereby letting air into the rusted metal intermittently may maintain the necessary iron concentration for a prolonged period of time.

6.4.3 Wet/dry experiments

Experiments were carried out as detailed in Section 6.3.2 using one layer of corroded nails, and letting the reactor drain and the material dry out for different time periods, to examine the change in Fe dissolution. Figure 6.5 shows the results of a sample of these experiments, using a flow rate of 0.6 l/min, and drying times of 1 hour. The amount of iron dissolved from the hydrous ferric oxide surface was much smaller than in the previous tests, due to the significant decrease in surface area by using only the nails. The concentration remained reasonably stable for the first 3 hours experimental time, after an initial increase in concentration from the first 2 retention times. After a drying period of 1 hour the first sample taken showed a significant decrease in iron concentration, most likely due to the particulate iron being washed off the material. However, the subsequent concentrations increased to above that of the stable values recorded before drying, indicating the potential benefits of incorporating wet/dry periods into the process. It should be noted that the second drying period for test 2 did not result in such a high increase, implying the drying time may need to be increased for each subsequent drying period.

During the longer term experiments (see Figure 6.6), the same flow rate was used (0.6 l/min) and samples were taken 400 minutes after the drying period (of 1 hour). The plots from both sets of experiments are similar in that the concentrations are low and remain steady for the first portion of the experimental run, and there is an increase in concentration after the drying time. However, the final samples taken in these long term tests show a significant decrease in dissolved iron concentration. This agrees with the previous long term tests using the packed bed of all sizes of iron. The drying times therefore would need to occur at regular intervals, and as suggested above, each subsequent drying period would need to have a longer drying time.

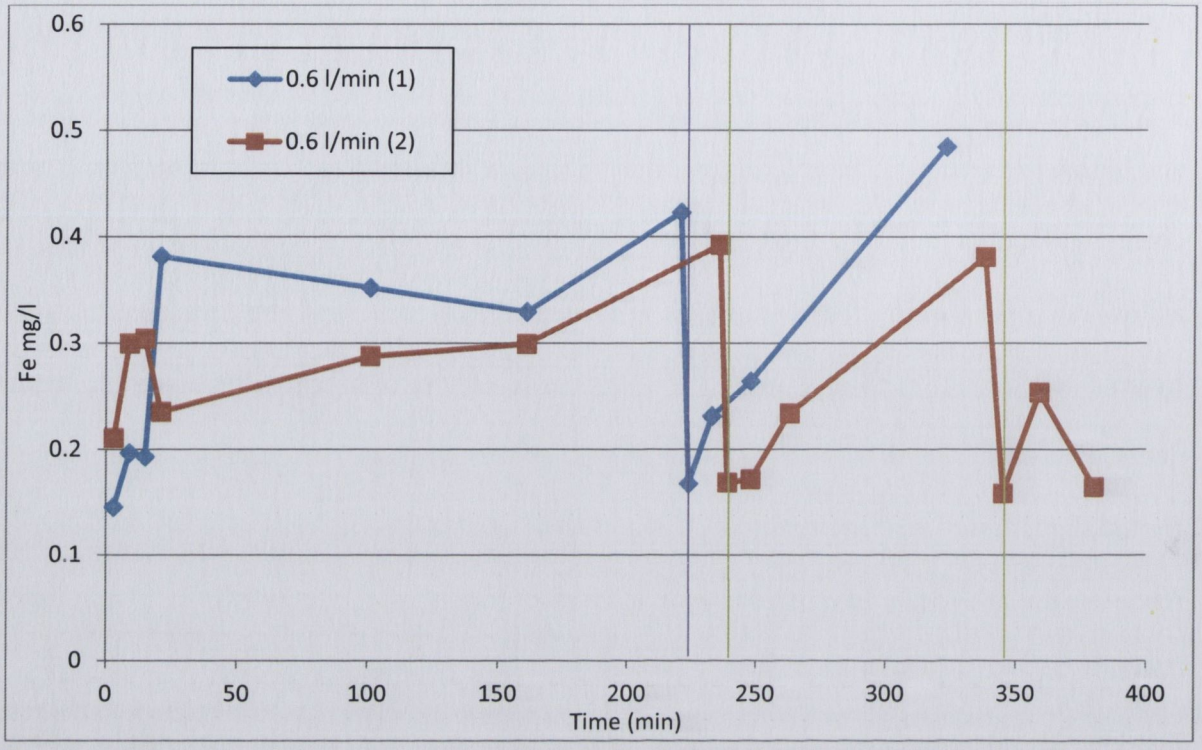

Figure 6.6 *Iron dissolution over time with periodic drying (1 hour drying time: purple line test 1; green lines test 2)*

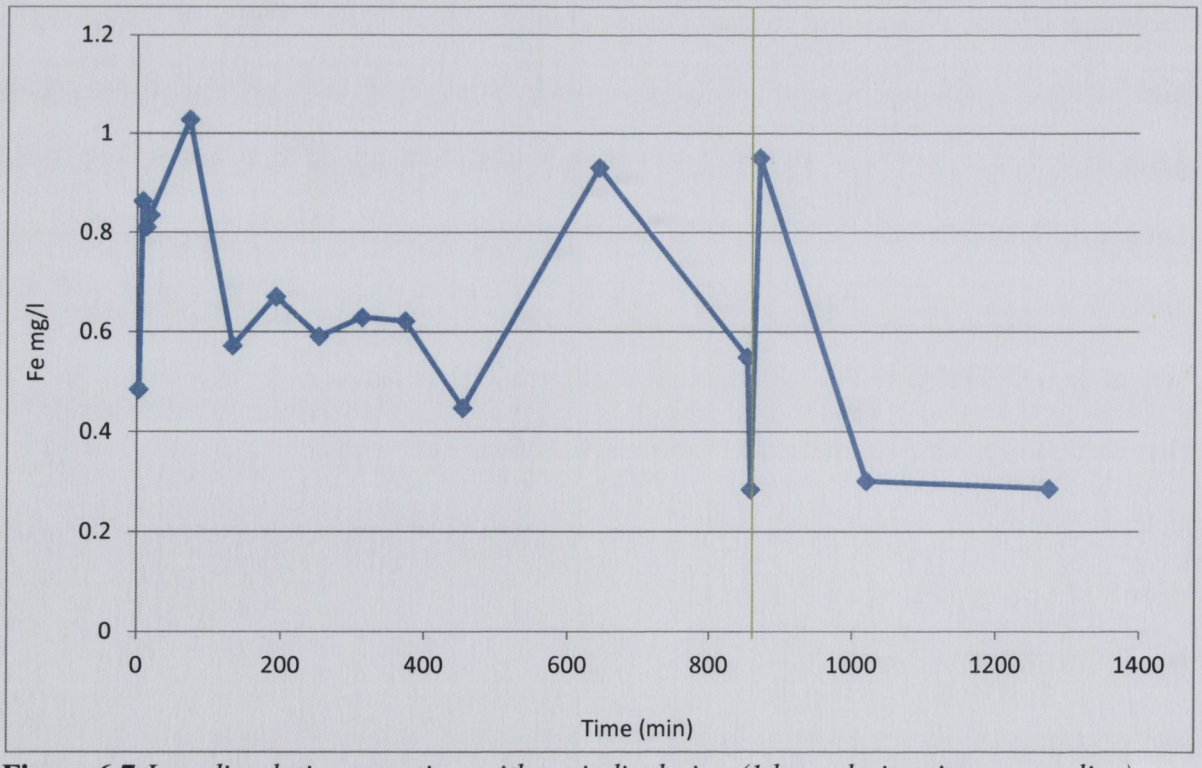

Figure 6.7 *Iron dissolution over time with periodic drying (1 hour drying time: green line)*

The purpose of these experiments was to investigate the possible use of an iron dissolution system in the field for the iron requirement of the SORAS process. As experiments showed significant amounts of resulting dissolved iron, it could be an option where iron is not present in the water to be treated, or if additional iron is needed for higher initial arsenic concentrations in order to optimise the design kinetic. The concept would be to have two (or more) columns filled with corroded iron materials, having one releasing dissolved iron to water passing through it, while the other dries and re-rusts, and alternating between them to maintain the iron release. An advantage of using such a system in conjunction with the SORAS process is that the reactor can only be used during daylight hours, hence the iron material could be left drying at night.

6.4.4 Arsenic adsorption to zero valent iron

No experiments on iron dissolution were carried out using arsenic-spiked water however, in reality the water used in the reactor would most likely be contaminated with As. As mentioned in Section 2.3.3, zero valent iron can be used to remove arsenic from drinking water. Leupin and Hug (2005) and Nikolaidis *et al.* (2003) amongst others showed significant removal of As in column tests using ZVI and sand as adsorption media. Both studies observed leaching of Fe(II) from the ZVI, As(III) oxidation and As(V) adsorption onto the media. Nikolaidis *et al.* (2003) found that a column containing 73kg of iron filings could reduce As(III) (average 297 µg/l) to below 10 µg/l for up to 8 months, running at 2722 l/d. A column length to diameter ratio of 5 is suggested to prevent plugging. Leupin and Hug (2005) found a number of columns in series to be more effective as aeration of the water occurred when in contact with oxygen, promoting oxidation of both As(III) and Fe(II) and hence further adsorption and

precipitation. By taking this into consideration when designing the iron reactor, given there is arsenic present in the influent water, the SORAS reactor could be made smaller as the water be subjected to UV treatment would have a lower As concentration than originally expected. This will be discussed further in Section 7.

6.5 Modelling

6.5.1 PHREEQC

PHREEQC (version 2) is a computer program designed to perform a wide variety of low-temperature aqueous geochemical calculations. PHREEQC is based on an ion-association aqueous model and has capabilities for (1) speciation and saturation-index calculations; (2) batch-reaction and one-dimensional (1D) transport calculations involving reversible reactions, which include aqueous, mineral, gas, solid-solution, surface-complexation, and ion-exchange equilibria, and irreversible reactions, which include specified mole transfers of reactants, kinetically controlled reactions, mixing of solutions, and temperature changes; and (3) inverse modeling, which finds sets of mineral and gas mole transfers that account for differences in composition between waters, within specified compositional uncertainty limits (USGS, 1998). It was used to calculate the amount of iron release as $Fe(OH)_2$ to flowing water from a column of corroded iron metal.

The experiments were modeled using the transport calculation functions for irreversible reactions. To begin, the tap water solution parameters were entered (Table 6.1)

Parameter	Value	Unit
Temperature	10.5 - 14	°C
pH	6.89 - 7.94	-
Ca	15 - 23	mg/l
Cl	22 - 28	mg/l
Cu	0.1 - 1	mg/l
Fe	0.014 - 0.0596	mg/l
F	0.6 - 1	mg/l
O_2	7-10	mg/l
Mg	13 - 19	mg/l
Al	0.05 - 0.12	mg/l
P	0.013 - 0.027	mg/l
Alkalinity (as $CaCO_3$)	20 - 35	mg/l
Na	3.7 - 5.9	mg/l
ρ	1000	kg/m^3

Table 6.1 *Tap water parameters used in PHREEQC*

Next, the iron metal was input as a saturated solution of iron with a density of 3.57 g/cm^3. Then a surface for the solid was equilibrated with this solution according to the parameters given by Dzombak and Morel (1990) for hydrous ferric oxide (HFO):

Parameter	Symbol	Value	Unit
Specific surface area	A	600	m^2/g
Solid concentration	TOTFe	0.09 or 10^{-3}	g/L (mol Fe/90 g HFO) M (mol Fe/kg solvent)
Weak site	TOT(Fe^wOH)	$2x10^{-4}$	M (mol Fe/kg solvent)
Strong site	TOT(Fe^sOH)	$5x10^{-6}$	M (mol Fe/kg solvent)

Table 6.2 *HFO parameters (Dzombak and Morel, 1990)*

The Donnan diffuse layer with a low thickness value was used due to the high porosity of HFO (Dzombak and Morel, 1990). The wet and dry metal in the reactor was weighed to give the mass of water contained in these pores. Next, the transport function was used to introduce the two solutions to each other by entering the time step, column data and flow conditions. In order to model the dissolution of iron from the HFO, the rates and kinetics functions were used. The water density, dynamic viscosity and velocity, and the reactor diameter and retention time were input here. The method used by Mutoti *et al.* (2007a) to reduce Equation 6 was applied to the current reactor set-up to obtain the rate of soluble Fe generation. Mutoti *et al.* (2007a) showed that in a pipe distribution network, the change in Fe concentration in the flowing water was equal to the surface area multiplied by the retention time and divided by the volume, and multiplied by a constant Km (for each type of pipe material and water quality). This is the main parameter that was investigated in the calibration of the model. Stoichiometric coefficients of each species of iron (Fe_{+2}, $FeCO_3$, FeO, $Fe(OH)_2$, Fe_{+3},

$Fe(OH)_3$, FeOOH, Fe_2O_3) were added, and the Runge-Kutta ODE method was chosen to solve the incurring reactions.

The gas phase function was used to simulate the drying/air purging steps. The components of air and their partial pressures were entered, and the volume of gas (whether the reactor being allowed dry out, or air being pumped in) and the drying time step were also input here.

6.5.1 Model results

The model was first calibrated against the experiments which used only the nails packed into one layer in the reactor, as a more accurate value of surface area could be calculated from the geometrically standard nails compared to the swarf. Although the specific surface area of hydrous ferric oxide is given by Dzombak and Morel (1990), the mass of HFO in the experiments is clearly less than that of the total mass of iron pieces, hence the specific surface area was calculated based on an estimated mass of HFO. It should be noted that this estimation may have contributed to some of the errors within the model.

Figure 6.7 shows the model output (as moles of iron per kilogram solvent (water)) plotted against the experimental data from these tests. There is reasonable comparison between the experimental data and model output, with relatively steady levels of iron until the drying period when the concentrations increases.

In an attempt to model the other experiments (using the reactor packed of all size iron pieces), this model grossly underestimated the resulting dissolved iron concentrations (by a factor of 100 on average), indicating that the model requires further calibration. This is most likely due to the limitations of PHREEQC, as it is a software based on equilibrium calculations and has fixed capabilities in estimating the constant changing of the surface and sample, ie. the complicated and numerous reactions involved in the corrosion and Fe(II) production,

including short-lived intermediary species. The chloride and dissolved oxygen concentrations could have also played a part in the further corrosion of the metal, thus altering expected results. Other trace metals associated with the scrap iron could have caused some interference with the ICP analysis, also giving possible errors in experimental results.

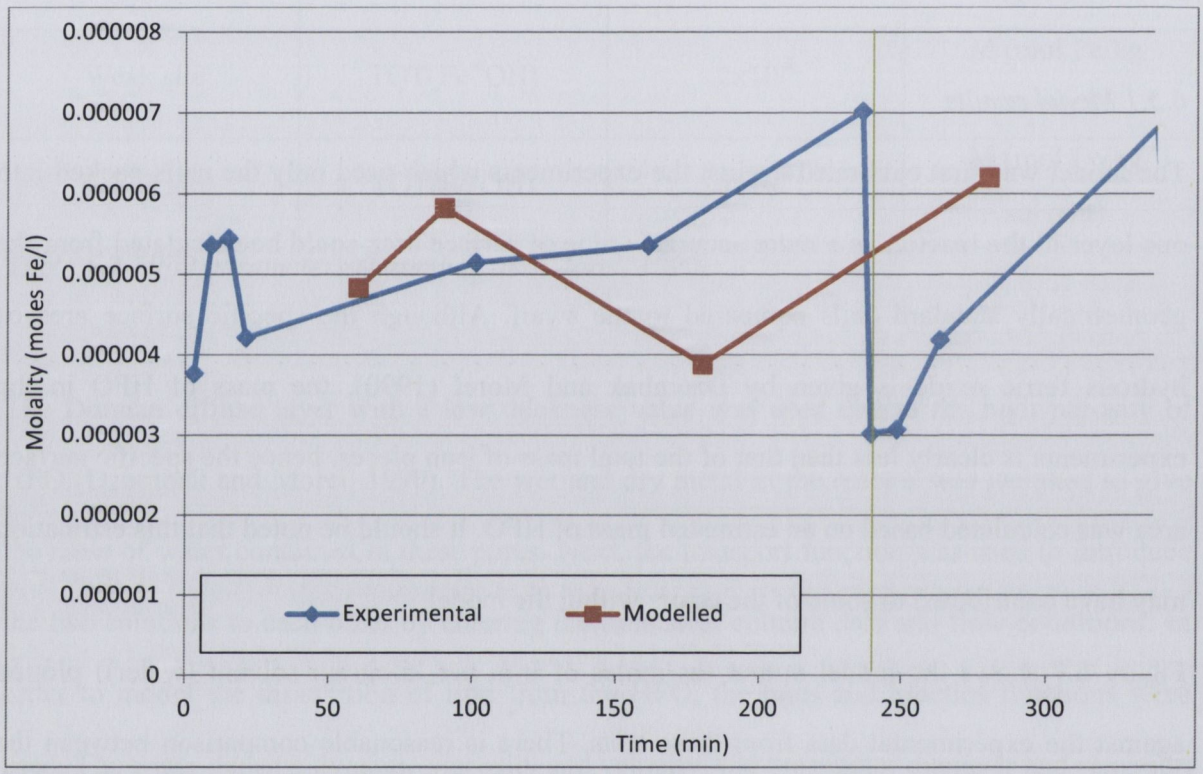

Figure 6.8 *Plot of modelled and experimental results of Fe (molality) against time. (1 hour drying period indicated by green line)*

Once a calibrated model is developed, it can be then used so as to vary wetting and drying times, flow rate and mass of required iron, in order to get the optimum process without the need for further experimentation. This model would likely be produced by using a more suitable software such as ACCUCHEM.

CHAPTER 7: ENGINEERING DESIGN FOR RURAL WATER SUPPLY

7.1 Introduction

There are advantages and disadvantages to treating water at both community scale and household level. As mentioned previously the use of SODIS at household level has not been taken up by users as hoped, hence this research into a village scale system. There are numerous other factors that must be taken into consideration when designing a water treatment system at any level in developing countries. The continuous risk of pathogenic contamination during transportation, handling and storage due to unhygienic practices is a major issue in itself. Regardless of the efficacy of the treatment process, microbial contamination that causes waterborne diseases can occur, rendering the actual treatment futile (WHO, 2002). Table 7.1 details the advantages and disadvantages of household and community systems, indicating some of the considerations required to be addressed in implementing water treatment in a developing county scenario.

Household Treatment	
Advantages	**Disadvantages**
High removal of contaminants	Efficiency depends on user knowledge
Generally low capital and running cost (varies)	Need for continued purchase of consumables
Usually simple to operate	Depends on individual dedication and participation
Good quality water	Limited volumes produced
No need to travel to get water	Storage in the home where contamination can occur
Community Treatment	
Advantages	**Disadvantages**
High removal of contaminants	Need for committee/individual in charge of system
Low running costs, consumables bought in bulk	High capital costs and need for water fees to be collected on regular basis
One time installation	Can have higher technical difficulty
Large volumes produced	Need to travel to collect water
Individuals do not bear responsibility of water quality as it is distributed amongst the community	Space requirement

Table 7.1 *Advantages and disadvantages of household and community water treatment*

The various treatment methods available must be chosen on a case-by-case basis, with user acceptability in mind, particularly with regard to females in the community, as they are the group who use the water most for cooking and cleaning etc.

In order to apply the results of this research to the practical design for a full-scale arsenic removal system, a number of parameters must be taken into consideration, namely:

- The target population
- The per capita daily water requirement (drinking and cooking)
- The variation in intensity of solar radiation received per day
- The raw water concentrations of arsenic and iron
- Other raw water quality parameters (competitive species e.g. PO_4)
- The threshold UV dose required
- The removal rate coefficient
- The system flow rate

From these, the size of the required reactor system can be calculated. An example of this is outlined in the following sections, based on a hypothetical village in the Bengal Basin region. The village has a target population of 500 inhabitants, with a potable water requirement of 10 litres per capita per day (as stated previously, arsenic-free water is only required for drinking and cooking).

7.2 Sizing of continuous flow CPC SORAS reactor

Based on the results found in large scale testing (Section 4.9), an average of 7.5 kJ_{UV}/l was needed to remove any arsenic concentration up to 1000 µg/l, as long as there was required iron in the raw water feeding the reactor (i.e. 10 mg/l Fe required for1000 µg/l As). If naturally

present iron is not sufficient, the use of iron salts would be recommended, or an iron dissolution reactor similar to that tested in Section 6.3 (this will be discussed further in Section 7.4). At the tested flow rate of 10 l/min, the research has shown that 75 kJ_{UV}/min of solar radiation is required to fall on the reactor for effective arsenic removal down to less than 10 µg/l, which equates to 1250 Watts.. Sample UV data from India (although not in the region of interest) reported by Balasaraswathy *et al.* 2002, shows an average UV-A value of 35 W/m^2 from 9am to 5pm (see Figure 7.1). Hence using this value for the design of the system means that the overall size of the irradiated area required for effective arsenic removal at a flow rate of 10 l/min is 35.7 m^2. This equates to 15 of the standard 10 tube reactors (as tested in this research) joined in series. Each reactor has 10 x 1.5 m long tubes, hence giving a total length of tubing for this village of 225 m. At the tube diameter of 48 mm and flow rate of 10 l/min, this would mean a hydraulic retention time of 37.5 minutes for water passing through the reactor. It is believed that this irradiation time would be sufficient given the conservative UV value used, as Hug *et al.* (2001) reported average values of 70 W/m^2 (although no detailed data was given).

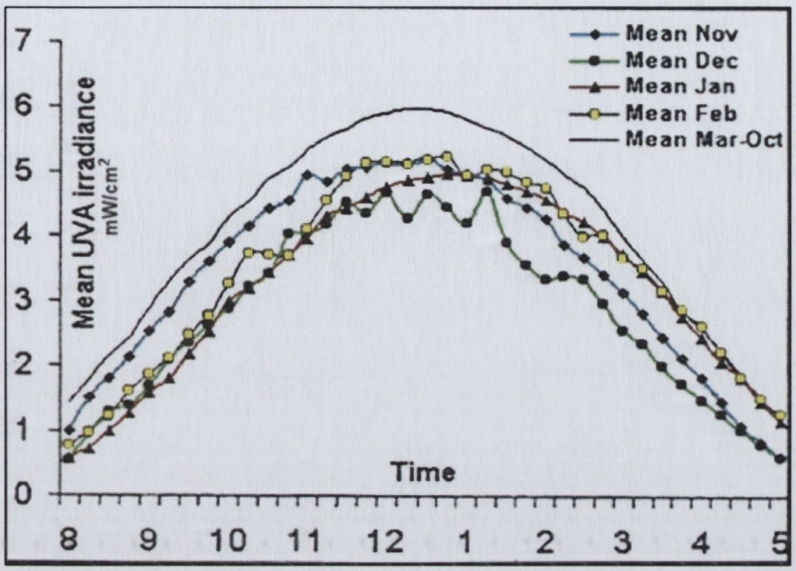

Figure 7.1 *Light intensity data for southern India* (Balasaraswathy *et al.*, 2002)

The reactor would need to be inclined at an angle according to the location's latitude (e.g. 22° 32' for Calcutta, India) and directed due south for maximum sunlight capture. Water would be pumped from an arsenic contaminated tube well to a small reservoir just above the inlet to the reactor, to promote gravitational flow of water through the system controlled by an outlet valve. This pump would need an electricity supply, or use could be made of a solar powered pump given the clear suitability of the region for solar applications. At the beginning of each day (~9am), the manual valves to the inlet and outlet of the reactor would be opened and adjusted to the design flow rate of 10 l/min. The reactor would be given sufficient irradiation time for the water contained in the tubes to receive the required UV dose (based on UV intensity. The reactor would then run at this fixed flow rate with minimal operator interference until 5pm, with treated water exiting to a clarification system (Section 7.3) for the precipitate removal. To overcome the issue of sedimentation of precipitate that would occur overnight within the reactor tubes, a number of options could be utilized. The reactor could be allowed

to empty at the end of the daylight hours, and refilled the next day, though would require additional manpower and waste a certain amount of water. The reactor could be flushed each morning with a higher flow rate to dislodge any sediment, but more energy would be needed. The simplest option would be to close the outlet valve at the end of the day, and then allow the treated water to discharge to clarification under darkness, thereby refilling the reactor with contaminated water ready for the next day's treatment, with little to no sedimentation. As discussed in Section 4.11, periodic cleaning of the reactor tubing would be needed, however as this was not investigated fully on the large scale, observations would have to be made on a pilot system for intervals at which cleaning would need to occur.

The proposed system would be similar in appearance to that shown in Figure 7.1, an example of a full scale CPC reactor system implemented in Ndulyani village in Kenya for solar disinfection (Gill and Price, 2010).

Figure 7.2 *Full scale solar disinfection system in Kenya (Gill and Price, 2010)*

7.3 Suggested design of coagulation-flocculation-clarification system for SORAS precipitate

Using the design information in Sections 5.2.1 and 5.2.2 previously, and the results from coagulation-flocculation and fall velocity tests, the following is an example of a full scale treatment system for use in conjunction with the SORAS continuous flow reactor. As this system is intended for use in developing countries, the appropriate design should be easily built and maintained, with a minimum energy requirement. The suggested design is therefore an around-the-end baffled channel for flocculation and a simple rectangular tank as a sedimentation chamber.

Appropriate hydraulic conditions need to be designed up front of the sedimentation basin in order to allow effective flocculation. A simple open channel baffled flocculator has been chosen as offering the most appropriate solution. Figure 7.2 shows a plan view of a baffled channel. Haarhoff and van der Walt reported optimum geometric ratios for channel design of slot ratio (p) = 1, overlap ratio (q) = 4.5, and depth ratio (r) = 2, for a G value of 50 s^{-1}. As the G value for flocculation calculated in the jar tests carried out in Section 5.3.3.1 was 45 /s, these ratios were used in the design of the suggested baffled channel. The discharge from the SORAS reactor is 10 l/min, and a velocity of 0.1 m/s, so for gentle mixing, the cross sectional area of the channel would need to be greater than that of the reactor tubes. For example, if the area was doubled – giving ~15000 mm^2, the channel width would be 80 mm and depth 160 mm. The overall tank width and length would be 480mm and 1120 mm respectively, containing 14 channels with 13 baffles.

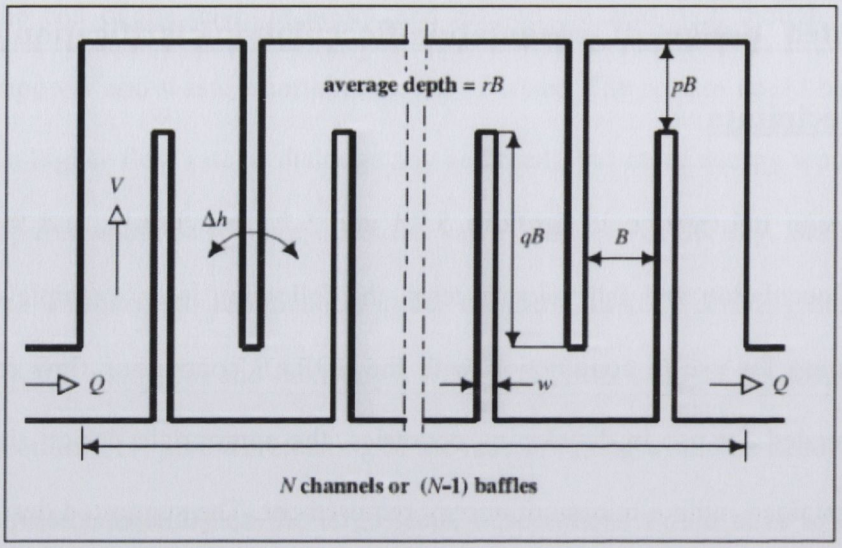

Figure 7.3 *Plan view of baffled channel flocculator. (N = number of channels, therby fixing the number of baffles at (N-1); B = the channel width between baffles; p = the slot ratio (with respect to B); q = the overlap ratio (with respect to B); r = the depth ratio (with respect to B); w = the baffle thickness; Δh = head loss across one turn (m); Q = flow rate (m^3/s)) (Haarhoff and van der Walt, 2001)*

The settlement tank has been designed using the settling velocity and the mean flow rate and general practice suggests factoring up by a factor of 2 to take into account turbulence, wind drag and effects of sunlight creating thermal currents. Basic design and sizing details for full scale treatment include: retention time: 2-4 hours, velocity of flow: not greater than 30 cm/min (horizontal flow), tank dimensions: L:B = 3 to 5:1 (generally L= 30 m, maximum 100 m, breadth= 6 m to 10 m) and circular: diameter not greater than 60 m (generally 20 to 40 m), depth 2.5 to 5.0 m, surface overflow rate: 12000 to 30000 L/d/m^2 tank area, and slopes: rectangular 1% towards inlet, and circular 8% (Metcalf and Eddy, 2003). Based on a flow rate through the CPC reactor of 10 l/min and a settling velocity of the precipitate of 0.015 mm/s, the surface area of the sedimentation basin would need to be approximately 20 m^2. The dimensions of a simple rectangular tank would be 4.5 m(length) x 1.5 m(breadth) x 1.5

m(depth), which is relatively small for a full scale treatment scenario. This surface area could even be dramatically reduced if using 20 mg/l *Moringa oleifera* or 20 mg/l *Moringa oleifera* and 20 mg/l potato starch, to 6 m^2 and 3.5 m^2 respectively, based on their settling velocities. It should be noted however, that if such coagulants / flocculant aids were to be incorporated into the design these would require separate preparation processes to get the material into the correct form for addition into the raw water which adds another level of complexity to the overall design and maintenance of such a system. Katayon *et al.* (2006) investigated storage of *Moringa oleifera* solutions for use in coagulation processes for turbidity removal. It was concluded that the solutions (as made up in the current study – see Section 5.2) did not require refrigeration or to be kept in closed containers, as it had no effect on efficiency, and could be stored for up to one month before a decrease in efficiency was observed. In practice, the *Moringa oleifera* solution would be suspended in a container above the inlet to the baffled channel, releasing the appropriate volume and concentration of the coagulant at the required time. For example, a high concentration stock solution being added dropwise via a small hole in a plastic container, sized to hold a full day's coagulant requirement, therefore only needing daily refilling. Both the sedimentation tank and baffled channel would be constructed from metal or plastic.

An alternative to this system - which was not investigated experimentally - would be a sand filtration unit. Filtration as a method of arsenic removal was discussed in Section 2.5.4, and

due to the nature of the precipitate formed during the SORAS process, a sand filter could increase sediment removal efficiency, and also at a low cost.

7.4 Iron dissolution reactor

As suggested in Chapter 6, if iron concentrations in the inlet water were not sufficient for adequate removal of the initial arsenic concentrations, the use of corroded iron metal for iron dissolution could be utilised. The iron reactor would be similar to what was tested in Section 6.3, with two or more columns being used, one having water flowing through it while the other(s) allowed to dry and re-corrode, alternating when the resulting dissolved iron concentration drops below the level required. By reducing the flow rate through a reactor that contains a large amount of iron, a feed could be supplied to the inlet with high concentrations resulting in the correct amount, rather than all the water needing to be passed through the metal.

7.5 Optimisation of system

The option of having the iron reactor as a pre-treatment stage, or coagulation with *Moringa oleifera* as a post-treatment step, or both, could change the design of the SORAS reactor. Arsenic adsorption onto the scrap iron could remove significant amounts before being

oxidised using UV (Section 6.4.4), in addition to supplying dissolved iron. As shown in Section 5.4.2, *Moringa oleifera* can also remove arsenic and not just simply coagulate the already adsorbed particles. Using these addition elements jointly, whereby a lower As concentration is entering the solar reactor, and (more importantly) a higher concentration can be permitted in the effluent, the actual SORAS rig would be smaller (ie. UV threshold would not need to be reached). The technical difficulty in building the appropriate iron and coagulation elements is relatively low as described previously, and would be more cost effective in comparison with a larger solar reactor, as the glass tubing and aluminium reflectors are more expensive. However, the practicality of this would have to be investigated, as a supply of scrap iron and *Moringa oleifera* would need to be readily available.

As stated previously, water treatment options in developing countries should be chosen on a case-by-case basis, taking the appropriateness, sustainability and efficacy of the technology, cost, and user acceptability into account.

CHAPTER 8: CONCLUSIONS

8.1 Conclusions of research

8.1.1 The use of SORAS in a continuous flow reactor

The results from both small and large scale reactor testing have indicated the potential for the utilisation of a continuous flow SORAS system at village level in a developing country. Inlet water arsenic concentrations of up to 1000 µg/l were reduced to below the MCL of 10 µg/l, requiring up to 10 mg/l iron. The compound parabolic collector (CPC) was found to be the most effective reflector profile in laboratory scale experiments, when compared against a parabolic reflector, V-shaped reflector and flat plate reflector.

Citrate (in the form of both sodium citrate and natural lemon juice), when used in batch scale tests, enhanced the SORAS process by one third as had been found previously by other researchers. However, citrate was found to have the opposite effect (i.e. a detrimental effect on the process) in the continuous flow reactor studies. This is believed to be due to the increased levels of dissolved oxygen concentrations in the continuous flow reactor due to the continued recirculation of the water, compared to the quiescent conditions in the batch study. In such conditions the dissolved iron decreases the rate of Fe(III) reduction, thereby decreasing the amount of ROS being generated for As oxidation.

The arsenic removal kinetic was found to be biphasic, in that the initial drop in As concentration (first 0.2 hours irradiation time) resulted in a much steeper removal kinetic than for the following period, whereby arsenic removal proceeded at a more gentle rate. Generally

during the first phase, the rate of removal increases with iron dose, yet during the second phase, the removal rate showed a hysteresis effect with respect to the As:Fe molar ratio up to a point.

The impact of other typical water quality parameters on the process was also investigated. PO_4 and SiO_3 both had an adverse effect on removal as was expected due to their competition with arsenic for the photooxidation products, as reported by other authors. Generally, this negative effect increases with ion dose, with the process demonstrating much higher levels of sensitivity to PO_4 concentrations compared to SiO_3. Experiments using varying initial pH of samples were also conducted, with the lower pH range resulting in the greatest removal efficiency, which agrees with previous published research. Interestingly, the pH tended to an equilibrium value in all tests, irrespective of the starting value. Temperature also had an effect on removal, with higher temperatures showing better removal rates, which was attributed to more effective adsorption of As(V) onto the iron. Experiments which involved either the removal of initial dissolved oxygen, or the constant aeration of the sample using a diffuser, also showed a difference in the removal rate. The aerated sample reaction kinetic was significantly higher than the deoxygenated sample, however the final As concentrations after 4 hours irradiation time were comparable. This was due to the (unavoidable) natural reaeration of the deoxygenated sample from the turbulent conditions in the reactor tubing.

The use of 10 mg/l TiO_2 as a photocatalyst greatly increased the removal efficiency, taking just one third of the irradiation time needed without TiO_2 for reduction of 1000 µg/l to below 10 µg/l, with 9 mg/l iron.

The continuous flow testing of the SORAS process in the large scale reactor conducted in natural sunlight proved more efficient than the experiments carried out in the small scale reactor. The optimum dosages found in this set of experiments for 1000, 500 and 100 µg/l initial arsenic (over 4 hours actual irradiation time) were 10, 8 and 5 mg/l iron respectively, compared to the small scale dosages of 12, 10 and 5 mg/l iron for 1000, 500 and 100µg/l initial arsenic respectively over 4 hours irradiation time. The threshold UV dose found for all initial arsenic concentrations was 7.5 kJ_{UV}/l (as long as the requisite iron dose was present). An investigation into the effect of varying temperature on the removal process was also carried out on the large scale experiments. Contrary to what was observed in the small scale tests, no difference in arsenic removal occurred in these experiments, although only a maximum 15°C change in temperature took place.

The results from the SORAS-SODIS combined experiments showed that more research would have to be done to determine the respective design kinetics if such a system was to be run in parallel, as both the *E. coli* and arsenic seemed to have an adverse effect on the other's removal efficiency. This was most likely due to competition of both contaminants for ROS. *E. coli* showed adequate removal, but at slower rates than previously reported from experiments without As or Fe present. The rate and final As concentrations showed a marked decrease in efficiency however, indicating that any raw water to be treated by the SORAS process should be checked for microbial contamination. However, the experimental conditions (ie. sample water used) were different to those without *E. coli* and therefore direct comparisons are not possible.

8.1.2 SORAS precipitate removal

As expected, the settling velocity of the As-Fe precipitate was extremely slow due to the nature of colloidal particles. During coagulation jar tests on effluent from the SORAS reactor, the optimum dosages of coagulants were found to be: aluminium sulphate – 20 mg/l; *Moringa oleifera* – 20 mg/l; Magnafloc LT22S 0.1 mg/l; potato starch – 20 mg/l. These dosages resulted in the largest floc sizes in the shortest flocculation time with optimal sedimentation. Larger samples of SORAS effluent were then used (after flocculation with the optimum coagulant doses found) in a fall velocity column test to determine the settling velocity of the different flocs formed, with and without the addition of coagulant aids. The fall velocity results indicated that for 50% removal of the precipitate, the combination of industrial coagulant aids (alum and Magnafloc) performed more effectively than the natural aids (*Moringa oleifera* and potato starch), with settling velocities (v_{50}) of 0.238 and 0.096 mm/s respectively. It is evident that the use of conventional coagulants would be preferred if possible, however the natural aids did yield a 6.4-fold increase in settling velocities (v_{50}) compared to samples flocculated without the addition of any chemical. This has therefore indicated a definite advantage of using natural, locally available coagulant aids in conjunction with the SORAS process.

8.1.3 Iron dissolution

Experimental results from passing clean water through a column filled with corroded iron pieces showed significant iron dissolution from corrosion scales, which could generate sufficient dissolved iron concentration for the optimal levels required for the SORAS process.

The results of the experiments where the iron was continually wetted and then dried showed that corrosion scales reformed when exposed to air, as expected. Hence, for the purpose of providing a constant source of soluble iron into the reactor, a parallel system of one column releasing iron to water while the other dries would seem to be an efficient design. This type of system could be utilised in areas where iron is not naturally present in groundwater. Although a numerical geochemical model was calibrated to some of the physical results, a more rigorous model needs to be developed to model such a process from which the optimum flow rates and wet-dry time periods can be tailored to produce the required iron release for any specific arsenic removal scenario.

In summary, the studies on the SORAS continuous flow system were successful; in particular the large scale tests in natural sunlight, particularly given that the UV intensities in Ireland could be half those in West Bengal. This indicates the potential of such a treatment process which could now be designed to remove arsenic down safe drinking water levels taking into account a spectrum of different local geographical and water quality parameters. To demonstrate this, an example of a full scale treatment system design was carried out for a hypothetical village in an arsenic affected region. This considered the required dissolved iron for the process and local variations in solar radiation from which the required size of the continuous flow reactor was calculated. The precipitate removal system using a flocculation channel and sedimentation basin was then also designed. As a combined system, with the pre-treatment of the iron reactor whereby a portion of arsenic is adsorbed, and post-treatment of coagulation to remove residual arsenic, the SORAS reactor size could be reduced. The UV

threshold might not have to be reached as the low level of remaining arsenic would be removed with the coagulant.

8.1 Recommendations for further research

- A full scale treatment system (such as that designed in Section 7.2) should be set up and tested in an arsenic affected region to determine the system efficiency in the field as well its long term sustainability and user acceptance
- The possibility of using a fixed photocatalyst on inserts inside a continuous flow SORAS reactor should be tested in controlled conditions
- More research is needed to determine the efficiency of the SORAS continuous flow process at a variety of different natural light intensities
- A numerical model to predict the SORAS reactions in a continuous flow reactor should be investigated (using ACUCHEM for example)
- Further investigations, including numerical modelling, are needed to optimise the iron dissolution process with respect to flow rate and wetting / drying times
- Further investigations are needed into the precipitate formation and settlement inside the reactor tubes as well as methods to remove such solids (for example, increasing the flow rate).
- Research needs to be carried out into the economics of manufacturing and installing such a system in the relevant arsenic effected countries as well as a cost benefit analysis of the materials used in the manufacture

REFERENCES

Abdo, M.S.E., Sedahmed, G.H., 1998. A new technique for removing hexavalent chromium from wastewater and energy generation via galvanic reduction with scrap iron. *Energy Convers. Mgmt. Vol. 39, No. 9,943-951*

Acra, A., Raffoul, Z., Karahagopian, Y., 1984. Solar disinfection of drinking water and oral rehydration solutions: Guidelines for household application in developing countries. *UNICEF* Illustrated Publications

Addy, S.E., Gaggil, A.J., van Genuchten, C.M., and Li, L., 2011. Locally-affordable arsenic remediation for rural South Asia using electrocoagulation. *Proceedings of the 35th WEDC International Conference, Loughborough, UK.*

Adeel, Z., 2002. The disaster of arsenic poisoning of groundwater in South Asia – a focus on research needs and UNU's role. *Glob. Env. Change 12, 69–72*

Ahmad, S.A., Khatun, F., Sayed, M.H.S.U., Khan, M.H., Aziz, M.R., Hossain, M.Z., Faruquee, M.H., 2006. Electrocardiographic Abnormalities among Arsenic-exposed Persons through Groundwater in Bangladesh. *Journal of Health, Population and Nutrition, Vol. 24, No. 2, 221-227*

Ahmad, Z. 2006. Principles of corrosion engineering and corrosion control. Butterworth-Heinemann

Ahmed, M.F., 2001. An Overview of Arsenic Removal Technologies in Bangladesh and India. In: Ahmed M. F., Ali, M.A. and Adeel, Z. (eds.), Technologies for Arsenic Removal from Drinking Water, Bangladesh University of Engineering & Technology (BUET) and United Nations University (UNU), May: 251-269.

Ajona, J.I., Vidal, A., 2000. The use of CPC collectors for detoxification of contaminated water: design, construction and preliminary results. *Solar Energy Vol. 68, No.1, 109-120*

Akhter, H., Butler, L., Branz, S., Cartledge, F., Tittlebaum, M., 1990. A study of the effects of hazardous inorganic wastes on the solidification/stabilization of different types of cements using high-resolution MAS NMR spectroscopy. *J. Haz. Mat. 24 145*

Andreae, M.O., 1980. Arsenic in rain and the atmospheric mass balance of arsenic. *J. Geophys. Res. 85, 4512–4518.*

APHA, 1998. Standard Methods for the Examination of Water and Wastewater. *Washington, DC, American Public Health Association.*

Argos, M., Kalra, T., Rathouz, P.J., Chen, Y., Pierce, B., Parvez, F., Islam, T., Ahmed, A., Rakibuz-Zaman, M., Hasan, R., Sarwar, G., Slavkovich, V., van Geen, A., Graziano, J. and Ahsan, H., 2010. Arsenic exposure from drinking water, and all-cause and chronic-disease mortalities in Bangladesh (HEALS): a prospective cohort study. *The Lancet Vol 10, p. 60481-60483*

ASTM, 2008. ASTM D2035-08 Standard practice for coagulation-flocculation jar test of water. ASTM International, West Conshohocken, PA.

Babu, R. and Chaudhuri, M., 2005. Home water treatment by direct filtration with natural coagulant. *Journal of Water and Health, 3 – 1.*

Badruzzaman, A.B.M., 2003. Leaching of arsenic from wastes of arsenic removal systems. *[WWW document]* Available at www.unu.edu/env/Arsenic/Dhaka2003/13-Badruzzaman.pdf Accessed January 2007

Baeumer, B., Benson, D.A., Meerschaert, M.M., Wheatcraft, S.W., 2001. Subordinated advection-dispersion equation for contaminant transport. *Water Resources Research, Vol 37, No. 6, p1543-1550*

Balasaraswathy, P., Kumar, U., Srinivas, C.R., Nair, S., 2002. UVA and UVB in sunlight, Optimal Utilization of UV rays in Sunlight for phototherapy. *Indian J Dermatol Venereol Leprol; 68:198-201*

Bates, M.N., Smith, A.H., Cantor, K.P., 1995. Case-control study of bladder cancer and arsenic in drinking water. *Am J Epidemiol 141,523–530.*

Benjamin, M.M., Sontheimer, H., Leroy, P., 1996. Corrosion of iron and steel. *Internal Corrosion of Water Distribution Systems. AWWA Research Foundation.*

Benson, L.V., Spencer, R.J., 1983. A Hydrochemical Reconnaissance Study of the Walker River Basin, California and Nevada. *USGS Open File Rep., 83–740. United States Geological Survey, Denver.*

Berg, M., Stengel, C., Trang, P.T.K., Viet, P.H., Sampson, M.L., Leng, M., Samreth, S., Fredericks, D., 2007. Magnitude of arsenic pollution in the Mekong and Red River Deltas - Cambodia and Vietnam. *Science of the Total Environment 372 413–425*

Bhattacharya, P., Jacks, G., Nordqvist, S., Mukherjee, A.B., 2002. Metal contamination at a wood preservation site: characterization and experimental studies on remediation. *Science of the Total Environment 290 (1–3), 165–180.*

Bissen, M., Vieillard-Baron, M.M., Schindelin, A.J., Frimmel, F.H., 2001. TiO2-catalyzed photooxidation of arsenite to arsenate in aqueous samples. *Chemosphere 44 751-757*

Biterna M., Arditsoglou, A., Tsikouras' E., Voutsa, D., 2007. Arsenate removal by zero valent iron: Batch and column tests *Journal of Hazardous Materials Volume 149, Issue 3 Pages 548-552*

Blanco, J., Malato, S., Fernandez, P., Vidal, A., Morales, A., Trincado, P., Oliveira, J.C., Minero, C., Musci, M., Casalle, C., Brunotte, M., Tratzky, S., Dischinger, N., Funken, K.H., Sattler, C., Vincent, M., Collares-Pereira, M., Mendes, J.F., Rangel, C.M., 1999. Compound parabolic concentrator technology development to commercial solar detoxification applications. *Solar Energy 67(4-6):317 –330.*

Bode, A.M., Dong, Z., 2002. The paradox of arsenic: molecular mechanisms of cell transformation and chemotherapeutic effects. *Critical Reviews in Oncology/Hematology 42 5–24*

Bratby, J. 2006. Coagulation and flocculation in water and wastewater treatment. *IWA Publishing.*

BSI, 1990. BS 1377-1 Methods for test for soils for civil engineering purposes. Consolidation and permeability tests in hydraulic cells and with pore pressure measurement.

Bundschuh J. et al, 2011. One century of arsenic exposure in Latin America: A review of history and occurrence from 14 countries. *Sci Total Environ*, article in press. doi:10.1016/j.scitotenv.2011.06.024

Buxton, G.V., Greenstock, C.L., Helman, W.P., and Ross, A.B., 1988. Critical Review of Rate Constants for Reactions of Hydrated Electrons, Hydrogen Atoms and Hydroxyl Radicals in Aqueous Solution. *J. Phys. Chem. Ref. Data 17 513-886*

Caceres, L., Gruttner, E., Contreras, R., 1992. Water recycling in arid regions—Chilean case. *Ambio 21, 138–144.*

Campbell, J.P., Alvarez, J.A., 1989. Acute arsenic intoxication. *American Family Physician Vol. 40, no. 6, pp. 93-98*

Campos, J.R., Vieira, M.B.S., Villela, L.M.O., 1984. Comparison of the efficiency of various natural forms of starch when used as flocculants in potable water treatment. *Revista DAE 44, 137 Brazil*

Chakraborti, D., Mukherjee, S.C., Pati, S., Sengupta, M.K., Rahman, M.M., Chowdhury, U.K., Lodh, D., Chanda, C.R., Chakraborti, A.K., Basu, G.K. 2003 Arsenic groundwater contamination in Middle Ganga Plain, Bihar, India: A future danger? *Environmental Health Perspective 111, 1194–2201.*

Chakraborti, D., Sengupta, M.K., Rahman, M.M., Ahamed, S., Chowdhury, U.K., Hossain, M.A., Mukherjee, S.C., Pati, S., Saha, K.C., Dutta, R.N., Quamruzzaman,Q., 2004. Groundwater arsenic contamination and its health effects in the Ganga-Meghna-Brahmaputra plain. *Journal of Environmental Monitoring. 6 (6), 74–83*

Chakraborty A.K., and Saha K.C., 1987. Arsenical dermatosis from tubewell water in West Bengal. *Indian J Med Res., 85: 326–334.*

Chapelon, A., Herrmann, 2004. The AQUACAT project/detoxification and potabilisation of water by solar photocatalysis in semi-arid countries. *J.M. Applied Catalysis B: Environmental, 50, 1-5.*

Chappell, W.R., *et al* (editors), 2003. Arsenic exposure and health effects V: Proceedings of the fifth International Conference on Arsenic Exposure and Health Effects, July 14-18, 2002, San Diego, California.

Chapra, S.C., 1997. Surface Water Quality Modeling. *McGraw-Hill, New York.*

Chen, C.J., Chen, C.W., Wu, M.M., Kuo, T.L., 1992. Cancer Potential in Liver, Lung, Bladder and Kidney Due to Ingested Inorganic Arsenic in Drinking Water. *British Journal of Cancer BJCAAI, Vol. 66, No. 5, p 888-892.*

Chen, C.J., Hsueh, Y.M., Lai, M.S., Shyu, M.P., Chen, S.Y., Wu, M.M., Kuo, T.L., Tai, T.Y., 1995. Increased Prevalence of Hypertension and Long-term Arsenic Exposure. *Hypertension.* 25, 53-60

Chinnici, F., Spinabelli, U., Riponi, C., Amati A., 2005. Optimization of the determination of organic acids and sugars in fruit juices by ion-exclusion liquid chromatography *Journal of Food Composition and Analysis 18, 121-130*

Chu, P., Rafferty, M., Delfino, T., Gitschlag, R., 1991. Comparison of fixation techniques for soil containing arsenic. *Am. Chem. Soc.*

Clark, R.M. and Grayman, W.M., 1998. Modeling water quality in drinking water distribution systems. *AWWA, Denver.*

Conroy, R.M., Elmore-Meegan, M., Joyce, T., McGuigan, K.G., Barnes, J., 1996. Solar disinfection of drinking water and diarrhoea in Maasai children: a controlled field trial. *Lancet 348, 1695-1697*

Cornejo, L., Lienqueo, H., Arenas, M., Acarapi, J., Contreras, D., Yáñez, J., Mansilla, H.D., 2008. In field arsenic removal from natural water by zero-valent iron assisted by solar radiation. *Environmental Pollution, 156 (3), pp. 827-831*

Crecelius, E.A., 1975. The geochemical cycle of arsenic in Lake Washington and its relation to other elements. *Limnol. Oceanog. 20, 441–451.*

Criaud, A., Fouillac, C., 1989. The distribution of arsenic(III) and arsenic(V) in geothermal waters: Examples from the Massif Central of France, the Island of Dominica in the Leeward Islands of the Caribbean, the Valles Caldera of New Mexico, USA, and southwest Bulgaria. *Chemical Geology 76, 259–269*

Dannan, M., Dally, S., Conso, F., 1984. Arsenic induced encephalopathy. *Neurology 34, 1529*

Das, D., Chatterjee, A., Mandal, B.K., Samanta, G., Chakraborti, D., Chanda, B., 1995. Arsenic in groundwater in six districts of West Bengal, India: the biggest calamity in the world. *Analyst 120 917-924*

Davey, J.C., Bodwell, J.E., Gosse, J.A., Hamilton, J.W., 2007. Arsenic as an Endocrine Disruptor: Effects of Arsenic on Estrogen Receptor–Mediated Gene Expression In Vivo and in Cell Culture. *Toxicological Sciences 98(1), 75–86*

Davey, J.C., Nomikos, A.P., Wungjiranirun, M., Sherman, J.R., Ingram, L., Batki, C., Lariviere, J.P., Hamilton, J.W., 2008. Arsenic as an Endocrine Disruptor: Arsenic Disrupts Retinoic Acid Receptor–and Thyroid Hormone Receptor–Mediated Gene Regulation and Thyroid Hormone–Mediated Amphibian Tail Metamorphosis. *Environmental Health Perspectives Vol 116 No 2*

Del Campo, G., Berregi, I., Caracena, R., Santos, I.J., 2006. Quantitative analysis of malic and citric acids in fruit juices using proton nuclear magnetic resonance spectroscopy *Analytica Chimica Acta 556, 462-468*

Del Razo, L.M., Arellano, M.A., Cebrian, M.E., 1990. The oxidation states of arsenic in well-water from a chronic arsenicism area of northern Mexico. *Environ. Pollut. 64, 143–153.*

Delowar, H.K.M., Yoshida, I., Harada, M., Uddin, I., 2005. Effect of arsenic-contaminated water on food chain in Bangladesh: Analysis of arsenic in soil, water and plants. *Journal of Food Agriculture and Environment Vol. 3, no. 2, pp. 282-286.*

Dennett K.E., Amirtharajah A., Moran T.F. & Gould J.P., 1996. Coagulation: its effect on organic matter. *Journal of American Water Works Association,* 88, 129-141.

Dharmappa, H. B., Verink, J., Fujiwara, O. and Vigneswaran, S., 1993. Optimal design of a flocculator. *Water Research* 27 3, pp. 513–519

Dhekane, N. Y., Ambawane, G. B., Patil, B. N. & Pagar, S. D., 1970. Nirmali seed as a coagulant. *J. Instn Engrs India (PHE Div.) 50(10), 108–112.*

Diaz, A., Rincon, N., Escorihuela, A., Fernandez, N., Chacin, E., Forster, C.F., 1999. A preliminary evaluation of turbidity removal by natural coagulants indigenous to Venezuela. *Process Biochemistry, Volume 35, Issues 3-4, Pages 391-395*

Dikshit, A. K., Pallamreddy, K., Reddy, L.V.P. and Saha, J. C., 2000. Arsenic in groundwater and its sorption by kimberlite tailings. *Journal of Environmental Science and Health, Part A, 35: 1, 65 — 85,*

Dixit, S. and Hering, J.G., 2003. Comparison of Arsenic(V) and Arsenic(III) Sorption onto Iron Oxide Minerals: Implications for Arsenic Mobility. *Environ. Sci. Technol. 37, 4182-4189*

Dodd, M. C., Vu, N. D., Ammann, A., Le, V. C., Kissne, R., Pham, H. V., Cao, T. H., Berg, M., Gunten, U. V., 2006. Kinetics and mechanistic aspects of As(III) oxidation by aqueous chlorine, chloramines, and ozone: relevance to drinking water treatment. *Environ. Sci. Technol. 40, 3285−3292,*

Du Preez, M., McGuigan, K.G., Conroy, R.M., 2010. Solar Disinfection of Drinking Water In the Prevention of Dysentery in South African Children Aged under 5 Years: The Role of Participant Motivation. *Environ. Sci. Technol., 44 (22), pp 8744–8749*

Dutre, V. and Vandecasteele, C., 1998. Immobilization mechanism of arsenic in waste solidified using cement and lime. *Environ. Sci. Technol. 32 2782*

Eary L.E., and Schramke, J.A., 1990. Rates of inorganic oxidation reactions involving dissolved oxygen. *In Chemical modeling of aqueous systems, eds. Melchior, D.C. and Bassett, R.L. American Chemical Society, Washington DC.*

EAWAG, 2002. [WWW document] – Solar water disinfection. A water treatment process used at household level. Available at http://www.sodis.ch/methode/anwendung/ausbildungsmaterial/dokumente_material/manual_e.pdf Accessed January 2008

EAWAG, 2002. Solar Water Disinfection a guide for the application of SODIS *Swiss Federal Institute of Environmental Science and Technology [WWW document]* Available at www.sodis.ch/files/SODIS_Manual_english.pdf Accessed December 2007

Eliassen, R.; Pereda, C.; Romeo, A.J. & Skrinde, R.T., 1956. Effects of pH and Velocity on Corrosion of Steel Water Pipes. *Journal AWWA, 48:8:1005.*

Emett M.T., and Khoe, G.H., 2001. Photochemical oxidation of arsenic by oxygen and iron in acidic solutions. *Wat Res Vol. 35, No. 3, pp 649-656*

EPA (Ireland), 2002. Water treatment manuals: Coagulation, flocculation & clarification. *EPA. [WWW document]* Available at http://www.epa.ie/downloads/advice/water/drinkingwater/epa_water_treatment_mgt_coag_flocc_clar2.pdf Accessed May 2009

EPA (US), 1992. [WWW document] - Toxicity characteristic leaching procedure method. Available at http://www.epa.gov/wastes/hazard/testmethods/sw846/pdfs/1311.pdf Accessed February 2007

EPA (US), 2000. [WWW document] – Arsenic compounds. Hazard summary- created in April 1992; revised in January 2000. Available at http://www.epa.gov/ttn/atw/hlthef/arsenic.html Accessed January 2008

EPA (US), 2000. Arsenic Removal from Drinking Water by Ion Exchange and Activated Alumina Plants. *EPA [WWW Document]* Available at: http://www.epa.gov/nrmrl/pubs/600r00088/600r00088.pdf Accessed May 2010

EPA (US), 2000a. Technologies and Costs for Removal of Arsenic from Drinking Water *EPA 815-R-00-028 [WWW document]* Available at www.epa.gov/safewater/arsenic/pdfs/treatments_and_costs.pdf Accessed on November 2007

EPA (US), 2001. Treatment of arsenic residuals from drinking water removal processes. *[WWW document]* Available at www.epa.gov/nrmrl/pubs/600r01033/600R01033.pdf Accessed February 2007

Fan, M., Brown, R.C., Sung, S.W., Huang, C.P., Ong, S.K., van Leeuwen, J., 2003. Comparisons of Polymeric and Conventional Coagulants in Arsenic(V) Removal. *Water Environment Research, Volume 75, Number 4, pp. 308-313(6)*

Feenstra, L., van Erkel, J., Vasak, L., 2007. Arsenic in groundwater: overview and evaluation of removal methods. *Special Report SP nr. 2007-2, Interbational Groundwater Resources Assessment Centre (IGRAC)*

Ferguson, M.A., Hering, J.G., 2006. TiO2-photocatalyzed As(III) oxidation in a fixed-bed, flow-through reactor. *Environ Sci Technol 40 4261-4267*

Fernandez, P., Blanco, J., Sichel, C., Malato, S., 2005. Water disinfection by solar photocatalysis using compound parabolic collectors. *Catalysis Today 101 345-352*

Ficker, E., Kuryshev, Y.A., Dennis, A.T., Obejero-Paz, C., Wang, L., Hawryluk, P., Wible, B.A., Brown, A.M., 2004. Mechanisms of Arsenic-Induced Prolongation of Cardiac Repolarization. *Mol Pharmacol 66:33–44*

Ficklin W.H., 1983. Separation of arsenic(III) and arsenic(V) in ground waters by ion-exchange. *Talanta, 30 (5), pp. 371-373.*

Fostier, A.H., do Socorro Silva Pereira, M., Rath, S., Guimaraes, J.R., 2008. Arsenic removal from water employing heterogeneous photocatalysis with TiO2 immobilized in PET bottles. *Chemosphere Volume 72 Issue 2 pages 319-324*

Frankenberger Jr., W., T., 2001. Environmental chemistry of arsenic. Marcel Dekker Inc.

Fujii, R., Swain,W.C., 1995. Areal Distribution of Selected Trace Elements, Salinity, and Major Ions in Shallow Ground Water, Tulare Basin, Southern San Joaquin Valley, California. *US Geol. Surv. Water-Resour. Investig. Rep. 95–4048.*

Fytianos, K., Voudrias, E., Raikos, N., 1998. Modelling of phosphorous removal from aqueous and wastewater samples using ferric iron. *Environmental Pollution 101 123-130*

Garcia, M.G., d'Hiriart, J., Giullitti, J., Lin, H., Custo, G., del V. Hidalgo, M., Litter, M.I., Blesa, M.A., 2004a. Solar light induced removal of arsenic contaminated groundwater: the interplay of solar energy and chemical variables. *Solar Energy 77, 601-613.*

Garcia-Sanchez, A. and Alvarez-Ayuso, E., 2003. Arsenic in soils and waters and its relation to geology and mining activities (Salamanca Province, Spain) *Journal of Geochemical Exploration, Volume 80, Issue 1, Pages 69-79*

Germolec, D.R., Spalding, J., Boorman, G.A., Wilmer, J.L., Yoshida, T., Simeonova, P.P., Bruccoleri, A., Kayama, F., Gaido, K., Tennant, R., Burleson, F., Dong, W., Lang, R.W., Germolec, D.R., Spalding, J., Yu, H.S., Chen, G.S., Simeonova, P.P., Humble, M.C., Bruccoleri, A., Boorman, G.A., Foley, J.F., Yoshida, T., Luster, M.I., 1998. Arsenic Enhancement of Skin Neoplasia by Chronic Stimulation of Growth Factors. *American Journal of Pathology, Vol. 153, No. 6*

Geucke, T., Deowan, S.A., Hoinkis, J., Patzold, C., 2009. Performance of a small-scale RO desalinator for arsenic removal. *Desalination, 238 (1-3), pp. 198-206.*

Ghurye, G., and D. Clifford. 2001. Laboratory Study on the Oxidation of Arsenic III to Arsenic V. *US EPA/600/R-01/021. National Risk Management Research Laboratory, Office of Research and Development, Cincinnati, OH.*

Gill, L.W. and Price, C., 2010. Preliminary observations of a continuous flow solar disinfection system for a rural community in Kenya. *Energy, 35, p4607-4611*

Gill, L.W., 2006. Report on WatSan Activities in northern Katanga province of Democratic Republic of Congo. *GOAL and Trinity College Dublin*

Guillard, C., Disdier, J., Monnet, C., Dussaud, J., Malato, S., Blanco, J., Maldonado, M.I., Herrmann, J.M., 2003. Solar efficiency of a new deposited titania photocatalyst: chlorophenol, pesticide and dye removal applications. *Applied Catalysis B: Environmental 46 319–332*

Gupta, B.S., Chatterjee, S., Rott, U., Kauffman, H., Bandopadhyay, A., DeGroot, W., Nag, N.K., Carbonell-Barrachina, A.A., Mukherjee, S., 2009. A simple chemical free arsenic removal method for community water supply--a case study from West Bengal, India. *Environmental Pollution. Vol 157, Iss 12, p 3351-3353*

Gupta, S.K. and Chen, K.Y., 1978. Arsenic Removal by Adsorption. *Journal Water Pollution Control Federation, Vol. 50, No. 3 pp. 493-506*

Hamel, N. and Zinia, B.K.N., 2001. A study of treatment technologies and leaching characteristics of arsenic contaminated sludge. *[WWW document]* Available at www.unu.edu/env/Arsenic/Hamel.pdf Accessed January 2008

Haarhoff, J. and van der Walt, J.J., 2001. Towards optimal design parameters for around-the-end hydraulic flocculators. *Journal of Water Supply: Research and Technology – Aqua, 50.3, 149-159*

Hao, Z.W., Xu, X.H., Wang, D.H., 2005. Reductive denitrification of nitrate by scrap iron filings. *Journal of Zhejiang University SCIENCE 6B(3):182-186*

Harper, T.R. and Kingham, N.W., 1992. Removal of Arsenic from Wastewater Using Chemical Precipitation Methods. *Water Environment Research, Vol. 64, No. 3, pp. 200-203*

Hering, J.G., Chen, P., Wilkie, J.A., Elimelech, M., Liang, S., 1996. Arsenic removal by ferric chloride. *J. AWWA 88 155-167*

Hering, J.G., Chen, P., Wilkie, J.A., Elimelech, M., Liang, S., 1997. Arsenic removal from drinking water during coagulation. *J. Environ. Eng. 123 800-807*

Hockberger, P.E., 2000. The discovery of the damaging effect of sunlight on bacteria. *Journal of Photochemistry and Photobiology B: Biology 58 185–191*

Hopenhayn-Rich, C., Biggs, M.L., Fuchs, A., Bergoglio, R., Tello, E.E., Nicolli, H., Smith, A.H., 1996. Bladder Cancer Mortality Associated with Arsenic in Drinking Water in Argentina. *Epidemiology, Vol. 7, No. 2, pp. 117-124*

Hopenhayn-Rich, C., Biggs, M.L., Smith, A.H., 1998. Lung and kidney cancer mortality associated with arsenic in drinking water in Cordoba, Argentina. *International Journal of Epidemiology 27 561-569*

Hsueh, Y.M., Cheng, G.S., Wu, M.M., Yu, H.S., Kuo, T.L., Chen, C.J., 1995. Physiological factors and environmental carcinogenesis: multiple risk factors associated with arsenic induced skin cancer: effects of chronic liver disease and mal-nutritional status. *Human Experimental Toxicology 14 464–465.*

Hug, S.J., and Leupin O., 2003. Iron-catalyzed oxidation of arsenic (III) by oxygen and by hydrogen peroxide: pH dependent formation of oxidants in the Fenton reaction. *Environ Sci Technol 37:27–34*

Hug, S.J., Canonica, L., Wegelin, M., Gechter, D., von Gunten, U., 2001. Solar oxidation and removal of arsenic at circumneutral pH in iron containing waters. *Environ. Sci. Technol. 35, 2114-2121.*

Huie, R. E.; Shoute, L. C. T.; Neta, P., 1991. Temperature dependence of the rate constants for reactions of the carbonate radical with organic and inorganic reductants. *Int. J. Chem. Kinet. 23, 541-552.*

Hussam, A., and Munir, A.K.M., 2007. A simple and effective arsenic filter based on composite iron matrix: Development and deployment studies for groundwater of Bangladesh, *Journal of Environmental Science and Health, Part A,42:12,1869 — 1878*

International Agency for Research on Cancer, 2004. Monographs on the evaluation of carcinogenic risk to humans. Volume 84. Some drinking-water disinfectants and contaminants, including arsenic. *WHO Press.*

Jahn, S. 1981. *Traditional water purification in tropical developing countries; existing methods and potential application*, German Agency for Technical Cooperation.

Jahn, S. 1986. Proper use of African coagulants for rural water supply: Research in the Sudan and a guide for new projects. *Deutsche Gesellschaft fur Technische Zusammenarbeit (GTZ), Eschborn, Federal Republic of Germany,* 351.

Johnston, R. and Heijen, H., 2001. Safe Water Technology for Arsenic Rremoval. *In: Technologies for Arsenic Removal From Drinking Water, BUET Dhaka.*

Kartinen Jr., E.O. and Martin, C.J., 1995. An overview of arsenic removal processes. *Desalination 103, 79-88*

Katayon, S., Megat Mohd Noor, M.J., Asma, M., Abdul Ghani, L.A., Thamer, A.M., Azni, I., Ahmad, J., Khor, B.C. and Suleyman, A.M. 2006. Effects of storage conditions of Moringa oleifera seeds on its performance in coagulation. *Bioresour. Technol., 97: 1455–1460.*

Kessel, M., Liu,S.X., Xu, A., Santella, R., Hei, T.K., 2002. Arsenic induces oxidative DNA damage in mammalian cells. *Molecular and Cellular Biochemistry 234/235: 301–308*

Khan, Z., & Thiem, L.T., 2008. Optimizing coagulation process for a low turbidity, low temperature water. *Electronic Journal of Environmental, Agricultural and Food Chemistry*, 7, 12, 2599-2610.

Khoe, G.H., Emett, M.T., Robins, R.G., 1997. Photoassisted oxidation of species in solution. *U.S. Patent No. 5688378. C.R.C. for Waste Management and Pollution Control.*

Kinniburgh, D.G. and Smedley, P.L., (editors) 2001. Arsenic contamination of groundwater in Bangladesh. *British Geological Survey.*

Kinniburgh, D.G. and Smedley, P.L., 1999. Groundwater studies of arsenic contamination in Bangladesh. *British Geological Survey and Department of Public Health Engineering, Bangladesh.*

Kitchin, K.T., Ahmad, S., 2003. Oxidative stress as a possible mode of action for arsenic Carcinogenesis. *Toxicology Letters 137 3 _ 13*

Klaning, U. K., Bielski, B. H. J., Sehested, K., 1989. Arsenic(IV) a pulseradiolysis study. *Inorg. Chem. 28, 2717-2724.*

Korte, N.E., Fernando, Q., 1991. A Review of Arsenic (III) in Groundwater *CRC Critical Reviews in Environmental Control CCECAU, Vol. 21, No. 1, p 1-39*

Kostal, J., Yang, R., Nu, C.H., Mulchandani, A., Chen, W., 2004. Enhanced arsenic accumulation in engineered bacterial cells expressing ArsR. *Appl. Environ. Microbiol. 70 (8) 4582-4587*

Kudish, A.I., Lyubansky, V., Evseev, E.G. and Ianetz, A. 2005. Inter-comparison of the solar UVB, UVA and global radiation clearness and UV indices for Beer Sheva and Neve Zohar (Dead Sea), Israel. *Energy, 30, pp. 1623–1641.*

Kumari, P., Sharma, P., Srivastava, S., Srivastava, M.M., 2006. Biosorption studies on shelled *Moringa oleifera* Lamarck seed powder: Removal and recovery of arsenic from aqueous system. *International Journal of Mineral Processing, Vol. 78, Iss. 3, pp131-139*

Kuo, T.L., 1968. Arsenic content of artesian well water in endemic area of chronic arsenic poisoning. *Rep Inst Pathol Natl Taiwan Univ. 20:7–13.*

La Mer, V. 1966. Filtration of colloidal dispersions flocculated by anionic and cationic polyelectrolytes. *Discussions of the Faraday Society, 42, 248-254.*

Lai, M.S., Hsueh, Y.M., Chan, C.J., Shyu, M.P., Chen, S.Y., Kuo, T.L., Wu, M.M., Tai, T.Y., 1994. Ingested inorganic arsenic and prevalence of diabetes mellitus. *American Journal of Epidemiology Vol. 139, no. 5, pp. 484-492*

Lakshmanan, D., Clifford, D. and Samanta, G., 2008. Arsenic Removal by Coagulation with Aluminum, Iron, Titanium, and Zirconium. *Journal AWWA, Vol. 100, Iss. 2, Pages 76-88*

Lara, F., Cornejo, L., Yanez, J., Freer, J., Mansilla, H.D., 2006. Solar-light assisted removal of arsenic from natural waters: effect of iron and citrate concentrations. *J. Chem. Technol. Biotechnol. 81, 1282-1287.*

Leupin, O.X., and Hug, S.J., 2005. Oxidation and removal of arsenic (III) from aerated groundwater by filtration through sand and zero-valent iron. *Water Research, 39, 1729-1740*

Lin, T.F. and Wu, J.K. 2001. Adsorption of arsenite and arsenate within activated alumina grains: Equilibrium and kinetics. *Water Research, 35 (8), pp. 2049-2057.*

Lu, M.C., Anotai, J., Liao, C.H., Ting, W.P., 2004. Dechlorination of hexachlorobenzene by zero-valent iron. *Practice Periodical of Hazardous, Toxic, and Radioactive Waste Management 8, 2, 136-140*

Luo, Z.D., Zhang, Y.M., Ma, L., Zhang, G.Y., He, X., Wilson, R., Byrd, D.M., Griffiths, J.G., Lai, S., He, L., Grumski, K., Lamm, S.H., 1997. Chronic arsenicism and cancer in Inner Mongolia - consequences of well-water arsenic levels greater than 50 mg l_1. *Arsenic Exposure and Health Effects. Chapman Hall, London, pp. 55–68.*

Luster, M.I., 1997. Arsenic can mediate skin neoplasia by chronic stimulation of keratinocyte-derived growth factors. *Mutation Research 386 209-218*

Mahata, J., Basu, A., Ghoshal, S., Sarkar, J.N., Roy, A.K., Poddar , G., Nandy, A.K., Banerjee, A., Ray, K., Natarajan, A.T., Nilsson, R., Giri, A.K., 2003. Chromosomal aberrations and sister chromatid exchangesin individuals exposed to arsenic through drinking water in West Bengal, India. *Mutation Research 534 133–143*

Malato Rodriguez, S., Blanco Galvez, J., Maldonado Rubio, M.I., Fernandez Ibanez, P., Alarcon Padilla, D., Collares Pereira, M., Farinha Mendes, J., Correia de Oliveira, J., 2004. Engineering of solar photocatalytic collectors. *Solar Energy, 77, 513-524*

Malato, S., Blanco, J., Cáceres, J., Fernández-Alba, A.R., Agüera, A., Rodríguez, A., 2002. Photocatalytic treatment of water-soluble pesticides by photo-Fenton and TiO2 using solar energy. Catalysis Today, Volume 76, Issues 2-4, Pages 209-220

Malato, S., Fernández-Ibáñez, P., Maldonado, M. I., Blanco, J. & Gernjak, W., 2009. Decontamination and disinfection of water by solar photocatalysis: Recent overview and trends. *Catalysis Today, 147, 1-59.*

Manning, B.A., Hunt, M.L., Amrhein, C., Yarmoff, J.A., 2002. Arsenic(III) and Arsenic(V) Reactions with Zerovalent Iron Corrosion Products *Environ. Sci. Technol., 36 (24), 5455 -5461*

Matheson, L.J., Tratnyek, P.G., 1994. Reductive dehalogenation of chlorinated methanes by iron metal. *Environ. Sci. Technol. 28 2045-2053*

Matthews, R.W., 1992. Photocatalytic oxidation of organic contaminants in water: An aid to environmental preservation. *Pure &Appl. Chem., Vol. 64, No. 9, pp. 1285-1290*

Mäusezahl, D., Christen A., Pacheco G.D., Tellez F.A., Iriarte M., 2009. Solar drinking water disinfection (SODIS) to reduce childhood diarrhoea in rural Bolivia : a cluster-randomized, controlled trial. *PLoS Medicine ; vol. 6, no. 8*

Mays, L. 1999. Water distribution systems handbook. McGraw-Hill

Mazumder, D.N., Das Gupta, J., Santra, A., Pal, A., Ghose, A., Sarkar, S., 1998. Chronic arsenic toxicity in west Bengal--the worst calamity in the world. *J Indian Med Assoc. 96(1):4-7, 18.*

Mazumder, D.N.G., Haque, R., Ghosh, N., De, B.K., Santra, A., Chakraborti, D., Smith, A.H., 1998. Arsenic levels in drinking water and the prevalence of skin lesions in West Bengal, India. *Int. Epidemiol. Assoc. 17 871–877*

Mazumder, D.N.G., Haque, R., Ghosh, N., De, B.K., Santra, A., Chakraborti, D., Smith, A.H., 2000. Arsenic levels in drinking water and the prevalence of respiratory effects in West Bengal, India. *International Journal of Epidemiology 29 1047-1052*

McArthur, J.M., Ravenscroft, P., Safiullah, S., Thirlwall, M.F., 2001. Arsenic in groundwater: testing pollution mechanisms for sedimentary aquifers in Bangladesh. *Water Resources Research, 37(1), 109-117.*

McLoughlin, O. A., 2006. An Examination of the Parameters Involved in the Design of a Continuous Flow Solar Disinfection Process. *PhD Thesis, Dept. of Civil, Structural & Environmental Engineering. Dublin, Trinity College Dublin.*

McLoughlin, O.A., Kehoe, S.C., McGuigan, K.G., Duffy, E.F., Al Touati, F., Gernjak, W., Oller Alberola, I., Malato Rodriguez, S., 2004. Solar disinfection of contaminated water: a comparison of three small-scale reactors. *Solar Energy 77 657-664*

McNeill, L.S., and Edwards, M., 1995. Soluble arsenic removal at water treatment plants. J Am Water Works Assoc. *Vol. 87 Iss.4, p. 105–113.*

McNeill, L.S., and Edwards, M., 2001. Iron pipe corrosion in distribution systems. *Journal AWWA, Vol 93, No. 7, p88-100*

Meharg, A., 2005. Venomous Earth - How Arsenic Caused The World's Worst Mass Poisoning. Macmillan Science

Meng, X. G., Korfiatis, G. P., Bang, S. B., Bang, K. W., 2002. Combined effects of anions on arsenic removal by iron hydroxides. *Toxicol. Lett., 133, 103-111.*

Meng, X. G., Korfiatis, G. P., Christodoulatos, C., Bang, S. B., 2001. Treatment of arsenic in Bangladesh well water using a household co-precipitation and filtration system. *Wat Res Vol 35, Iss 12, p. 2805-2810*

Metcalf and Eddy, Inc. 2003. Wastewater engineering: Treatment and reuse 4th Edition. McGraw-Hill

Métral, J., Charlet, L., Bureau, S., Mallik, S.B., Chakraborty, S., Ahmed, K.M., Rahman, M.W., Cheng Z., and van Geen, A., 2008. Comparison of dissolved and particulate arsenic distributions in shallow aquifers of Chakdaha, India, and Araihazar, Bangladesh. *Geochem. Trans., 9 , p. 1*

Mhaisalkar, V. A., Paramasivam, R. and Bhole, A. G., 1991. Optimizing physical parameters of rapid mix for coagulation–flocculation of turbid waters. *Water Research* 25 1, pp. 43–52

Millero, F. J., Sotolongo, S., 1989. The oxidation of Fe(II) with H2O2 in seawater. *Geochim. Cosmochim. Acta 53 (8), 1867–1873.*

Milton, A.H., Hasan, Z., Shahidullah, S.M., Sharmin, S., Jakariya, M.D., Rahman, M., Dear, K., Smith, W., 2004. Association between nutritional status and arsenicosis due to chronic arsenic exposure in Bangladesh. *International Journal of Environmental Health Research, 14:2, 99 – 108*

Milton, A.H., Rahman, M., 2002. Respiratory effects and arsenic contaminated well water in Bangladesh. *International Journal of Environmental Health Research, 12:2, 175 - 179*

Milton, A.H., Smith, W., Rahman, B., Hasan, Z., Kulsum, U., Dear, K., Rakibuddin, M., Ali, A., 2005. Chronic Arsenic Exposure and Adverse Pregnancy Outcomes in Bangladesh. *Epidemiology. 16(1):82-86*

Misstear, D.B., 2010. An investigation into the optimization of a solar photocatalytic continuous flow disinfection system. *PhD Thesis, Dept. of Civil, Structural & Environmental Engineering. Dublin, Trinity College Dublin.*

Mitra, S.R., Mazumder, D.N.G., Basu, A., Block, g., Haque, R., Samanta, S., Ghosh, N., Hira Smith, M.M., von Ehrenstein, O.S., Smith, A.H., 2004. Nutritional Factors and Susceptibility to Arsenic-Caused Skin Lesions in West Bengal, India. *Environ Health Perspect 112:1104-1109.*

Morton, W.E., Caron, G.A., 1989. Encephalopathy: An uncommon manifestation of workplace arsenic poisoning? *American Journal of Industrial Medicine Vol. 15, no. 1, pp. 1-5.*

Mukherjee, A., Fryar, A.E., Thomas, W.A., 2009. Geologic, geomorphic and hydrologic framework and evolution of the Bengal basin, India and Bangladesh. *Journal of Asian Earth Sciences, Volume 34, Issue 3, Pages 227–244*

Mukherjee, P., Chatterjee, D., Jana, J., Maity, P.B., Goswami, A., Saha, H, Sen, M., Nath, B., Shome, D., Joyti Sarkar, M., Bagchi, D., 2007. Household water treatment option: removal of arsenic in presence of natural Fe-containing groundwater by solar oxidation. *Trace Metals and other Contaminants in the Environment, Volume 9, 603-622.*

Murcott, S., 1999. Appropriate remediation technologies for arsenic contaminated wells in Bangladesh. *[WWW document]* Available at: http://phys4.harvard.edu/~wilson/arsenic/re mediation/arsenic removal/murcott.html Accessed November 2007.

Murcott, S., Dunn, A., Harleman, D.R.F. 1996. Chemically Enhanced Wastewater Treatment for Agricultural Reuse in Mexico. *International Association of Water Quality 1996 Biennial Conference. June 23- 28. Singapore*

Mutoti, G., Dietz, D., Imran, S.A., Taylor, J.S., Cooper, C.D., 2007(a). Development of a novel iron release flux model for distribution systems. *Journal American Water Works Association 99:1*

Mutoti, G., Dietz, D., Imran, S.A., Uddin, N., Taylor, J.S., 2007(b). Pilot-scale verification and analysis of iron release flux model. *Journal of Environmental Engineering 133, 2, 173-179*

Muyibi Suleyman, A. and Evison, L. M., 1995. Optimizing physical parameters affecting coagulation of turbid water with Moringa Oleifera seeds. *Water Research* 29 12, pp. 2689–2695

National Research Council, 2001. Final Report of the Arsenic Cost Working Group to the National Drinking Water Advisory Council USA.

National Research Council, USA, 2001. Arsenic in drinking water risk estimate, 2001 update. National Academy Press

Navntoft, C., Araujo, P., Litter, M.I., Apella, M.C., Fernández, D., Puchulu, M.E., Hidalgo, M.D.V., and Blesa, M.A., 2007. Field tests of the solar water detoxification SOLWATER reactor in Los Pereyra, Tucumán, Argentina. *Journal of Solar Energy Engineering*, 129, *p.127*

Ndabigengesere, A. and Narasiah, K. S. 1998a. Use of Moringa Oleifera Seeds as a Primary Coagulant in Wastewater Treatment. *Environmental Technology,* 19, 789 - 800.

Ndabigengesere, A. and Narasiah, K. S. 1998b. Quality of water treated by coagulation using Moringa Oleifera seeds. *Wat. Res. Vol. 32, No. 3, pp781-791*

Ndabigengesere, A., Narasiah, K. S. and Talbot, B. G. 1995. Active agents and mechanism of coagulation of turbid waters using Moringa Oleifera. *Water Research, Vol. 2, p703-710.*

Ngai, T., Dangol B., Murcott, S., Shrestha, R.R., 2006. Kanchan Arsenic Filter. *Massachusetts Institute of Technology (MIT) and Environment and Public Health Organization (ENPHO). Kathmandu, Nepal*

Nguyen, C.M., Bang, S., Cho, J., Kim, K.W., 2009. Performance and mechanism of arsenic removal from water by a nanofiltration membrane. *Desalination, 245 (1-3), pp. 82-94.*

Nishimura, T., Wang, Q., Umetsu, Y., 1996. Removal of arsenic from process liquors by oxidation of iron(II), arsenic(III) and sulfur(IV) with oxygen. *Iron Control and Disposal ; Ottawa; Canada; 20-23 Oct. 1996. pp. 535-548.*

Nickson, R.T., McArthur, J.M., Ravenscroft, P., Burgess W.G., and Ahmed, K.M., 2000. Mechanism of arsenic release to groundwater, Bangladesh and West Bengal. *Appl Geochem, 15, pp. 403–413*

Nicolli, H.B., Suriano, J.M., Peral, M.A.G., Ferpozzi, L.H., Baleani, O.A., 1989. Groundwater contamination with arsenic and other trace-elements in an area of the Pampa, province of Co′ rdoba, Argentina. *Environ. Geol. Water Sci. 14, 3–16.*

Nikolaidis, N.P., Dobbs, G.M., Lackovic, J.A., 2003. Arsenic removal by zero-valent iron: field , laboratory and modelling studies. *Water Research, 37, 1417-1425*

Ning, R.Y., 2002. Arsenic removal by reverse osmosis. *Desalination. Vol 143 Iss 3, p 237-241*

Nordstrom, D.K., 2002. Worldwide occurrences of arsenic in groundwater. *Science 296 2143-2145*

Ogihara, T., Asano, T., Katagiri, H., Sakoda, H., Anai., M., Shojima, N., Ono, H., Fujishiro, M., Kushiyama, A., Fukushima, Y., Kikuchi, M., Noguchi, N., Aburatani, H., Gotoh, Y., Komuro, I., Fujita, T., 2004. Oxidative stress induces insulin resistance by activating the nuclear factor-κB pathway and disrupting normal subcellular distribution of phosphatidylinositol 3-kinase. *Diabetologia 47:794–805*

Pacheco, J.E., Tyner, C.E., 1990. Enhancement of processes for solar photocatalytic detoxification of water. *Solar eng 163-169*

Parker, D.S., Kaufman, W.J., Jenkins, D., 1972. Floc Breakup in Turbulent Flocculation Processes. *Journal of the Sanitary Engineering Division*, Vol. 98, No. 1, pp. 79-99

Penniston, K.L., Nakada, S.Y., Holmes, R.P., Assimos, D.G., 2008. Quantitative assessment of citric acid in lemon juice, lime juice, and commercially-available fruit juice products. *J Endourol. 22:567–570.*

Pi, J., Kumagai, Y., Sun, G., Yamauchi, H., Yoshida, T., Iso, H., Endo, A., Yu, L., Yuki, K., Miyauchi, T., Shimojo, N., 2000. Decreased serum concentrations of nitric oxide metabolites among Chinese in an endemic area of chronic arsenic poisoning in inner Mongolia. *Free Radical Biology & Medicine, Vol. 28, No. 7, pp. 1137–1142*

Plumlee, G.S., Smith, K.S., Montour, M.R., Ficklin, W.H., Mosier, E.L., 1999. Geologic controls on the composition of natural waters and mine waters draining diverse mineral deposit types. *Environmental Geochemistry of Mineral Deposits. Part B: Case Studies. Chapter 19, pp. 373–432*

Pokhrel, D. and Vivaraghavan, T., 2006. Arsenic removal from an aqueous solution by modified fungal biomass. *Water Research 40 549-552*

Polya, D. A., Gault, A. G., Diebe, N., Feldman, P., Rosenboom, J. W., Gilligan, E., Fredericks, D., Milton, A. H., Sampson, M., Rowland, H. A. L., Lythgoe, P. R., Jones, J. C., Middleton, C. and Cooke, D. A. 2005. Arsenic Hazard in shallow Cambodian groundwaters. *Mineralogical Magazine*, 807-823.

Qian, Y., Castranova, V., Shi, X., 2003. New perspectives in arsenic-induced cell signal transduction. *Journal of Inorganic Biochemistry Volume 96, Issues 2-3, Pages 271-278*

Rahman, M., Tondel, M., Ahmad, S.A., Axelson, O., 2002. Diabetes Mellitus Associated with Arsenic Exposure in Bangladesh. *American Journal of Epidemiology Vol. 148, No. 2 198-203*

Ratnaweera, H., Hiller, n., Bunse, U., 1999. Comparison of the coagulation behavior of different Norwegian aquatic NOM sources. *Environment International, Vol 25, Iss 2-3, p347-355*

Reichard, J.F, Schnekenburger, M., Puga, A., 2007. Long term low-dose arsenic exposure induces loss of DNA methylation. *Biochemical and Biophysical Research Communications Volume 352, Issue 1, Pages 188-192*

Ribeiro, A.B., Mateus, E.P., Ottosen, L.M., and Bech-Nielsen, G., 2000. Electrodialytic Removal of Cu, Cr, and As from Chromated Copper Arsenate-Treated Timber Waste *Environ. Sci. Technol., Vol 34 Iss 5, p 784–788*

Rincon, A.G., Pulgarin, C., 2003. Photocatalytical inactivation of *E. coli*: effect of (continuous-intermittent) light intensity and of (suspended-fixed) TiO2 concentration. *Applied Catalysis B: Environmental 44 263-284*

Robert, D., Malato, S., 2002. Solar photocatalysis: a clean process for water detoxification. *The Science of the Total Environment 291 85-97*

Roberts L.C., Hug S.J., Ruettimann T., Billah M., Khan A.W., Rahman M.T., 2004. Arsenic removal with Iron(II) and Iron(III) in waters with high silicate and phosphate concentrations. *Environmental Science and Technology*, 38, 307-315.

Robertson, F.N., 1989. Arsenic in groundwater under oxidizing conditions, south-west United States. Environ. *Geochem. Health 11, 171–185.*

Rossini M., Garcia Garrido J. & Galluzzo M., 1999. Optimization of the coagulation-flocculation treatment: influence of rapid mix parameters. *Water Research*, 33, 1817-1826.

Rossman, T.G., Meyn, M.S., and Troll, W., 1975. Effects of sodium arsenite on the survival of UV-irradiated Escherichia coli: inhibition of a recA-dependent function. *Mutat Res. Nov;30(2):157-62.*

Rossman, T.G., Meyn, M.S., and Troll, W., 1977. Effects of arsenite on DNA repair in Escherichia coli. *Environ Health Perspect. 19: 229–233.*

Rush, J.D., Bielski, B.H.J., 1985. Pulse radiolytic studies of the reactions of HO_2/O_2^- with Fe(II)/Fe(III) ions. The reactivity of HO_2/O_2^- with ferric ions and its implication on the occurrence of the Haber-Weiss reaction. *Journal of Physical Chemistry Volume 89, Issue 23, Pages 5062-5066*

Saccani, G., Gherardi, S., Trifirò, A., Soresi Bordini, C., Calza, M., Freddi, C., 1995. Use of ion chromatography for the measurement of organic acids in fruit juices. *Journal of Chromatography A, Volume 706, Issues 1-2, Pages 395-403*

Salih, F.M., 2002. Enhancement of solar inactivation of *Escherichia coli* by titanium dioxide photocatalytic oxidation. *Journal of Applied Microbiology 92 920-926*

Sancha, A.M., 2006. Review of coagulation technology of removal of arsenic: Case of Chile. *J Health Popul Nutr 24(3) 267-272*

Sarin, P., Snoeyink, V.L., Bebee, J., Jim, K.K., Beckett, M.A., Kriven, W.M., Clement, J.A., 2004(b). Iron release from corroded iron pipes in drinking water distribution systems: effect of dissolved oxygen. *Water Research 38 1259-1269*

Sarin, P., Snoeyink, V.L., Bebee, J., Kriven, W.M., Clement, J.A., 2001. Physio-chemical characteristics of corrosion scales in old iron pipes. *Wat. Res. Vol. 35, No. 12, pp 2961-2969*

Sarin, P., Snoeyink, V.L., Lytle, D.A., Kriven, W.M., 2004(a). Iron Corrosion Scales: model for scale growth, iron release, and colored water formation. *Journal of Environmental Engineering 130, 4, 364-373*

Sarkar, S., Gupta, A., Biswas, R.K., Deb, A.E., Greenleaf, J.E. and SenGupta, A.K., 2005. Well-head arsenic removal units in remote villages of Indian subcontinent: field results and performance evaluation. *Water Res., Vol. 39, p. 2196–2206*

Sato, Y., Kang, M., Kamei, T., Magara, Y., 2010. Performance of nanofiltration for arsenic removal. *Water Research Vol 36, Iss 13, p3371-3377*

Schneiter, W.R., Middlebrooks, J.E., 1983. Arsenic and fluoride removal from groundwater by reverse osmosis. *Environment International Vol 9, Iss 4, p.289-291*

Schulz, C. R. and Okun, D. A., 1984. Surface Water Treatment for Communities in Developing Countries. *John Wiley & Sons, New York.*

Scott, K., Green, J., Do, H., McLean, J., 1995. Arsenic removal by coagulation. *Am. Water Works 88 155*

Sedlak, D. L., and Hoigné, J., 1993. The Role of Copper and Oxalate in the Redox Cycling of Iron in Atmospheric Waters. Atmos. Environ. *27A, 2173-2185.*

Selecky, M., White, B. and Grunenfelder, G., 2005. Arsenic Treatment for Small Water Systems. Olympia, WA.

Sharma, V.K., 2004. Use of iron(IV) and iron (V) in water and wastewater treatment. Water Science and Technology Vol. 49 No. 4 pp 69-74

Sherwood Lollar, B., 2005. Environmental Geochemistry, Volume 9: Treatise on Geochemistry Elsevier Science

Singh, N., Ma, L.Q., Srivastava, M., Rathinasabapathi, B., 2006. Metabolic adaptation to arsenic-induced oxidative stress in *Pteris vittata* and *Pteris ensiformis. L, Plant Sci. 170 274-282*

Smedley, P.L. and Kinniburgh, D.G., 2002. A review of the source, behaviour and distribution of arsenic in natural waters. *Applied Geochemistry 17 517–568*

Smedley, P.L., 1996. Arsenic in rural groundwater in Ghana. *J. Afr. Earth Sci. 22, 459–470.*

Smet, J. 2002. Small community water supplies: technology, people and partnership. *IRC International Water and Sanitation Centre.*

Smith, A.H., Arroyo, A.P., Guha Mazumder, D., Kosnett, M.J., Hernandez, A.L., Beeris, M., Smith, M.M., Moore, L.E., 2000. Arsenic-induced skin lesions among Atacameño people in northern Chile despite good nutrition and centuries of exposure. *Environ. Health Perspect. 108 pp. 617–620.*

Smith, R. M., Martell, A. E., Eds. 1979. Critical Stability Constants. Plenum Press, New York.

Soignet, S.L., Frankel, S.R., Douer, D., Tallman, M.S., Kantarjian, H., Calleja, E., Stone, R.M., Kalaycio, M., Scheinberg, D.A., Steinherz, P., Sievers, E., Coutre, S., Dahlberg, S., Ellison, R., Warrell Jr., R.P., 2001. United States Multicenter Study of Arsenic Trioxide in Relapsed Acute Promyelocytic Leukemia. *Journal of Clinical Oncology, Vol 19, No 18 pp 3852-3860*

Squibb, K.S., Fowler, B.A., 1983. The toxicity of arsenic and its compounds. *Biological and Environmental Effects of Arsenic, Elsevier*

Stollenwerk, K.G., Breit, G.N., Welch, A.H., Yount, J.C., Whitney, J.W., Foster, A.L., Uddin, M.N., Ahmed, N., 2007. Arsenic attenuation by oxidized aquifer sediments in Bangladesh *Science of the Total Environment, 379 (2-3), pp. 133-150.*

Stuglik, Z. and Zagorski, Z.P., 1981. Pulse radiolysis of neutral iron(II) solutions: oxidation of ferrous ions by HO radicals. *Radiat. Phys. Chem. 17, pp. 229–233*

Stumm, W. *and* Lee, G.F., 1961. Oxygenation of ferrous iron. *Ind. Eng. Chem,, 53:143 146*

Takeuchi, M., Kawahata, H., Gupta, L.P., Kita, N., Morishita, Y., Onoc, Y., Komai, T., 2007 Arsenic resistance and removal by marine and non-marine bacteria. *Journal of Biotechnology 127 434–442*

Tang, Z., Hong, S., Xiao, W., Taylor, J., 2006. Characteristics of iron corrosion scales established under a blend of ground, surface, and saline waters and their impacts on iron release in the pipe distribution system. *Corrosion Science 48 322-342*

Tondel, M., Rahman, M., Magnuson, A., Chowdhury, L.A., Faruquee, M.H., Ahmed, S.A., 1999. The relationship of arsenic levels in drinking water and the prevalence rate of skin lesions in Bangladesh. *Environ. Health Perspect. 107 727–729*

Tseng, C.P., 2004. The potential biological mechanisms of arsenic-induced diabetes mellitus. *Toxicology and Applied Pharmacology 197 67– 83*

Tseng, W.P., 1977. Effects and Dose-Response Relationships of Skin Cancer and Blackfoot Disease with Arsenic. *Environmental Health Perspectives, Vol. 19, pp. 109-119*

Tseng, W.P., Chu, H.M., How, S.W., Fong, J.M., Lin, C.S., Yeh, S., 1968 Prevalence of skin cancer in an endemic area of chronic arsenicism in Taiwan. *J Natl Cancer Inst. 40(3):453-63.*

Tsuda, T., Babazono, A., Yamamoto, E., Kurumatani, N., Mino, Y., Ogawa, T., Kishi, Y., Aoyama, H., 1995. Ingested Arsenic and Internal Cancer: A Historical Cohort Study Followed for 33 Years. *American Journal of Epidemiology Vol. 141, No. 3: 198-209*

Tyrovola, K., Nikolaidis, N.P., Veranis, N., Kallithrakas-Kontos N., and Koulouridakis, P.E., 2006. Arsenic removal from geothermal waters with zero-valent iron — effect of temperature, phosphate and nitrate. *Water Res, 40, pp. 2375–2386.*

Tzou, YM, Wang, S.L., Wang, M.K., 2005. Fluorescent light induced Cr(VI) reduction by citrate in the presence of TiO_2 and ferric ions Colloids and Surfaces. *Physicochemical and Engineering Aspects. Vol 253, p.15-22.*

UNICEF, 2011. Making economic sense for arsenic mitigation: a case study of Comilla District, Bangladesh. *United Nations.*

US Army Corps of Engineers, 2001. Engineering manual EM 1110-1-4012 Precipitation/Coagulation/Flocculation. *Washington, DC. (WWW document* Available at: http://www.scribd.com/doc/19646601/EM-111014012-Precipitation-Coagulation-Flocculation-Web Accessed May 2010

USGS, 1999. [WWW document] – USGS PHREEQC Welcome page. Available at http://wwwbrr.cr.usgs.gov/projects/GWC_coupled/phreeqc/ Accessed February 2009

Vaishya, R.C. and Gupta, S.K., 2003. Arsenic Removal from Groundwater by Iron Impregnated Sand. *J. Env. Eng. Vol. 129, Iss. 1, p. 89-92*

Varsanyi, I., Fodre, Z., Bartha, A., 1991. Arsenic in drinking water and mortality in the southern Great Plain, Hungary. *Environ. Geochem. Health 13, 14–22.*

Vera, E., Sandeaux, J., Persin, F., Pourcelly, G., Dornier, M., Ruales, J., 2007. Deacidification of clarified tropical fruit juices by electrodialysis. Part I. Influence of operating conditions on the process performances. *Journal of Food Engineering, Volume 78, Issue 4, Pages 1427-1438*

Von Ehrenstein, O.S., Mazumder, D.N.G., Hira-Smith, M., Ghosh, N., Yuan, Y., Windham, G., Ghosh, A., Haque, R., Lahiri, S., Kalman, D., Das, S., Smith, A.H., 2006. Pregnancy Outcomes, Infant Mortality, and Arsenic in Drinking Water in West Bengal, India *American Journal of Epidemiology Vol. 163, No. 7 662–669.*

Wang, L.F., Huang, J.Z., 1994. Chronic arsenism from drinking water in some areas of Xinjiang, China. *Arsenic in the environment 27 159-172*

Wang, L.K., Hung, Y.T., Shammas, N.K., 2004. Physicochemical treatment processes (Handbook of environmental engineering). *Humana Press Inc.,U.S.*

Wasserman, G.A., Liu, X., Parvez, F., Ahsan, H., Factor-Litvak, P., van Geen, A., Slavkovich, V., LoIacono, N. J., Cheng, Z., Hussain, I., Momotaj, H., and Graziano, J., 2004. Water Arsenic Exposure and Children's Intellectual Function in Araihazar, Bangladesh. *Environ Health Perspect 112:1329-1333*

Water Environment Federation, 2005. Clarifier Design: WEF Manual of Practice No. FD-8. *McGraw-Hill Professional*

Wauson, E.M., Langan, A.S., Vorce1, R.L., 2002. Sodium Arsenite Inhibits and Reverses Expression of Adipogenic and Fat Cell-Specific Genes during *in Vitro* Adipogenesis. *Toxicological Sciences 65, 211–219*

Wegelin, M., Canonica, S., Mechsner, K., Fleischmann, T., Pesaro, F., Metzler, A., 1994. Solar water disinfection: scope of the process and analysis of radiation experiments. *J Water SRT- Aqua Vol. 43, No. 3, pp 154-169*

Wegelin, M., Gechter, D., Hug, S.J., Mahmud, A., Motaleb, A., 2001. SORAS - a simple arsenic removal process. *Presented at 26th WEDC Conference. [WWW document]* Available at:http://www.physics.harvard.edu/~wilson//arsenic/remediation/sodis/SORAS_Paper.html Accessed November 2006.

Welch, A.H., Lico, M.S., 1998. Factors controlling As and U in shallow ground water, southern Carson Desert, Nevada. *Appl. Geochem. 13, 521–539.*

White, D.E., Hem, J.D., Waring, G.A., 1963. Data of Geochemistry, 6th ed. M. Fleischer, (Ed). Chapter F. Chemical Composition of Sub-Surface Waters. *US Geol. Surv. Prof. Pap. 440-F.*

Wickramaslnghe, S.R., Han, B., Zimbron, J., Shen ,Z., Karim, M.N., 2004. Arsenic removal by coagulation and filtration: comparison of groundwaters from the United States and Bangladesh. *Desalination, Vol.169 p. 231–244.*

Williams, M., Fordyce, F., Paijitprapapon, A., Charoenchaisri, P., 1996. Arsenic contamination in surface drainage and groundwater in part of the southeast Asian tin belt, Nakhon Si Thammarat Province, southern Thailand. *Environ. Geol. 27, 16–33.*

Wist, J., Sanabria, J., Dierolf, C., Torres, W. & Pulgarin, C., 2002. Evaluation of photocatalytic disinfection of crude water for drinking-water production. *Journal of Photochemistry and Photobiology A: Chemistry, 147, 241-246.*

World Bank, 2005. Arsenic contamination of groundwater in south and east Asian countries *[WWW document]* Available at www.siteresources.worldbank.org/INTSAREGTOPWATRES/Resources/ArsenicVolII_WholeReport.pdf Accessed January 2007

World Health Organization, 2002. Managing Water in the Home: Accelerated Health Gains from Improved Water Supply. Geneva: World Health Organization, Document No. WHO/SDE/WSH/02.07.

World Health Organization, 2006 Guidelines for drinking-water quality, third edition, incorporating first addendum *[WWW document]* Available at: http://www.who.int/water_sanitation_health/dwq/gdwq3rev/en/index.html Accessed November 2006.

Yang, C.Y., Chang, C.C., Tsai, S.S., Chuang,H.Y., Ho, C.K., Wu, T.N., 2003. Arsenic in drinking water and adverse pregnancy outcome in an arseniasis-endemic area in northeastern Taiwan. *Environmental Research 91 29–34*

Yoshida, T., Yamanchi, H., Jun, G.F., 2004. Chronic health effect in people exposed to arsenic via the drinking water: dose–response relationship in review. *Toxicol. Appl. Pharmacol. 198 243–252*

Yu, H.S., Liao, W.T., Chang, K.L., Yu, C.L., Chen, G.S., 2002. Arsenic Induces Tumor Necrosis Factor α Release and Tumor Necrosis Factor Receptor 1 Signaling in T Helper Cell Apoptosis. *J Invest Dermatol 119:812-819.*

Zaw, M., Emett, M.T., 2002. Arsenic removal from water using advanced oxidation processes. *Toxicol. Lett. 133, 113-118*

Zepp, R.G., Faust, B.C., and Hoigne, J., 1992. Hydroxyl radical formation in aqueous reactions (pH 3-8) of iron(II) with hydrogen peroxide: the photo-Fenton reaction, *Environ Sci Technol 26, pp. 313–319*

Zhang, T.D., Chen, G.Q., Wang, Z.G., Wang, Z.Y., Chen, S.J., Chen, Z., 2001. Arsenic trioxide, a therapeutic agent for APL. *Oncogene 20, 7146-7153*

Zhang, W., Singh, P., Paling, E., Delides, S., 2004. Arsenic removal from contaminated water by natural iron ores. *Minerals Engineering, 17, 4, 517-524*